


THE PETROCHEMISTRY OF METABASITES FROM
A PRECAMBRIAN AMPHIBOLITE-GRANULITE
TRANSITION ZONE, SOUTH NORWAY.

by

PETER W. L. CLOUGH, B.Sc. F.G.S.

Thesis submitted to the University of Nottingham
for the degree of Doctor of Philosophy,
September, 1977.



CONTENTS

	<u>Page</u>
<u>Chapter 1:</u>	<u>Introduction</u>
A. Location	1
B. Geological outline and previous research	1
C. Objectives	3
D. Nomenclature of metamorphosed mafic rocks	6
<u>Chapter 2:</u>	<u>Field relations and petrography</u>
A. Introduction	8
B. Field relations	9
C. Sampling	11
D. The orthopyroxene isograd and sub-division of the terrain	11
E. Mineral assemblages	13
F. Textural relationships	16
G. Discussion	18
H. Conclusions	20
<u>Chapter 3:</u>	<u>Major element chemistry</u>
A. Introduction	22
B. Major element characterisation of the metabasites	23
C. Intra-terrain major element variation	25
D. CIPW norms	29
E. Major element variation diagrams	30
The AFM diagram	30
Differentiation indices	31
Alkali element variation	34
F. Conclusions	38
<u>Chapter 4:</u>	<u>Trace element chemistry</u>
A. Introduction	40
B. Comparisons with basalt and metabasite trace element data	41

	<u>Page</u>
C. Intra-terrain trace element variation	42
D. The transition metals	43
The problem of Nickel	47
Scandium	49
E. The 'incompatible' elements	51
F. Discussion	53
G. Conclusions	55
 <u>Chapter 5:</u>	
<u>The 'lithophile' elements, K,Rb,Ba & Sr</u>	
A. Introduction	57
B. Element ratios in the metabasites	58
C. Discussion	64
D. Conclusions	66
 <u>Chapter 6:</u>	
<u>The presumed immobile elements, Ti,P,Zr,Y & Nb</u>	
A. Introduction	68
B. Y/Nb ratios	71
C. The Zr-Ti/100-Y.3 diagram	71
D. Floyd-Winchester diagrams	72
E. Diagrams using 'mobile' elements	74
F. Discussion	76
The tholeiitic-alkalic affinities of the metabasites	76
Zr as an immobile element	78
G. Conclusions	79
 <u>Chapter 7:</u>	
<u>Petrochemistry: Summary and discussion</u>	
A. Primary characteristics	81
B. Metamorphic fractionation	83
 <u>Chapter 8:</u>	
<u>Mineral chemistry</u>	
A. Introduction	90
B. Analytical techniques	91
C. Hornblendes	91
D. Pyroxenes	93
E. Biotites	93
F. Coexisting minerals	94
G. Discussion	96

	<u>Page</u>
H. The garnetiferous metabasites	98
Petrography	99
Garnet analyses	100
Chemical control of garnet formation	100
Discussion	101
I. Conclusions	104
<u>Acknowledgements</u>	106
<u>References</u>	107

Appendix 1:

Modal analyses

Appendix 2:

Analytical techniques

 X-ray fluorescence

 Electron Microprobe

Appendix 3:

Analytical data

 Major elements

 Trace elements

 Niggli norms

 CIPW norms

 Element ratios

Summary

The metabasites of the Arendal-Tvedestrand district were originally minor igneous intrusions, but are now characterised by wholly metamorphic mineral assemblages and textures, which are diagnostic of a prograde amphibolite-granulite facies transition. The main mineralogical changes with increasing grade of metamorphism (zone A to zone C) are decreases in modal hornblende and biotite, with increased pyroxenes.

Major and trace element analyses for 176 metabasites are presented, and show the overall chemistry to be analogous to that of basaltic rocks. K and Rb vary systematically across the transition zone, declining in abundance with increased grade of metamorphism. In other respects, zones A and B are chemically homogeneous. Zone C (Tromsø) metabasites are characterised by low TiO_2 , K_2O , P_2O_5 , H_2O , Zr, Ni, Sr, Ba, Rb, and high Na_2O , (MnO), Zn, and oxidation ratios relative to the mainland suite. In part, these abundances are related to an original igneous fractionation in which a fairly strong iron-enrichment was accompanied by increased levels of TiO_2 , P_2O_5 and 'incompatible' elements, and decreases in transition trace elements. The relative absence of iron-rich differentiates in zone C accounts for the lower levels of P_2O_5 and TiO_2 in this zone.

Secondary fractionation accompanied the metamorphism, and resulted in K and Rb redistribution throughout the terrain and the Na_2O enhancement in zone C. Ba, Sr and Zr appear to be depleted in this zone. These chemical changes are also noted in the acid-intermediate charnockitic suite of the transition zone, which is genetically distinct from the metabasites.

'Stable' element discrimination diagrams (when used with caution in view of these fractionation patterns) show the suite to be originally tholeiitic.

Preliminary microprobe data support the concept of chemical equilibrium in the metabasites. Almandine-rich garnets are sporadically developed in the suite, and their growth is not directly related to the host-rock chemistry.

Chapter 1: Introduction.

A. Location.

The study area is located along the Skagerrak coast of South-east Norway, approximately 200 kilometres south-west of Oslo (Figure 1.1). The region includes the coastal towns of Tvedestrand and Arendal and further inland, the villages of Vegårshei and Ubergsmöen. Tromsø and several smaller off-shore islands are also within the considered terrain.

B. Geological outline and previous research.

The area forms part of the Bamble sector of the Precambrian Fennoscandian shield, and consists of a high grade metamorphic sequence. The rocks are overlain by lower Palaeozoic sediments in the east and separated in the north-west from the adjacent Telemark complex by the Porsgrunn-Kristiansand fault (Morton et al 1970), previously known as the "Great Friction Breccia" (Bugge 1928)(Figure 1.1).

The Bamble sector is assigned to the Proterozoic 1200-900 Ma Sveconorwegian zone (Kratz et al 1968). Systematic K-Ar age dating by O'Nions et al (1969) in northern Bamble has revealed that a metamorphic maximum occurred at 1160-1200 Ma, and that later K-Ar mica dates of 1100-900 Ma (e.g. Neumann 1960, Kulp and Neumann 1961) are cooling ages. Rb-Sr and U-Pb dates on the nearby Levang gneiss dome (O'Nions and Baadsgaard 1971) have shown that parts of the complex underwent an earlier (Svecofennian) metamorphic event at about 1600 Ma.

There is therefore a broad correlation with the Grenville

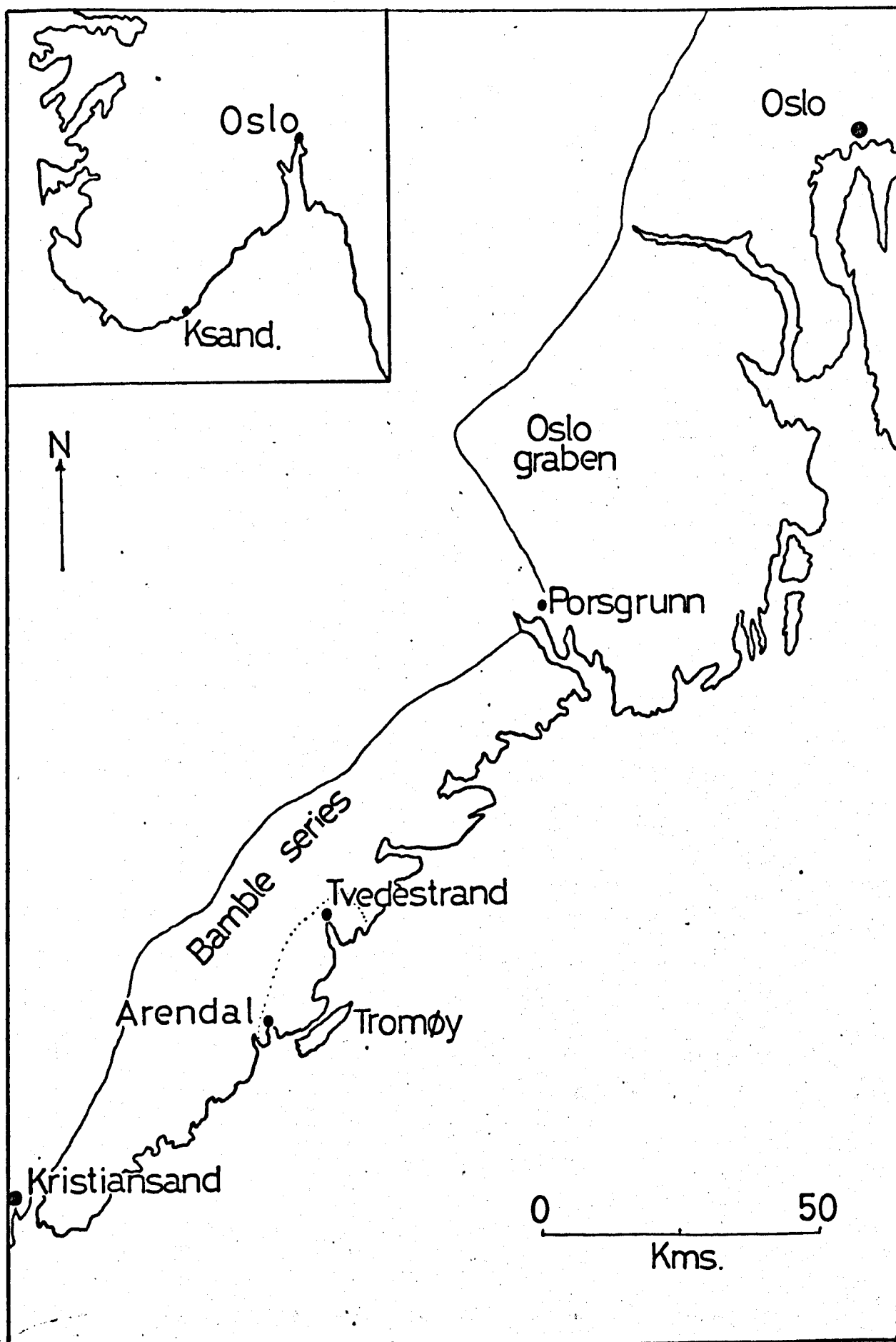


Figure 1.1: Location of the area.

province of North America (Patchett and Byland 1977) at ca. 1100 Ma, with some older dates emerging from both areas (Krogh and Davis 1969). Systematic Rb-Sr studies on samples from the Arendal-Tvedestrand district are currently in progress (Field and Råheim) but no data are yet available.

The principal lithologies in the Arendal-Tvedestrand area are metasediments, including pelitic rocks, metabasites, granitic gneisses and associated migmatites and pegmatites. Acid and intermediate charnockitic rocks are characteristic of much of the coastal area and the off-shore islands. Quartzites, graphitic schists and marbles are not abundant. A group of small late-stage, gabbro intrusions (hyperites) occurs throughout the area.

Upper amphibolite facies assemblages dominate much of the sector, with a granulite facies culmination occurring to the south of Tvedestrand around Arendal (Figure 1.2). Staurolite and muscovite are absent and the amphibolite facies rocks are assigned to the sillimanite-almandine-orthoclase subfacies, following Turner and Verhoogen (1960). The pelitic and semi-pelitic rocks are frequently cordierite-bearing. The granulite facies zone is demarcated from the adjacent amphibolite facies by the presence of orthopyroxene in the metabasites, which are otherwise dominantly of hornblende and plagioclase. Besides forming a stable phase in these higher grade metabasites, orthopyroxene also occurs in equilibrium as a component of many of the granulite facies acid-intermediate charnockites. The assemblage olivine + plagioclase is unrecorded. Thus, according to the criteria of Green and Ringwood (1967) and Heier (1973a) the granulites belong to a low to intermediate pressure group. Metamorphic maxima in the range

**3RD PARTY COPYRIGHT
MATERIAL EXCLUDED
FROM DIGITISED THESIS**

**PLEASE REFER TO THE
ORIGINAL TEXT TO SEE
THIS MATERIAL**

Figure 1.2: Geological sketch map of the Arendal-
Tvedestrand district.

700°- 800°C at 2 - 8 kbars. have been estimated for the terrain (Touret 1968, Cooper 1971).

The structural evolution of the Bamble sector has been long and complex, although much is now known of the relative timing of events, and there is a published framework (Starmer 1972 a, b). The essential fabric consists of a regional foliation, sub-vertical, and trending broadly parallel with the Skagerrak Coast. The amphibolite-granulite facies transition, marked by the orthopyroxene isograd, runs parallel to this dominant main phase foliation, which is common to both facies. (Figure 1.2).

The approximate position of the orthopyroxene isograd has been described by previous workers (Touret 1971, Andrae 1974) and is revised in the present study, which is based on an area geologically mapped (Scale 1:15000) by Field (1969), Beeson (1971) and Cooper (1971). These maps will shortly be available in published form with an accompanying report on the geology of the area. (Norges Geologisk Unders. report series; Field, in preparation). For more detailed accounts of the geology of the Tvedestrand-Arendal district reference may be made to the work of Field, Beeson and Cooper (op. cit.) and to the surveys by Bugge (1940, 1943) and Touret (1962, 1968). Descriptions of the geology of other parts of the Bamble sector are summarised by Morton et al (1970), and Starmer (1969 a, b; 1972 a, b).

C. Objectives.

By 1972 the mapping and preliminary geochemical work by Cooper (1971) and Field (1969) had revealed several features

which combined to suggest that further, in depth, geochemical studies were warranted. At approximately the same time there was a considerable resurgence of international interest in the chemistry of granulite terrains, (e.g. Sighinolfi 1971, Tarney et al 1972, Drury 1973, 1974, Sheraton et al 1973, Heier 1973 (a, b), 1976, Tarney 1976). These works refined and extended the earlier studies of for example Lambert and Heier (1968), Sighinolfi (1969) and Whitney (1969) which had suggested that many granulite terrains were characterised chemically by relative deficiencies in certain lithophile elements, notably the alkaline metals. These were presumed to have been mobilised and enriched into formerly overlying amphibolite facies rocks either by transport in granitic melts (e.g. Sighinolfi 1971) or by fluid diffusion processes. (Beach and Fyfe 1972, Drury 1972, 1973, 1974.).

Thus, a consequence of these granulite studies was that important data on chemical fractionation in the crust were obtained, leading to hypotheses concerning:

- a) The nature of the lower continental crust (Heier 1964, 1973a, b, Smithson and Brown 1977).
- b) The evolution of the Precambrian crust (e.g. Tarney 1976).

The amphibolite-granulite facies zone in the Arendal-Tvedestrand district appeared to offer a unique set of advantages for undertaking the present study:

- i) The transition zone had been geologically mapped.
- ii) It was considered by both Field (1969) and Cooper (1971) to represent a prograde transitional sequence preserving an

increase in grade from the orthopyroxene isograd towards the coast and the Island of Tromsø where the lowest structural levels are exposed. On Tromsø many of the rocks are genuinely anhydrous.

- iii) Retrogression was minor, and a single dominant foliation could be recognised as contiguous across the transition. Thus, later events had not obscured the prograde crystallisation.
- iv) The acid-intermediate gneisses of highest grade (Tromsø gneisses) are charnockitic, and were found to be characterised by the lowest K and Rb values known for granulites (Cooper 1971). This work has since been extended recently and the data are thought to be indicative of extreme fractionation (Cooper and Field 1977).
- v) Preliminary data suggested that the metabasites in the granulite facies also had these chemical features of lower alkali elements relative to their amphibolite facies equivalents. Research on chemical fractionation in granulite terrains had often emphasized gross chemical variation in acid-intermediate suites, and it was often concluded that mafic material seemed to retain its pre-metamorphic chemistry (e.g. Lambert and Heier 1968, Lewis and Spooner 1973). Further studies have failed to completely clarify this position; Drury (1974) showed some chemical variation in mafic granulites (n=9) and amphibolites (n=32) from the Lewisian, but for Central Australia, Collerson (1975) concluded that only acidic rocks had been involved in crustal fractionation processes.

The question arises therefore, that if genetically distinct basic rocks are affected by chemical fractionation, can this be reconciled with material transport via

granitic melts? (c.f. Heier 1973 a, b).

- vi) The terrain is of low to intermediate pressure.
It had previously been suggested that fractionation was restricted to medium or high pressure series (Lambert and Heier 1968).
- vii) The metamorphism is of established Proterozoic age (O'Nions et al 1969), while the majority of previous granulite studies have been on Archaean rocks. If crustal fractionation processes are important in the Proterozoic, then some constraints are placed on hypotheses deemed applicable only to Archaean crustal formation.
- viii) Since the work of Engel and Engel (1962) and Binns (1964), no comprehensive attempt has been made to investigate a series of metabasites from a progressive amphibolite - granulite transition zone.

Thus, the present work is an attempt to characterise in detail the petrochemistry of the metabasic rocks from across the amphibolite-granulite transition in the Arendal-Tvedestrand region. Although less important in terms of volume than the acid and intermediate components of the terrain, the metabasites are nevertheless highly significant in its evolution and petrochemical character. Certain details of the metabasite chemistry have already been published (Field and Clough 1976) and a reprint of this work is included at the back of this thesis.

D. Nomenclature.

The term 'amphibolite' is used consistently by most authors in referring to a rock, essentially of hornblende and plagioclase

in subequal proportions, irrespective of origin. Sometimes, however, this is synonymous with "basic rocks of the amphibolite facies". In this terrain a further difficulty arises, due to the transition into granulite facies assemblages. 'Pyribolite' has been used (e.g. Starmer 1972a), though not extensively, for these granulite facies orthopyroxene - hornblende-plagioclase rocks, and another alternative is 'basic granulite' (e.g. Drury 1974). To avoid using more than one term to describe these rocks from across the transition zone 'metabasite' is used in this study for assemblages of hornblende - plagioclase \pm orthopyroxene. This practice corresponds to the nomenclature recommended by Miyashiro (1967). The term is particularly apt due to the wholly metamorphic nature of the textures in the group, and their undoubted igneous origin. (See Chapter 2).

The gabbro intrusions which occur throughout the terrain, but which are only partially metamorphosed, and were intruded later in the sequence of events (e.g. Starmer 1969b), are referred to as 'hyperites'. This usage follows Brøgger (1935), and later authors (Frødesen (1968a, b), Elliott 1973, Field and Elliott 1974).

CHAPTER 2.

Field relations and petrography.

A. Introduction

The metabasites considered in this thesis are important constituents of the terrain, and account for approximately 10% by volume of the surface outcrop. They are well-distributed throughout the transition.

The distinction between the metabasite suite and two groups must be emphasized. Firstly, whilst mafic material frequently occurs in complex association with migmatites throughout the terrain, such rocks have been excluded from the present survey. Secondly, the metabasites may be readily distinguished in time and origin from the hyperites and their attendant dykes. These bodies were emplaced at a late stage in the evolution of the terrain, and are characterised by corona development and occasional veins of chloroapatite and albitite (Bugge 1965, Starmer 1969a). The hyperite dykes are frequently found to transgress the surrounding gneisses, including metabasites, sometimes at high angles (Field 1969). Additionally, the presence of relict ophitic or coronitic textures is a decisive characteristic of the hyperites, such features being completely absent from the metabasite group. Although amphibolitization of hyperite is common, particularly at the margins of the intrusive stocks (Elliott 1973) it is an incomplete process often patchy or abrupt in transition to normal hyperite facies. With suitable caution a complete discrimination between the metabasites and the later hyperites is possible in the field.

B. Field relations

The Bamble sector affords good rock exposure, a consequence of the glaciated fjord coastline, and strong, but not mountainous relief. Recently cut road sections occur throughout the area.

The metabasites are found as layers and lenses of variable thickness, ranging from a few centimetres to over 30 metres in width of outcrop. They occur as both massive and schistose bodies, the latter being slightly the more frequent, reflecting the ubiquitous presence of prismatic hornblende. Massive varieties are most common in the granulite facies, and are usually finer-grained. Where a foliation is developed it is continuous with the regional fabric in the country gneisses.

Workers in adjacent areas of the Bamble sector have concluded that the metabasites were originally minor igneous intrusions. (Pettersson 1964, Touret 1968, Starmer 1972a). The same conclusion has been formed in the Arendal-Tvedestrand district in the present study and by Field (1969). Although there is an overall conformability of lithological units throughout the sector, positive field evidence for discordant intrusion of the metabasites has been verified in some outcrops (e.g. figures 2.1, 2.2) where slightly oblique contacts between a metabasite and the country foliation are occasionally preserved. Such contacts are sharp and are particularly prominent where the wall rock is a quartzite. In these instances transgressive apophyses have also been recorded. Moreover, in northern Bamble, Pettersson (1964)

has described xenoliths of quartzite in an amphibolite.

Nowhere is there a thin layered sequence that might be indicative of a sedimentary origin for some of the mafic rocks (c.f. Orville 1969, Kamp 1970). Marbles and calc-silicates are present, but are poorly developed and largely restricted to the environs of Arendal. Metabasites are rarely in association with these groups, and sampling in these areas has been avoided.

Although the metamorphic evolution of the Bamble sector was complex and protracted, (O'Nions and Baadsgaard 1971) the relative timing of major events is now known, (e.g. Starmer 1972 a, b). All workers are agreed that the metabasites already existed during the development of the main regional foliation and metamorphism; they both contain this dominant foliation and have acquired wholly metamorphic textures and assemblages. This re-emphasizes the distinction between this group and the later hyperites, in which relict ophitic textures are such a prominent feature.

Field relationships therefore suggest that the metabasites as a suite were essentially a series of basic dykes or sills intruded into a gneiss/supracrustal sequence before the thermal maximum. There is no evidence in the Arendal-Tvedestrand district for the syn-kinematic intrusion of primary amphibolite as described by Watterson (1968) in Greenland. Similarly, no evidence has been found for the existence of more than one generation of (metabasite) intrusion, although this possibility cannot be excluded on field evidence alone.

Figures 2.1 - 2.5 illustrate some typical aspects of the field occurrence of the metabasites in the Arendal-Tvedestrand area.

C. Sampling.

Sampling points have been divided sub-equally between the amphibolite facies and the granulite facies, and since the focus has been upon one lithological unit, a grid system has not been employed. The frequency of fresh exposure has facilitated a wide and a really representative selection of sampling points. The precise locations of 176 metabasite samples which have been chemically analysed are given on the 1:50000 map included in the folder at the back of this thesis. Thin sections of these form the basis of the ensuing comments on petrography. The representative areal sampling has been supplemented in four sub-areas by relatively dense sample selection. 42 samples were originally collected from the mainland transition zone, as a pilot study (Field 1969), and these have been fully integrated into the present survey.

The collection of fresh unweathered rocks, usually from the central portion of the metabasite outcrop has been emphasized.

D. The orthopyroxene isograd and sub-division of the terrain.

The first occurrence of orthopyroxene in metabasites towards the Skagerrak coast is gradual, but the "best-fit" of the incoming of the mineral has been determined and is shown on the maps of figures 1.2 (Chapter 1), and 2.6. This presentation is a slight modification of the positions figured by Touret (1968, 1971) and Andrae (1974). Of the 94 samples to the south-east of this divide, 14 (15%) are not



Figure 2.1: Thin, discordant apophyses of metabasite in quartzite wall rock.



Figure 2.2: Discordant metabasite with small apophysis preserved (to right of coin).



Figure 2.3: Metabasite with charnockitic gneiss wall rock (Zone B).



Figure 2.4: Garnetiferous metabasite from zone A.



Figure 2.5: Thin metabasites in acid gneiss sequence (Zone C).

orthopyroxene bearing, and orthopyroxene-free samples have been found up to 11 kilometres up-grade from the isograd. Conversely, rare isolated occurrences of granulite facies assemblages, including rocks with charnockitic affinities, are known from the environs of Vegårshei, well to the west of the orthopyroxene isograd in the present area. (Touret 1967, Morton et al, 1970, Beeson 1971). This occasional presence of orthopyroxene-bearing metabasites within areas which are otherwise characteristic of the upper amphibolite facies has been confirmed in the current study. (6/82 samples west and north-west of the isograd (figure 2.6) contain orthopyroxene). This imprecision of the isograd is either due to minor chemical variations within the metabasite lithological unit, or to local fluctuations in the pressure-temperature gradient, perhaps associated with variable pH_2O .

While the facies boundary forms a natural two-fold division of the Arendal-Tvedestrand district, a three-fold zonal division, based on both mineralogical and geographical criteria, is used in this study. The three zones, A, B and C are outlined in figure 2.6 and table 2.1.

82 out of the 176 analysed samples are assigned to zone A, north-west of the orthopyroxene isograd which separates zones A and B. Zone A is thus equated with the amphibolite facies of the Tvedestrand-Arendal district. The 94 granulite facies rocks are subdivided into "mainland" samples (zone B, $n = 62$) and those from the island of Tromsø (zone C, $n = 32$). This off-shore island contains the highest grade rocks of the study area and thus both geographically and geologically provides a convenient unit for discussion of the metabasite petrochemistry

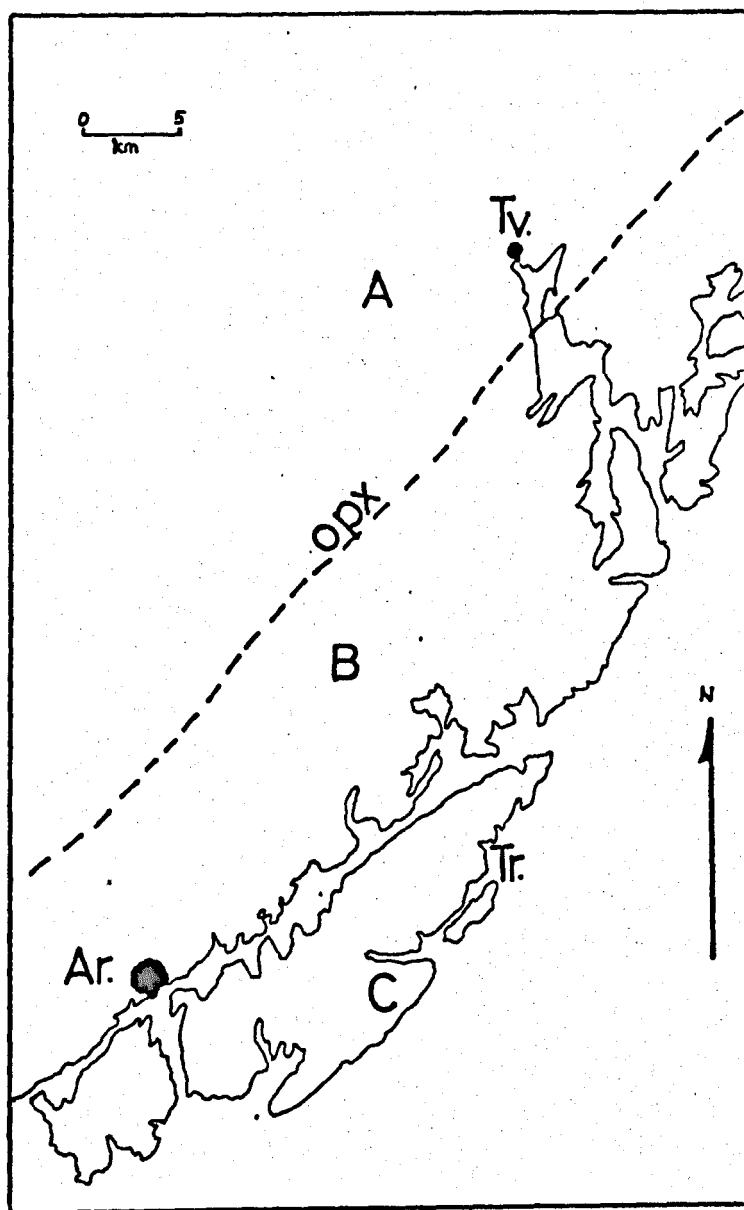


Figure 2.6: Subdivision of the terrain into metamorphic zones A, B and C.
Ar. = Arendal; Tv. = Tvedestrand;
Tr. = Tromsø.

Zone	Description	Characteristic Metabasite assemblages	Other minerals and comments
A	"Amphibolite facies - Mainland"	hb - pl _± bi	cpx and gt sporadic; opx-bearing metabasites are infrequent and uncharacteristic
B	"Granulite facies - Mainland"	hb - pl - opx _± bi	17% of Zone B metabasites are opx-free; cpx is more frequent; gt remains sporadic, and bi shows a small decline in occurrence
C	"Granulite facies - Tromsø"	hb - pl - opx - cpx _± bi	Garnet very rare; biotite considerably less abundant. Clinopyroxene now a characteristic mineral
Key: opx = orthopyroxene; hb = hornblende; cpx = clinopyroxene; pl = plagioclase; bi = biotite; gt = garnet:			

TABLE 2.1: Generalised Zonal Mineralogies in the Metabasites

at some distance up-grade from the isograd. Recently documented analyses of the Tromøy acid-intermediate charnockitic gneisses suggest that the separation of Tromøy from the mainland granulite facies terrain may also be justified on purely geochemical grounds. (Cooper and Field, 1977; Field, unpublished data). This subdivision of the terrain is maintained in the ensuing chapters on chemistry.

E. Mineral assemblages.

Modal analyses for the metabasites are tabulated in Appendix 1. The mineral assemblages are divided into two broad groups, corresponding to the facies division in which orthopyroxene is the index mineral.

1. hornblende-plagioclase (\pm biotite) (Zone A)
2. hornblende-plagioclase - (orthopyroxene) \pm
(clinopyroxene) \pm (biotite) (Zones B and C).

The assemblage characteristics of the three zones are also summarised in table 2.1, and each zone is now discussed in turn.

Zone A: The hornblende-plagioclase \pm biotite assemblage shows its maximum expression in the metabasites of zone A. Hornblende ranges from 28% to 74%, with a well defined mean value of 55% in the mode. Plagioclase is usually, though not exclusively subordinate, averaging 34.5%. Biotite ranges from 0 - 30%, and 67% of the group have greater than 1% of this mineral. However, only 30% attain 10% modal biotite.

Of the 82 metabasites, 7 contain minor amounts of clinopyroxene ($\leq 5\%$) and 6 contain garnet ($\leq 17\%$). A single hornblende-plagioclase-cummingtonite-garnet rock has been recorded. 6 of the metabasites contain the granulite facies index mineral, orthopyroxene, although in 4 samples it attains less than 10%. These 6 rocks are widely distributed within zone A.

The hornblende is typically green to dark green in colour, although rare brown-green to brown varieties have been noted, including in two of the orthopyroxene-bearing samples. The plagioclase feldspar ranges in anorthite content from An₃₀ to An₆₅; there is a mean value approximating to the andesine-labradorite boundary at An₅₀. Plagioclase is seldom completely fresh in the metabasites and sericitization is widespread but usually partial. The textures of the metabasites are described and illustrated separately below.

Zone B. Hornblende-plagioclase-orthopyroxene is the characteristic assemblage of zone B, although orthopyroxene is absent in a significant minority of metabasites (11/62 = 17%). It is present in only accessory quantities or in highly altered condition in a further 9 samples. In the remaining, the average modal value is 12%. With the incoming of orthopyroxene there is a concomitant decline in the average modal hornblende value to 39%. The range of hornblende frequency is from 3% to 65%. The plagioclase mode and anorthite content are comparable with the Zone A values.

The occurrence of biotite and the sericitization of plagioclase are slightly less prominent in zone B. Clinopyroxene is more frequently found, occurring in one-

third of the Zone B samples, though seldom attaining 10% of the mode. Garnet ($\leq 18\%$) remains sporadic in distribution. (7/62 samples).

Hornblende is more variable in colour in zone B, and brown varieties, though still subordinate to green and green-brown forms, are more frequent.

Zone C. Orthopyroxene is more widely established in this zone, and is characteristically found in association with clinopyroxene. Orthopyroxene (0 - 24%) averages ca 12%, while the mean modal value for clinopyroxene is ca 5%. (range = 0 - 14%). Pyroxenes are not appreciably more abundant than in zone B, therefore, and hornblende remains the dominant mafic mineral. The amphibole is present as 15 - 68% of the mode, averaging 38%. Plagioclase (25% - 57%; mean 43%) is thus approximately equally developed with hornblende, but is generally subordinate to the combined modal proportions of the mafic minerals.

Garnet has not been recorded in the analysed metabasites from Tromøy, but is known to occur in one locality on the northern coast of the island, (grid ref: 49006482).

A most interesting mineralogical feature of the Zone C metabasites is the significantly lower anorthite content of their plagioclases compared with the mainland zones. The An % ranges from An₁₅ to An₄₄, averaging An₂₉ (Calcic oligoclase). This feature was previously noted by Cooper (1971), and will be discussed again in Chapter 3.

The hornblendes are typically dark green. The increased tendency to a brown colouration noted between zones A and B is apparently not continued into zone C. Biotite is much less frequently developed in zone C, and sericitization of the plagioclase is further reduced.

Accessory minerals.

The most persistent accessories are opaque ore minerals, with ilmenite being the most common. Apatite is well-distributed and particularly notable in zone B samples; quartz and sphene have a dispersed and irregular distribution throughout the Arendal-Tvedestrand district. Both are extremely rare in zone C, however. K-feldspar (microcline) has been noted locally, and where present is usually found in metabasites closely associated with granitic gneiss. It is also associated with the rocks showing the greatest sericitization of the plagioclase. In sample 7128 K-feldspar occurs as 10.3% of the mode.

Other rare accessories include rutile, prehnite, zircon and pyrite, whilst chlorite and sericite form alteration products.

The occurrence and paragenesis of garnet is considered separately in Chapter 8.

F. Textural relationships.

The metabasites display wholly metamorphic textures. There is a complete absence of the relict ophitic or coronitic textures that are one of the distinguishing features of the hyperites.

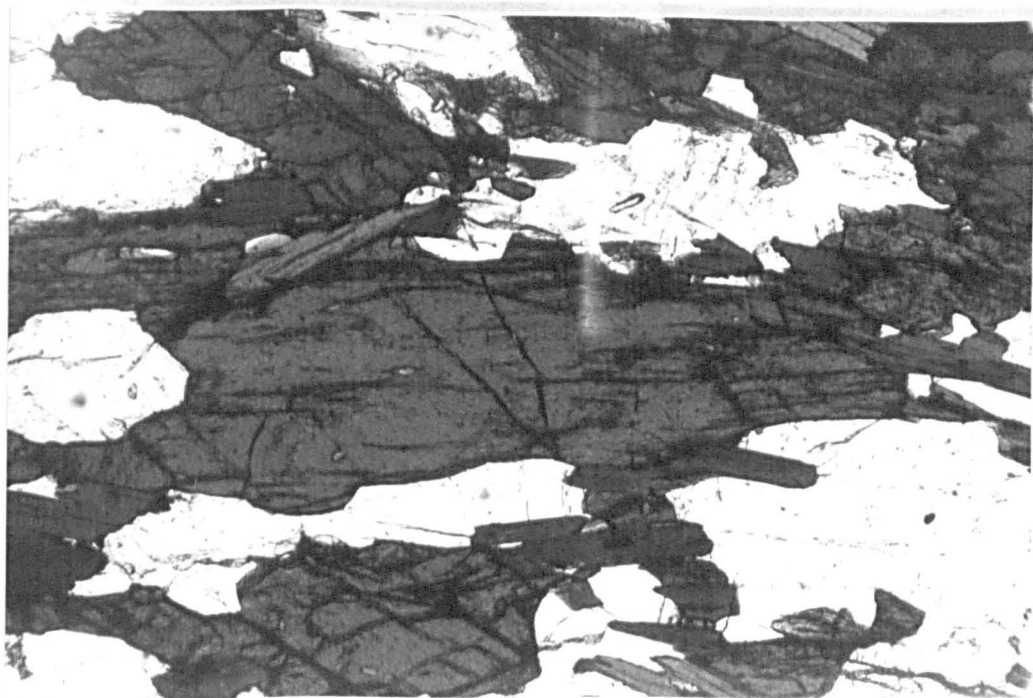


Figure 2.7: Schistose metabasite, zone A. (No. 786). (X 16)

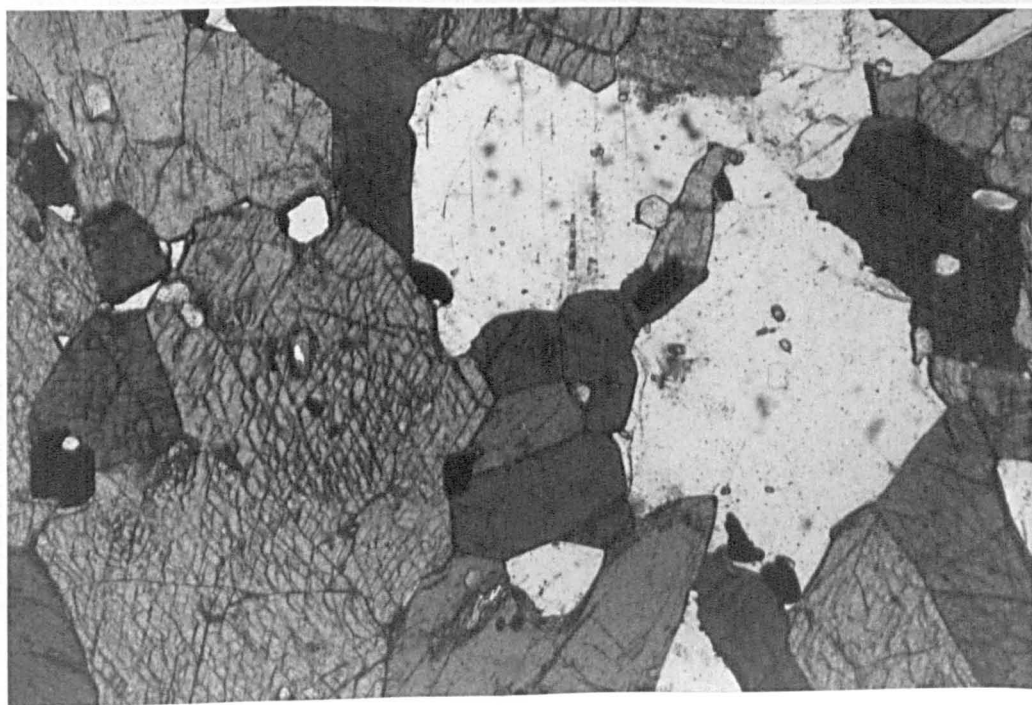


Figure 2.8: Biotite-free metabasite from zone A (No. 780)
Accessory ore and apatite. (X 16).

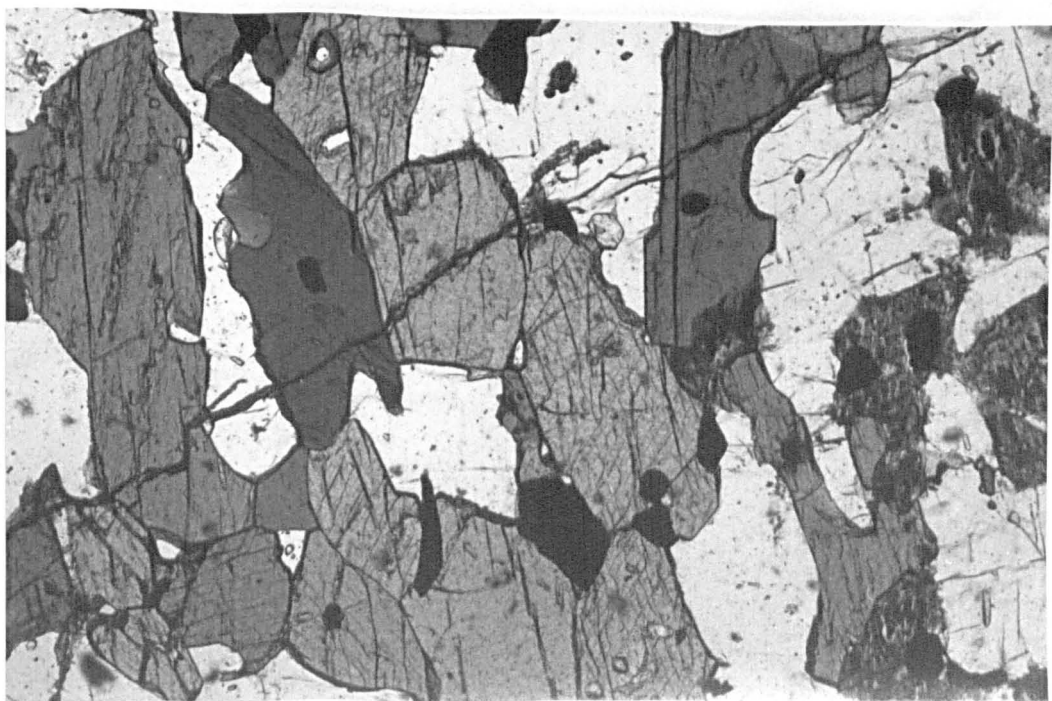


Figure 2.9: Metabasite from zone B (No. 705), with highly altered relict orthopyroxene. (Right of photograph.) (X 16)



Figure 2.10: Granoblastic texture in metabasite from zone B. Abundance of biotite is higher than usual for zone B. (X 16).

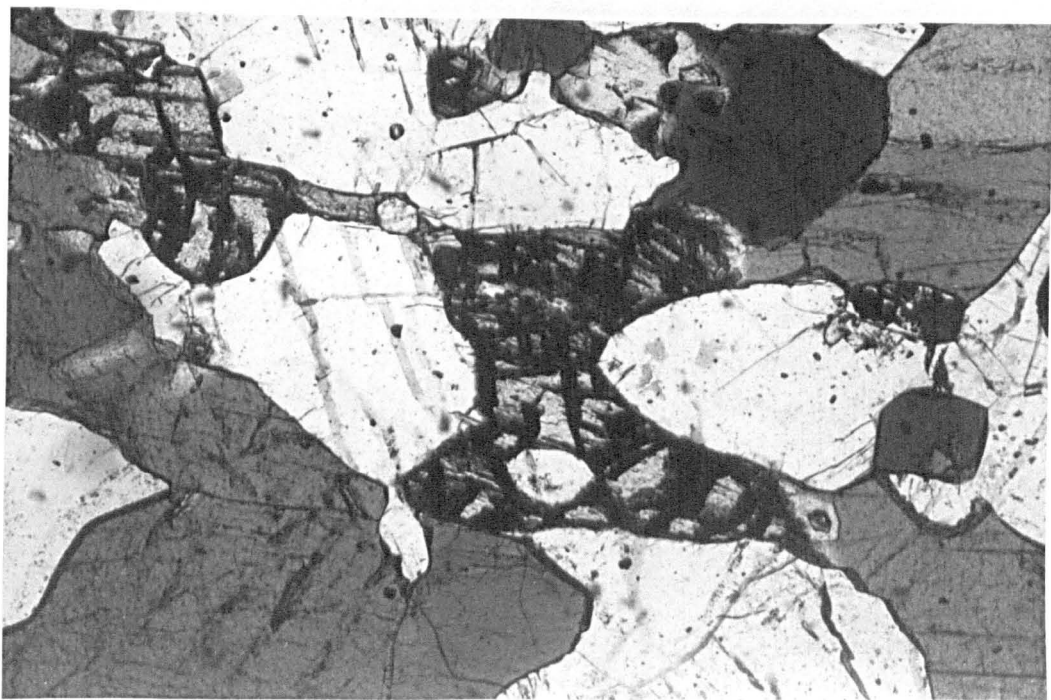


Figure 2.11: Zone C metabasite (No. 203). Alteration of orthopyroxene to chlorite and hornblende contrasts with the xenoblastic hornblende. (X 16).

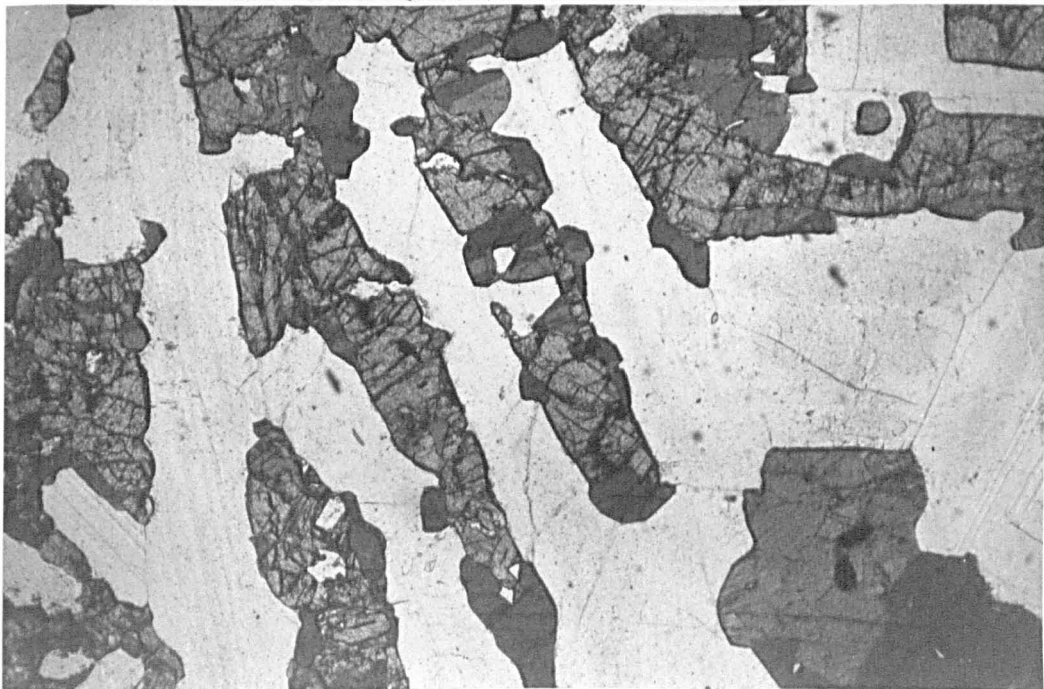


Figure 2.12: Hyperite sample with relict ophitic texture and partial coronas of hornblende after pyroxene. (X 10).

The photomicrographs of figures 2.7 to 2.11 illustrate the typical textural features of the metabasites, which characteristically vary with zone, and thus reflect the changes in metamorphic grade across the terrain. Figure 2.12 is a photomicrograph of a typical hyperite sample, for comparison.

Zone A: The samples of zone A are generally medium-grained sub-equigranular rocks, often with a nematoblastic schistosity (Harker 1939, p.201; Spry 1969, p.208). The sub-parallel elongation of the prismatic hornblende is frequently well-defined in this group. The plagioclase feldspar occurs as irregular, rounded xenoblastic grains, and the biotite, where present, as irregularly dispersed flakes. Inclusions of ore minerals and occasionally quartz are relatively common in the hornblendes. Xenoblastic plagioclase grains form irregular or rounded grain-boundaries against the prismatic and often poikiloblastic hornblendes. Closely comparable textural descriptions of metabasic rocks in the amphibolite facies of high-grade transition zones have been given by Engel and Engel (1962) for the Adirondacks and by Binns (1964) for Broken Hill.

Zones B and C: These two zones have important metabasite textures, based on hornblende-pyroxene relationships.

One or both pyroxenes generally occur as small xenoblastic or sub-idioblastic grains often coexisting under apparent textural equilibrium with discrete hornblendes. (Figures 2.10 & 2.11). The schistosity characteristic of the zone A samples is less well defined in these higher grade

zones, and granuloblastic textures with straight or curved grain boundaries are correspondingly more important. Triple junctions have occasionally been observed (figure 2.11).

Grains of biotite, where present, show an even distribution in these rocks.

No corona structure of hornblende around orthopyroxene has been noted in the metabasites. Nevertheless partial alteration of orthopyroxene along cleavages is a common feature, and the process is sometimes seen to be complete, leaving a relict or skeletal grain. The alteration products are a brownish chlorite and/or hornblende. This secondary hornblende is different in aspect from the discrete hornblendes described above (Figure 2.11)

G. Discussion.

The main problem centres on the question of whether the amphibolite-granulite facies transition is prograde or retrograde. The evidence published to date is somewhat conflicting.

Starmer (1972b) in the Risør area, north of Tvedestrand has suggested that some of the hornblendes in the granulite facies assemblages are secondary to orthopyroxene and represent an amphibolite facies regeneration. However, the figured specimen of Starmer (1972b, p.52f) suggests he was considering a hyperite specimen. Certainly, his view contrasts with Touret (1968), who described the pyroxenes and hornblendes as having formed contemporaneously.

The latter view is supported by the petrographic

relationships observed during the current survey. The dominant textures of the metabasites, described and illustrated above, are analogous to those of prograde terrains. Two classical examples from the literature which correspond in many details to the Arendal-Tvedestrand metabasites are the transition zones at Broken Hill (Binns 1964), and Emeryville-Colton in the Adirondacks (Engel and Engel 1962). The granuloblastic granulite facies assemblages in zone C in South Norway are essentially the culmination of the terrain, and there is no reason to suspect that the discrete, apparently coexisting hornblende formed later than the orthopyroxene. Reaction rims of hornblende around orthopyroxene are absent. The alteration that does occur in the pyroxene grains is frequently incipient, along cleavage planes, and is often chlorite instead of, or as well as, hornblende. Such alteration is not typical of a pervasive amphibolite-facies retrogression (c.f. Drury 1972, 1973, 1974). The problem of the relative timing of hornblende and pyroxene in granulite terrains has been discussed at length by Schriver (1973a, b). None of Schriver's criteria for retrograde hornblende development is present in the metabasites.

The existence of rare, localised "granulite facies" assemblages including charnockitic rocks (Touret 1967; Beeson 1971) in zone A has previously been mentioned. While this may be evidence for a more extensive retrogression, an alternative explanation is the occurrence of either local thermal maxima, during a single progressive metamorphism or of "dry spots" with reduced pH_2O . The "granulite facies" assemblages in zone A are not notably more retrogressed than their equivalents at deeper levels in the terrain.

The hyperite bodies, being only partially metamorphosed, form a critical time horizon in the metamorphic evolution of the region, occurring in both the amphibolite facies and the granulite facies. Distinct variation in the character of the hyperite coronas occurs between the two facies. In the granulite facies, the orthopyroxene aggregates (after olivine) are invariably surrounded by a corona of garnet which is idioblastic against plagioclase (Cooper 1971). By contrast amphibole or amphibole-spinel symplectite coronas, with imperisistently developed garnet are characteristic of the amphibolite facies intrusions. The lack of hornblende at higher grades is thought to reflect the different metamorphic conditions, and path of recrystallisation, direct to granulite facies, shown by these rocks (Cooper. op. cit). The hyperites are therefore essentially syn-metamorphic and provide further evidence that the facies variation is progressive. There is no need to invoke an extensive amphibolite facies retrogression in the terrain, as implied by Starmer (1972b).

H. Conclusions.

1. Field considerations support an intrusive igneous origin for the metabasite suite. This group and the later hyperite dykes are distinguishable in the field.
2. The amphibolite-granulite facies transition has been delineated by the incoming of orthopyroxene in the metabasites. A three-fold division of the terrain has been made.
3. The principal assemblages of the suite are hornblende-plagioclase \pm biotite and hornblende-plagioclase-

orthopyroxene \pm clinopyroxene \pm biotite. Garnet, quartz, and potash feldspar are less common. Ore minerals are widespread, and apatite and sphene are other important accessories.

4. The principal mineralogical changes with increasing grade are a decline in modal biotite and hornblende, and an increase in pyroxenes. The anorthite content of the plagioclase decreases significantly in zone C. (Tromø).
5. The granulite facies samples in this study display stable assemblages of orthopyroxene and hornblende in apparent equilibrium. There are textural similarities with the progressive amphibolite-granulite transitions in the Adirondacks and Broken Hill.

Chapter 3: Major Element Chemistry.

A. Introduction.

In this chapter, the bulk major element chemistry of the metabasites is defined, and comparisons are made with the overall chemistry of basalts (Manson 1967) and also with some metabasite analogues. Intra-terrain abundance differences by zone are considered, and igneous variation diagrams are used to examine whether such changes might be superimposed upon, or have been caused by, igneous differentiation.

The twelve "standard oxides", SiO_2 , Al_2O_3 , TiO_2 , Fe_2O_3 , MgO , CaO , Na_2O , K_2O , MnO , P_2O_5 , and H_2O have been determined. With the exception of FeO and H_2O , all analyses were obtained by X-Ray Fluorescence, using a Philips PW1212 spectrograph. Except for Sodium, a fusion bead specimen preparation technique (Harvey et al 1972) was used. Sodium was determined using a pressed powder method similar to that described by Leake et al. (1969). FeO analyses were obtained by the method of Wilson (1955) and H_2O by a modified Penfield procedure. Accuracy and precision were monitored by simultaneous analysis of 6 U.S.G.S. International standards, DTS-1, BCR-1, PCC-1, GSP-1, G-2 and AGV-1, and the results are in good agreement with recently published values (e.g. Abbey 1973, Flanagan 1973). Four replicate determinations were made for each sample. Details of analytical procedures, together with tables of accuracy and precision are given in Appendix 2.

All individual analyses, together with percentage totals, selected element ratios, niggli numbers and CIPW norms are tabulated in Appendix 3.

B. Major element characterisation of the metabasites.

The overall distributions of values for each major oxide are presented in the histogram plots of figures 3.1 to 3.3. Table 3.1 summarises the data with respect to mean, median, maximum, minimum and standard deviation for each element.

The mean SiO_2 content of the Norwegian metabasites (47.9%) is slightly lower than that established for all basalts (49.3%) (Manson 1967). However, with only two exceptions the analyses satisfy Manson's chemical screen for basaltic rocks which specifies under 56.0% SiO_2 . The frequency distribution is less comparable, as the cumulative frequency curves of figure 3.4 illustrate. Moreover, in contrast to the positively skewed metabasite distribution, Ahrens (1964) has described a negatively skewed distribution for SiO_2 in 400 basalts. Ahren's distribution has been attributed to the effects of mild differentiation in some of his sample.

All the Norwegian metabasite samples fit the constraints of Manson's (1967) basalt screen for the following oxides: Al_2O_3 , FeO , CaO , MgO , TiO_2 , Na_2O , K_2O , H_2O and MnO . Comparisons of the metabasite mean values with those of "all basalts", and "all dolerites" (Manson, op. cit., Table VI) also show strong similarities except that the mean CaO is slightly lower and the iron content slightly higher in the metabasites. (Table 3.2).

An interesting feature of K_2O is the pronounced asymmetry of its distribution, causing a marked discrepancy between the mean and median values. Figure 3.5 emphasizes this asymmetric

TABLE 3.1

Summary major element data for South Norwegian Metabasites.

Oxide	1.	2.	3.	4.	5.
SiO ₂	47.89	47.76	42.72	56.31	2.33
Al ₂ O ₃	15.80	15.89	12.54	20.32	1.29
TiO ₂	1.93	1.85	0.51	5.25	0.76
Fe ₂ O ₃	3.52	3.43	0.17	9.12	1.40
FeO	9.68	9.58	4.19	14.73	1.88
MgO	6.88	7.05	2.22	10.55	1.41
CaO	8.97	9.17	6.01	11.85	1.07
Na ₂ O	2.77	2.76	0.87	5.01	0.72
K ₂ O	1.30	1.09	0.20	3.91	0.78
MnO	0.22	0.21	0.12	0.56	0.08
P ₂ O ₅	0.35	0.25	0.03	2.14	0.33
H ₂ O	0.62	0.60	0.14	2.21	0.31
*FeO	12.86	12.92	7.66	18.31	1.93

n = 176

* Total Fe calculated as FeO.

1. = Mean.

2. = Median.

3. = Minimum.

4. = Maximum.

5. = Standard Deviation.

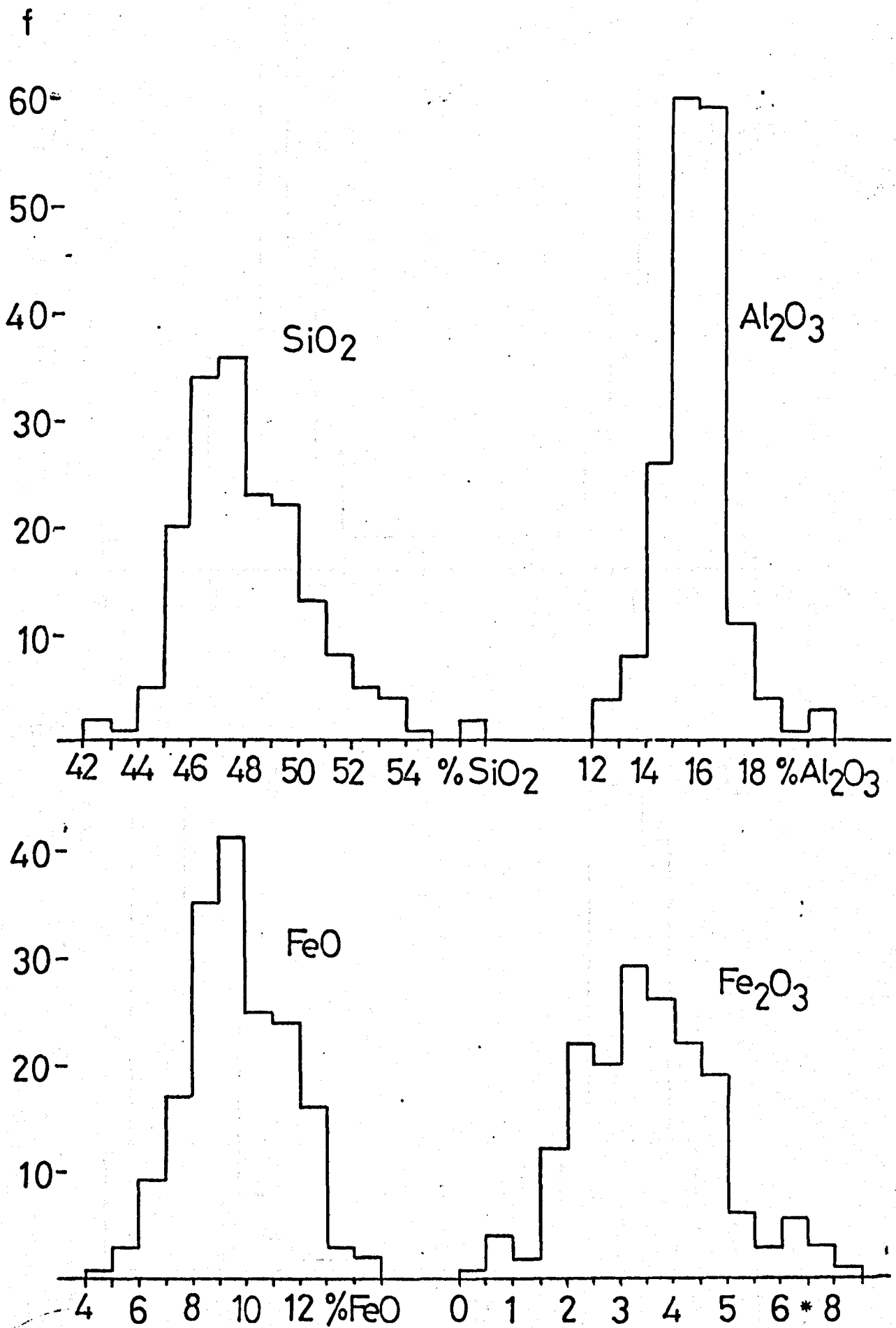


Figure 3.1: Frequency histograms for SiO₂, Al₂O₃, FeO and Fe₂O₃ in 176 metabasites. Oxides as wt. %. f = frequency. * Fe₂O₃ scale is non-linear at high values.

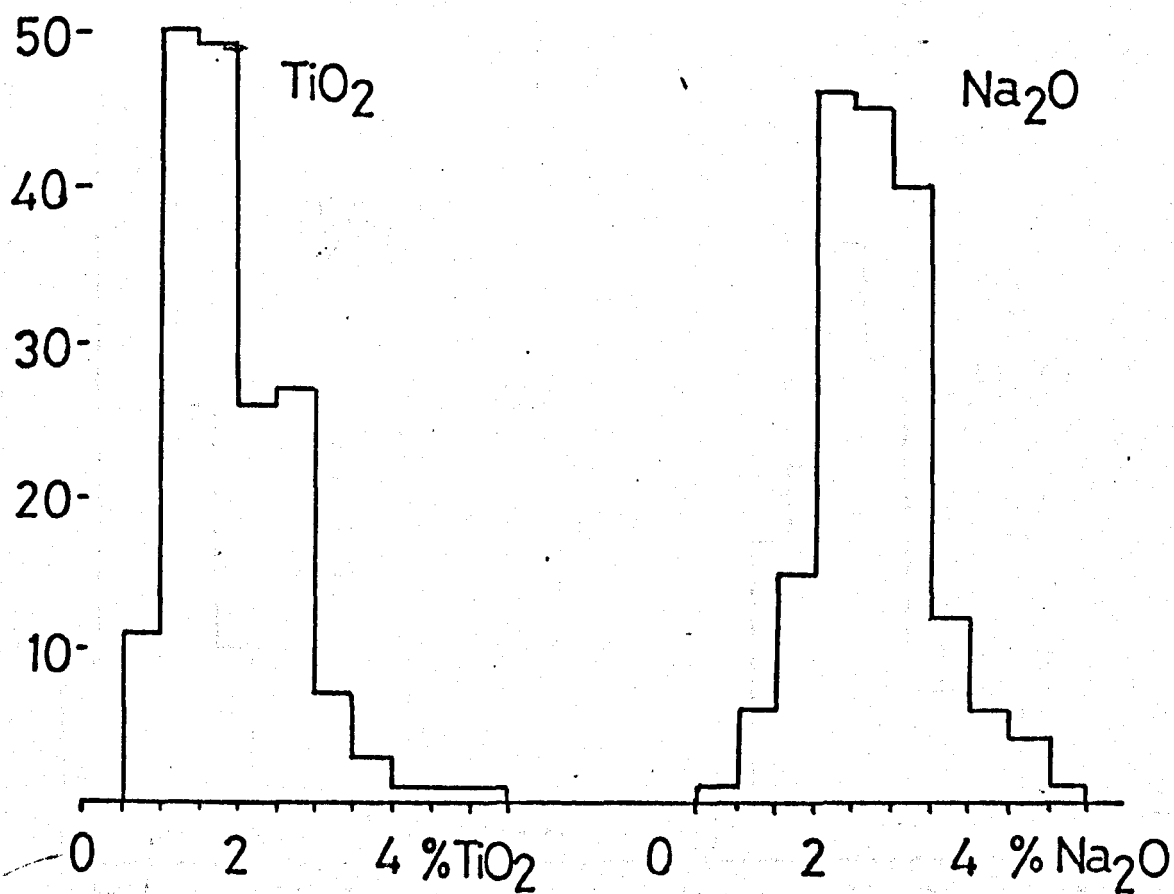
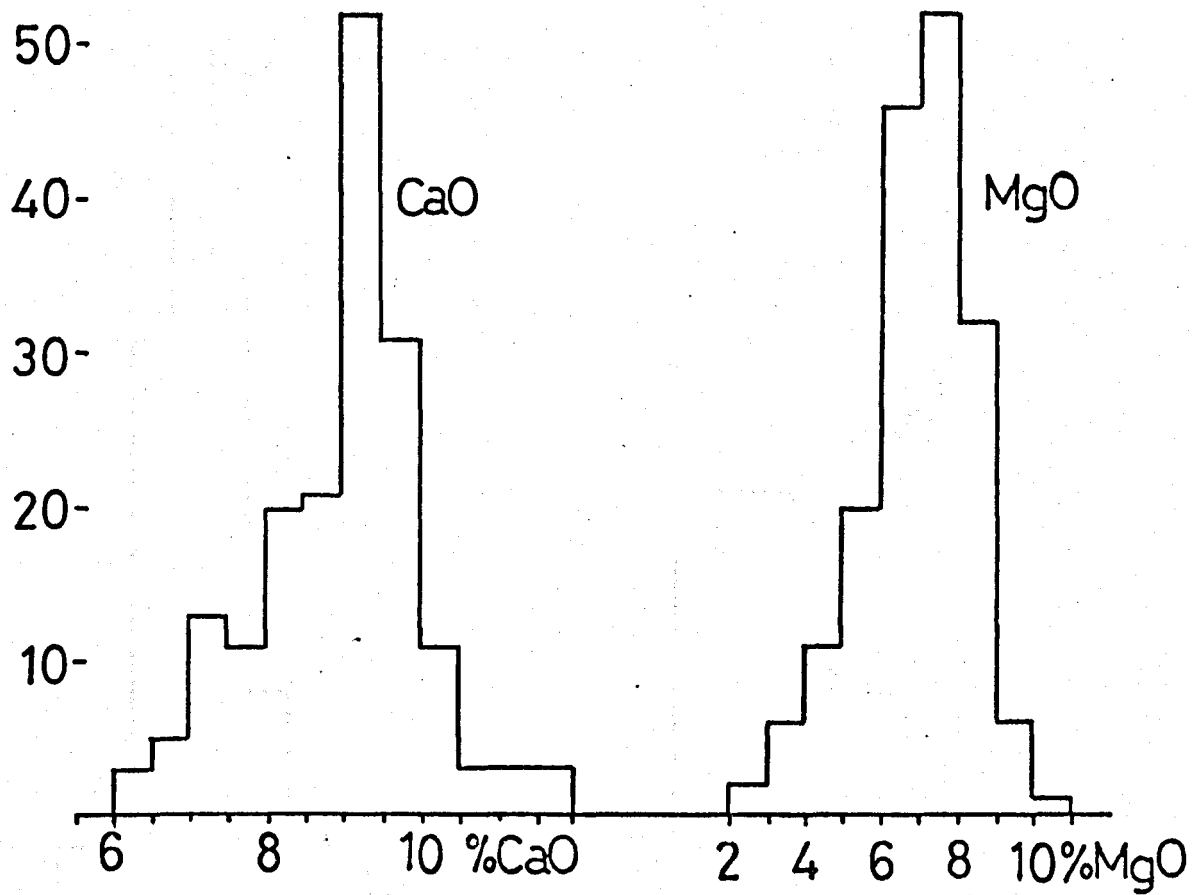


Figure 3.2: Frequency histograms for CaO, MgO, TiO₂ and Na₂O.
(oxides as wt. %.)

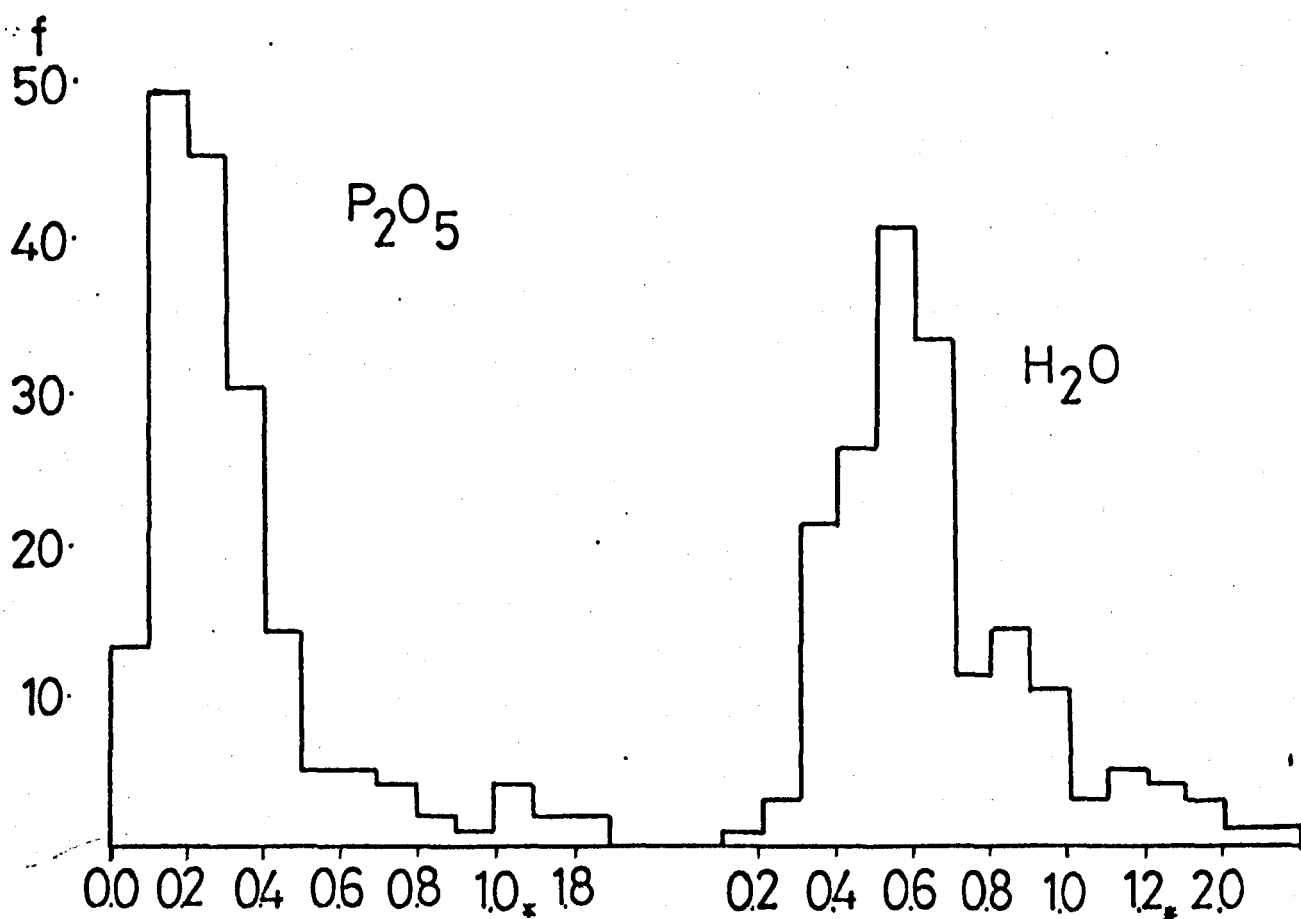
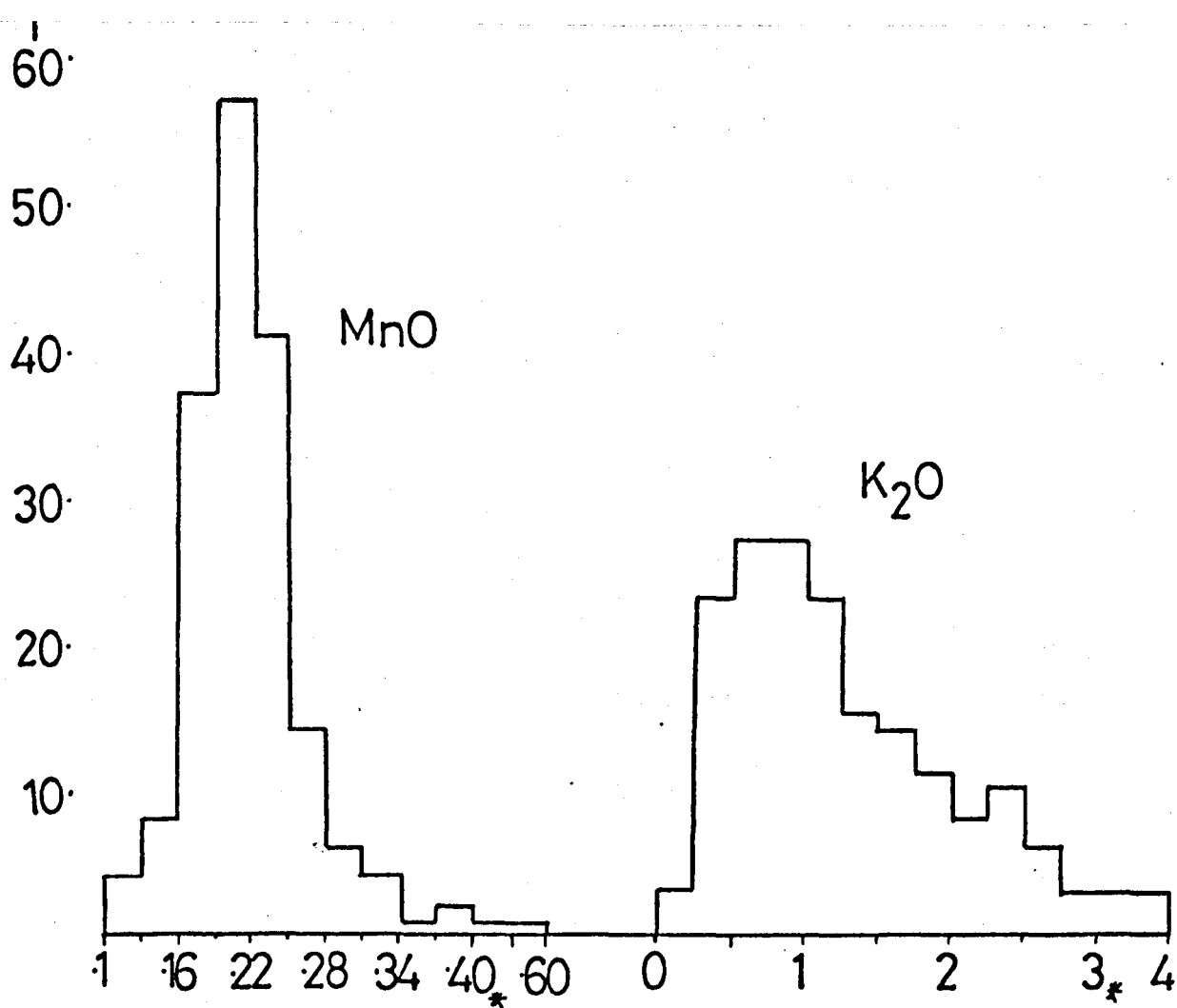


Figure 3.3: Frequency histograms for MnO, P₂O₅, K₂O, and H₂O. (oxides as wt. %.) * All horizontal scales are non-linear at high values.

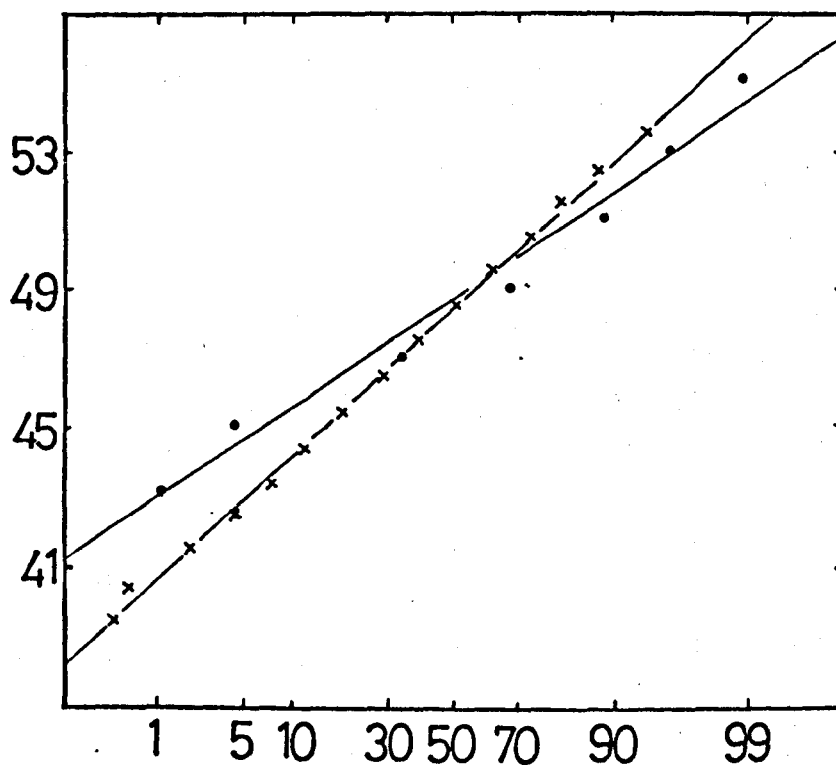


Figure 3.4: SiO_2 frequency distribution in South Norwegian metabasites compared with that in all basaltic rocks.

Vertical axis: SiO_2 wt. %.

Horizontal axis : Cumulative frequency %.

Crosses = " all basaltic rocks" $n=1996$, (Manson 1967).

Closed circles = South Norwegian metabasites ($n = 176$).

TABLE 3.2

Comparison of mean Metabasite chemistry with overall basalt chemistry, as compiled by Manson (1967).

Oxide	1	2	3
SiO ₂	47.89	49.3	50.6
Al ₂ O ₃	15.80	16.0	15.3
TiO ₂	1.93	2.0	1.5
Fe ₂ O ₃	3.52	3.2	2.4
FeO	9.68	7.8	8.9
MgO	6.88	6.6	6.4
CaO	8.97	9.9	10.1
Na ₂ O	2.77	2.8	2.4
K ₂ O	1.30	1.0	0.9
MnO	0.22	0.17	0.18
P ₂ O ₅	0.35	0.32	0.26
H ₂ O	0.62	0.9	1.0

1. Metabasites (mean); Column 1, Table 3.1.
 2. "All basalts" (n = 1558))
 3. "All dolerites" (n = 417))
- Manson (1967).

distribution. In some instances such distribution curves have been used to infer the existence of two populations with respect to potash abundance (e.g. Oxburgh 1964) . The reasons for the distribution in the South Norway metabasites are discussed later in the text and in Field and Clough (1976).

P_2O_5 displays a similarly prominent asymmetric distribution, partly due to a few extremely high values. One of these ($P_2O_5 = 2.14\%$) exceeds Manson's basalt chemistry screen. His criteria are also exceeded by a small proportion of samples in the Fe_2O_3 distribution (10/176 with $Fe_2O_3 > 6.0\%$). Despite this, and the very wide spread of Fe_2O_3 values, the means for the two series (Table 3.2) are similar. It is interesting to note that metabasites from an amphibolite-granulite transition in the Inner Hebrides (Drury 1974) show extremely high Fe_2O_3 values. The mean values for both the amphibolites and the granulite facies basic rocks described by Drury (1974, Table 3) exceed the strict requirements of Manson's upper criterion for this oxide. Thus the fact that a small percentage of the Norwegian metabasites exceed the constraints for Fe_2O_3 may not be of great significance, particularly as the oxidation ratio may have been modified during metamorphism.

These data show that the major element chemistry of the metabasites corresponds closely with that of basaltic igneous rocks. The great majority of the Norwegian rocks adhere in all respects to the limits of chemical variation ascribed to basalts by Manson (1967). On empirical grounds this is to be expected, since any rock composed primarily of hornblende and plagioclase will approximate to a basalt chemistry

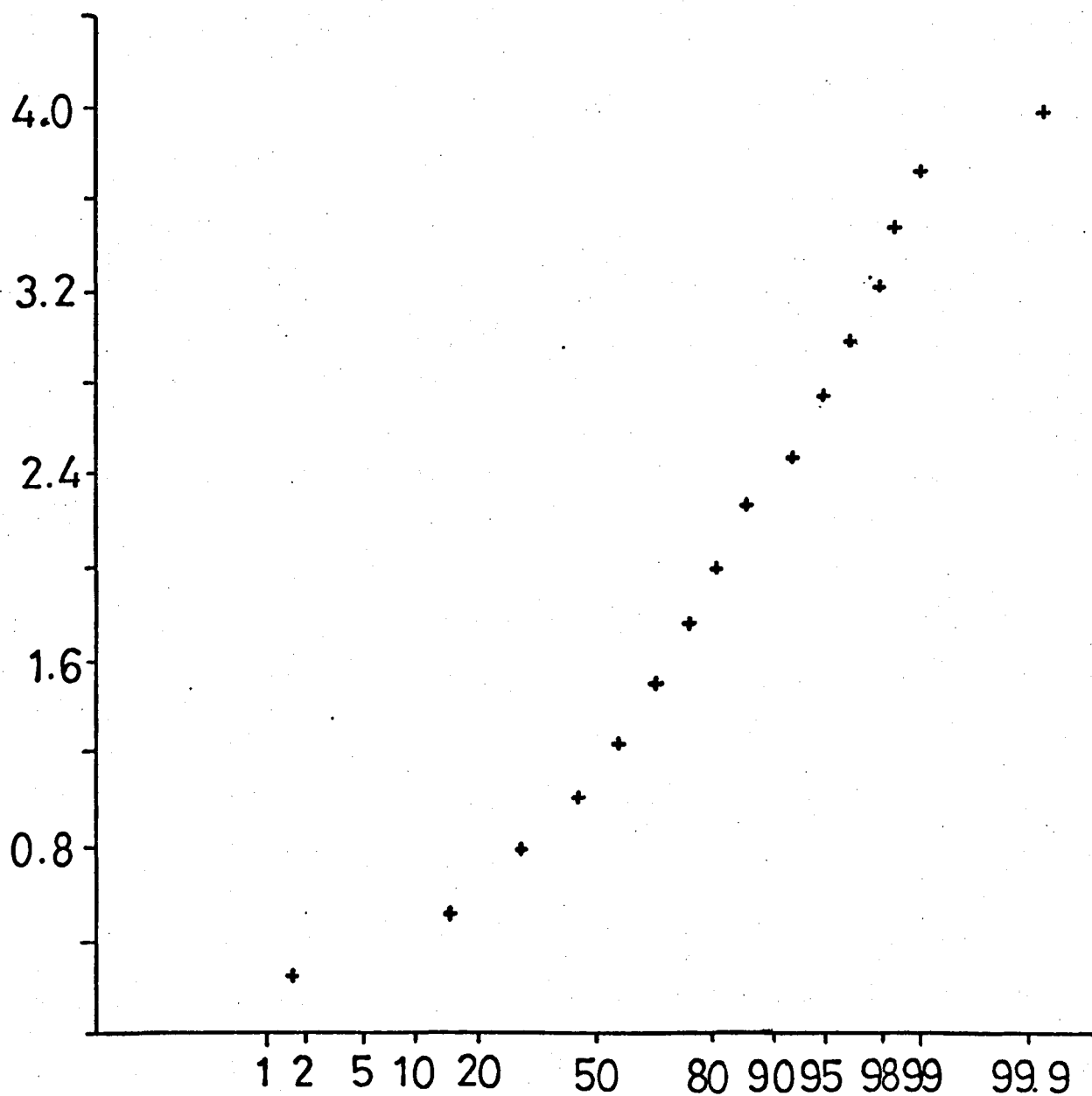


Figure 3.5: Cumulative frequency diagram for K₂O, in 176 metabasites.
Vertical axis = K₂O wt. %. Horizontal axis = Cumulative frequency %

(cf. Orville 1969). The presence of ortho- or clinopyroxene will not radically affect the composition field, but biotite for example would tend to lower the CaO value, and raise K₂O %. This effect may be noted in table 3.2.

Table 3.3 is a comparison of the mean metabasite major element chemistry with recently published compilations of metabasic rocks from other terrains. There are no obvious differences between the metabasites and these broadly analogous suites.

C. Intra-terrain major element variation.

The bulk major element chemistry of the metabasites, described for the whole suite in the previous section is now examined with respect to zones A, B and C, which were defined in chapter 2. A summary of the mean and median values for each zone is given in table 3.4.

i) Zone A v. Zone B.

The data show that the amphibolite facies-granulite facies transition on the mainland (zones A and B) is not characterised by marked major element chemical variation. There are no obvious variations between the populations of zone A and B for SiO₂, Al₂O₃, Fe₂O₃, FeO, MgO, CaO, Na₂O, MnO, and H₂O. This congruence has been verified by comparisons of zonal histograms and median values rather than by the Student t test, since the samples are not always gaussian in distribution. The mean values for these elements in table 3.4 should be taken as broadly representative of the consistence of the overall chemistries of the group.

TABLE 3.3

Comparison of mean Metabasite chemistry (S. Norway) with other, recently analysed, metabasic suites.

Oxide	1.	2.	3.	4.	5.	6.	7.	8.
SiO ₂	47.89	49.70	50.16	51.05	48.40	52.22	47.42	48.9
Al ₂ O ₃	15.80	13.75	14.53	14.13	15.88	13.85	15.12	14.5
TiO ₂	1.93	1.41	1.10	1.03	1.53	0.78	2.37	1.06
Fe ₂ O ₃	3.52	6.07	2.55	4.23	3.64	5.55	4.31	2.14
FeO	9.68	8.61	10.27	8.04	5.43	4.97	10.41	9.03
MgO	6.88	6.59	6.72	7.63	7.45	7.26	5.67	6.27
CaO	8.97	6.26	10.48	8.95	8.42	8.76	9.73	8.74
Na ₂ O	2.77	2.46	1.92	2.55	4.32	3.09	3.47	2.51
K ₂ O	1.30	1.01	0.36	1.03	0.41	0.61	0.62	0.45
MnO	0.22	0.24	0.21	0.20	0.18	0.16	0.23	0.21
P ₂ O ₅	0.35	0.12	0.04	0.25	0.24	0.13	0.64	0.07
H ₂ O	0.62	-	1.32	-	4.08*	2.08	-	3.34

1. = South Norwegian Metabasites (this study, n = 176).
2. = Weighted mean of 32 amphibolites + 9 granulite facies basic rocks, Coll and Tiree, Inner Hebrides. (Drury 1974).
3. = 23 amphibolites, Frederikshab, Greenland. (Rivalenti 1972; Rivalenti and Rossi, 1972).
4. = 54 amphibolites, Neria (Kalsbeek and Leake 1970).
5. = 39 metabasalts (Appennine ophiolites). (Ferrara et al, 1976)
(* = Loss on Ignition).
6. = 11 basic hornblende gneisses, Assynt. (Sheraton et al. 1973, Table 3).
7. = Wilson and Leake (1972) 31 'epidiorites', Tayvallich.
8. = 162 Canadian amphibolites (Goodwin, 1968).

TABLE 3.4

Intra-terrain major element variation for South Norwegian
Metabasites

	A		B		C		A+B	
SiO ₂	48.15		47.63		47.87		47.89	
Al ₂ O ₃	16.07		15.46		15.51		15.87	
TiO ₂	1.87	(1.80)	2.27	(2.03)	1.43	(1.40)	2.04	(1.88)
Fe ₂ O ₃	3.39		3.43		4.04		3.40	
FeO	9.86		10.23		8.60		9.92	
MgO	6.97		6.62		7.15		6.82	
CaO	8.97		9.02		8.88		8.99	
Na ₂ O	2.53		2.64		3.62		2.58	
K ₂ O	1.47	(1.34)	1.26	(0.90)	0.94	(0.75)	1.38	(1.20)
MnO	0.21		0.20		0.26		0.21	
P ₂ O ₅	0.30	(0.25)	0.48	(0.30)	0.22	(0.22)	0.37	(0.27)
H ₂ O	0.63		0.69		0.49		0.65	
*FeO	12.72		13.37		12.24		13.00	

*FeO Total Fe calculated as FeO.

A = Mainland, Amphibolite facies (n = 82)

B = Mainland, Granulite facies (n = 62)

C = Tromsø, Granulite facies (n = 32).

Figures in parentheses are median values.

However, there are obvious differences for the K_2O , TiO_2 and P_2O_5 mean values between the two zones, and histograms for these three oxides are plotted by zone in figures 3.6a and 3.6b. From these diagrams it is clear that the differences in mean TiO_2 and P_2O_5 between the two mainland zones are largely due to an asymmetric distribution of values. For both elements zone B contains a small but important proportion of very high values (e.g. P_2O_5 : 7/62 samples in Zone B $>1.0\%$). Since this asymmetry invalidates the use of the t-test, median values (Table 3.4) are the best criterion for comparison between zones A and B. It is clear that if this parameter is taken as a measure of location, the apparent differences in TiO_2 and P_2O_5 abundance between the mainland zones largely disappear.

The case for real differences in K_2O between zones is stronger. There is little doubt that the abundance levels show a small but real decrease between A and B (Table 3.4, Figure 3.6a). The decline in this oxide may be noted in the median values (1.34 to 0.90) as well as in the mean chemistry for the zones.

Thus, with the exception of K_2O , it becomes possible to combine the bulk chemistries of zones A and B to give an overall expression of metabasite chemistry on the mainland. This is presented in column 4 of Table 3.4.

ii) Zone C v. Zones (A + B).

A comparison of zone C (Tromøy) with the mainland reveals some important geochemical distinctions. Although there are no appreciable differences in SiO_2 , Al_2O_3 , MgO and CaO , there

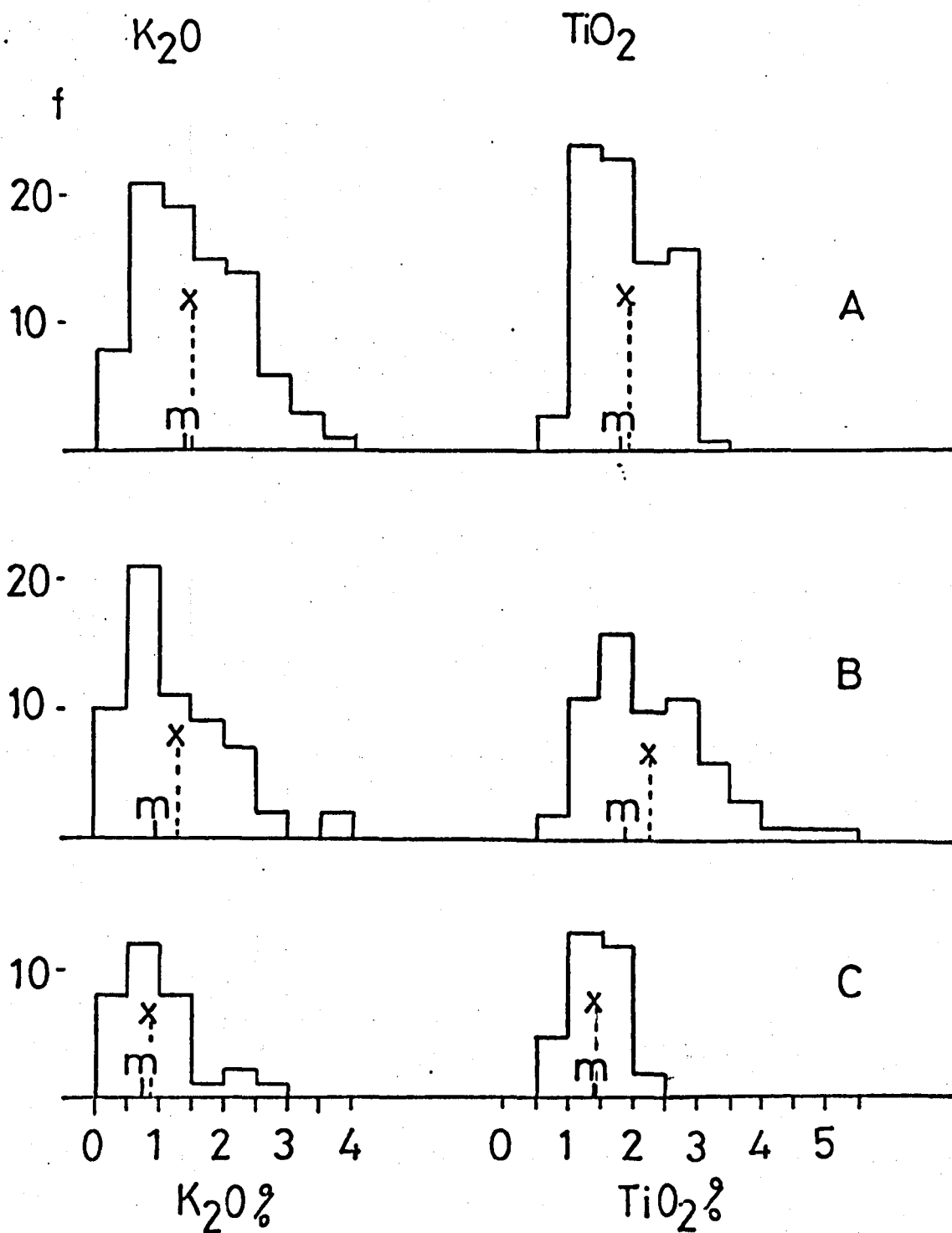


Figure 3.6a: Frequency histograms for K_2O and TiO_2 by metamorphic zone-(A, B and C). m = median, \bar{x} = mean, f = frequency.

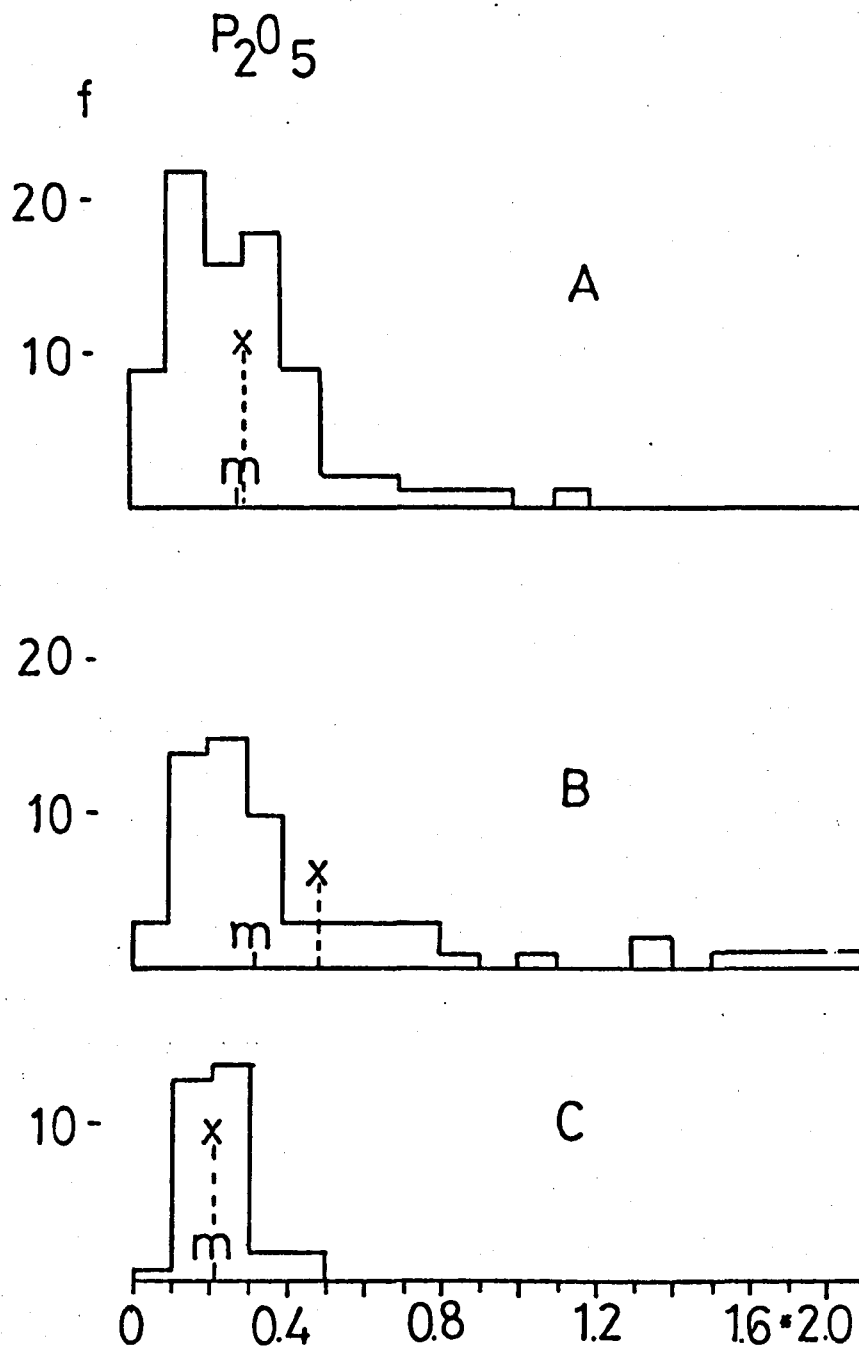


Figure 3.6b: Frequency histogram for P_2O_5 by metamorphic zone (A, B and C). Symbols as in figure 3.6 a.

are lower averages for TiO_2 , P_2O_5 , H_2O and K_2O than elsewhere. In addition, zone C displays higher Na_2O and possibly MnO than zones A and B; with higher Fe_2O_3 and lower FeO values there is also a clear trend to higher oxidation ratios in zone C, though there is little variation in total iron content.

Thus, all the recognised chemical changes with the exception of K_2O , occur between Zones A+B and Zone C, and are therefore geographically abrupt. Potash continues the trend to lower abundances at the higher grades of metamorphism, and is the only major oxide to display a gradual variation across the whole transition. This feature must be due either to systematic original (igneous) differences, or to consistent changes accompanying the metamorphism. Such changes are not unusual in high-grade terrains (e.g. Eade and Fahrig 1971). Each of the variations described above is now compared with those established for other high-grade transitional sequences.

- (a) In their pioneering study in the Adirondacks, Engel and Engel, (1958, 1960) described chemical changes associated with a prograde amphibolite facies to granulite facies metamorphism. The chemistry of amphibolites in the Amphibolite facies (at Emeryville) was compared with metabasites in the granulite facies culmination around Colton (Engel and Engel, 1962). Having made the assumption that there was no major variation in pre-metamorphic chemistry, Engel and Engel suggested that increasing grade of metamorphism resulted in decreases of K_2O , H_2O , the oxidation ratio and possibly SiO_2 . The

metabasites also showed overall increases in CaO and MgO towards Colton (granulite facies). The Adirondacks data also suggested small decreases with grade in both TiO₂ and P₂O₅ and a possible small increase in soda, though these features were not discussed at length by Engel and Engel (op.cit.).

Table 3.5 includes a summary of the established chemical variation in the Adirondacks compared with the Tromsø-Mainland variation in South Norway. The higher grade rocks in each area show apparent decreases in TiO₂, K₂O, P₂O₅ and H₂O. However, the oxidation ratio decreases with grade in the Adirondacks, but increases in South Norway, while Na₂O is much more markedly increased in the latter terrain. Relative enrichment of CaO and MgO is not prominent in the Bamble sector metabasites.

- (b) In a chemical study of retrogressive granulite facies - amphibolite facies metamorphism in the inner Hebrides, Drury (1974, Table 3) quotes average analyses of metabasites from both facies (9 samples from the granulite facies; 32 amphibolites). The most notable chemical variations in these rocks (Table 3.5) are a decrease in K₂O and an increase in Na₂O in the granulite facies, changes which also occur between Zone C and the mainland in South Norway. The slight decline in FeO and the increase in Al₂O₃ in the higher grade metabasites of the Inner Hebrides are not features of the Bamble transition.

No complete pattern of analogous chemical change with grade emerges therefore from these inter-terrain comparisons.

TABLE 3.5

Oxide	Adirondacks		South Norway		Inner Hebrides	
	Emeryville (A.F.)	Colton (G.F.)	Zones A+B	Zone C (High G.F.)	A.F.	G.F.
SiO ₂	48.20	47.89	47.89	47.87	49.7	49.7
Al ₂ O ₃	14.45	14.63	15.87	15.51	13.4	15.0
TiO ₂	1.89	1.56	2.04	1.43	1.37	1.53
Fe ₂ O ₃	3.50	1.85	3.40	4.04	6.03	6.21
FeO	10.35	11.20	9.92	8.60	8.84	7.79
MgO	6.62	7.41	6.82	7.15	6.5	6.9
CaO	10.25	11.54	8.99	8.88	6.39	5.80
Na ₂ O	1.94	2.19	2.58	3.62	2.2	3.40
K ₂ O	0.96	0.58	1.38	0.94	1.12	0.60
MnO	0.25	0.25	0.21	0.26	0.25	0.19
P ₂ O ₅	0.18	0.14	0.37	0.22	0.12	0.11
H ₂ O	1.31	0.72	0.65	0.49		

D. CIPW Norms.

The CIPW norms are tabulated in Appendix 3. There is an interesting division of the 176 samples based on these norms as follows:-

TABLE 3.6.

Normative characteristics of the South Norwegian Metabasites.

(CIPW classification).

NAME	No.	% of Suite
"Olivine Tholeiites" (No Ne; No qtz).	99/176	56.3%
"Quartz Tholeiites" (No ol.)	30/176	17.0%
"Alkali olivine basalts" (No hyp.)	47/176	26.7%

In the 30 quartz-normative samples, the average percentage of quartz in the norm is 4.2%. The 47 nepheline-normative rocks average 2.1% Ne, and in only 3 is 4.5% Ne exceeded. The majority of rocks are hypersthene-normative with neither quartz nor nepheline.

The bulk chemical changes described in the preceding section may also be ascertained by the normative classification. Zone C is dominated by "alkalic" normative compositions in comparison with zones A and B (Table 3.7).

Gill and Bridgwater (1976, p. 280) have drawn attention to the possible effects of non-isochemical metamorphism upon

TABLE 3.7

Normative characteristics by zone.

	Zone A (%)		Zone B (%)		Zone C (%)		Zones (A+B) (%)	
Qtz-normative (Q.Thol.)	17	21%	11	18%	2	6%	28	19%
Ne-normative (Alk. Ol. Bas)	19	23%	14	23%	14	44%	33	23%
Hyp-normative. (Ol Thol.)	46	56%	37	59%	16	50%	83	58%
Total	82	(100%)	62	(100%)	32	(100%)	144	(100%)
Ratio $\left(\frac{\text{Ne-normative}}{\text{Qtz-normative}} \right)$	1.12		1.27		7.00		1.18	

normative parameters. For example, the metasomatic addition of alkalis may lead to a reduction of quartz, hypersthene and the An/Ab ratio, and an increase in olivine in the hypothetical norm. Therefore, in view of the high grade of metamorphism affecting the metabasites, and also in consideration of the possible factors controlling their present chemistry, no petrogenetic implications should be drawn directly from these normative values.

E. Major element variation diagrams.

In the previous sections it has been demonstrated that the abundances of certain elements display a regional variation, and that differences are particularly prominent between zone C and the mainland. If these variations are to be ascribed to metamorphism, the assumption of a uniform initial composition must be made. Such an assumption is not necessarily valid, and hence the following igneous variation diagrams have been used in an attempt to distinguish any inherited chemical characters.

i) The AFM diagram (Figures 3.7, 3.8).

The metabasite data plot over a fairly large area of chemical variation, partly due to the large number of samples which provide a wide spectrum of chemistry.

The average values for each zone (A, B and C) plot very close to each other, though the slightly more alkalic character of zone C can be distinguished (Figure 3.8).

The original AFM variation may have been partially obscured if metamorphic redistribution of alkalis has occurred,

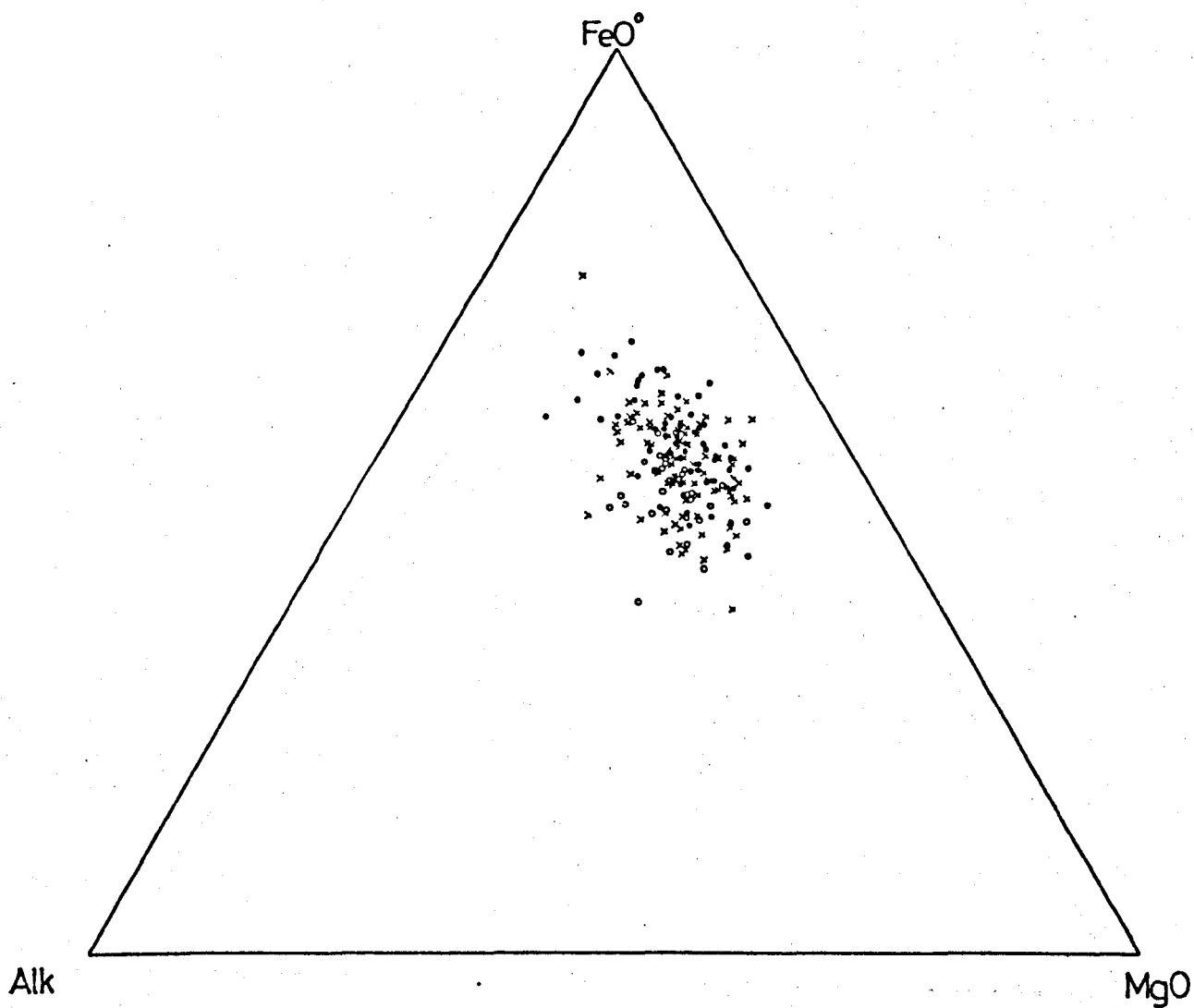


Figure 3.7: AFM diagram for 176 metabasites. Alk = $\text{Na}_2\text{O} + \text{K}_2\text{O}$; FeO^0 = Fe total as FeO; data in wt. %. Crosses = zone A samples; closed circles = zone B; open circles = zone C.

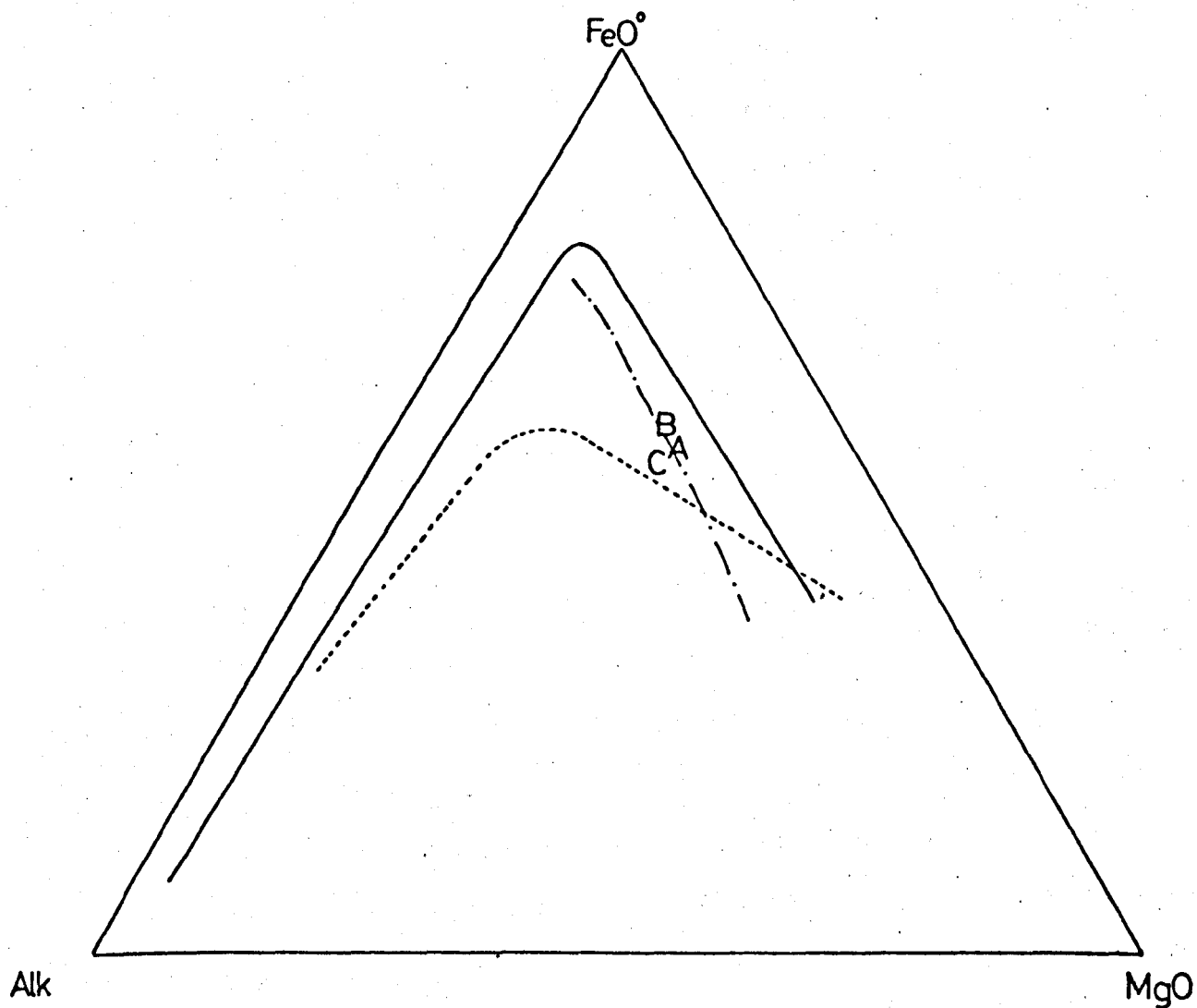


Figure 3.8: Schematic AFM diagram with generalised trend for the metabasites from figure 3.7. Solid line = Skaergaard trend. Dashed line = Tasmanian dolerites. Dashed-dotted line = Norwegian metabasites. A, B, and C refer to the average compositions by zone.

probably leading to increased scatter. Nevertheless, if the Fe/Mg ratios have remained unaltered, there is a broad trend towards iron enrichment, analogous to several differentiated basic suites including the mid-Atlantic tholeiitics (Thompson 1973) and the recently documented Dalradian metabasaltic rocks (Graham 1976a). The differentiation trends for Skaergaard (Wager and Brown 1968), and the Tasmanian dolerites (e.g. from Heier et al 1965) are plotted in figure 3.8 for additional comparison. This apparent fractionation pattern in the Norwegian metabasites is limited to an iron-enrichment, and no acid-alkalic residuals are found in the group. It is also pertinent to note that the trend of the metabasites is typical of tholeiitic provinces rather than alkalic basic rocks, which do not characteristically display such a marked variation in Fe/Mg (Kuno 1967).

ii) Differentiation indices.

Some of the most widely used indices of differentiation are based on parameters used in the AFM diagram, such as $(\text{FeO}^\circ + \text{Na}_2\text{O} + \text{K}_2\text{O})/(\text{FeO}^\circ + \text{MgO} + \text{Na}_2\text{O} + \text{K}_2\text{O})$ (e.g. Thompson 1973). However, in view of the possibility of alkali element mobility, indices using Na_2O and K_2O are avoided in this study. The two parameters chosen (niggli mg and niggli si) utilize both Fe/Mg variation and SiO_2 variation. In the metabasites mg varies from 0.18 to 0.66 and si from 89 to 160. The individual niggli values for each metabasite are tabulated in Appendix 3.

Figures 3.9 - 3.11 are scatter diagrams for si-al, si-fm and si-mg respectively, each zone being plotted separately to facilitate comparisons.

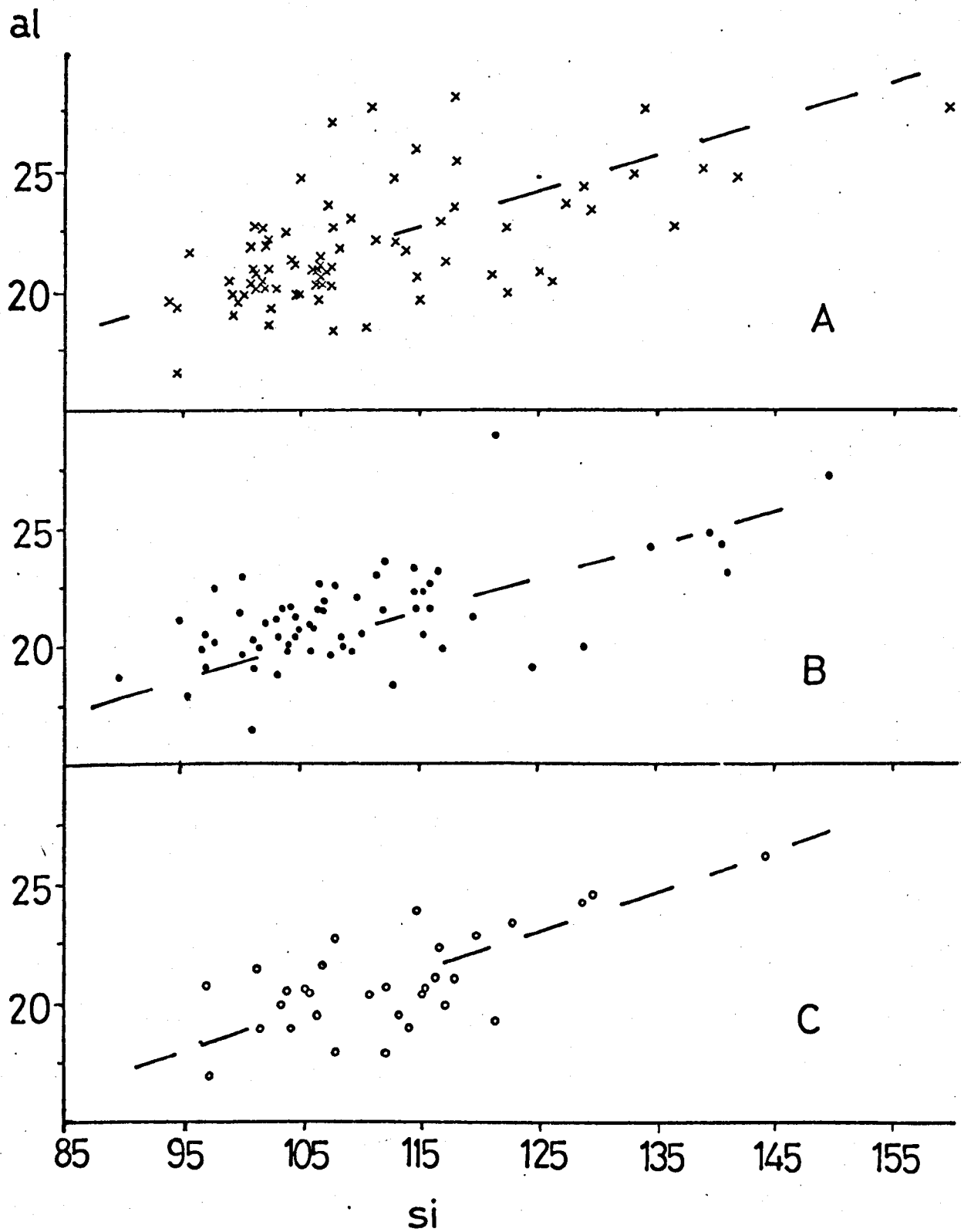


Figure 3.9: Niggli si v al for Norwegian metabasites by metamorphic zone. Crosses = zone A samples (n=82), closed circles = zone B samples (n=62), open circles = zone C samples (n=32).

There is a clear positive correlation between si and al (Figure 3.9), which is shown by the metabasites for all three zones (A, B and C). No differences in the zonal fields of variation are visible. Conversely, a negative correlation is shown by both the si-fm diagram (3.10) and the si-mg plot (3.11), although the latter relationship is not well defined in zone C. With this exception, the trends are described by the metabasites from each subdivision of the terrain.

Because the range of si values is relatively small (90-160), the variation curves are very shallow. However, the increasing al and decreasing fm are both characteristic of typical igneous differentiation sequences (e.g. Leake 1964, Correns 1969, Rivalenti 1970).

An important series of features is illustrated by the variation diagrams which use niggli mg as the index of differentiation. The range of mg (0.18 to 0.66) is substantially reduced to 0.40 - 0.60 when zone C is considered in isolation. This is an important constraint on the overall field of variation for this zone, and may also be noted in figure 3.11 (si-mg).

The mg-c diagram (3.12) shows some tendency for the metabasite suite to plot parallel to a trend first ascribed by Leake (1964) to systematic igneous variation. The slightly low average CaO content of the metabasites is reflected in the tendency of the rocks to plot just beneath the established trends for differentiated samples.

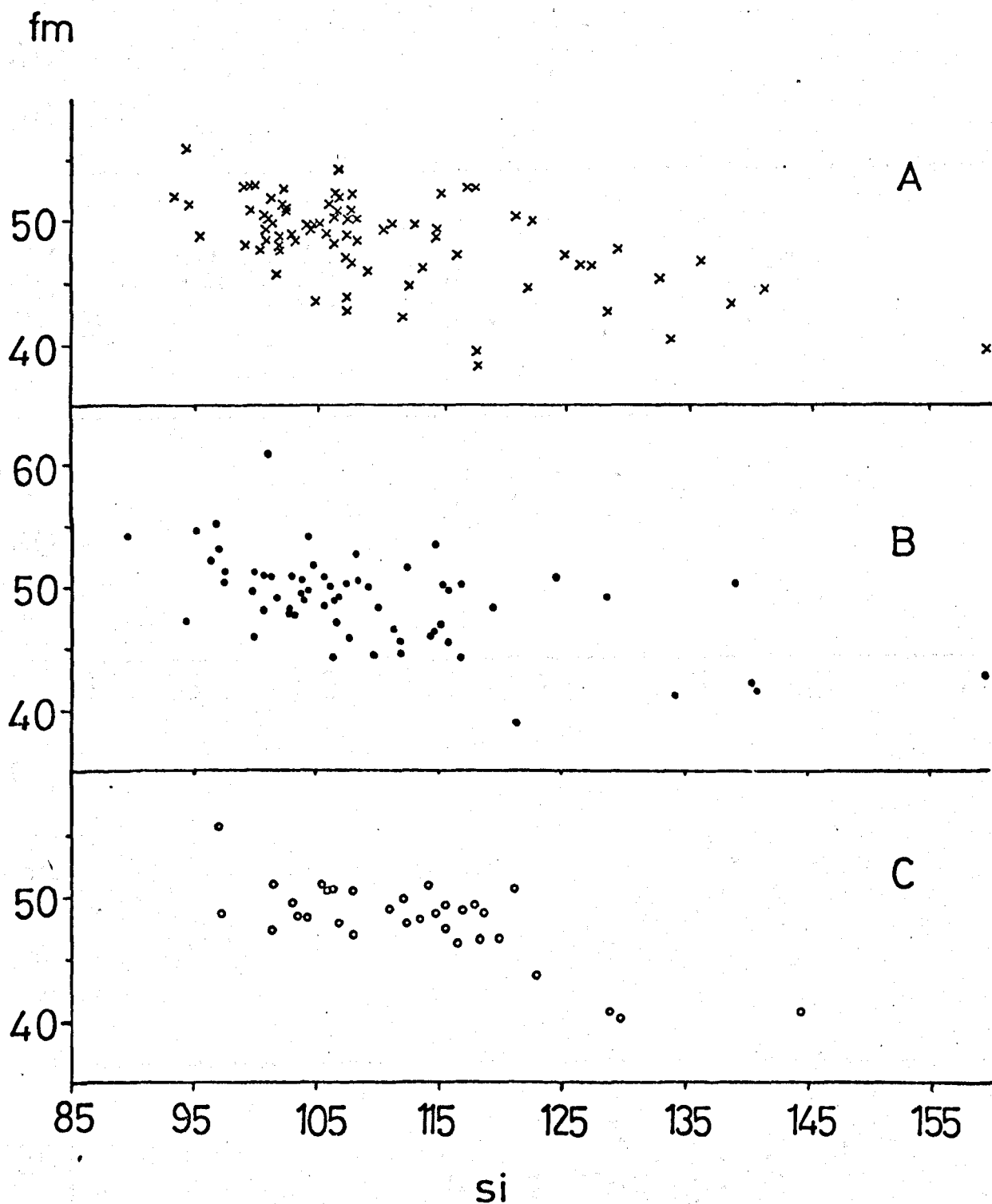
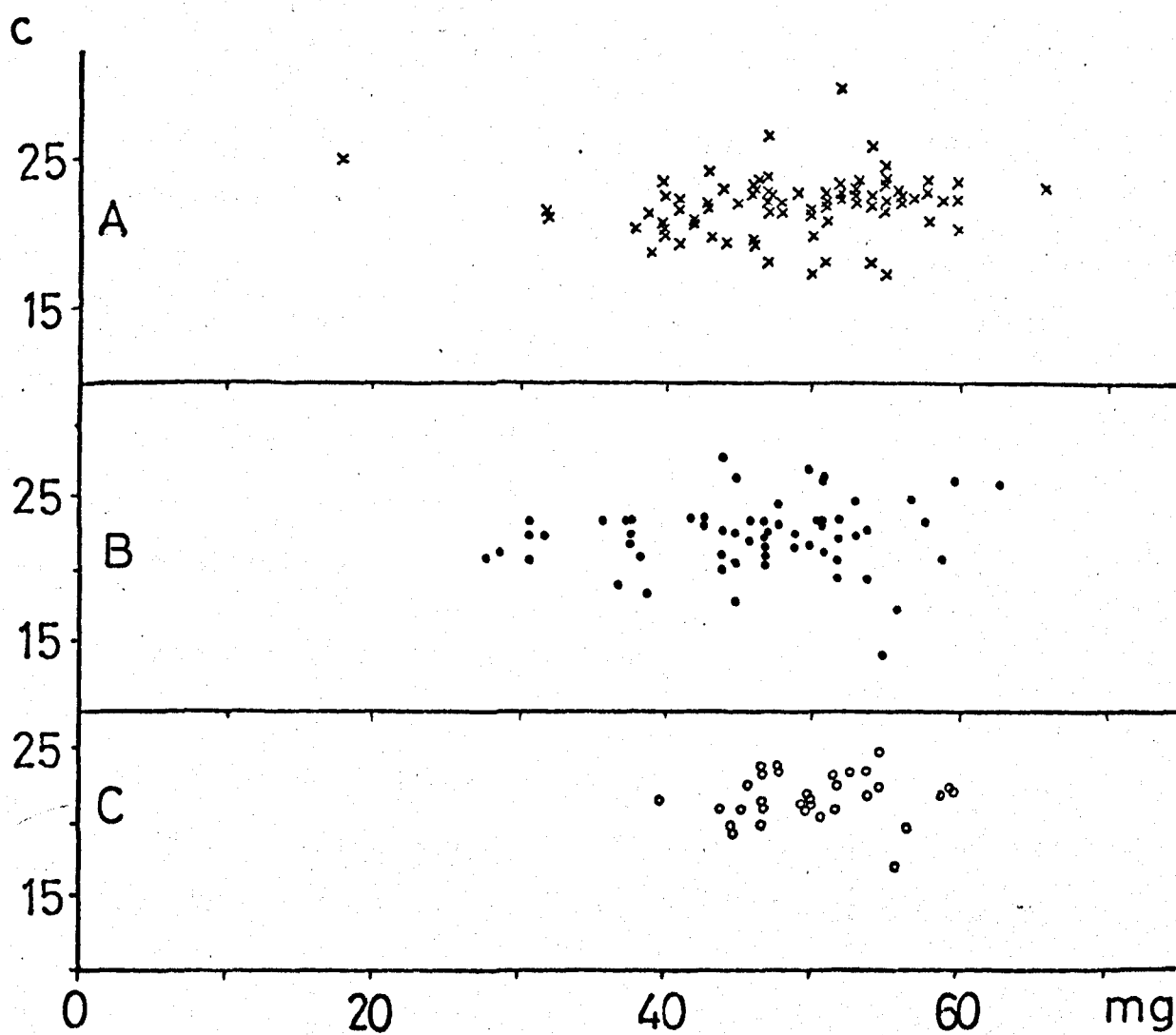
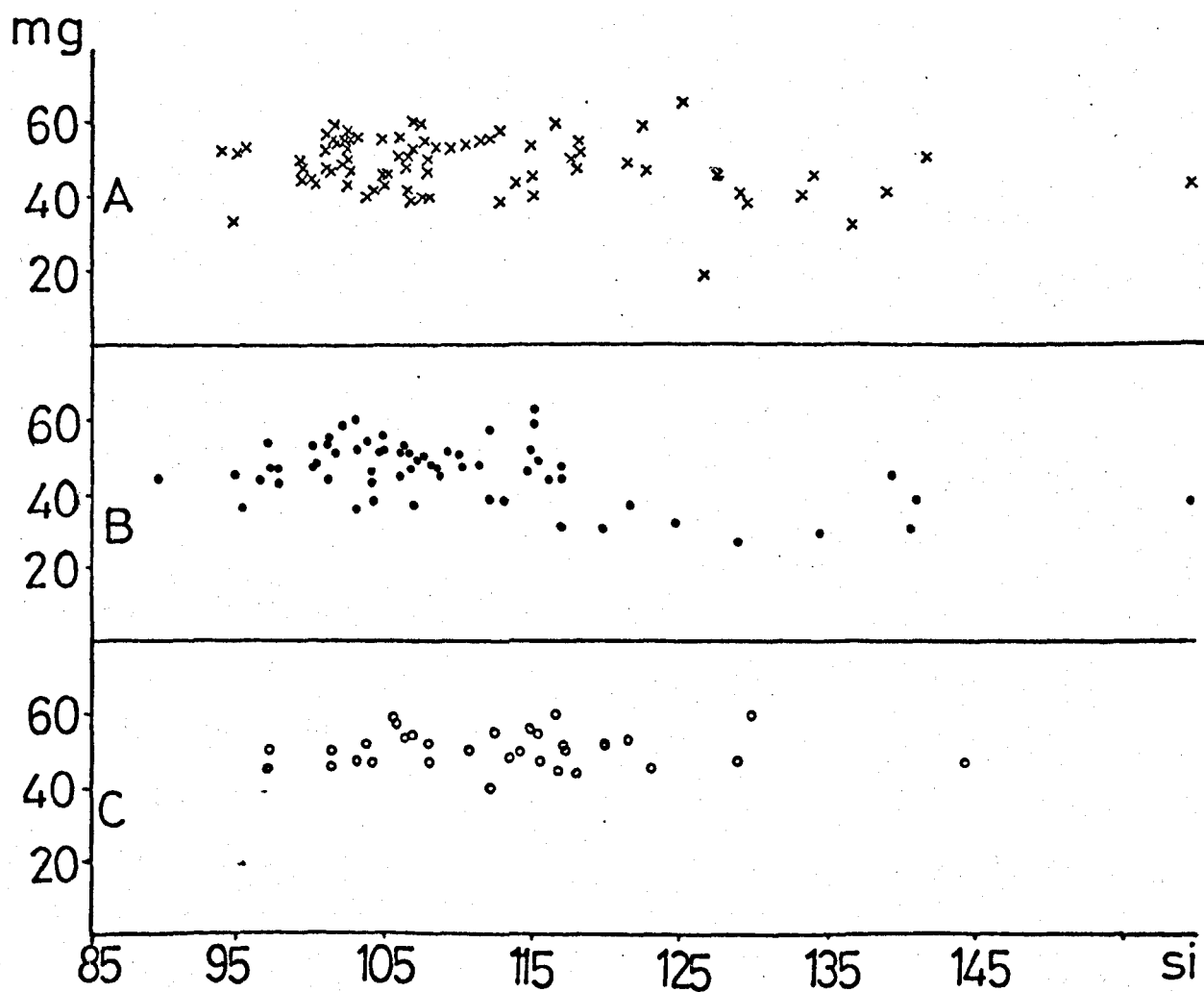


Figure 3.10: Niggli fm v si by metamorphic zone. Symbols as in figure 3.9.

Figures 3.11 and 3.12 (Overleaf): Niggli mg v si and c v mg.
 Symbols as in figure 3.9 (mg values $\times 10^2$)



Both the mg-p and the mg-ti diagrams (3.13 and 3.14) show well defined negative correlations for the suite as a whole, and also for each zonal subdivision. The "most differentiated" samples, with the lowest mg numbers generally display very high ti and p values.

Increases in both TiO_2 and P_2O_5 with concomitant iron-enrichment is again consistent with igneous fractionation. A well-known analogue is the Karroo dolerite province (Walker and Poldervaart 1949), including the Nuanetsi basalt succession (Cox et al 1967). However, extreme enrichments in these elements, interpreted as representing cumulus growth of ilmenite and apatite, are not particularly common, although Miyashiro et al (1970) have described ferrogabbroic differentiates from the Atlantic ridge with up to 7.0% TiO_2 . Muir (1954) quotes ferrodolerite analyses from Minnesota with an average P_2O_5 of 2.15%. The maximum TiO_2 and P_2O_5 values in the Norwegian metabasites are 5.25% and 2.14% respectively, and it is probable that a small proportion of the suite shows enrichments in these elements due to original cumulus fractionation. Graham (1976a) has recently described analogous enrichment patterns in Dalradian metabasaltic sills.

Another important aspect of figures 3.13 and 3.14 is the fact that negative correlations exist in zone C, although the mg-p curve is very shallow in this group. Thus despite the low range of mg values, similar differentiation trends to those on the mainland are preserved

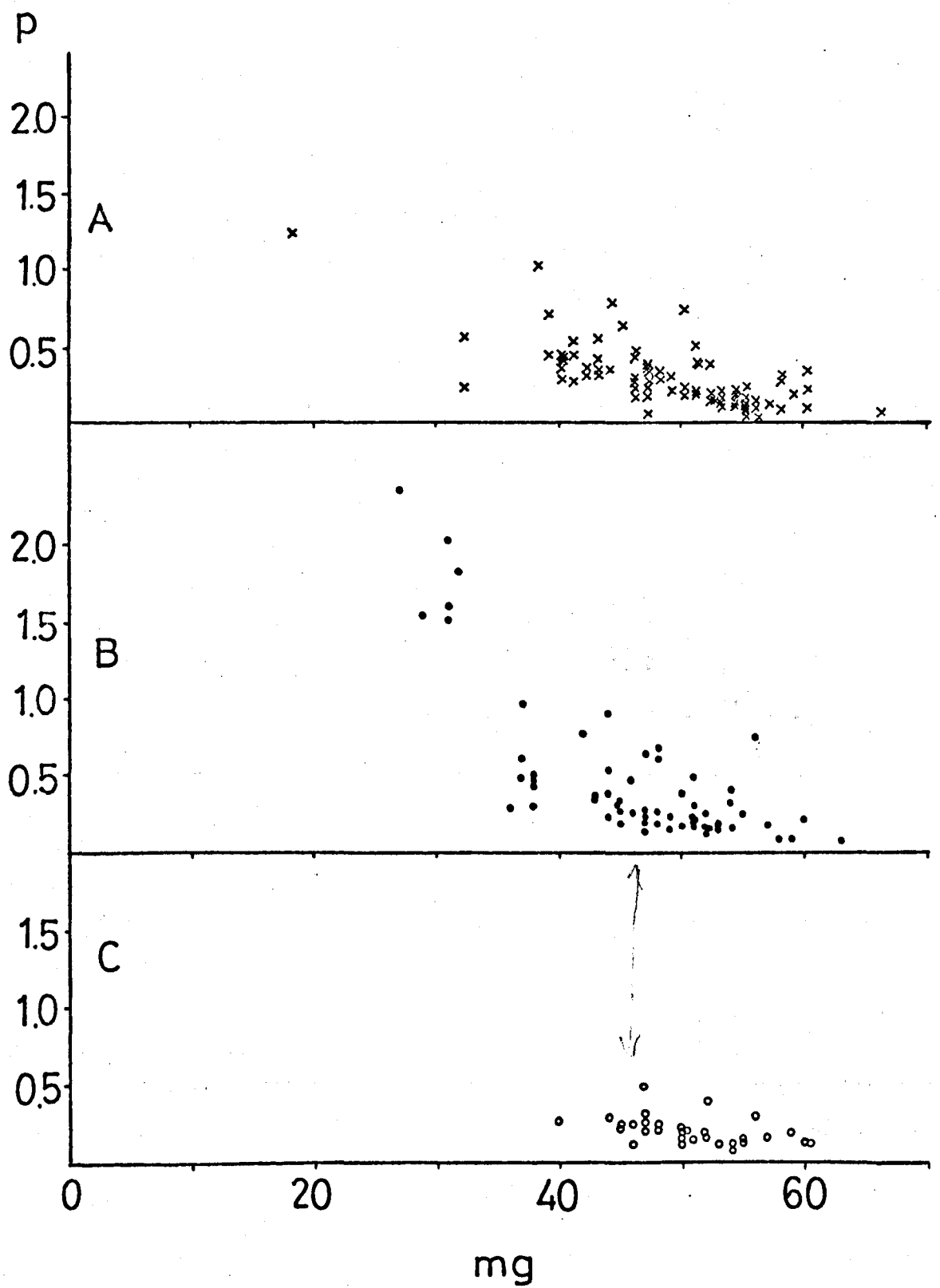


Figure 3.13: Norwegian metabasites: Niggli p v mg. Zonal symbols as in figure 3.9.

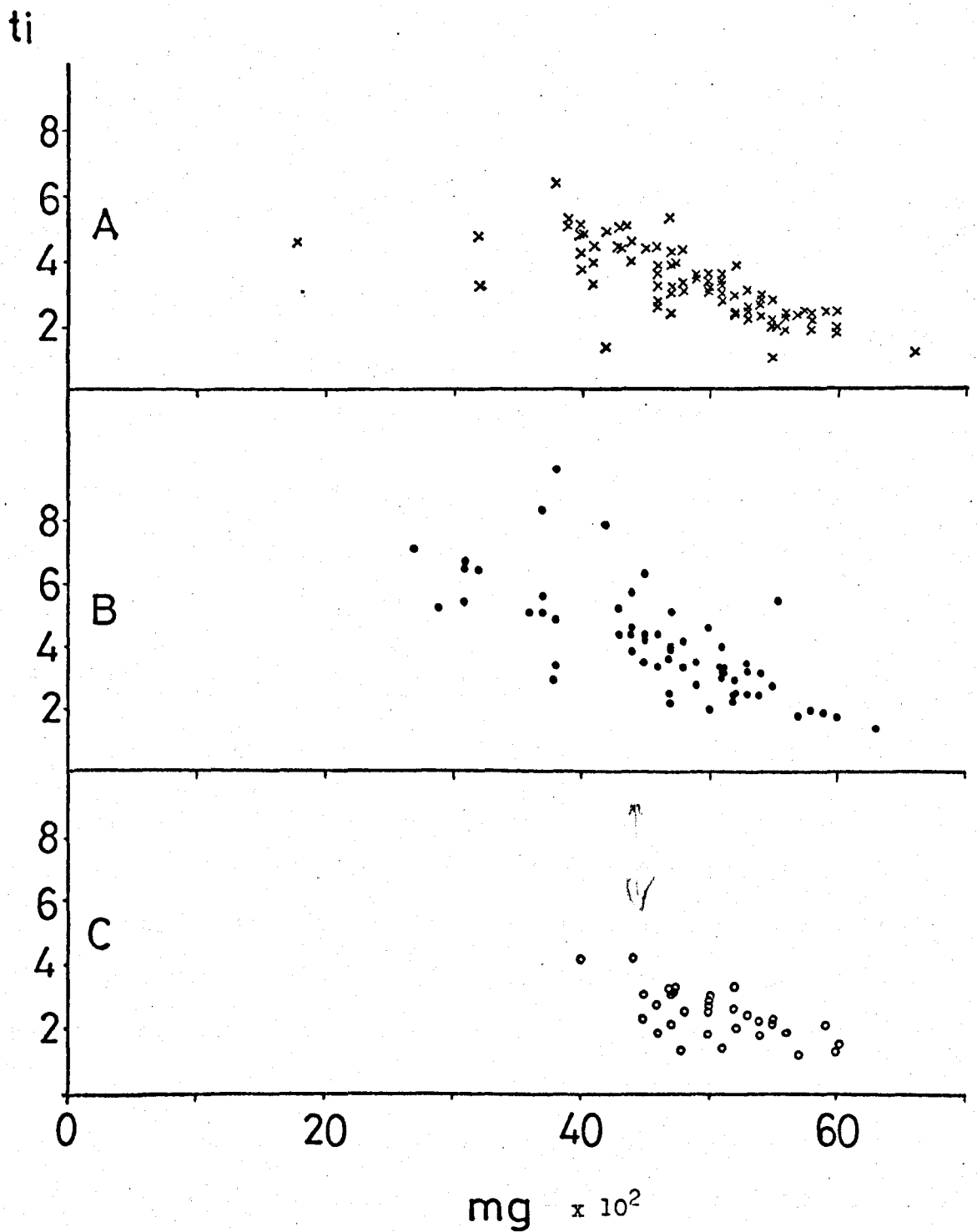


Figure 3.14: Norwegian metabasites: Niggli ti v mg by metamorphic zone. Symbols as in figure 3.9.

in zone C (Tromøy), with an absence of evolved samples being the most likely explanation for the low average P_2O_5 and TiO_2 values in zone C compared with A and B (Table 3.4). Hence, the regional variations in P_2O_5 and TiO_2 may be adequately explained as original (igneous) features and there is no reason to suspect that there has been metamorphic mobility of these elements.

The mg-MnO diagram (3.15) is inconclusive. Whilst zones A and B display shallow negative slopes, the zone C samples, with higher average MnO show more scatter.

iii) Alkali Element Variation Diagrams.

The total alkalis for the metabasite suite are, on average, high for a group of mafic rocks. ($Na_2O + K_2O$) has a mean value of over 4.0%. In addition, bulk chemical considerations in the previous sections have suggested that there is a systematic chemical gradient for K_2O across the transition, and also that soda is relatively enhanced in zone C. Thus, the Tromøy metabasites contain on average over 1% more Na_2O than the mainland samples. This is also reflected in the CIPW norms, the zone C metabasites showing a tendency to be Nepheline normative (Table 3.7). Moreover, mean normative plagioclase composition for zone C is 45% An compared with 57% An in zones A and B. The low anorthite content, from optical determinations, in the Tromøy metabasites was also described in chapter 2. Consequently all variation plots involving Na_2O and K_2O require cautious interpretation.

Diagrams involving alkali elements against differentiation indices (si-alk, mg-alk, mg- K_2O and mg- Na_2O) are presented in figures 3.16 to 3.19.

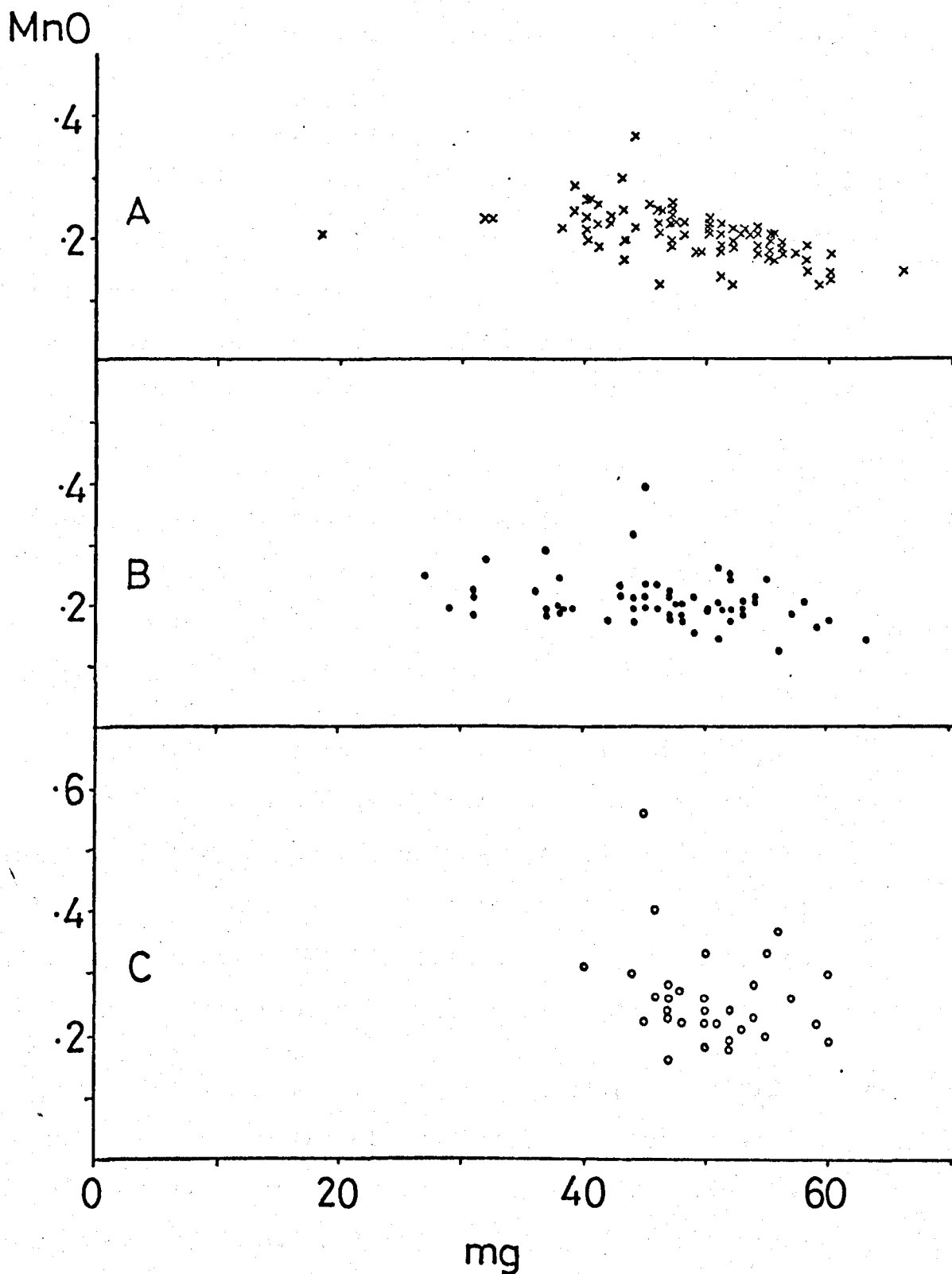


Figure 3.15: Norwegian metabasites: MnO % v niggli mg ($\times 10^2$)
Symbols as in figure 3.9.

The si-alk diagram (3.16) displays a shallow curve, with a slight tendency to increased alk with increasing SiO_2 , apparently characteristic for each zone. In contrast, there is no clear trend for the suite as a whole in the mg-alk diagram (3.17), although some trend to an increasing alk with decreasing mg occurs in zone B. K_2O and Na_2O , when plotted individually, show no correlations with mg. (3.18 and 3.19).

In figure 3.18 (mg- K_2O) the amount of dispersion on the vertical axis (K_2O) gradually increases from zone C through to zone A, and this reflects the variation in K_2O . There is no evidence that this zonal variation is related to an igneous differentiation.

Figure 3.19 illustrates the abnormally high Na_2O contents of the zone C metabasites compared with the mainland. The soda content of the metabasite suite appears unrelated to the differentiation index, and it is clear that zonal variation in this element cannot be ascribed to original differences due to igneous fractionation processes.

The total alkalis versus silica plot (Figure 3.20) has proved useful in the classification of fresh basic volcanic rocks. In particular it has been utilized in descriptions of Hawaiian lava chemistry (Tilley & Scoon 1961, MacDonald and Katsura 1964), and the latter authors have proposed a distinction between tholeiitic and alkalic basalts based on this diagram. Schwarzer and Rogers (1974), have successfully used the plot in a comparison of

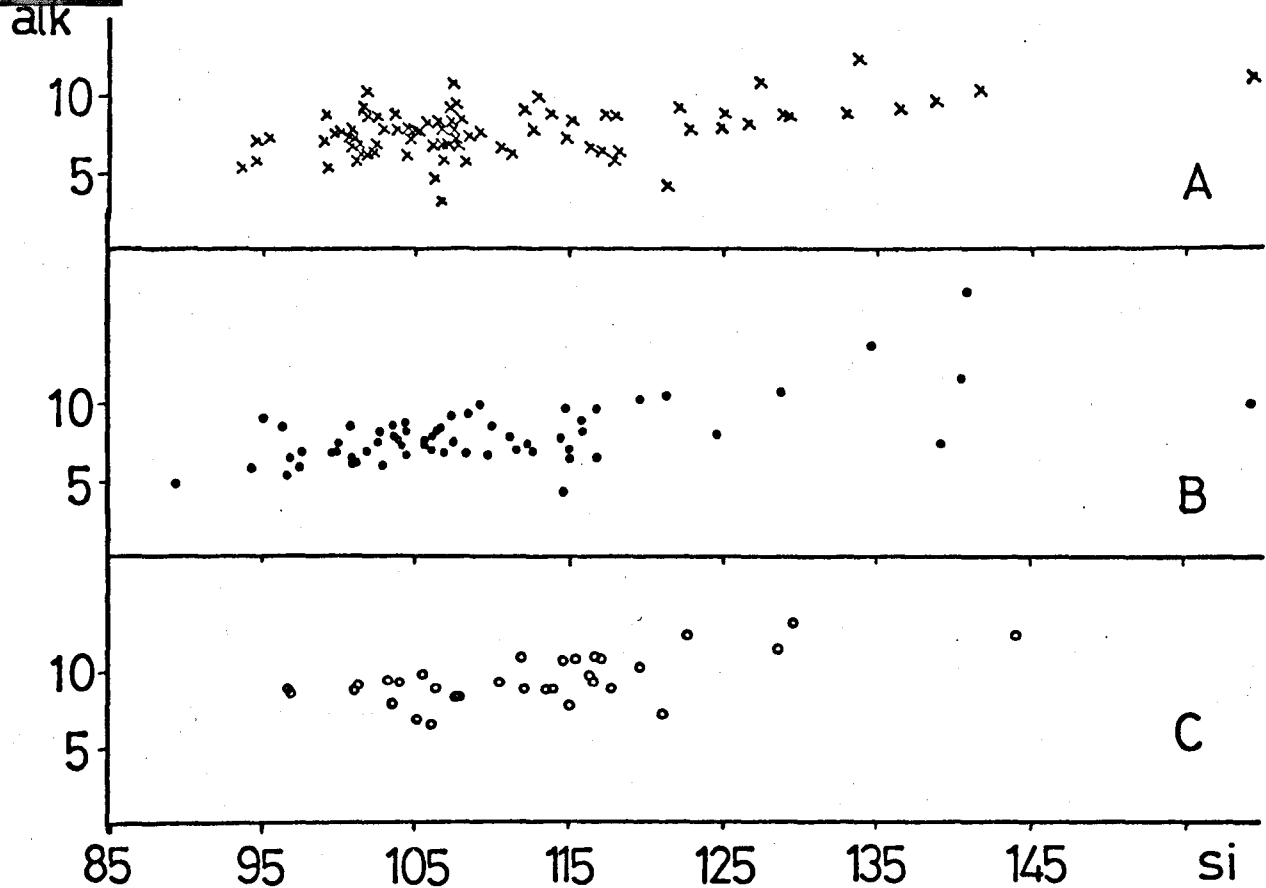


Figure 3.16: Niggli alk v si. Symbols as in figure 3.9.

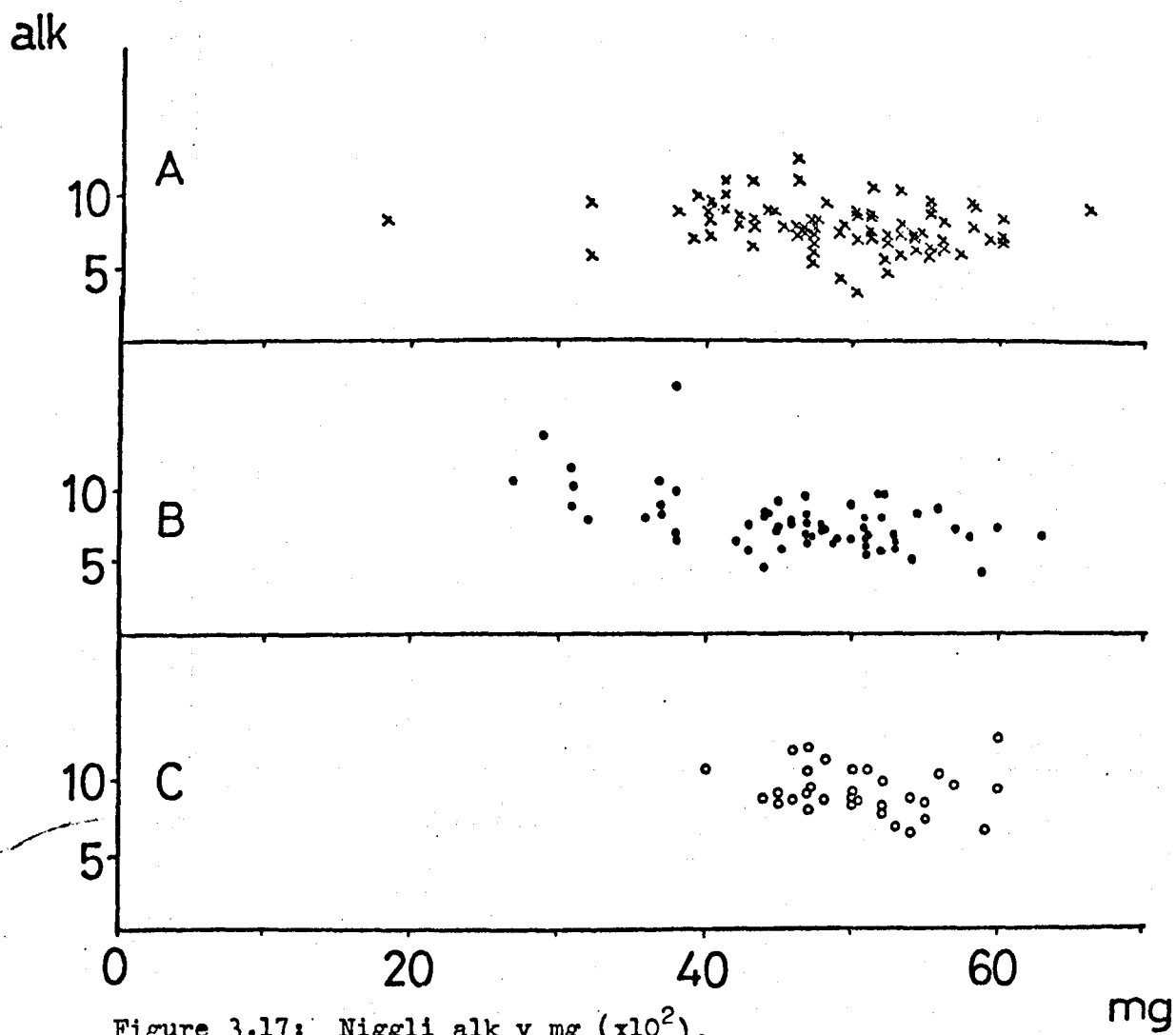


Figure 3.17: Niggli alk v mg ($\times 10^2$).

%K₂O

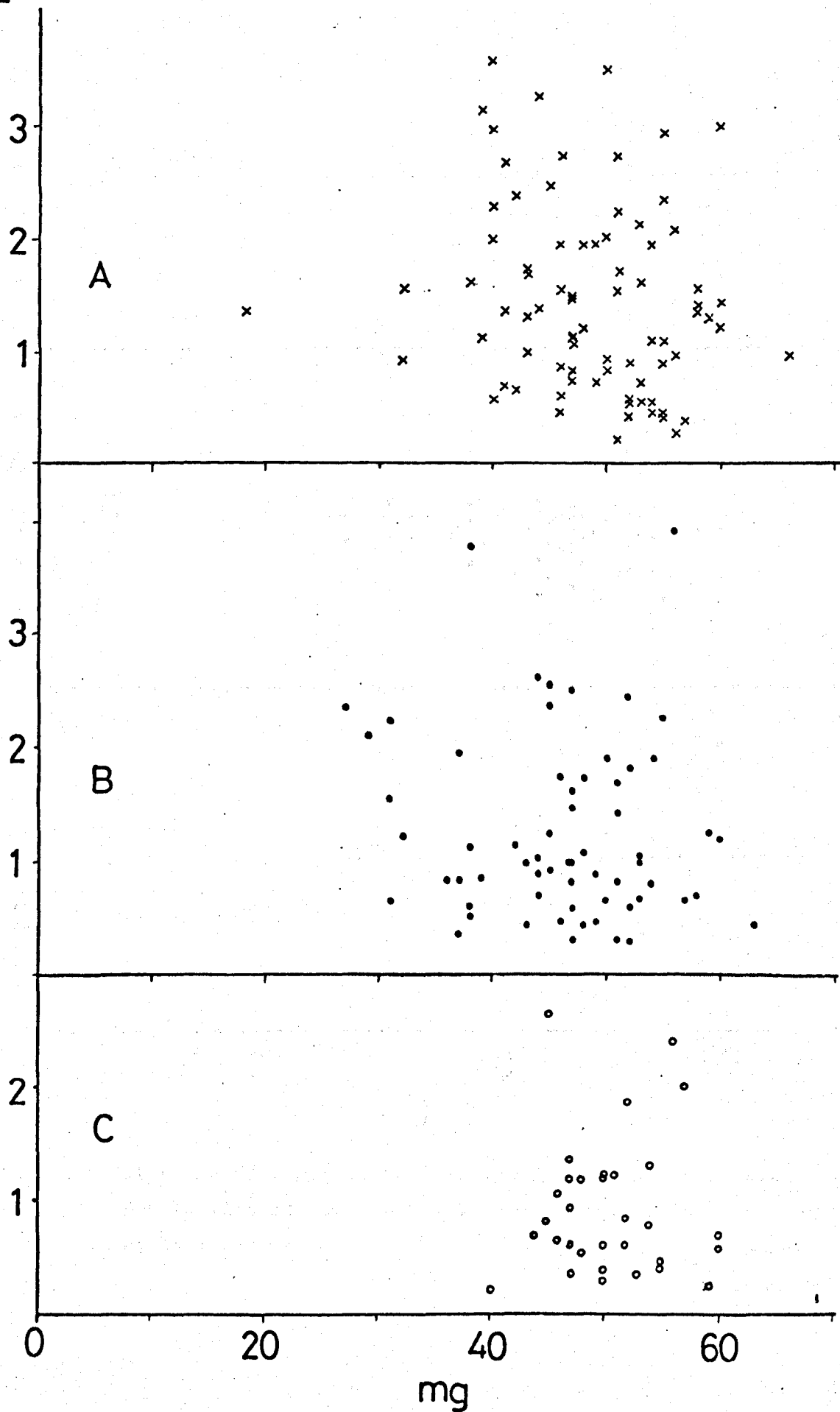


Figure 3.18: Norwegian metabasites: K₂O% v niggli mg (x10²)
Symbols as in figure 3.9.

%Na₂O

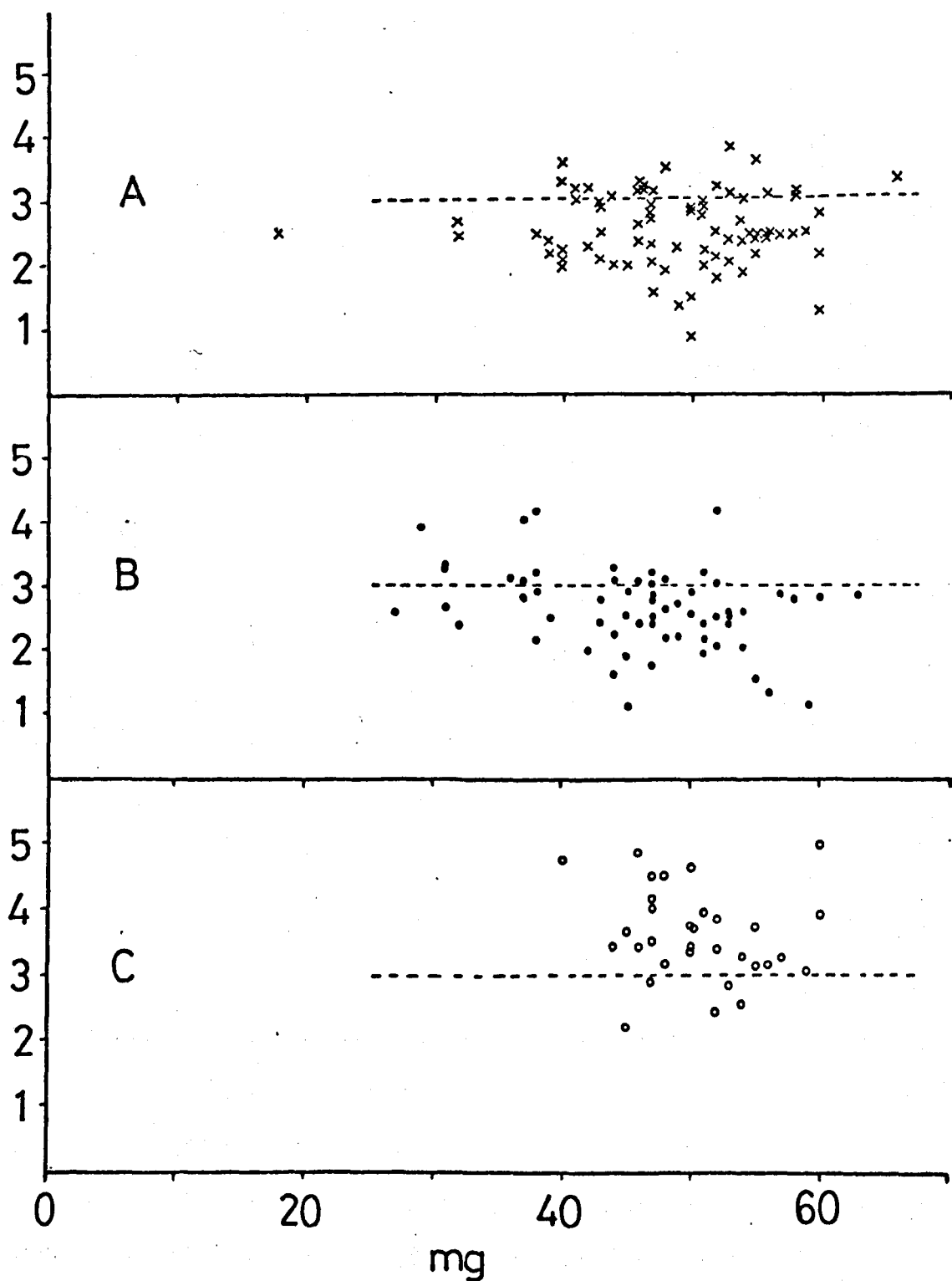


Figure 3.19: Na₂O% v niggli.mg ($\times 10^2$). Symbols as in figure 3.9. Broken line at 3.0% Na₂O illustrates high values in zone C metabasites.

alkalic basalts from several provinces. However, as Irvine and Baragar (1971) and Floyd and Winchester (1975) have pointed out, certain limitations apply to the diagram, particularly where alteration of the basalts has occurred. For example, the tholeiitic basalts from the Coppermine river area (Barager 1969) straddle the MacDonald and Katsura division. Thus, in examining metamorphosed basic rocks, the genetic implications of the diagram must be treated with caution, due to the possibility of alkali element redistribution already established.

Nearly 80% (139/176) of the South Norwegian metabasites plot on the alkalic side of the tholeiite-alkali basalt division. The 37 "tholeiitic" rocks are divided between the 3 zones, A, B and C as follows:-

Zone A: 20/82 samples (24%)

Zone B: 11/62 samples (18%)

Zone C: 5/32 samples (16%).

The unusual Na₂O distribution in the metabasites is also distinguished in the Na₂O-CaO scatter diagram (3.21). Whilst there is no major difference in the fields for zones A and B, the zone C metabasites partially separate out, to straddle the division used by Graham (1976a) to distinguish metabasites of a spilitic chemistry. The mean value for zone C lies exactly on this arbitrary division. Five zone B samples also cross the divide, though one (Spec. 750) only marginally. Of the remainder, one (7128) appears anomalous in containing large amounts of alteration, not visible in hand-specimen. It is perhaps

%Alk.

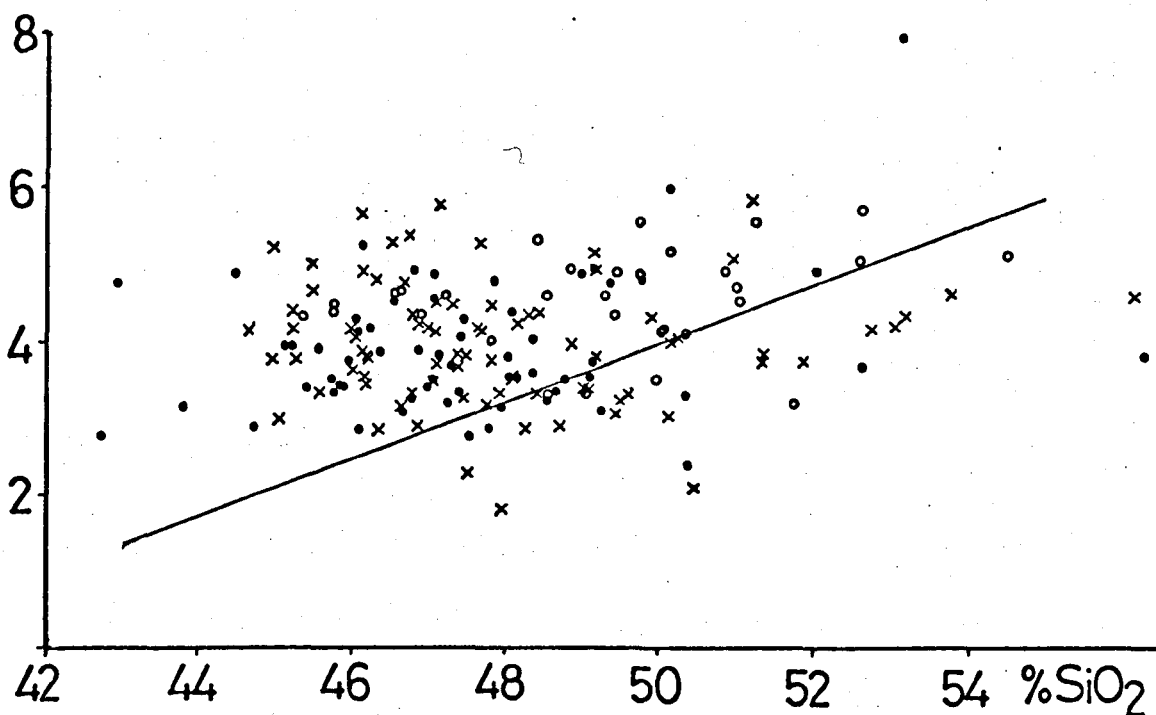


Figure 3.20: Total alkalis v SiO_2 . Symbols as in figure 3.9. The diagonal line is the alkalic-tholeiitic division of MacDonald & Katsura 1964, with the alkalic field above the line.

% Na_2O

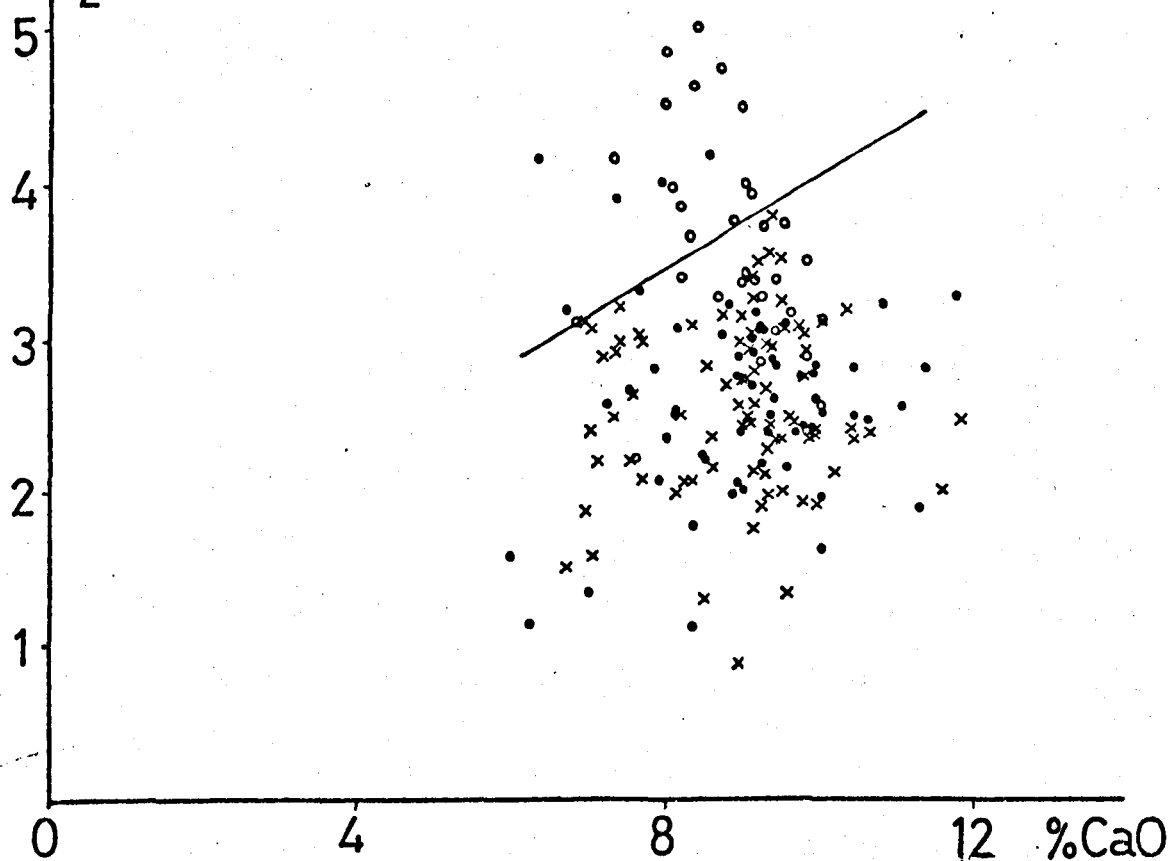


Figure 3.21: Na_2O v CaO . Diagonal line from Graham (1976). Symbols as in figure 3.9.

significant that 2 of the 3 remaining are samples from the mainland coast, and thus geographically very close to Tromøy (zone C).

The triangular $\text{CaO-Na}_2\text{O-K}_2\text{O}$ and normative Ab-An-Or diagrams also show these features (figures 3.22 - 3.24). In each case zone B sample 7128 plots well outside the normal field of variation (see note above). As shown in the schematic diagram (3.24) the zone C field of variation is clearly displaced to the Na_2O and Ab apices respectively. The small variations in mean chemistry for zones B and C can be attributed to the systematic K_2O variation between these mainland groups. It is the soda enhancement and not the lower K_2O of zone C which has the greater effect on the fields of chemical variation.

Pre-metamorphic variation in soda content in the terrain, perhaps associated with partial or complete spilitization (e.g. Smith 1968, Vallance 1969, Cann 1969) could provide a possible explanation for the Na_2O variation. However, strong evidence against this specific hypothesis is found when the geochemistry of other lithologies is considered. Independent work by Cooper (1971), and Cooper and Field (1977) has shown that the acid-intermediate charnockitic gneisses of Tromøy (zone C) are also significantly enriched in soda relative to the corresponding rock type on the mainland. (Field 1969, 1977 (in prep.); Beeson 1971, Field, Clough and Cooper (in prep.)). The $\text{Na}_2\text{O}/\text{CaO}$ and normative Ab/An ratios of the Tromøy gneisses are increased relative to the mainland and thus both the intrusive metabasites and their genetically divorced country rocks

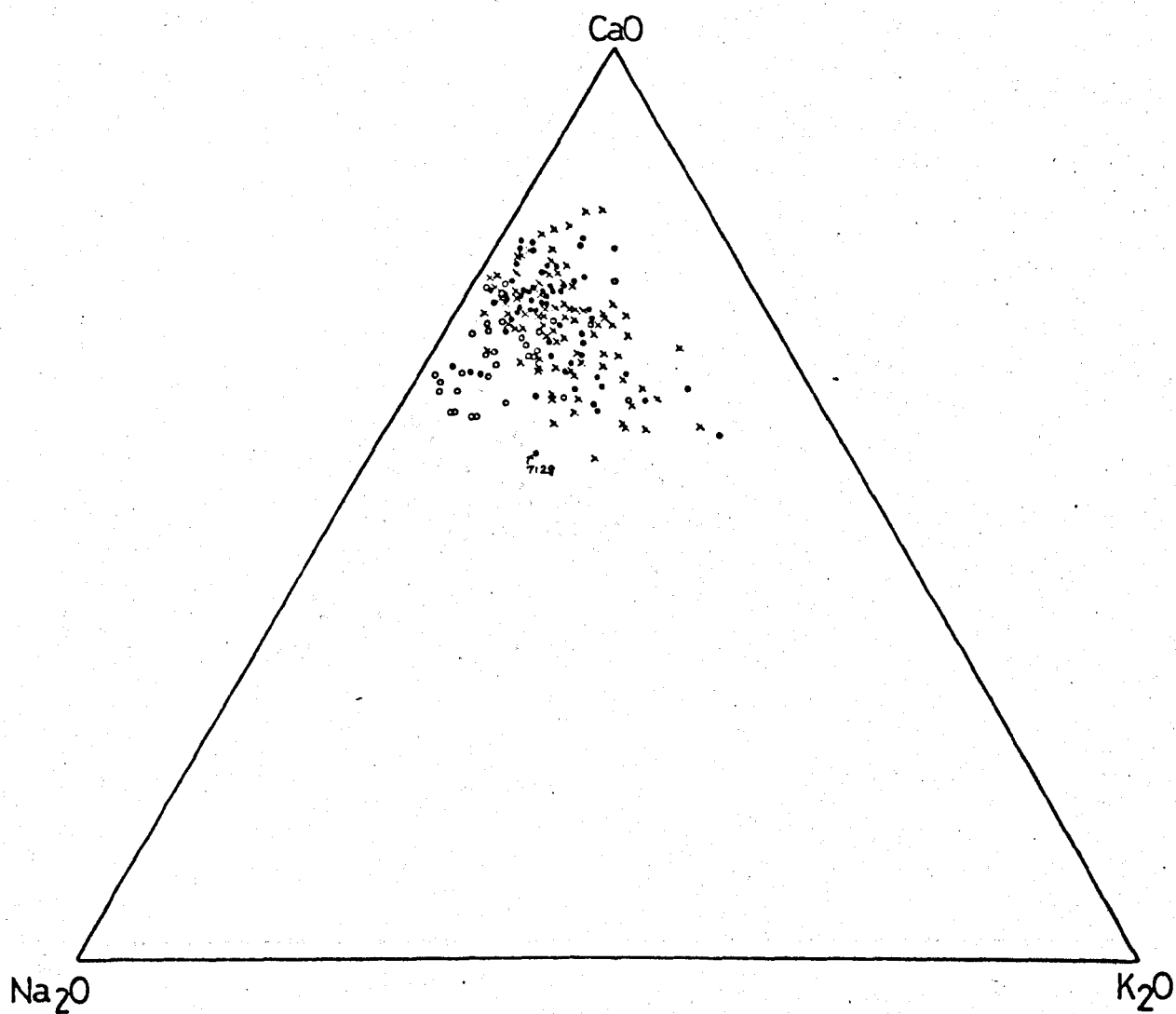


Figure 3.22: Ternary CaO-Na₂O-K₂O diagram. Data in wt.%. Symbols as in figure 3.9.

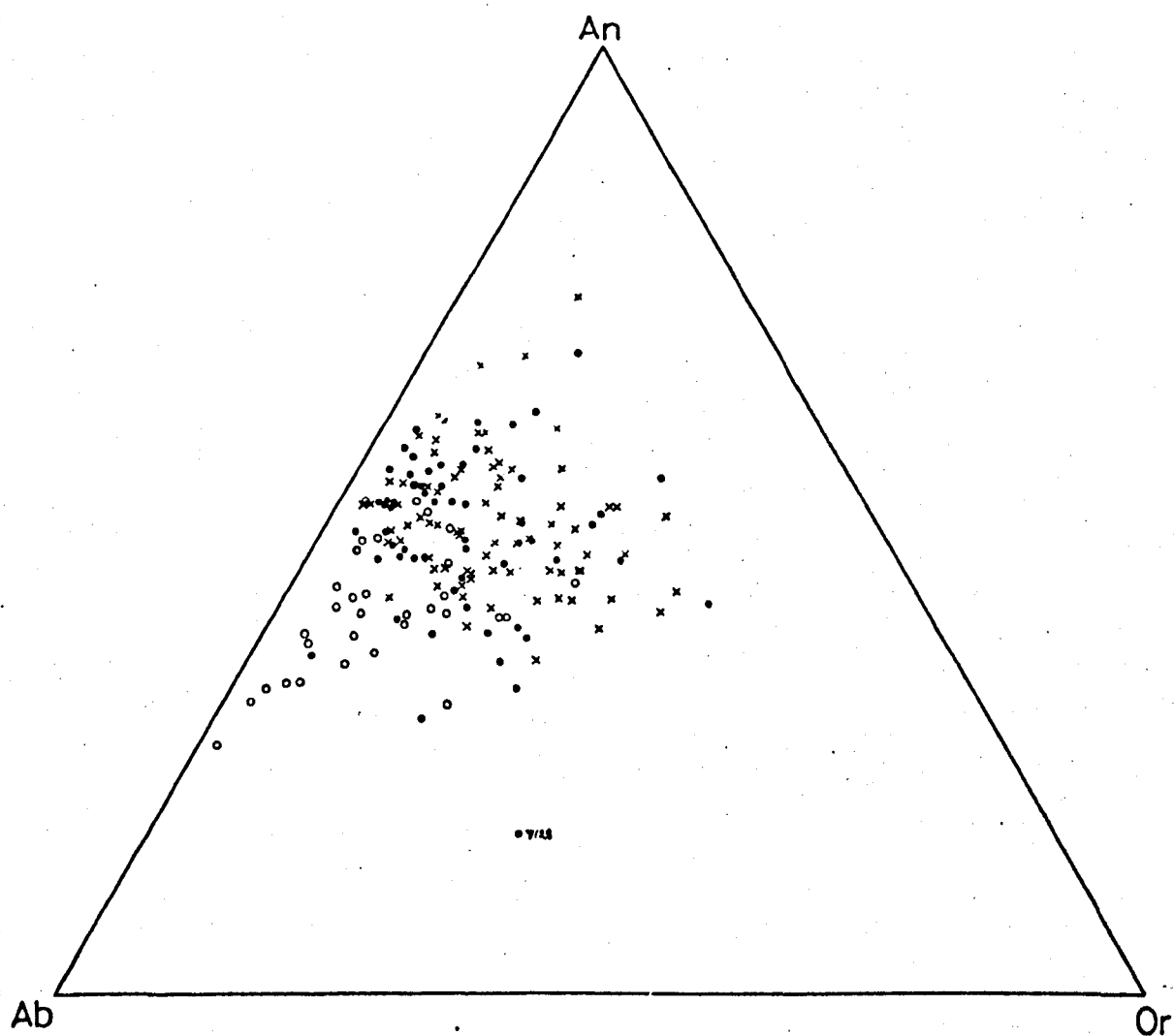


Figure 3.23: Ternary normative (An-Ab-Or) diagram. Symbols as in figure 3.9.

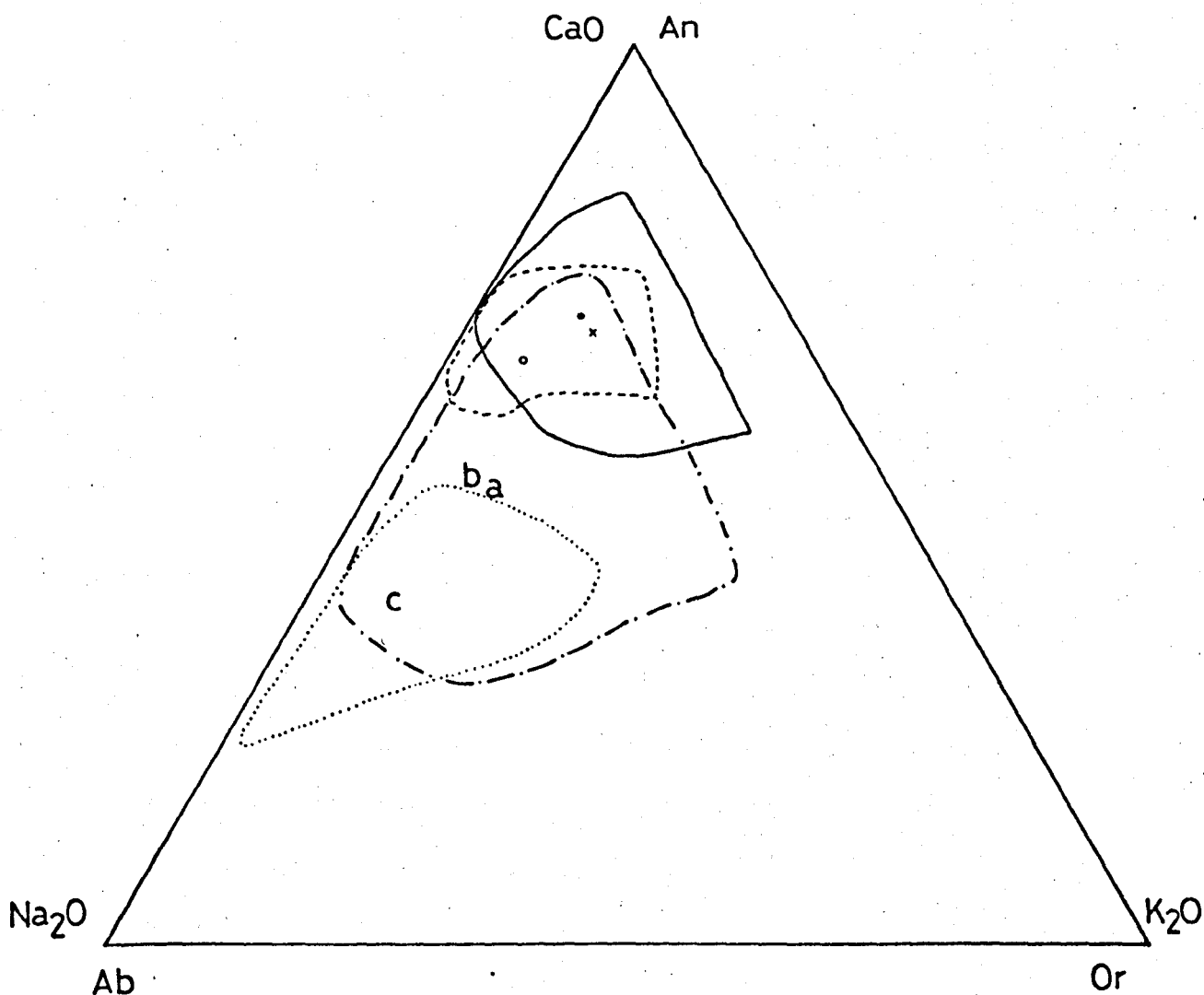


Figure 3.24: Schematic $\text{CaO-Na}_2\text{O-K}_2\text{O}$ and An-Ab-Or diagram:

$\text{CaO-Na}_2\text{O-K}_2\text{O}$: Solid line = field of variation for zones A + B; Dashed line = field for zone C. Cross = mean, zone A; closed circle = mean, zone B; open circle = mean, zone C.

An-Ab-Or: Dashed/dotted line = field of variation for zones A + B. Dotted line = field for zone C. a, b & c refer to the means for each zone.

show the same features of an enhancement of soda. This is possibly due to metasomatism (Cooper and Field, 1977), and the feature is discussed further later in the text (Chapter 7).

iv) The MgO-CaO-Al₂O₃ diagram.

This diagram has been applied by Viljoen and Viljoen (1969) and Viswanathan (1975) to distinguish highly primitive basaltic rocks with a komatiitic chemistry from other basaltic types. This is of particular interest in the present study due to the apparent association in India of rocks approaching basaltic komatiites with charnockites (Viswanathan 1975). However, despite a similar close association with charnockitic rocks in South Norway, none of the metabasites approach the komatiitic composition field in figure 3.25, and no rock has a low Al/Oa ratio characteristic of this primitive type. Since the CaO, MgO and Al₂O₃ abundance levels do not vary systematically through the three zones, A, B and C, it is unsurprising that no zonal separation of points occurs in figure 3.25.

F. Conclusions.

1. The vast majority of the metabasites are characterised by a major element chemistry which varies within the limits established by Manson (1967) for basalts. The normative parameters also suggest a wide range of basaltic chemistries is represented, but this may be due to secondary effects.
2. A zonal division of the metabasites shows that only K₂O of the major oxides varies systematically with metamorphic grade across the terrain. In other respects the chemistry of the mainland granulite facies samples is comparable with

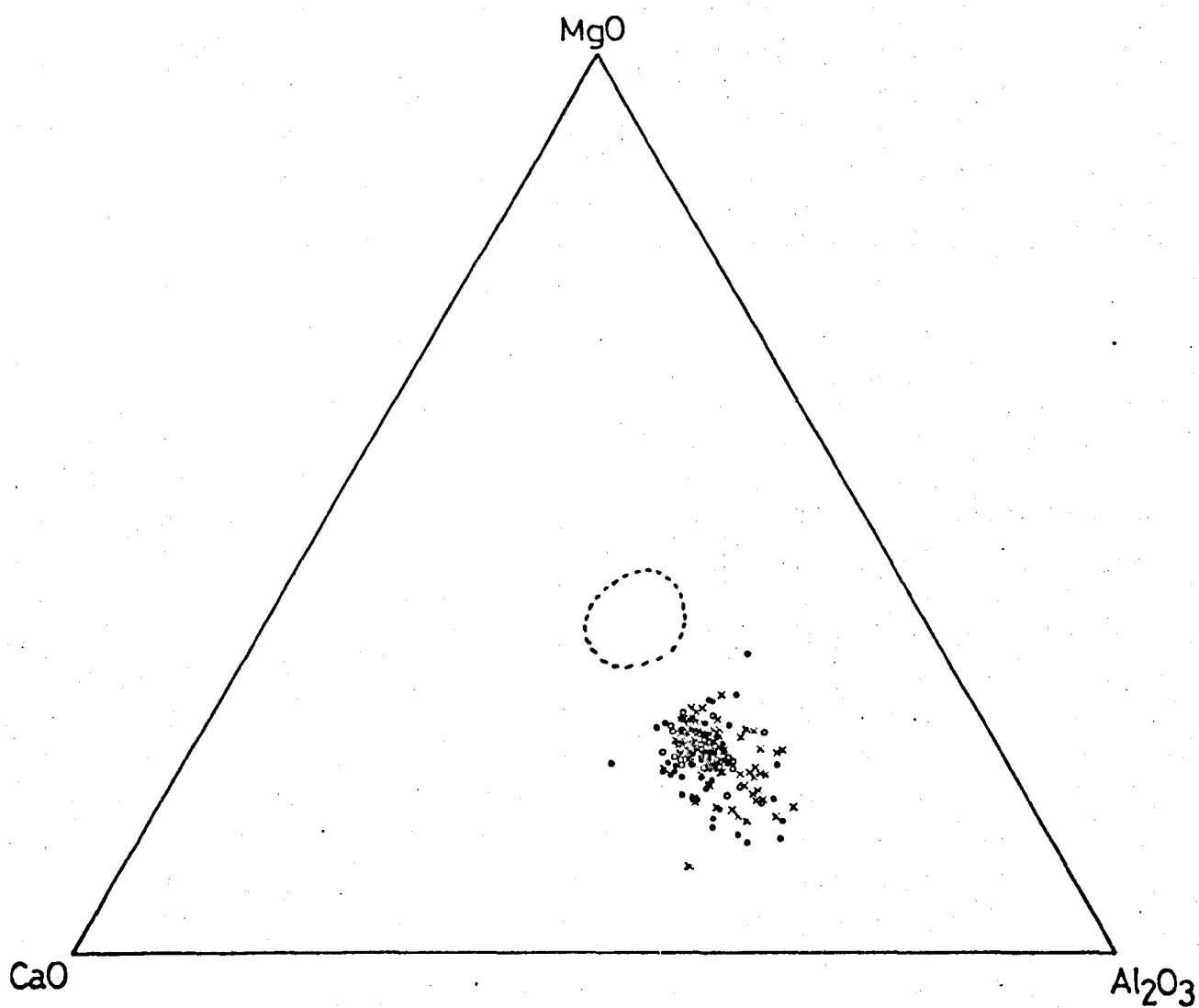


Figure 3.25: Ternary Al₂O₃-MgO-CaO diagram. Data in wt.%. Dashed line represents field of variation for rocks of komatiitic affinity.

that of the amphibolite facies.

3. The highest grade rocks (zone C) show chemical divergence from zones A and B: TiO_2 , P_2O_5 , H_2O and K_2O are lower; Na_2O , the oxidation ratio, and possibly MnO are higher. It is not clear from the overall major element chemistry whether these changes reflect original variation in (igneous) composition, or whether they occurred as a result of the metamorphism.
4. The metabasites display trends of major element variation analogous to differentiation trends in mafic igneous suites. The most notable features are strong enrichments in Fe, Ti and P. The zone C samples display limited Fe differentiation and this adequately explains the bulk chemical differences by zone in P_2O_5 and TiO_2 .
5. Variation diagrams do not adequately explain the present Na_2O and K_2O distributions in terms of original magmatic composition. The mg- K_2O diagram supports the concept of a systematic change in potash with metamorphic grade. There has also possibly been soda enhancement, focussed in zone C. High total alkalis are present throughout the suite.
6. The present major element chemistry does not clearly distinguish between an alkali basaltic or a tholeiitic source magma type for the metabasites.
7. None of the metabasites has a primitive komatiitic affinity.

Chapter 4: Trace Element Chemistry.

A. Introduction.

Prinz (1967) has recognised the difficulties in compiling representative average values for trace elements in rocks of basaltic composition. These include biased sample selection, with differentiates, accumulates, metamorphosed and altered rocks incorporated into estimates of basalts. Prinz (1967) remarks: "It is not uncommon to note dubious sample selection and unprecise definition of rock type in geochemical surveys with precise determinations". Additional factors affecting compilations of trace elements for comparison are non-representative areal sampling, and bias from samples with values below the detection limit. Consequently, Prinz suggests the median for quoting average values for trace elements in basalts.

In this chapter data for 13 elements (Sc, V, Cr, Co, Ni, Zn, Rb, Sr, Y, Ce, Ba, Zr and Nb) are presented. For the reasons outlined above, any comparison of the metabasite averages with basalts or metabasic analogues can only be an approximation, and these aspects of the data are therefore summarised briefly in the following text.

More detailed consideration is given to within-terrain trace element variation with respect to (a) the possible effects of primary igneous differentiation, and (b) the role of metamorphism in trace element fractionation/redistribution. This aspect of the study represents a contribution to the current ideas and debate concerning

possible element migrations under high-grade conditions. While it is well-recognised that alteration and low-grade metamorphism may lead to a redistribution of many elements (e.g. Vallance 1960, 1969; Matthews 1971, Hart 1969, 1970; Hart et al 1974), others (notably Ti, Zr, P, Nb and Y) are thought to be immobile (e.g. Pearce and Cann 1973), even under high-grades. Inter-element relationships concerning these "presumed mobile" and "presumed immobile" elements are also discussed in more detail in subsequent chapters.

All analyses were obtained using X-ray Fluorescence. The analytical details, accuracy and precision for trace elements are presented in Appendix 2 and the individual analyses are tabulated in Appendix 3.

B. Comparisons with Basalt and Metabasite trace element data.

The mean, median, maximum, minimum values and standard deviations for all analysed trace elements are presented in Table 4.1, while figures 4.1 to 4.4 are the corresponding histograms. No element follows a normal distribution, and notably asymmetric histograms occur for Rb, Ba, Y, Ce, Zr and Cr. All these elements have median values markedly lower than their arithmetic means.

A comparison of the metabasite trace element chemistry with selected data on basalts, including the data of Prinz (1967), is given in Table 4.2. Median values where available are quoted in parentheses. The metabasite data are broadly consistent with basaltic estimates, and there are no obviously anomalous mean/median differences.

TABLE 4.1

Summary trace element data for South Norwegian metabasites.
(n = 176).

Element	1.	2.	3.	4.	5.
Sc	42	42	85	18	8
V	295	296	1361	25	131
Cr	120	107	469	6	78
Co	47	47	86	5	15
Ni	84	84	205	14	37
Zn	140	116	924	4	110
Rb	41	20	225	1	44
Sr	198	195	437	10	83
Y	22	20	98	4	13
Ba*	212	170	1074	0 *	171
Ce*	44	35	214	0 *	32
Zr	147	110	976	22	130
Nb	14	13	67	5	7

1. = Mean.

2. = Median.

3. = Maximum.

4. = Minimum.

5. = Standard deviation.

* = Samples with values below detection limit included.

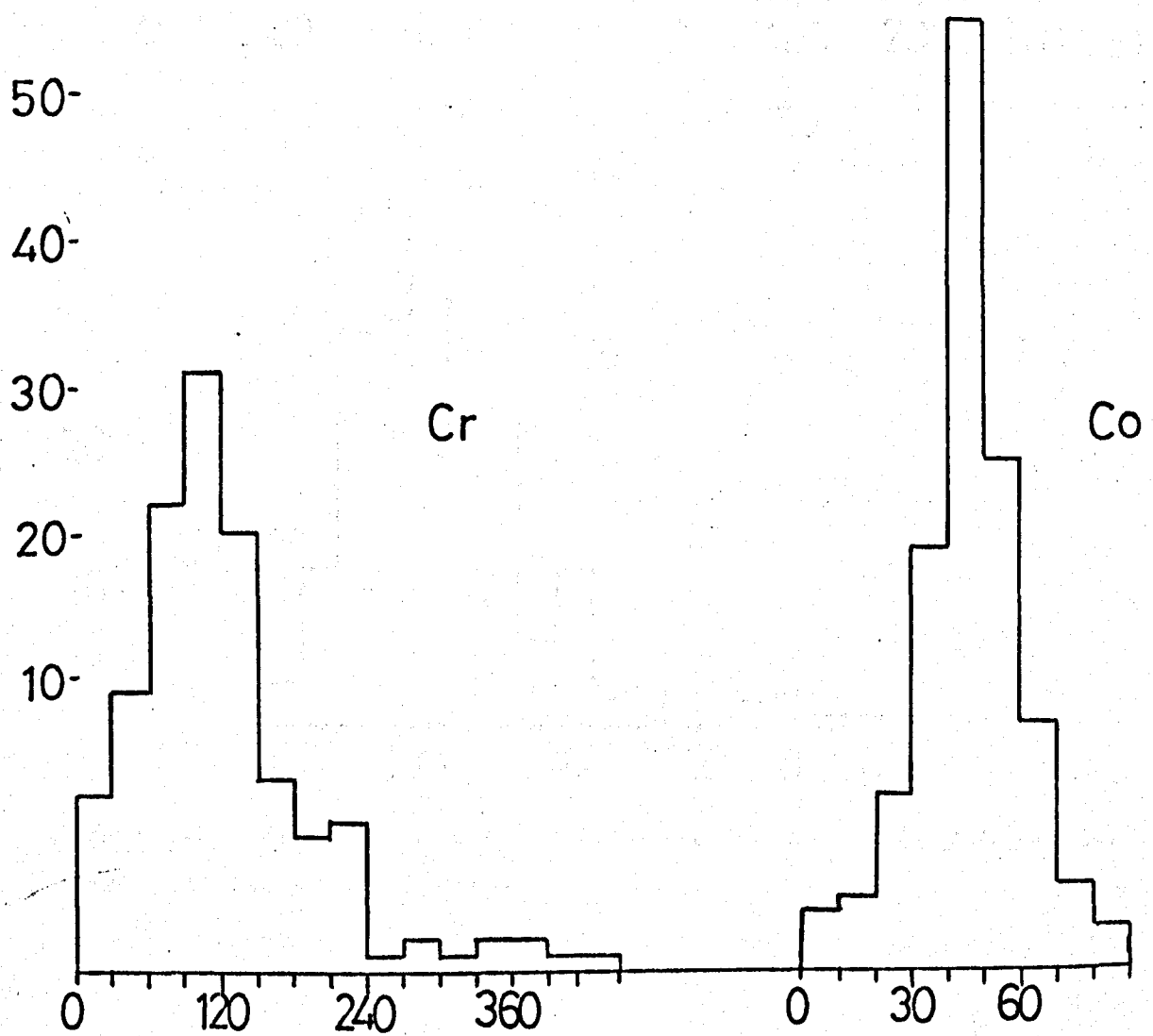
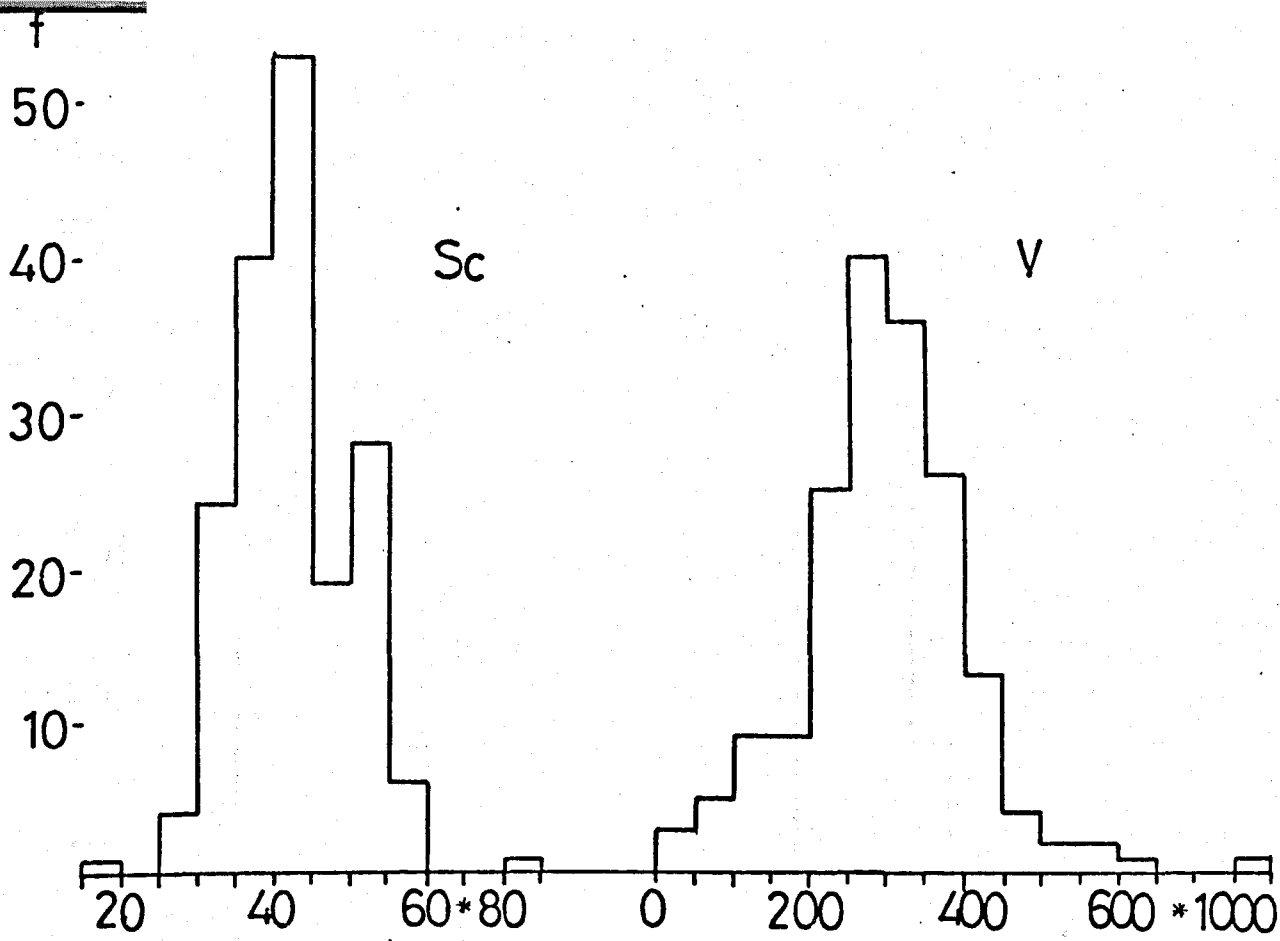


Figure 4.1: Frequency histograms for Sc,V,Cr and Co (p.p.m.). * Sc,V scales non-linear at high values.

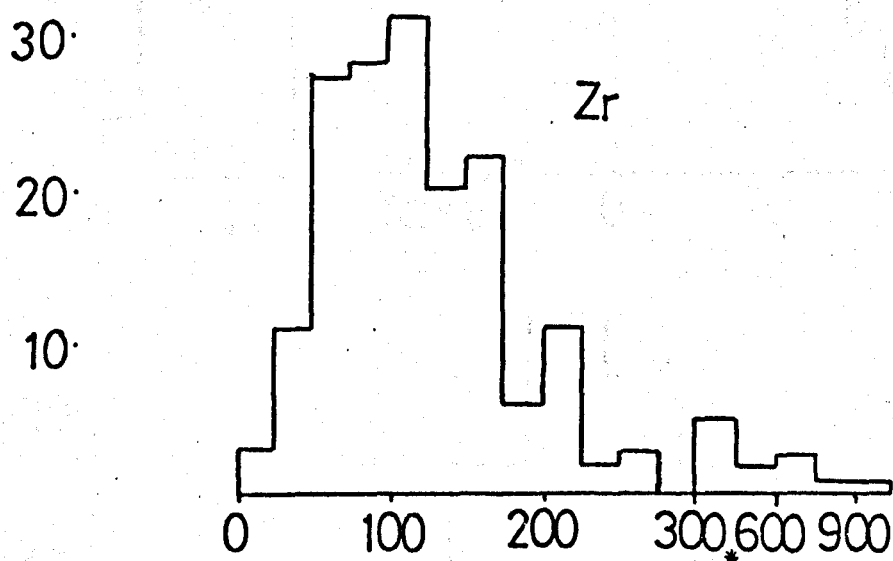
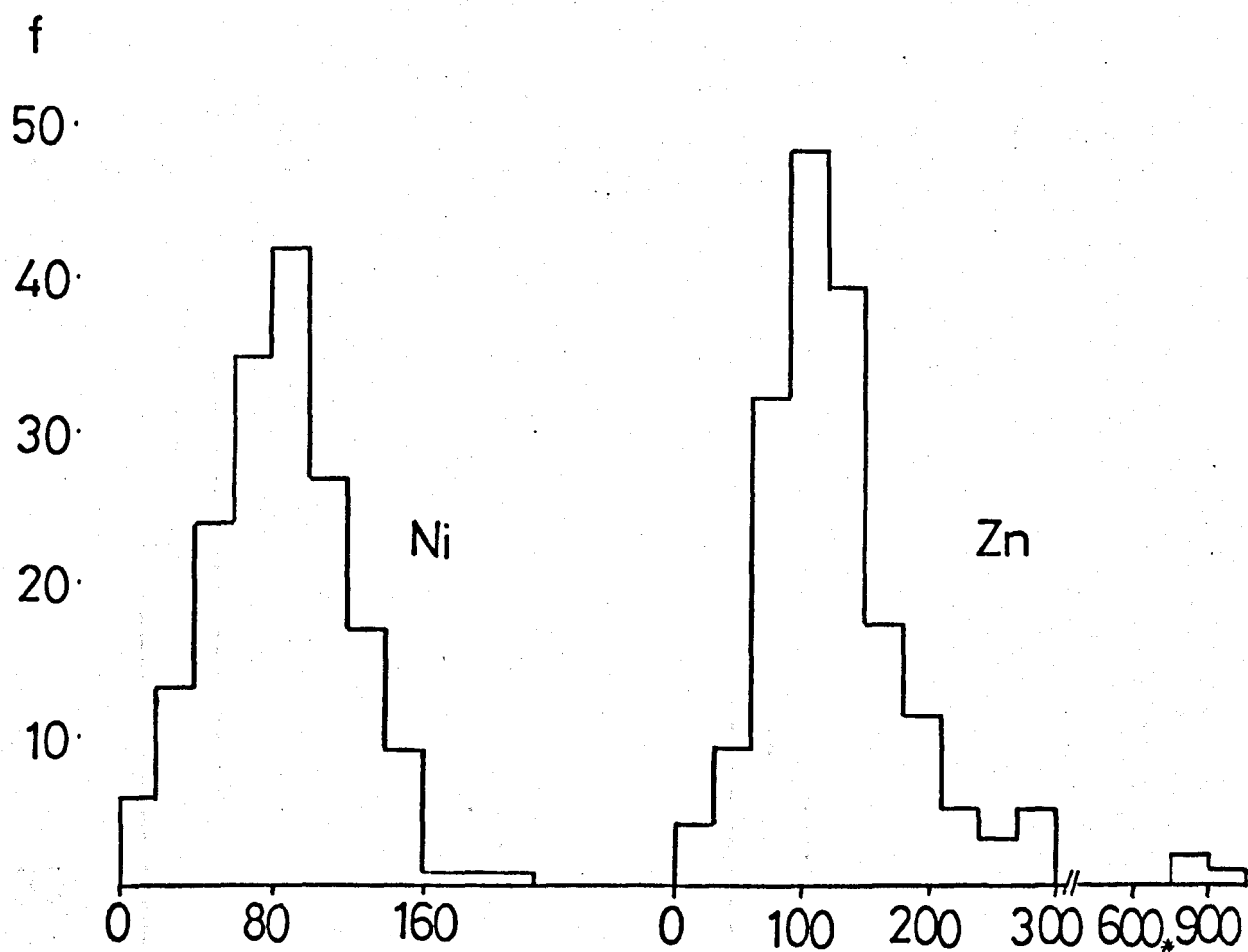
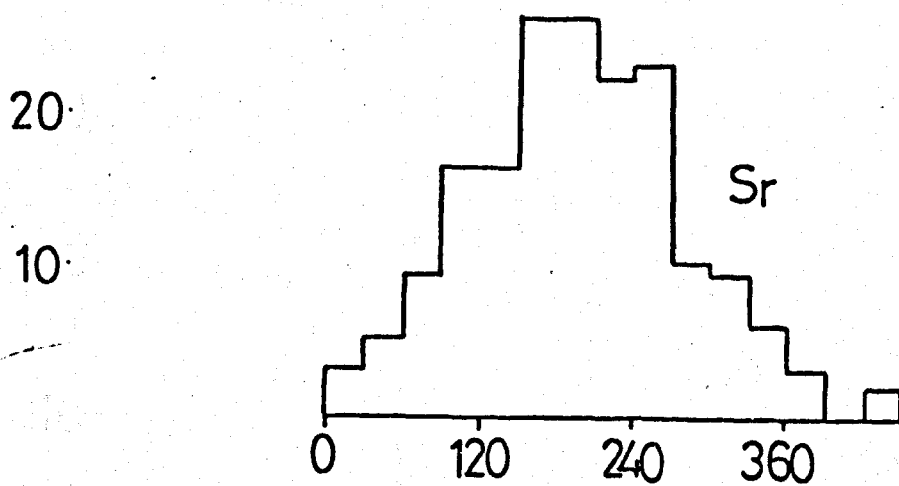
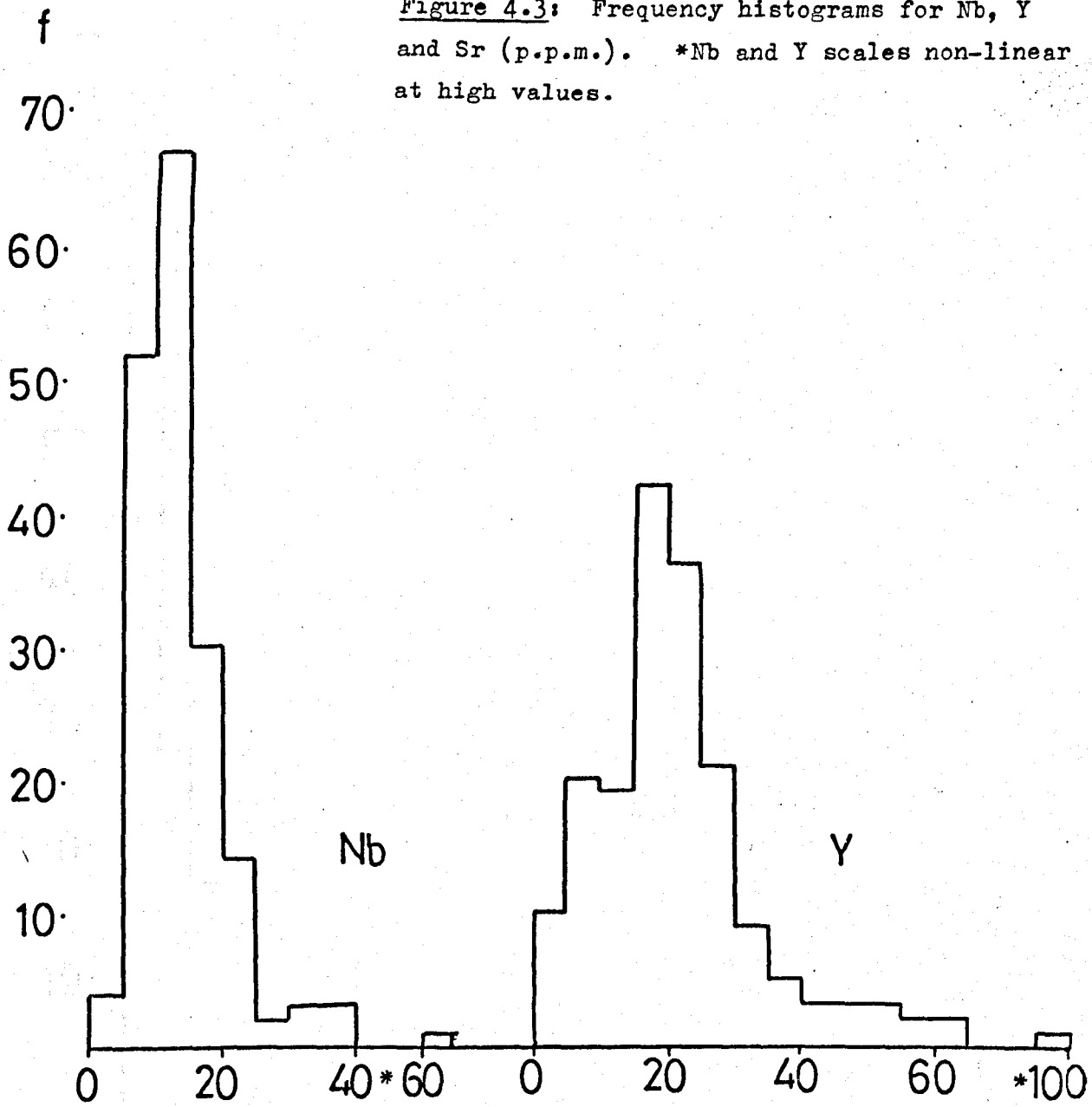
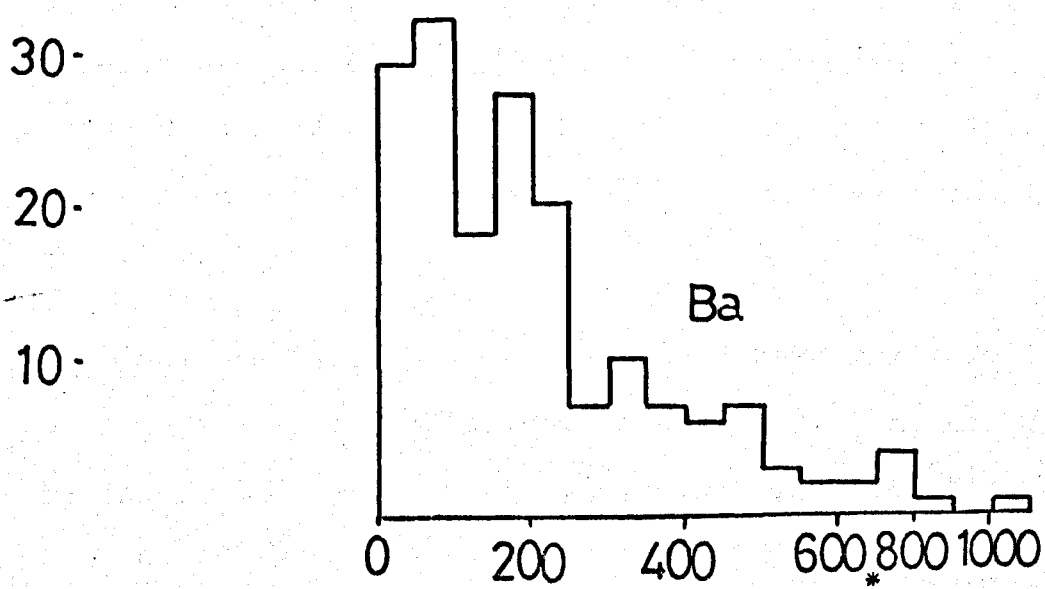
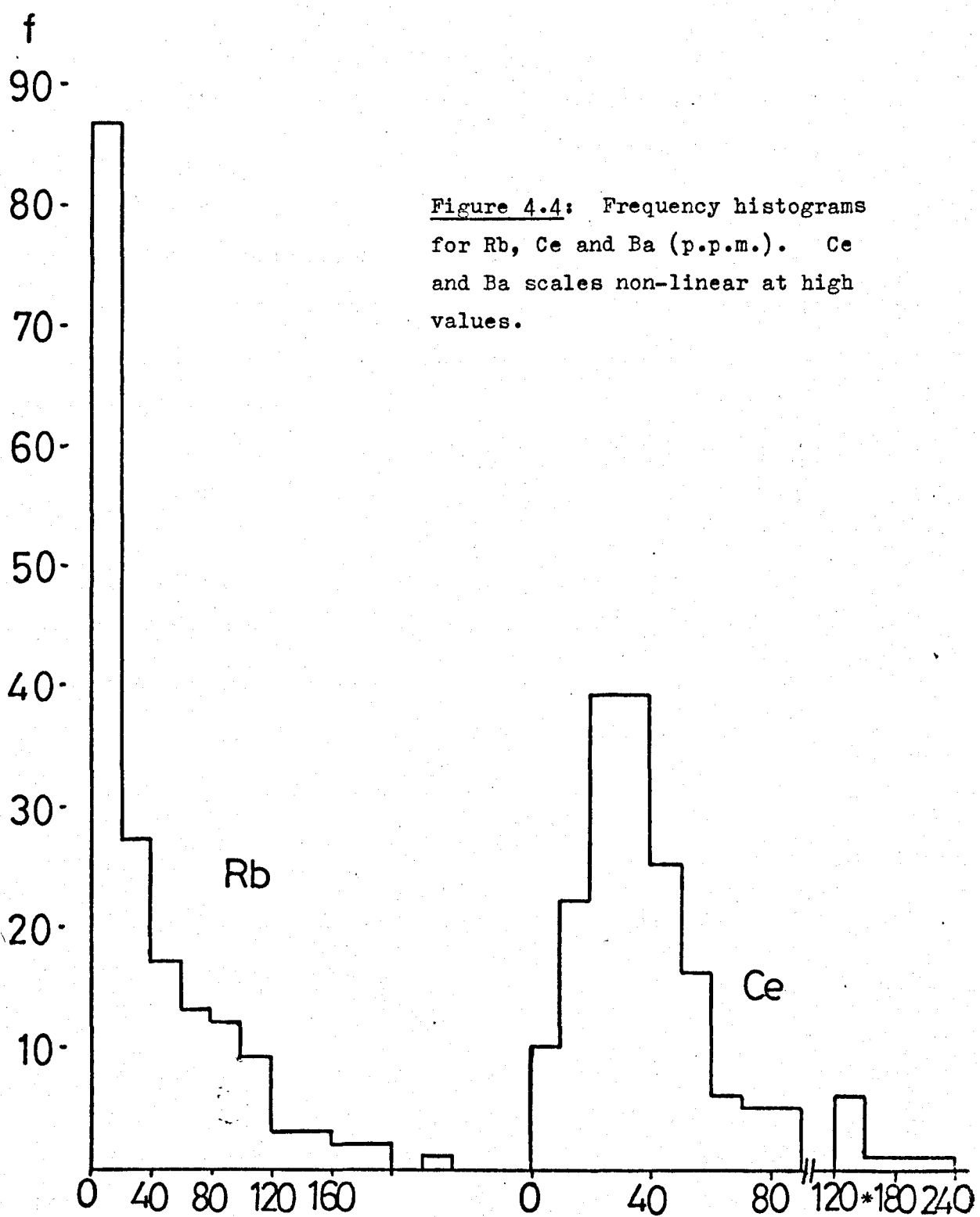


Figure 4.2: Frequency histograms for Ni, Zn, and Zr (p.p.m.). *Zn, Zr scales non-linear at high values.

Figure 4.3: Frequency histograms for Nb, Y and Sr (p.p.m.). *Nb and Y scales non-linear at high values.





Compared with the Nuanetsi basalts (Cox et al 1967), the metabasites are relatively low in the "incompatible" elements. However, the abundance levels are higher than the levels found in the primitive Baffin bay tholeiites (Clarke 1970), and Rb in particular is high in the metabasites relative to most tholeiite estimates. The mean value corresponds to Prinz'(1967) value for alkalic basalt. Of the transition metals, Cr is slightly low in the metabasite suite.

Table 4.3 is a comparison with recently published metabasic analogues and again, there is no major discordance in abundance levels.

C. Intra-terrain trace element variation.

(i) Zone A v. Zone B.

The summary data for trace element abundance levels by individual zones are presented in Table 4.4. As with major elements, there is no marked variation between zones A and B for most elements.

Ce, Zr, and to a lesser degree Y, are all higher in zone B when means are compared, but these differences are reduced by considering the median values. As figures 4.5 and 4.6 indicate, the differences in the means between zones A and B for these 3 elements largely reflect a small number of high values in the mainland granulite zone.

Rb, however, shows a clear increase from zone B to zone A in both median and mean values. The histograms in figure 4.7 are used for comparison in view of the pronounced asymmetry of the distributions. A systematic

TABLE 4.2

Comparison of mean trace element abundances for metabasites
with published values for basalts.

Element	1.	2.	3.	4.	5.	6.	7.
Sc	42 (42)	*31 (30)	*20 (15)	66		35	
V	295 (296)	251 (245)	236 (225)	615		260	
Cr	120 (107)	*160 (142)	*168 (140)	193		391	
Co	47 (47)	39 (40)	42 (40)	41		34	
Ni	84 (84)	*84 (75)	*98 (80)	84		323	
Zn	140 (116)			154			
Rb	41 (20)	*17 (5)	*41 (30)		2.5	50-110	
Sr	198 (195)	450 (400)	774 (700)	267	170	823	
Y	22 (20)	*30 (25)	*25 (25)	53	18	35	27
Ba	212 (170)	244 (200)	444 (400)	615	59	746	
Ce	44 (35)						59
Zr	147 (110)	108 (100)	138 (125)	352	69	224	
Nb	14 (13)					48	

All values are p.p.m.; figures in parentheses are median values.

1. = South Norwegian metabasites (n = 176).

2. = 'All tholeiitic basalts') Prinz (1967, Table II). *denotes the
 3. = 'All alkalic basalts') arithmetic mean includes values of
) zero for analyses below the level of
 sensitivity.

4. = 163 tholeiites; Coppermine river basalts (Barager 1969).

5. = 48 olivine tholeiites, Baffin Bay. (Clarke 1970).

6. = Nuanetsi basalts (Karoo). Cox et al. 1967).

7. = '282 Continental basalts' (Frey et al. 1968).

TABLE 4.3

Comparison of mean trace element abundances for metabasites
with means for analogues in different terrains.

Element	1.	2.	3.	4.	5.	6.
Sc	42 (42)	61	69			
V	295 (296)	396	282			
Cr	120 (107)	480	111	223	230	132 (126)
Co	47 (47)	60	39			92 (95)
Ni	84 (84)	147	75	118	94	106 (117)
Zn	140 (116)	104				169 (162)
Rb	41 (20)	85 (36)	21	30	8	11 (5)
Sr	198 (195)	188	243	151	215	366 (320)
Y	22 (20)	28	41	23	21	33 (24)
Ba	212 (170)	443 (105)	284	273	208	305 (242)
Ce	44 (35)	83		21	20	57 (45)
Zr	147 (110)	112	136	89	89	381 (276)
Nb	14 (13)	<2 - 18		7	5	28 (24)

All values are p.p.m.; figures in parentheses are median values.

1. = South Norwegian metabasites. (n = 176).

2. = Beartooth Mountains amphibolites. (van de Kamp 1969).

3. = Amphibolites, Mainland Lewisian. (Park 1966).

4. = 32 amphibolites) Lewisian, Inner Hebrides

5. = 9 'basic granulites') (Drury 1974).

6. = 31 Tayvallich 'epidiorites'. (Wilson and Leake 1972).

TABLE 4.4

Intra-terrain trace element variation for South Norwegian Metabasites.

Element	Zone			
	A	B	C	A+B
Sc	41 (40)	40 (40)	47 (48)	41 (40)
V	297 (294)	276 (278)	329 (333)	288 (287)
Cr	125 (108)	114 (103)	121 (125)	120 (107)
Co	47 (46)	46 (48)	46 (47)	47 (47)
Ni	89 (87)	85 (88)	66 (66)	88 (88)
Zn	135 (112)	128 (110)	172 (169)	131 (111)
Rb	52 (33)	41 (20)	16 (7)	
Sr	202 (193)	209 (215)	167 (142)	205 (202)
Y	20 (19)	26 (23)	19 (17)	23 (21)
Ba	241 (190)	254 (193)	108 (59)	247 (190)
Ce	38 (33)	58 (38)	32 (30)	47 (34)
Zr	126 (116)	208 (142)	79 (77)	162 (130)
Nb	13 (13)	16 (14)	12 (12)	15 (13)
n	82	62	32	144

Mean values; figures in parentheses are medians; all values in p.p.m.

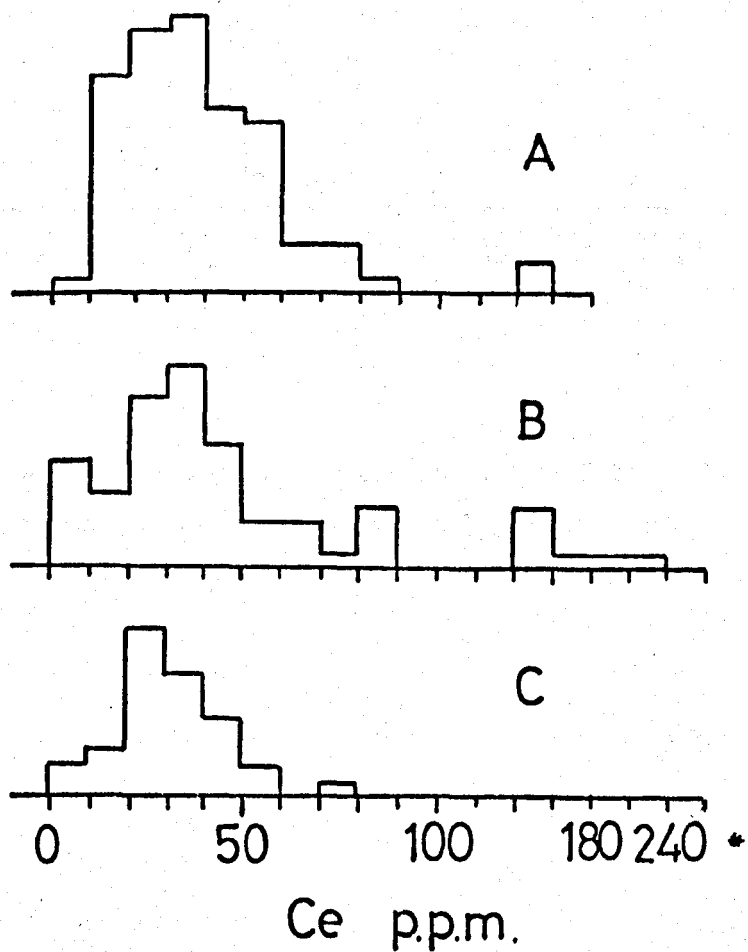
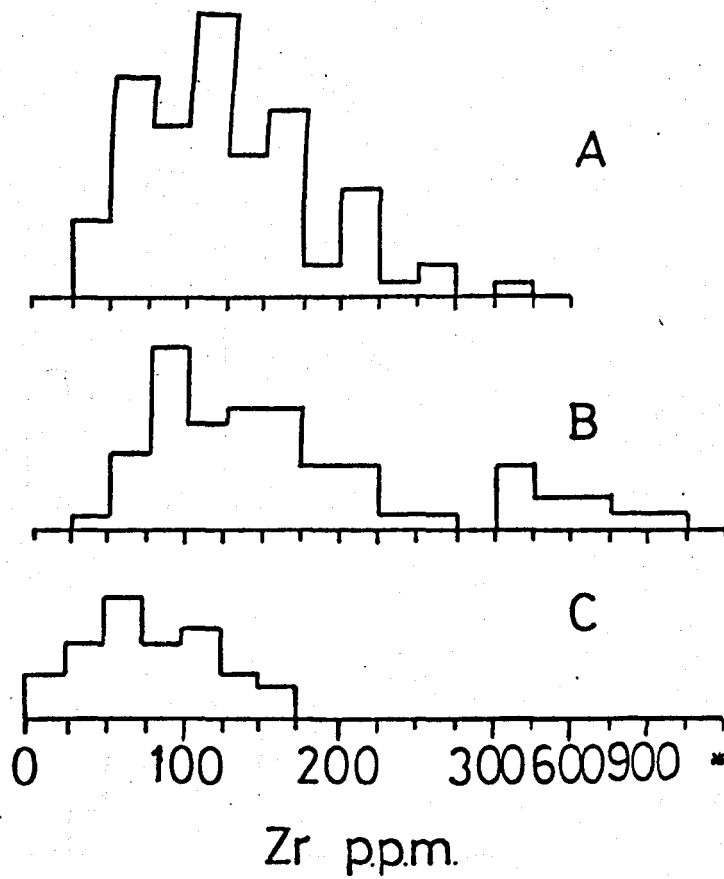


Figure 4.5: Frequency histograms for Zr and Ce by metamorphic zone (A,B and C). *Scales non-linear at high values.

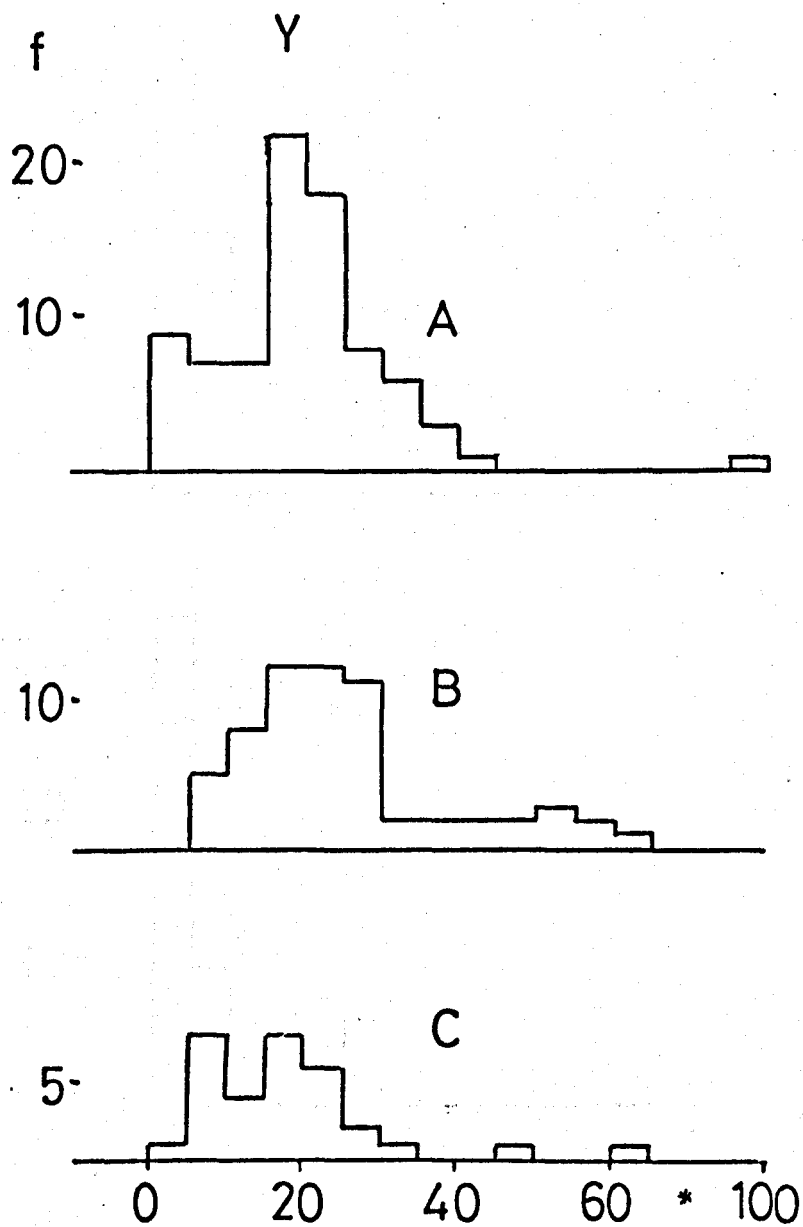


Figure 4.6: Frequency histograms for Y by metamorphic zone (A,B and C). Scale is non-linear at high values.

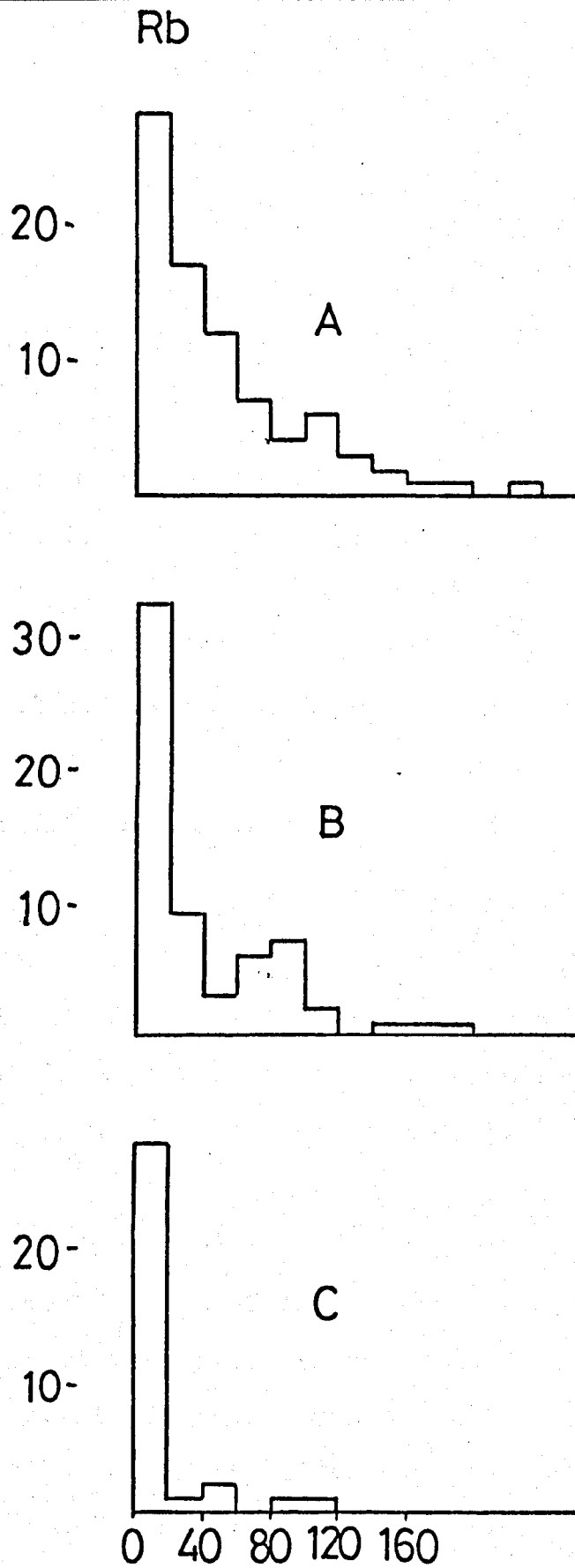


Figure 4.7: Frequency histograms for Rb p.p.m. by zone (A,B and C).

variation in Rb abundance according to metamorphic grade is not unexpected in view of the result for K₂O (Chapter 3), and the well-known diadochic relationship of these two elements (e.g. Ahrens et al, 1952).

With the exception of Rb, therefore, the trace element data for the two zones A and B has been combined as a broad expression of abundance levels on the mainland. (Column 4, table 4.4). This facilitates overall comparison with zone C, the Tromøy metabasites.

ii) Zone C v zones (A+B).

It is clear that zone C is characterised by lower abundances of Zr, Rb, Ba, Ni and probably Sr than the mainland. Zn appears to be increased in zone C (table 4.4). These changes are also shown by the zonal histograms, (figures 4.5, 4.7-4.9).

D. The Transition Metals.

The geochemistry of the transition metals which normally occur in trace quantities in the crust is complex and interesting. An important consideration in their geochemical affinities is crystal field theory (Burns 1970), the effects of which on certain trace element distributions are not fully documented. A brief summary of some of the problems of transition metal geochemistry is included in Lambert et al (1976, p.381).

(i) Vanadium, Cobalt, Chromium and Nickel.

The relationship of these four transition

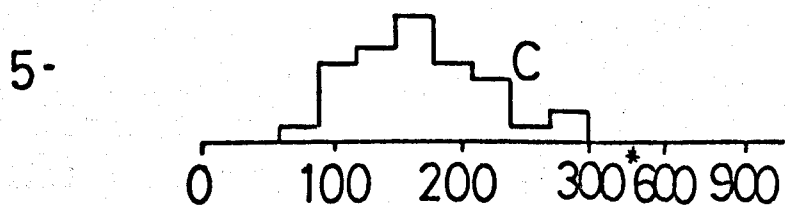
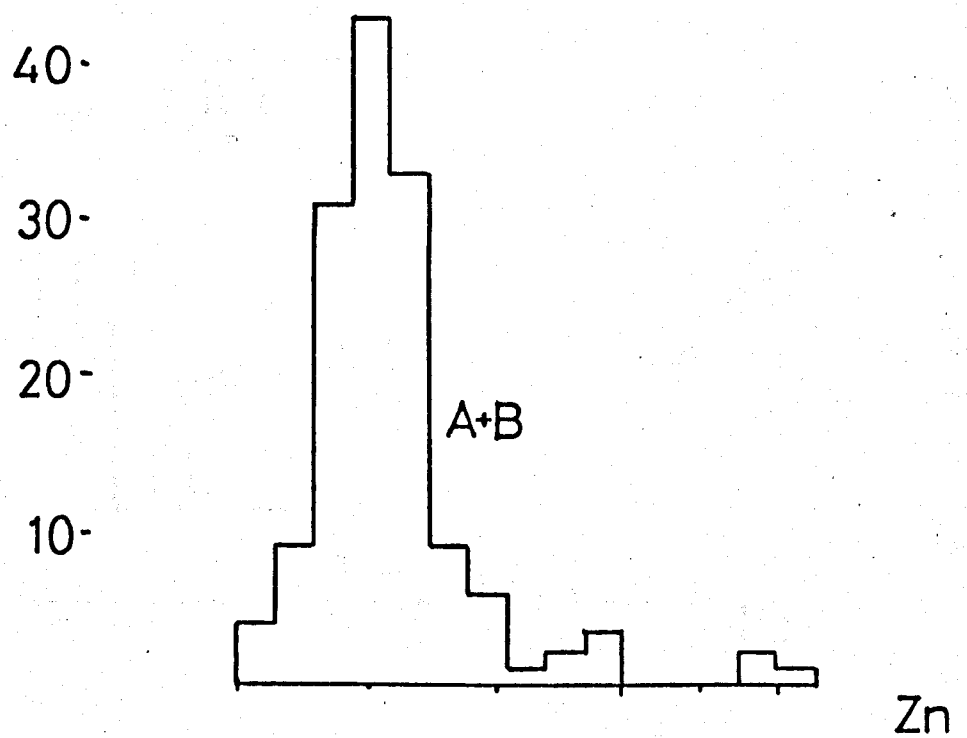
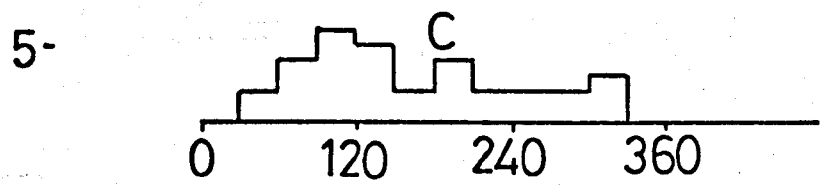
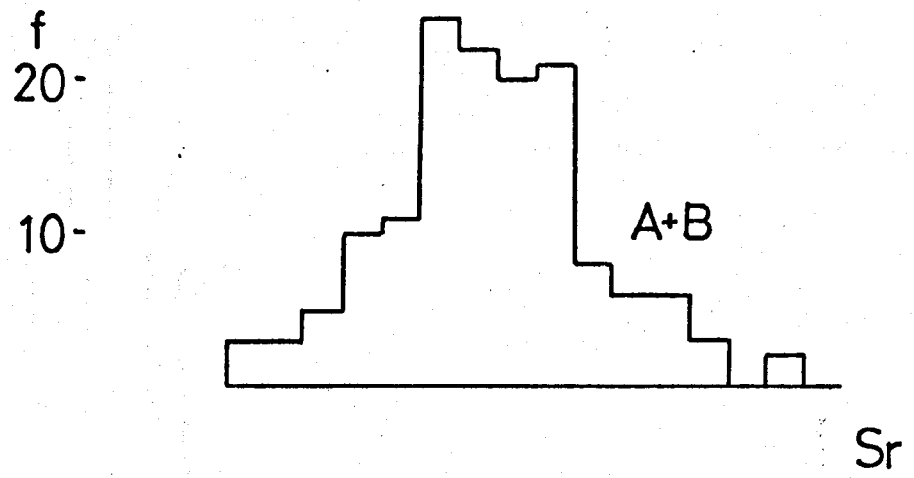


Figure 4.8: Zonal variation in Zn and Sr by histograms. Zn scale is non-linear at high values.

f

40.

30.

20.

10.

Figure 4.9: Zonal variation in
Ni and Ba by histograms. Ba
scale non-linear at high values.

A+B

Ni

C

0 80 160

A+B

Ba

C

0 200 400 600 * 1000

metals to the differentiation index, niggli mg, is presented in figures 4.10 to 4.12. Each zone (A, B and C) is plotted separately, and it should again be noted that mg is much less variable in zone C than in the two mainland zones. Zone B (Mainland granulite facies) shows proportionately the largest number of highly evolved, Fe-rich, Mg-poor samples.

mg-V and mg-Co. (4.10, 4.11)

The characteristics of these two scatter plots are very similar, and they may be summarised together. For each element in each zonal division, there is a random relationship for samples with mg greater than ca 0.40. The iron-rich differentiates however show quite sharp declines in both elements, and these effects are particularly well seen in the zone B plots.

mg-Cr and mg-Ni (4.12).

There are overall general trends to decreases in Cr and Ni with declining mg (and increased Fe). As for V and Co, the decreases are particularly visible in the extreme differentiates, but with Cr and Ni there is also a trend visible throughout the span of mg values. The trends are similar in all three metamorphic zones, but the Ni abundance level in zone C is anomalously low, particularly when the high range of mg values in that zone is considered.

The overall behaviour of Cr, Co and Ni with respect to the differentiation index is consistent with their

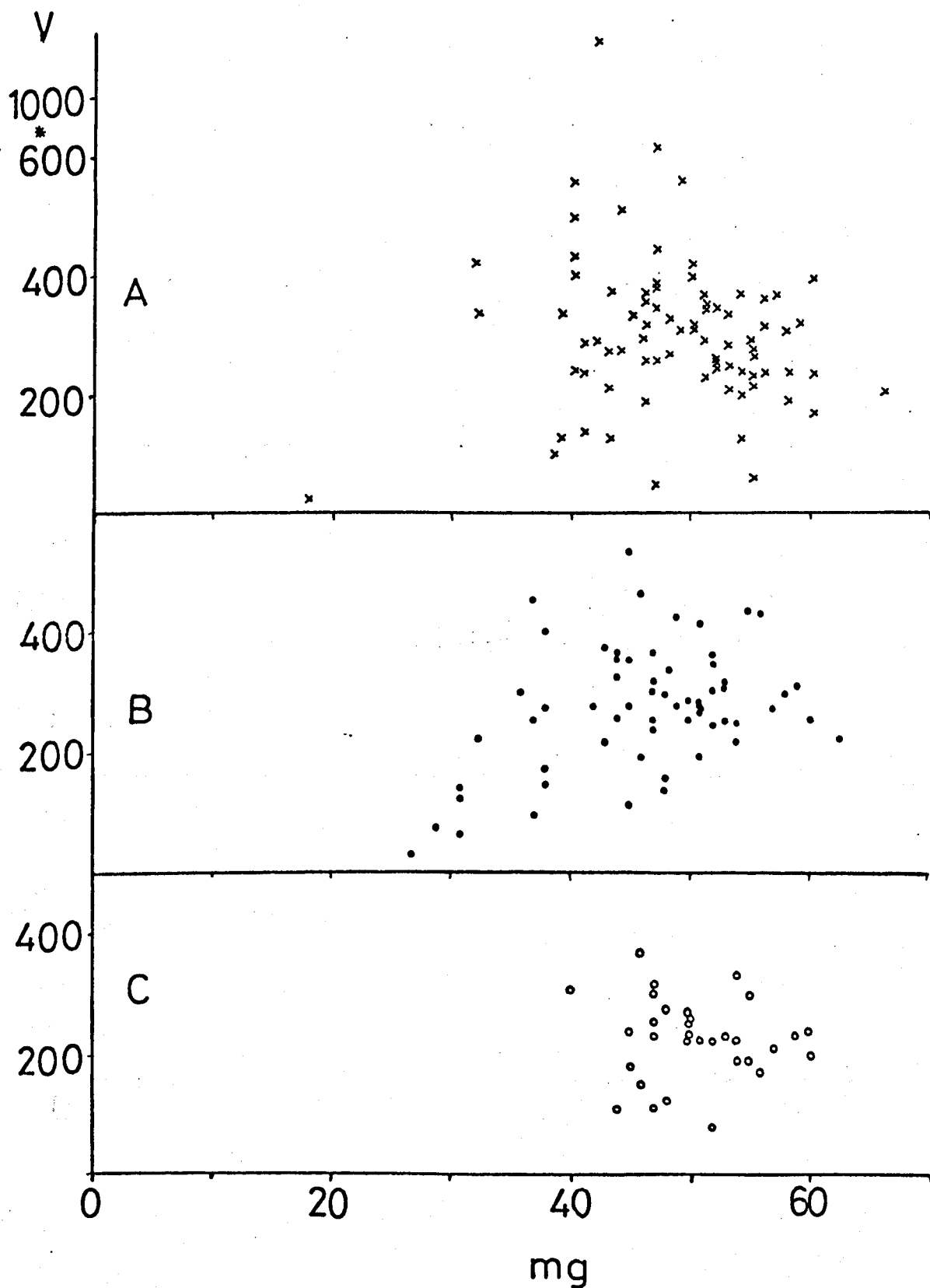


Figure 4.10: Norwegian metabasites: V p.p.m. v niggli mg.10². Symbols as in figure 3.9.

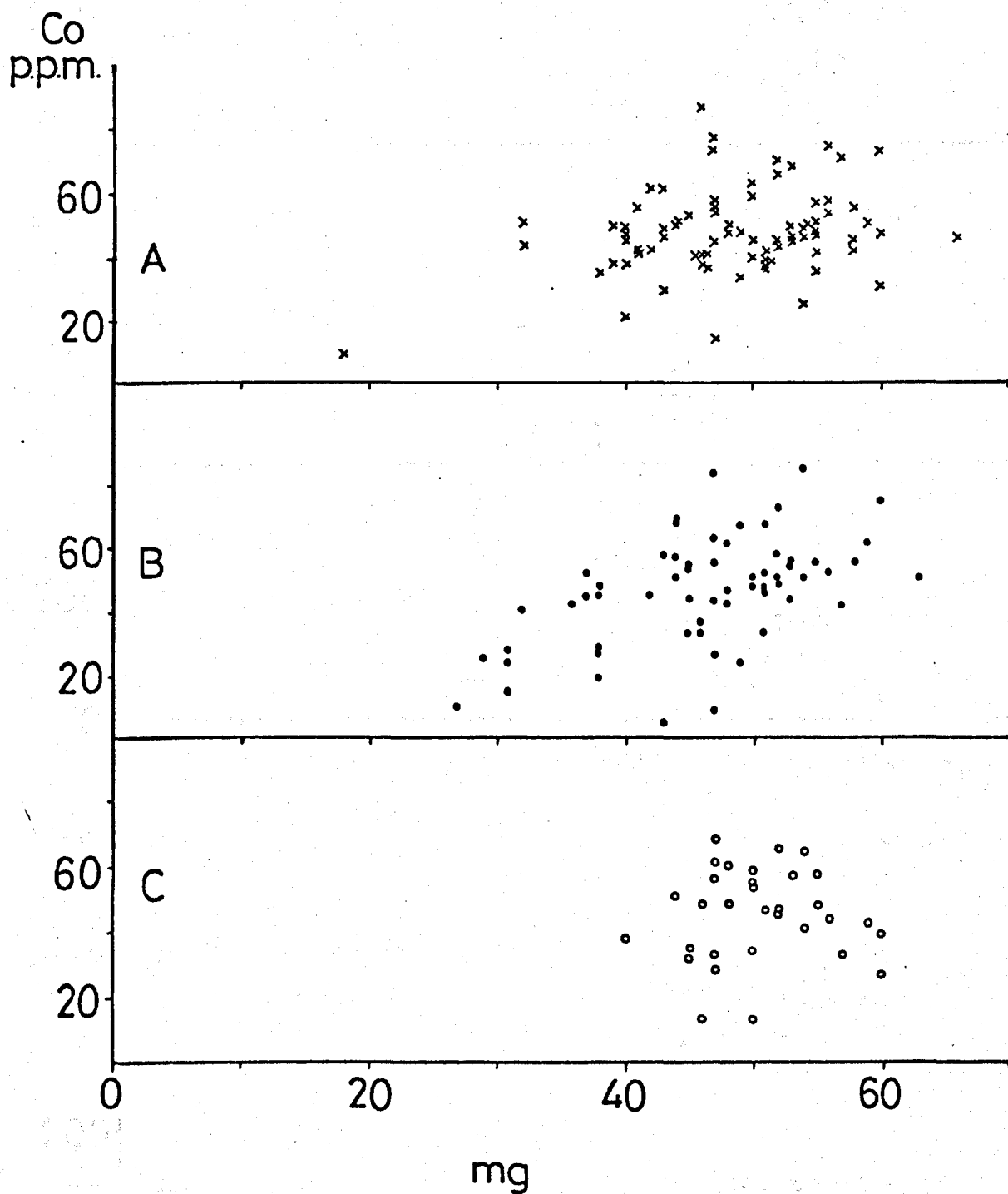
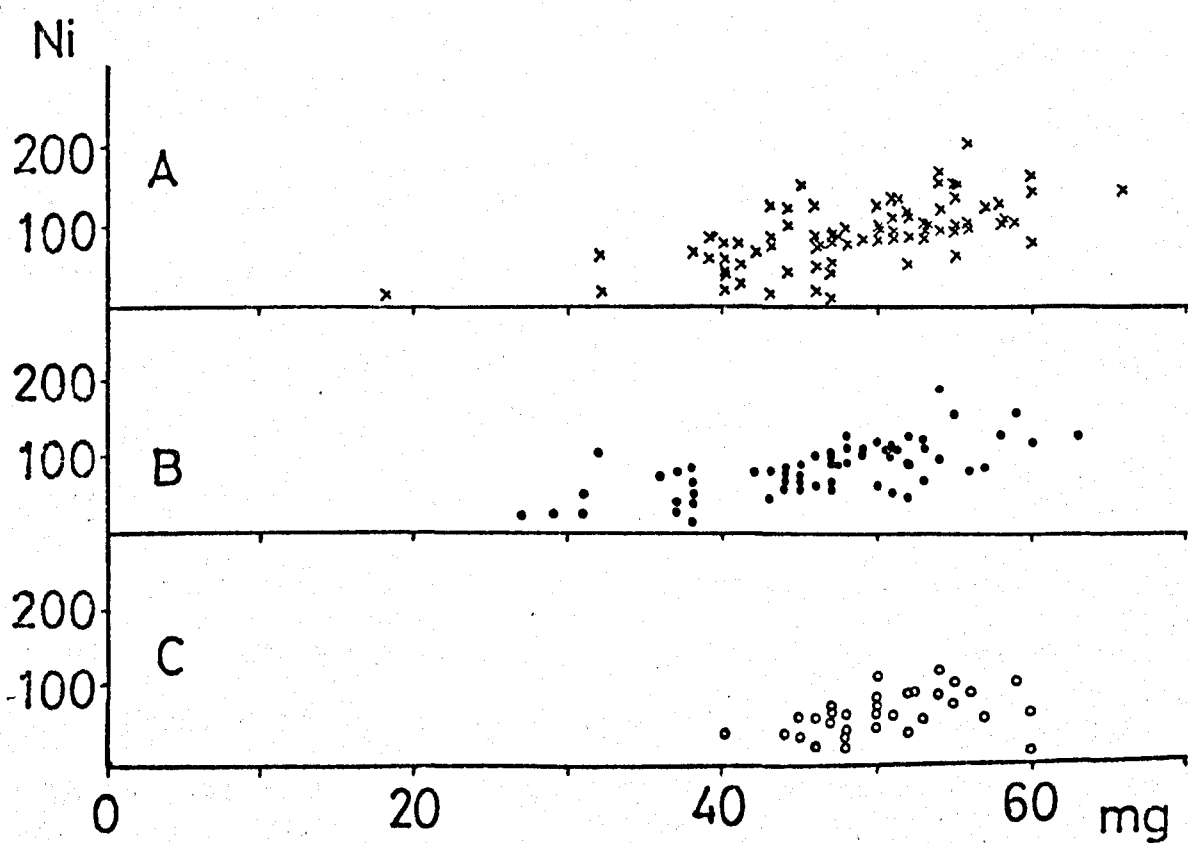
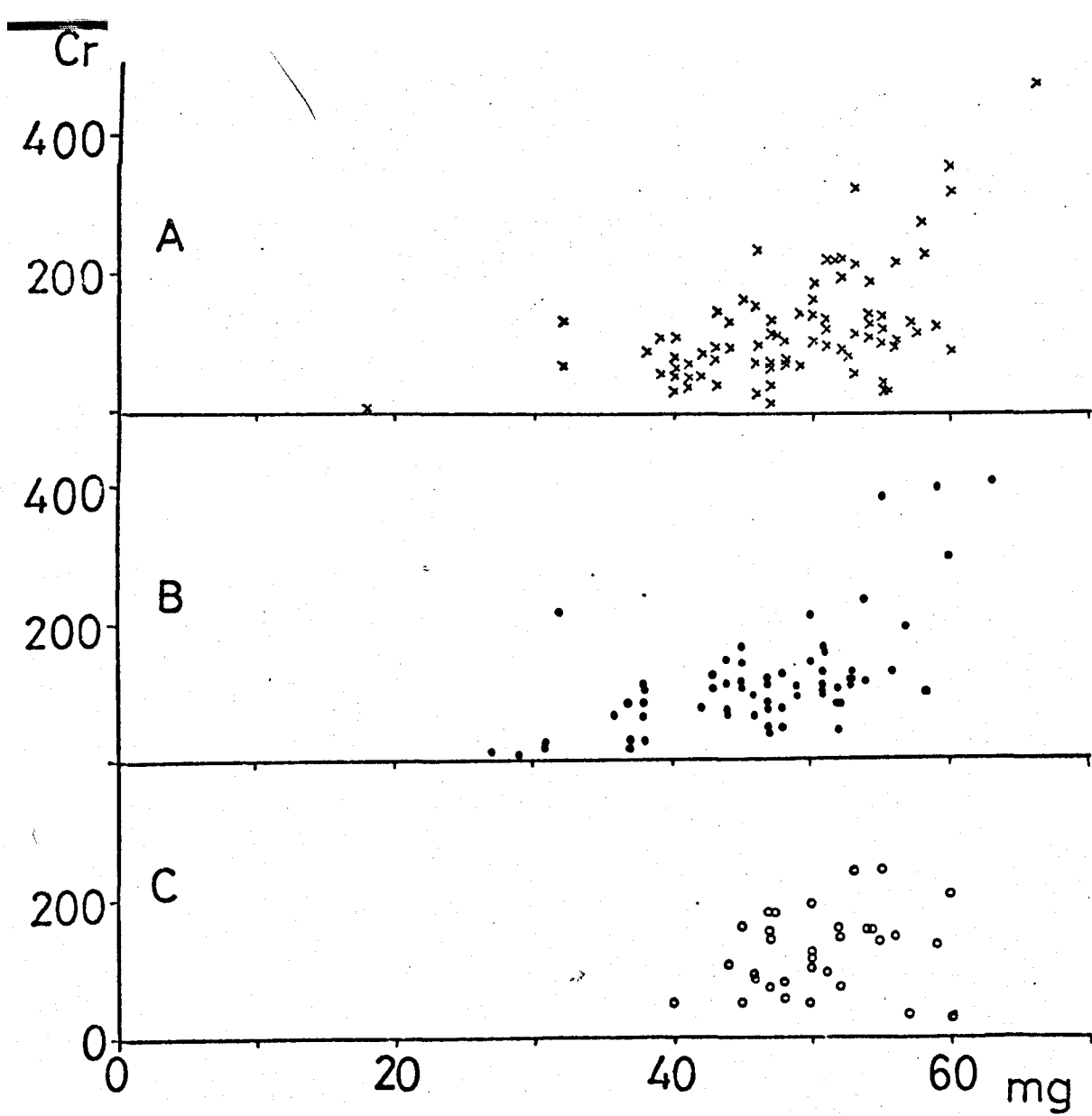


Figure 4.11: Norwegian metabasites: Co p.p.m. v niggli $\text{mg} \cdot 10^2$. Symbols as in figure 3.9.

Figure 4.12 (Overleaf): Norwegian metabasites: Cr v $\text{mg} \cdot 10^2$ and Ni v $\text{mg} \cdot 10^2$. Symbols as in figure 3.9.

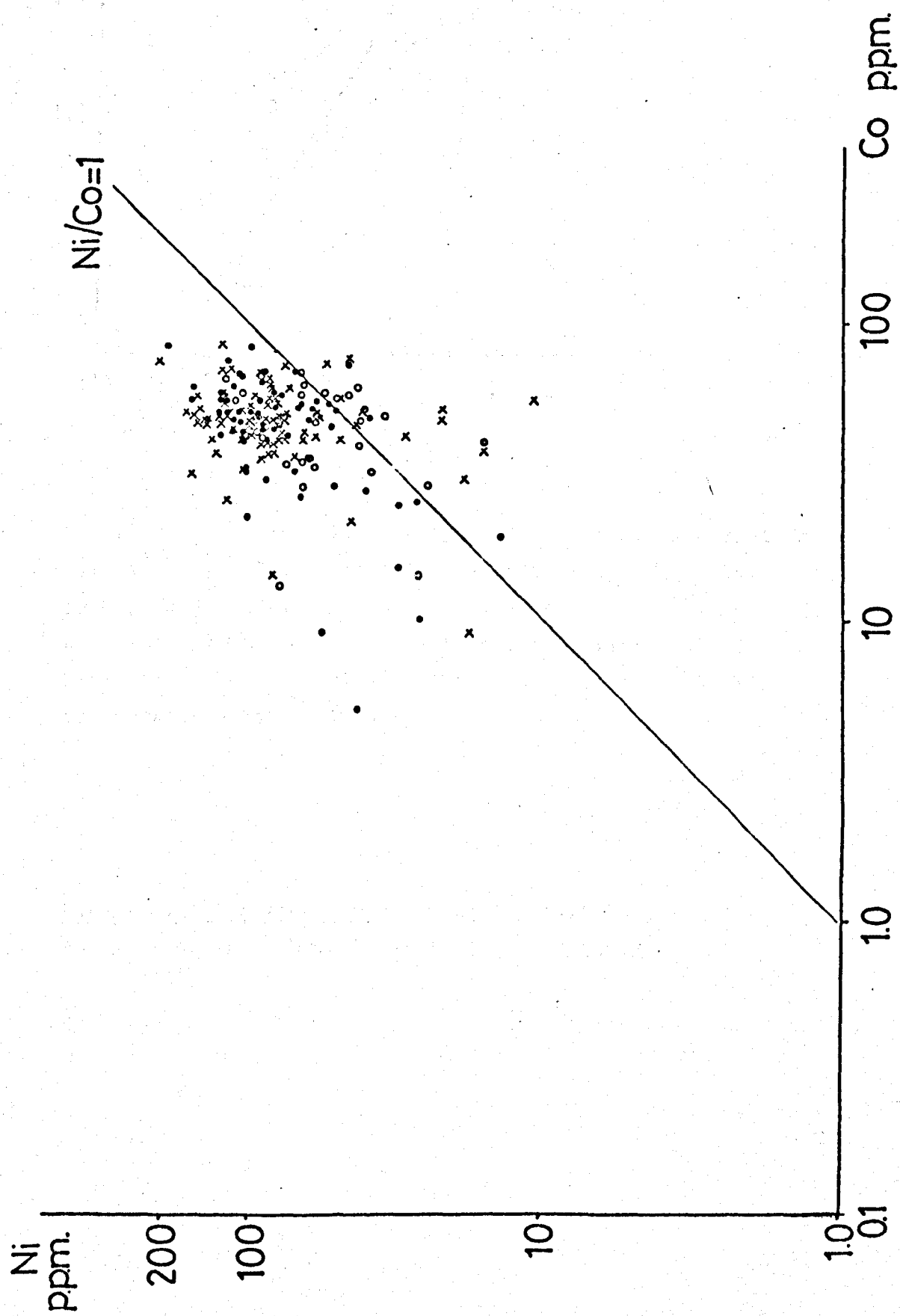


theoretically predicted behaviour (e.g. Taylor 1965, Burns 1970) in which Cr and Ni would be expected to be preferentially incorporated into the earlier stages of magmatic crystallisation than would Co.

The declining abundance levels of the transition metals may therefore be attributed to primary igneous mineral fractionation, prior to intrusion. A probable mechanism, particularly with regard to the Cr and Ni plots is the steady removal of olivine, a process which may eventually have led to the intrusion of ferrodolerites. The decrease in Co is also consistent with olivine fractionation. Vanadium however, is generally excluded from the olivine structure, and for instance, is known to be completely absent in Skaergaard olivines (Wager and Mitchell, 1951, Wager & Brown 1968). This element favours pyroxenes and early formed ore minerals (Taylor 1965). It is therefore postulated that the end stages of iron enrichment were also marked by removal of minor quantities of pyroxene and possibly also a non-titaniferous ore mineral such as magnetite.

Further aspects of transition metal inter-relationships are now considered using binary scatter diagrams (figures 4.13-4.16).

The Ni-Co diagram (figures 4.13 and 4.14) shows several features of interest. The majority of the metabasites are characterised by Ni and Co levels which plot within the general abundance field for basalts



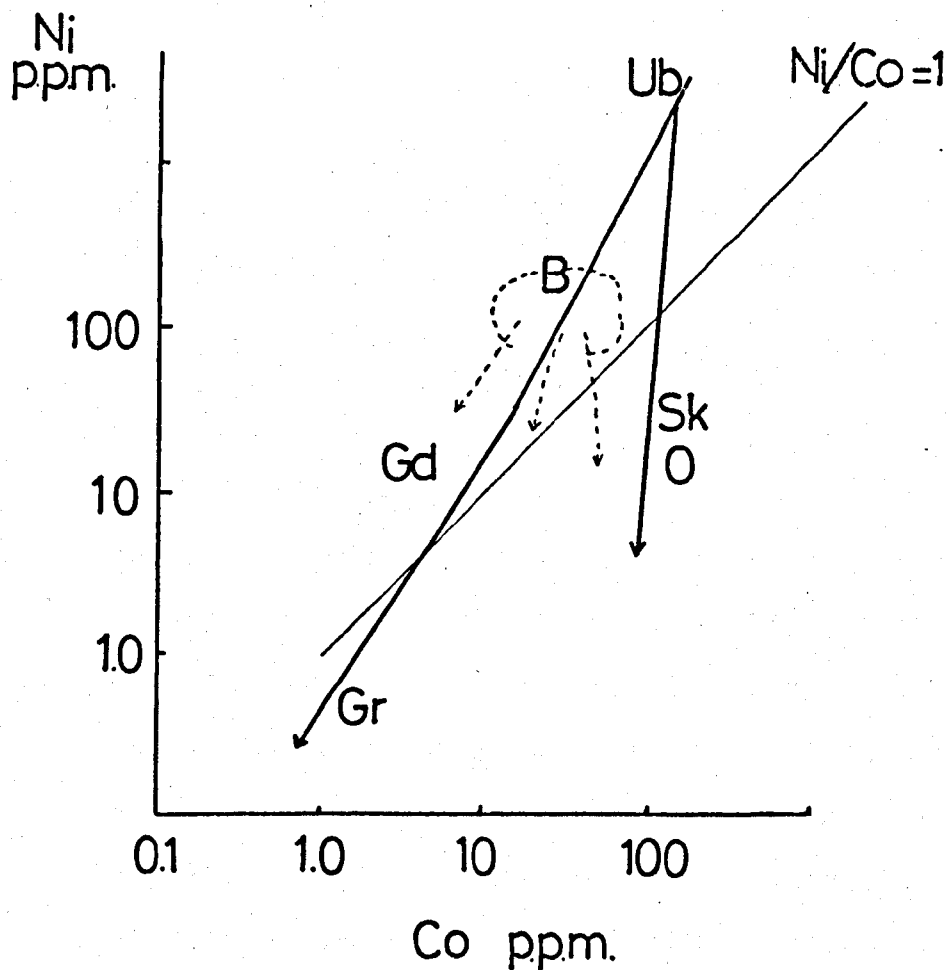


Figure 4.14: Schematic log-log Ni-Co diagram, illustrating fall in Ni/Co with igneous fractionation. Ub = Ultrabasic rocks, B = Basalts, Gd = Granodiorites, Gr = Granites, Sk O = Skaergaard olivines. (data from Taylor (1965)). Broken lines indicate field of variation and fractionation paths for the Norwegian metabasites.

Figure 4.13 (previous page): log-log Ni-Co diagram for the metabasites. Symbols as in figure 3.9.

(Carr and Turekian 1961; Taylor 1965). Systematic fractionation of basaltic magma by removal of olivine will normally result in a gradually reduced Ni/Co ratio with differentiation.

This generalisation is because Ni^{2+} tends to enter early magmatic fractions, concentrating in olivine relative to Co. (Burns 1970, p.171). However, the more 'evolved' metabasite samples have transition metal abundances more in keeping with some intermediate-acid igneous rocks (Wedepohl 1970), and these show a somewhat dispersed fractionation pattern on the Ni-Co diagram. In particular, whilst a proportion of points follow the theoretical fractionation trend outlined in the schematic diagram (4.14), a number trend over the $\text{Ni/Co} = 1$ divide. Ni/Co ratios under 1.0 are unusual in rocks of mafic composition, such values being more characteristic of granites (Taylor 1965). This relationship probably reflects an absence of fully systematic Co fractionation in the suite. However, in zone C there is an increased tendency to a low Ni/Co ratio, despite the lack of evolved samples in this zone. 10/32 samples in zone C have $\text{Ni/Co} < 1.0$, and this is a further indication of the low overall Ni abundance in the Tromsø metabasites relative to the mainland zones.

There are no obvious relationships between the element pairs V-Ni, Co-V, and Co-Cr. The correlation coefficients, r , for each element pair are very low, and do not reach

statistical significance at the 90% level of confidence. The plots are not illustrated.

Figures 4.15 and 4.16 are binary Ni-Cr and Cr-V diagrams, revealing clearer relationships. The Cr/Ni ratio (4.15) shows some tendency to decline with decreasing transition metal abundances (and increasing fractionation). The relative absence of low Cr/Ni ratios in zone C is again a function of the lower Ni abundances in this zone.

ii) The Problem of Nickel.

The existence of relatively low Ni values in the zone C metabasites is problematic. There is an overall average deficiency of over 20 ppm in this zone relative to the mainland, and the relationship between Ni and mg is less clearly defined in this portion of the granulite facies. In addition, from the absence of low-mg rocks in zone C it might be anticipated that Ni levels would be comparable, if not slightly higher, in zone C than on the mainland.

The reason for this deficiency is obscure. On empirical grounds, the Ni^{2+} ion is not expected to be susceptible to fractionation in metamorphic processes. Based on crystal field stabilization energy data, it has been predicted that Ni^{2+} would be relatively resistant to substitution into any intergranular aqueous phases existing during metamorphism. (Burns 1970).

ppm Ni

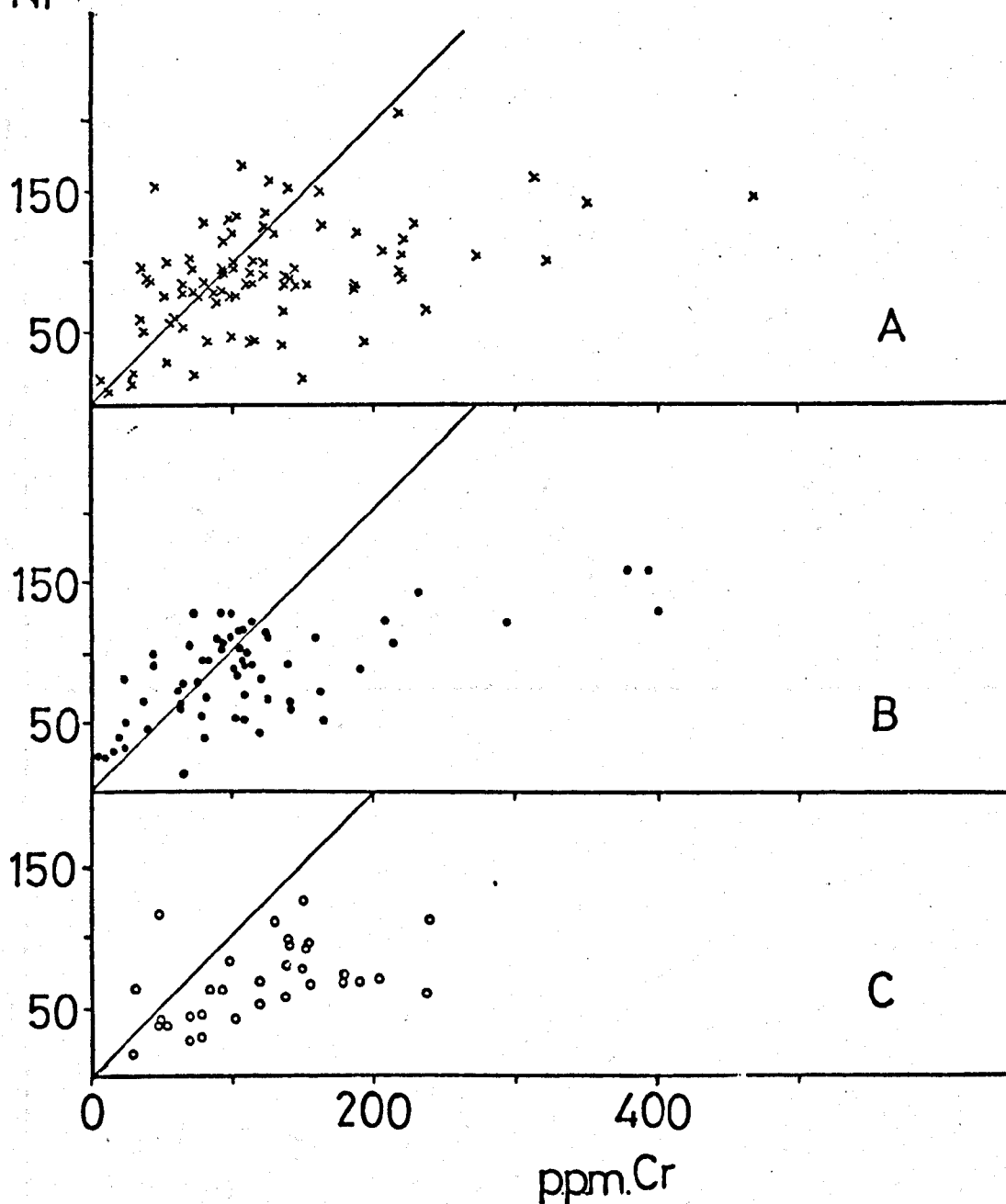


Figure 4.15: Ni p.p.m. v Cr p.p.m. by metamorphic zone.
Symbols as in figure 3.9. Diagonal line is $Ni/Cr = 1$.

Figure 4.16 (overleaf): Cr p.p.m. v V p.p.m. by zone.
Symbols as in figure 3.9. Diagonal line is $V/Cr = 2$.

Cr
ppm

400

300

200

100

A

300

200

100

B

200

100

C

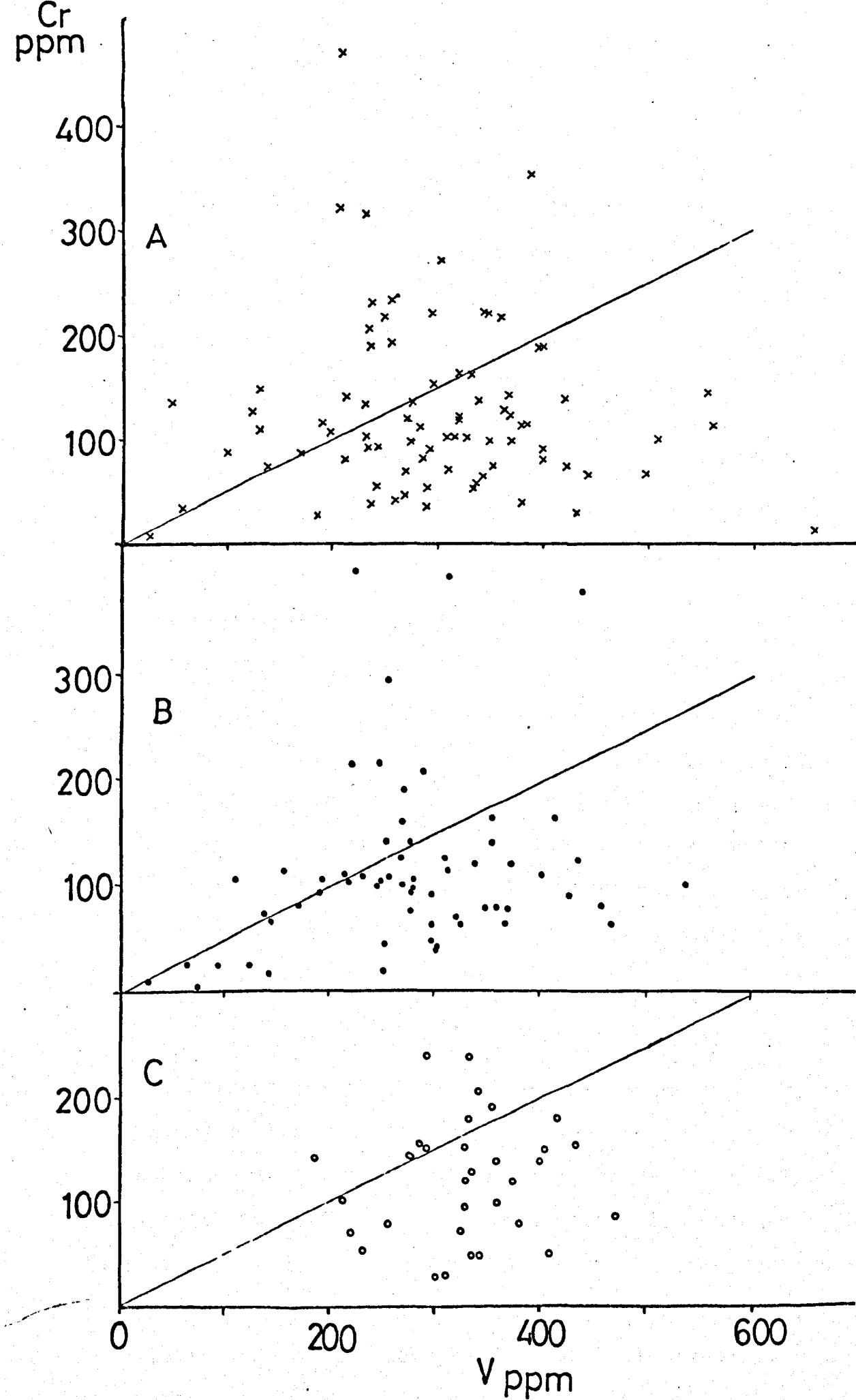
0

200

V ppm

400

600



Field and Elliott (1974), in a study of hyperite to amphibolite transitions in the Bamble sector, concluded that Ni remained static during amphibolite facies metamorphism. Several other workers who have studied element migration patterns in skarns and contact aureoles (e.g. Kretz 1960, Turekian and Carr 1960, Shaw 1963) have also noted its normally immobile behaviour in metasomatic environments. Ni is also known to be stable in serpentinization of peridotite (Wedepohl 1967, p.167).

The only evidence in support of metasomatic/metamorphic mobility of Ni in this terrain is an association in zone C between abnormally high soda and relatively low Ni (figure 4.17). There is no such association in zones A and B. If the Na_2O enhancement is due to a pervasive local metasomatism, it may be evidence for a concomitant depletion in Ni during metamorphism. The mechanism for such a depletion is not obvious however, and a spurious correlation between Ni and Na_2O in zone C is a possibility, even if Na_2O has been mobile.

An alternative explanation for the apparent nickel deficiency is that it reflects variation in primary igneous abundance levels. There is presently no evidence which might be used either to substantiate or confound this concept. In particular, there seems to be no reason to suppose that the Tromsø metabasites belong exclusively to a quite separate igneous suite, and it is likewise unnecessary to invoke a different magma source for

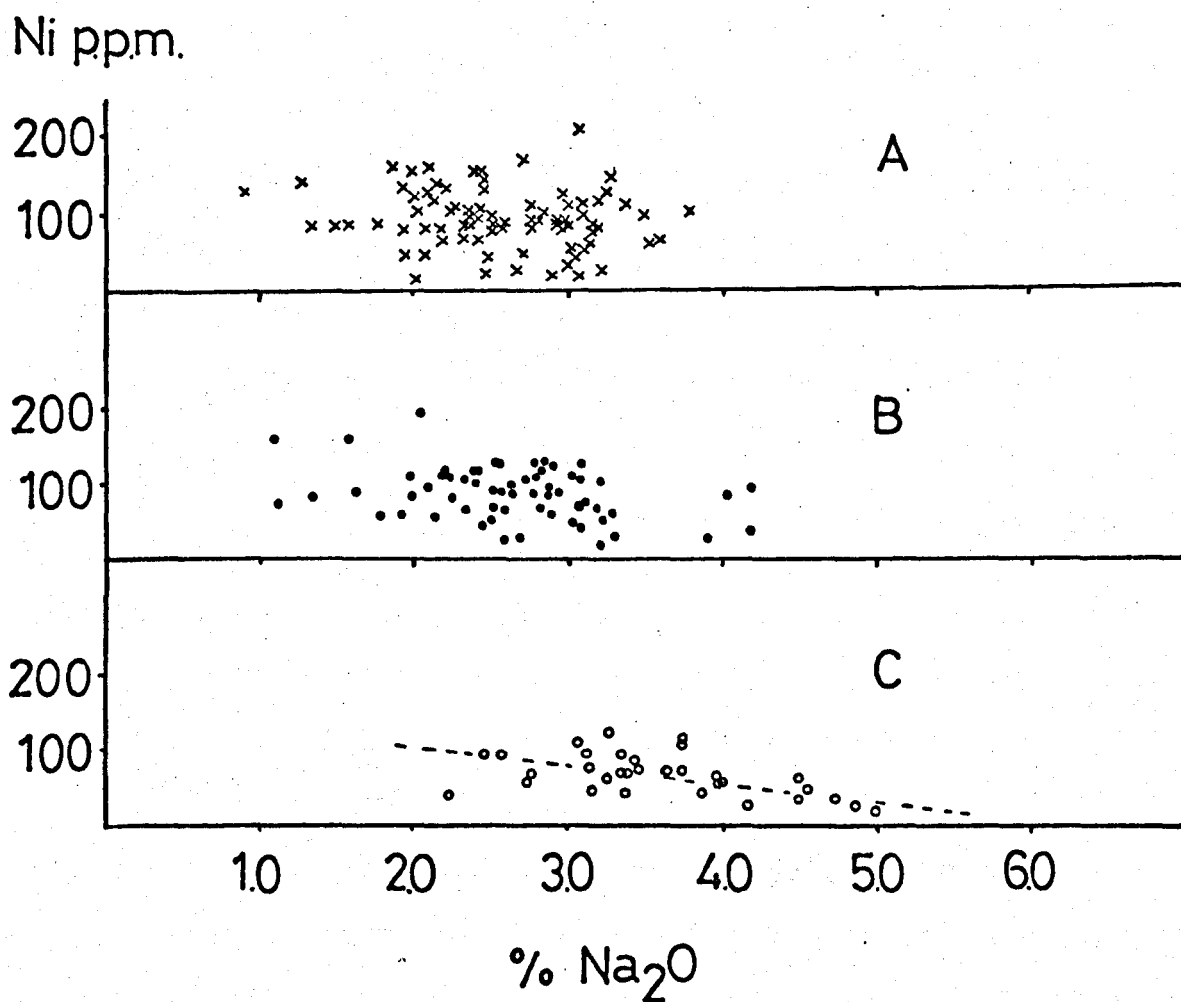


Figure 4.17: Ni v Na₂O for the metabasites by zone.
Symbols as in figure 3.9.

this group of rocks.

The Ni abundance remains therefore enigmatic, and it is possible that further knowledge of crystal field effects on this element are needed in order to completely explain its distribution.

iii) Scandium.

This interesting element is the first of the transition metals in Group III of the periodic table, and also has some crystallochemical similarities with Y and the light REE. The geochemistry of Sc has been reviewed by Norman and Haskin (1968), and certain Russian workers (e.g. Borisenko and Rodionov 1961), but comparatively little is known of its abundance in metamorphic terrains, or of its behaviour during metamorphism. Its lithospheric abundance has been estimated at 30 ppm (Fryklund and Fleischer 1963). It concentrates in the ferromagnesian minerals, excluding olivine, and is known to enter early magmatic pyroxenes. (Taylor 1965, Tilling et al 1969). It may also accumulate in late stage pegmatites (e.g. Phan 1967).

Any influence of differentiation is not particularly demonstrated by the mg-Sc plot (figure 4.18). For samples with mg > 0.40 no relationship exists, but the rocks with most marked iron enrichment (in zone B) do show a consistent, though small decline in Sc, amounting to a relative deficiency of 10 p.p.m. While fractionation of olivine would not affect Sc abundance in a magma, some removal of igneous pyroxene

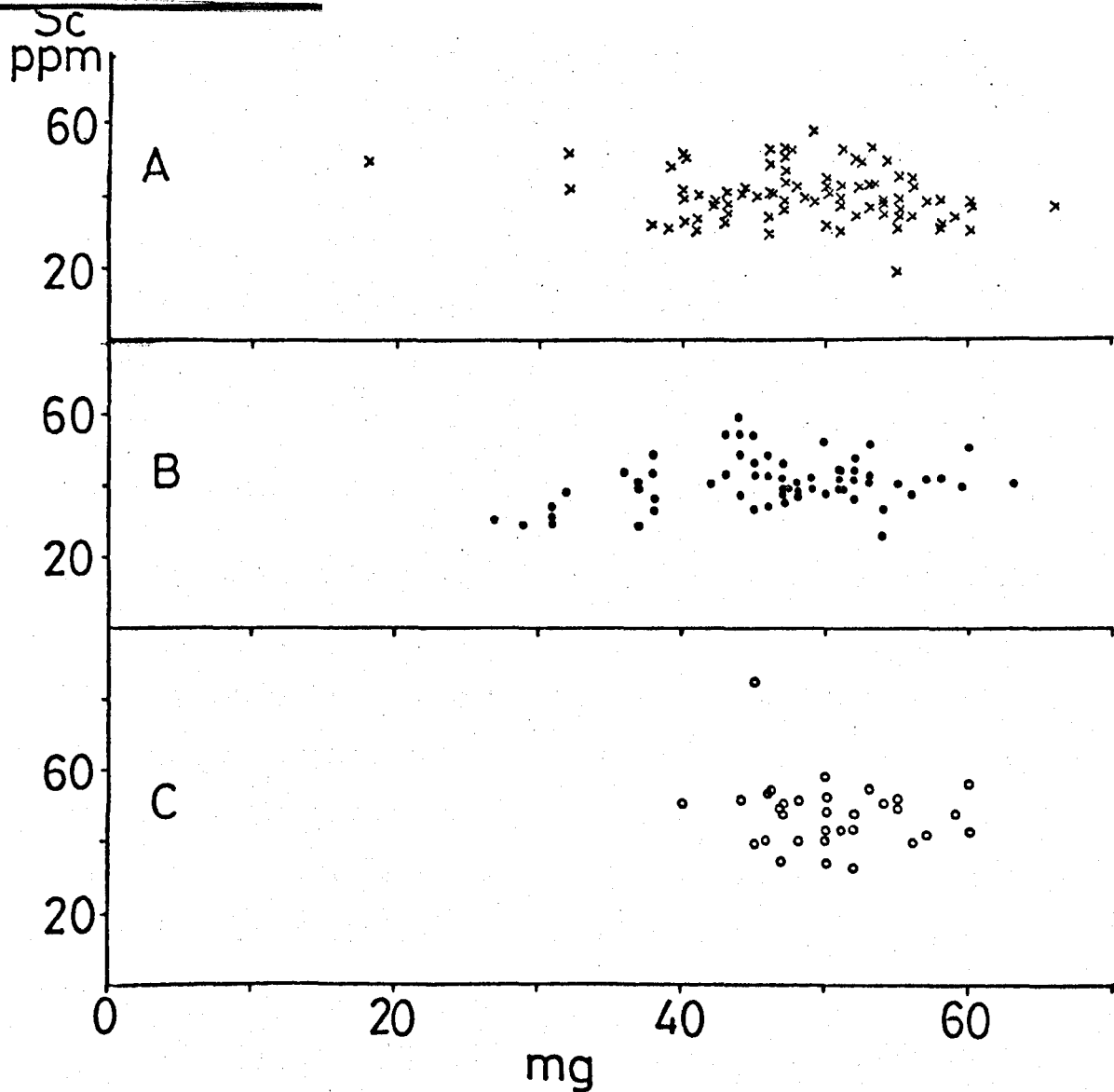


Figure 4.18: Norwegian metabasites: Sc p.p.m. v niggli $\text{mg} \cdot 10^2$
 Symbols as in figure 3.9.

in the later stages of differentiation could account for this small decline. The behaviour of Sc is therefore to some extent analogous to Vanadium (fig. 4.10), which is usually excluded from olivine, and which also declines in the low-mg samples.

The available Sc data for 16 hyperites and their metamorphic (amphibolitic) equivalents (Field and Elliott 1974) have been plotted as a histogram together with the metabasite data in figure 4.19. There is an excellent discrimination between the hyperites and the metabasites, based upon their Sc contents. (There is no field or microscopic textural evidence to support the classification of metabasite sample 7332 as a completely amphibolitized hyperite dyke, but it is the only metabasite to have such a low Sc level, causing it to fall in the hyperite range). These data, obtained in the same laboratory, suggest that a chemical distinction between the two suites, the metabasites and the later hyperites, can be confidently made using Sc abundances.

From this evidence it is clear that Sc is of some significance in the chemical evolution of the Bamble sector. Moreover, the existence of the extremely rare Scandium mineral, Thortveitite ($\text{Sc}_2\text{Si}_2\text{O}_7$) is documented for parts of the Bamble sector (Neumann 1961), where it occurs in some late stage pegmatites in quantities of minor economic significance.

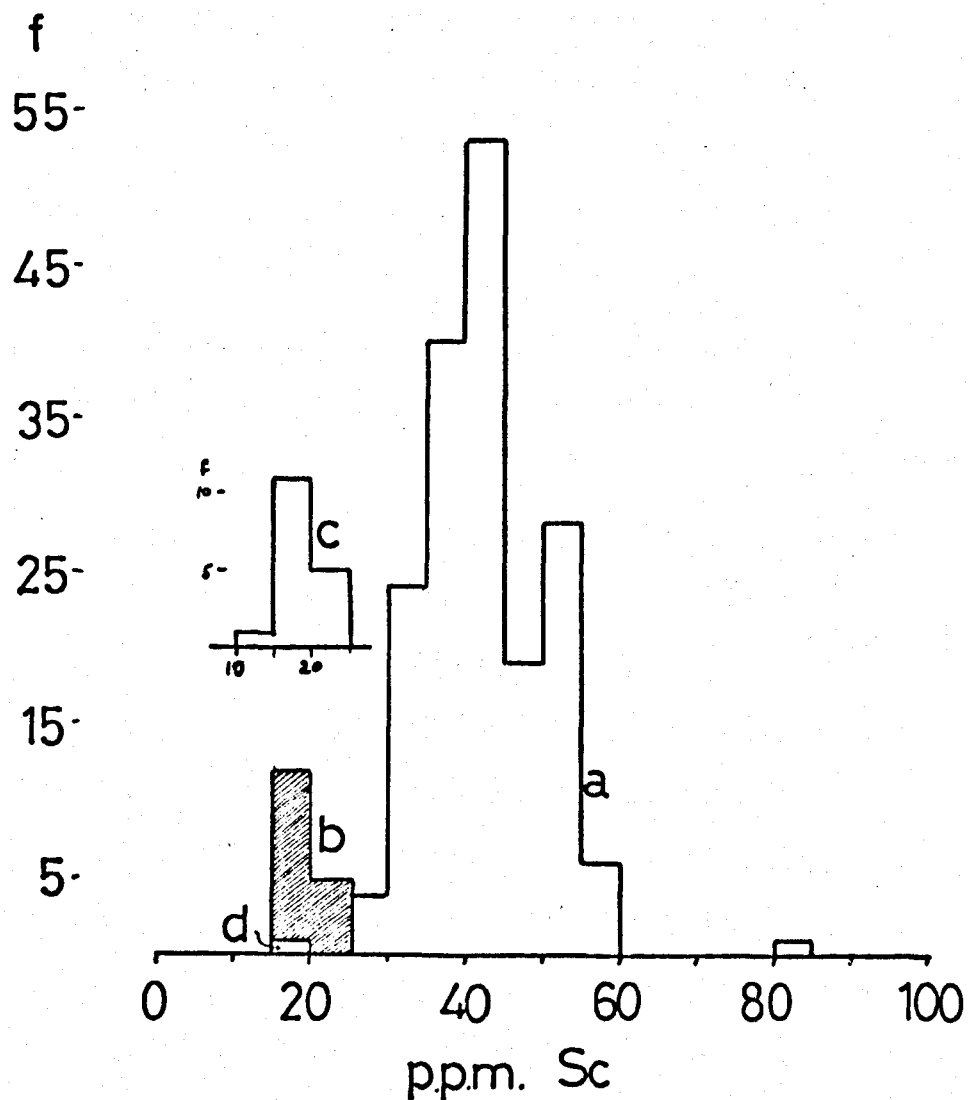


Figure 4.19: Comparison of Sc abundance in metabasites and hyperites (gabbros), from South Norway.

a = Metabasites, this study. (n=175).

b = Hyperites.

c = Amphibolitic margins to hyperites.

d = Metabasite sample 7332.

The data for b and c above, consisting of 16 pairs of hyperites and their metamorphic equivalents, are from Field and Elliott (1974).

While the metabasites have Sc values which are compatible with those reported for basic igneous intrusions, the gabbroic hyperites are clearly depleted in the element, relative to both the metabasites and to the literature values. The hyperite Sc range of 15-25 ppm is more characteristic of shales or granodioritic material than of ferromagnesian-rich basic intrusions. (Fryklund and Fleischer 1963; Taylor 1965). It is attractive to postulate a genetic association between this depletion and the extreme pegmatitic concentration which has resulted in the local occurrence of Thortveitite, but no further evidence is currently available. In the absence of further data on the hyperites, it is perhaps also premature to speculate on possible variations in magma chemistry between the metabasite source and the hyperite source, for the low Sc of the latter group may be associated with an unusual fractionation pattern. However, Fryklund and Fleischer (1963) have suggested that both rich and poor Sc provinces exist, and that these reflect inhomogeneous Sc domains in ^{the} upper mantle. The present data from Bamble, which show an almost complete separation of abundance levels between two successive (meta)-igneous provinces, would be consistent with this viewpoint, although further substantiation is necessary.

E. The "incompatible" elements.

Plots of Zr, Ce, Y, Zn, Nb, Ba, Sr and Rb against the differentiation index, n_{ig} , are presented in figures 4.20 to 4.26 respectively.

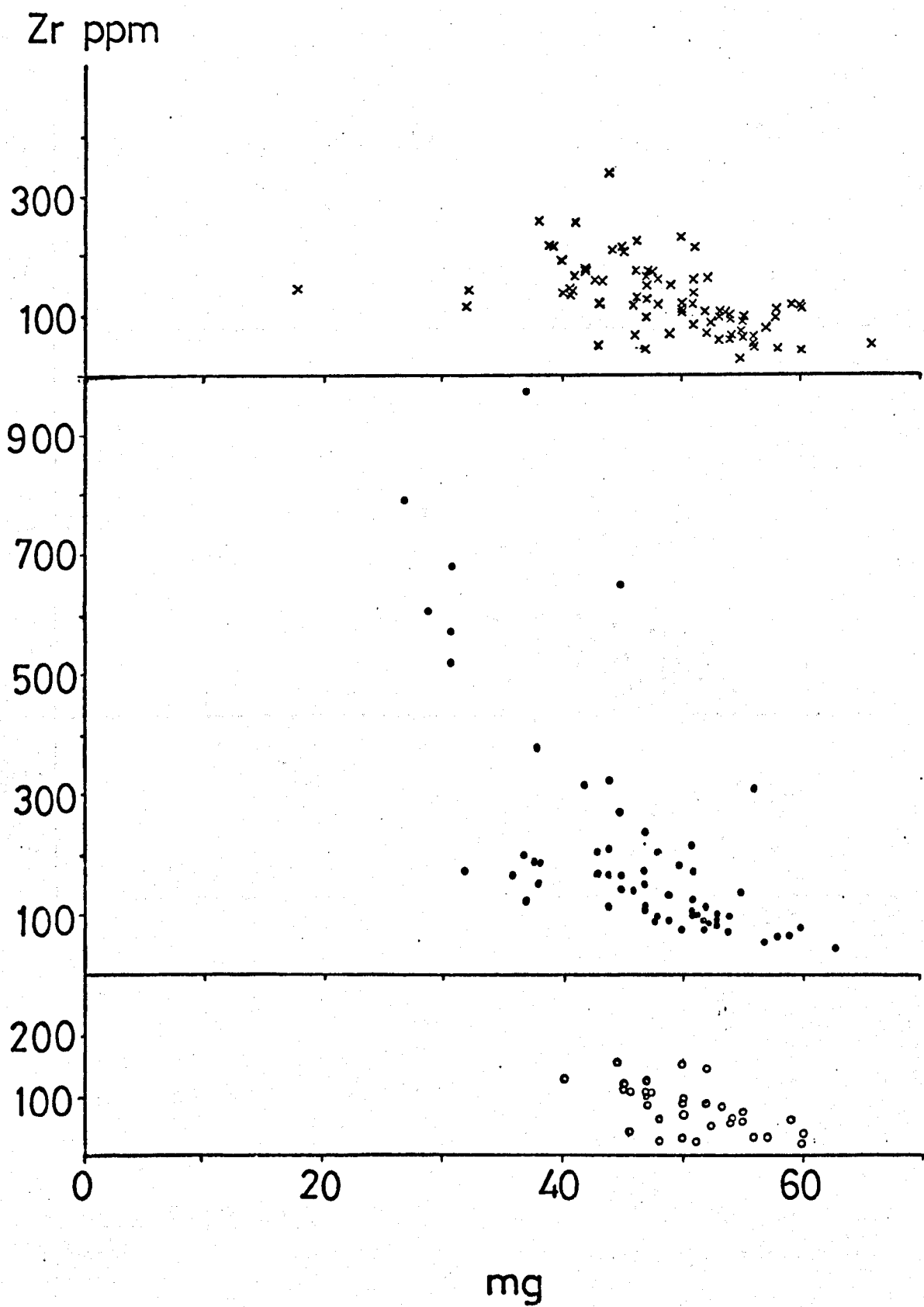


Figure 4.20: Zr p.p.m. v niggli $\text{mg} \cdot 10^2$

Ce

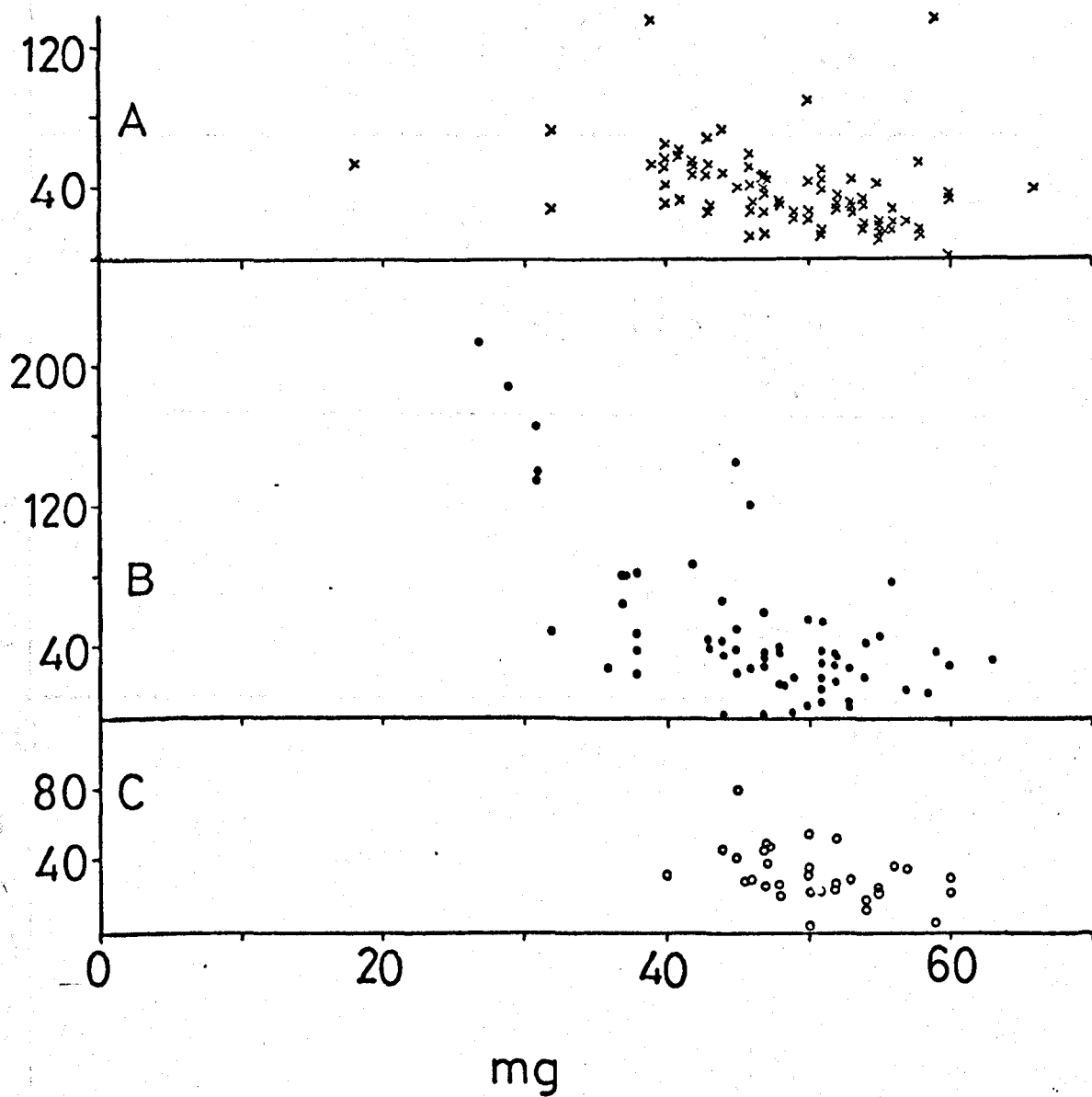
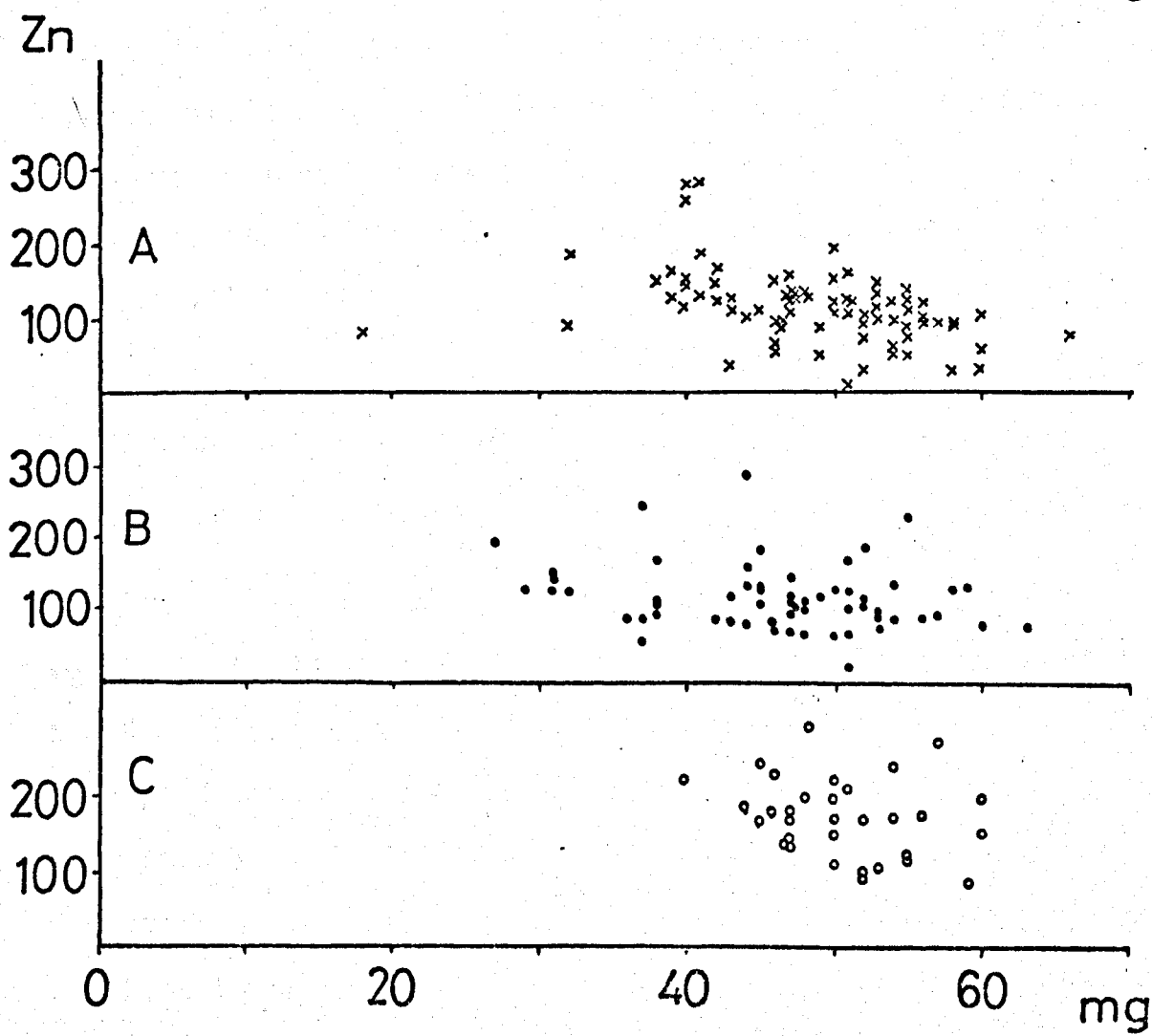
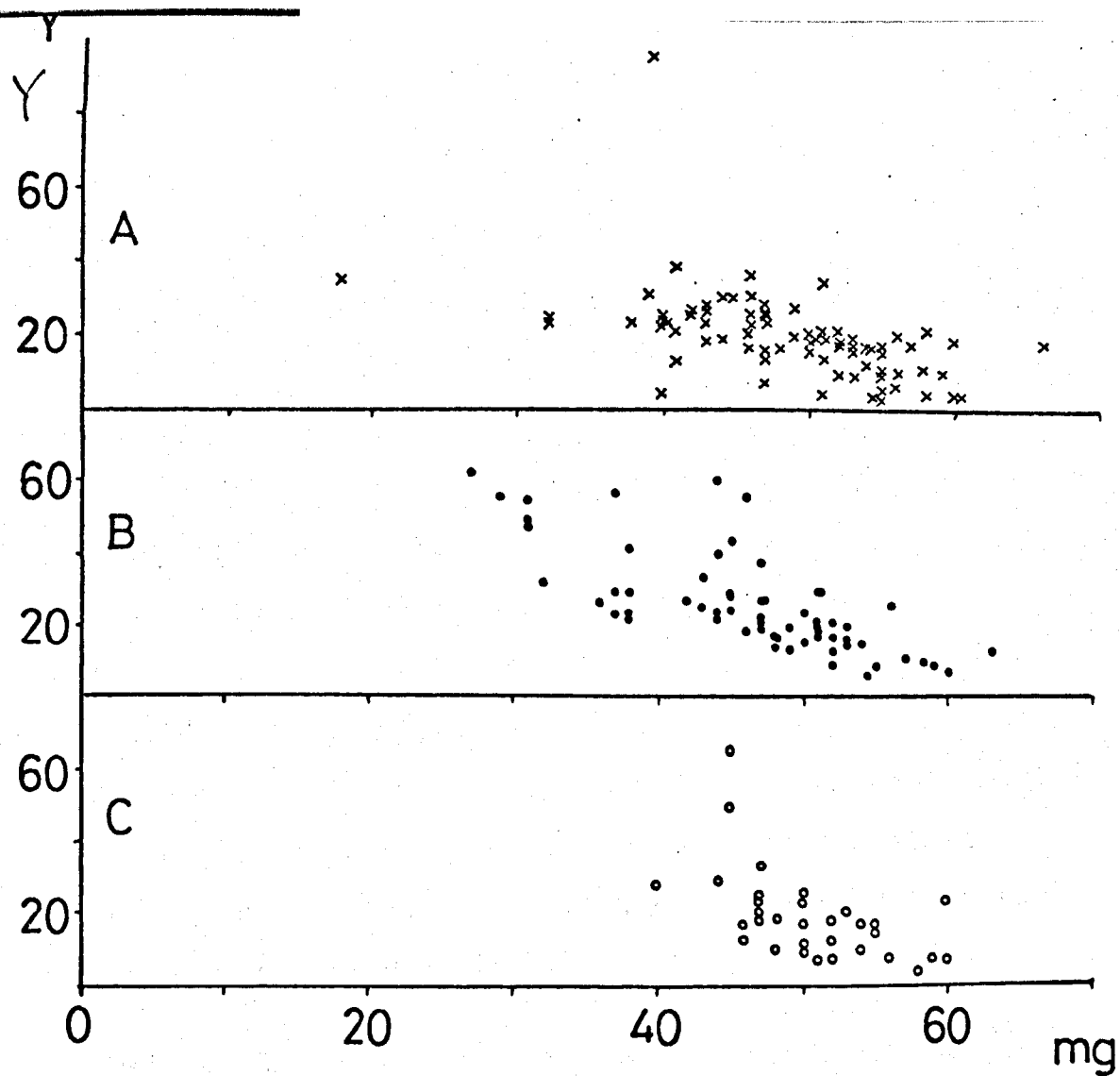


Figure 4.21: Ce p.p.m. v niggli $\text{mg} \cdot 10^2$

Figure 4.22(overleaf): Y p.p.m. v niggli $\text{mg} \cdot 10^2$ and Zn p.p.m. v niggli $\text{mg} \cdot 10^2$. (3 samples with anomolous Zn omitted.)



Zr, Ce and Y show regular increases with iron enrichment, and the rate of variation increases markedly in the low-mg group, particularly in the case of Zr. Abnormally high levels of up to 976 ppm Zr are found in this group. The Trompy metabasites (zone C) display a slightly reduced bulk level for Zr even taking into account the less differentiated character of this zone. Nevertheless, the negative correlation for mg vs Zr is still evident on Trompy. Ce and Y describe less rapid end-stage increases in abundance, and no discernable variations by metamorphic zone. Zn (4.22), when plotted against mg defines a more shallow curve, with no pronounced increase associated with lower mg values.

Neither Ba nor Nb shows any relationship for samples with $mg > 0.40$. However, rocks with lower mg in zone B have sharply increased abundances, again suggestive of some build-up of incompatible elements in the later stages of fractionation. The reduced level of Ba abundance in zone C (Table 4.4) is re-emphasised in figure 4.24.

Sr also shows a slightly reduced level in zone C, but no consistent relationship with the differentiation index, except for a weakly defined increase in the mg-poor samples.

In the mg-Rb plot, no trend is seen in any metamorphic zone. There is increased dispersion on the Rb axis in zones A and B compared to zone C, and these features are interpreted as being related to the systematic changes in abundance with metamorphic grade. Rb behaviour is analogous to that of K, and a discussion of K-Rb systematics is given in the following chapter and also in Field and Clough (1976).

Ba

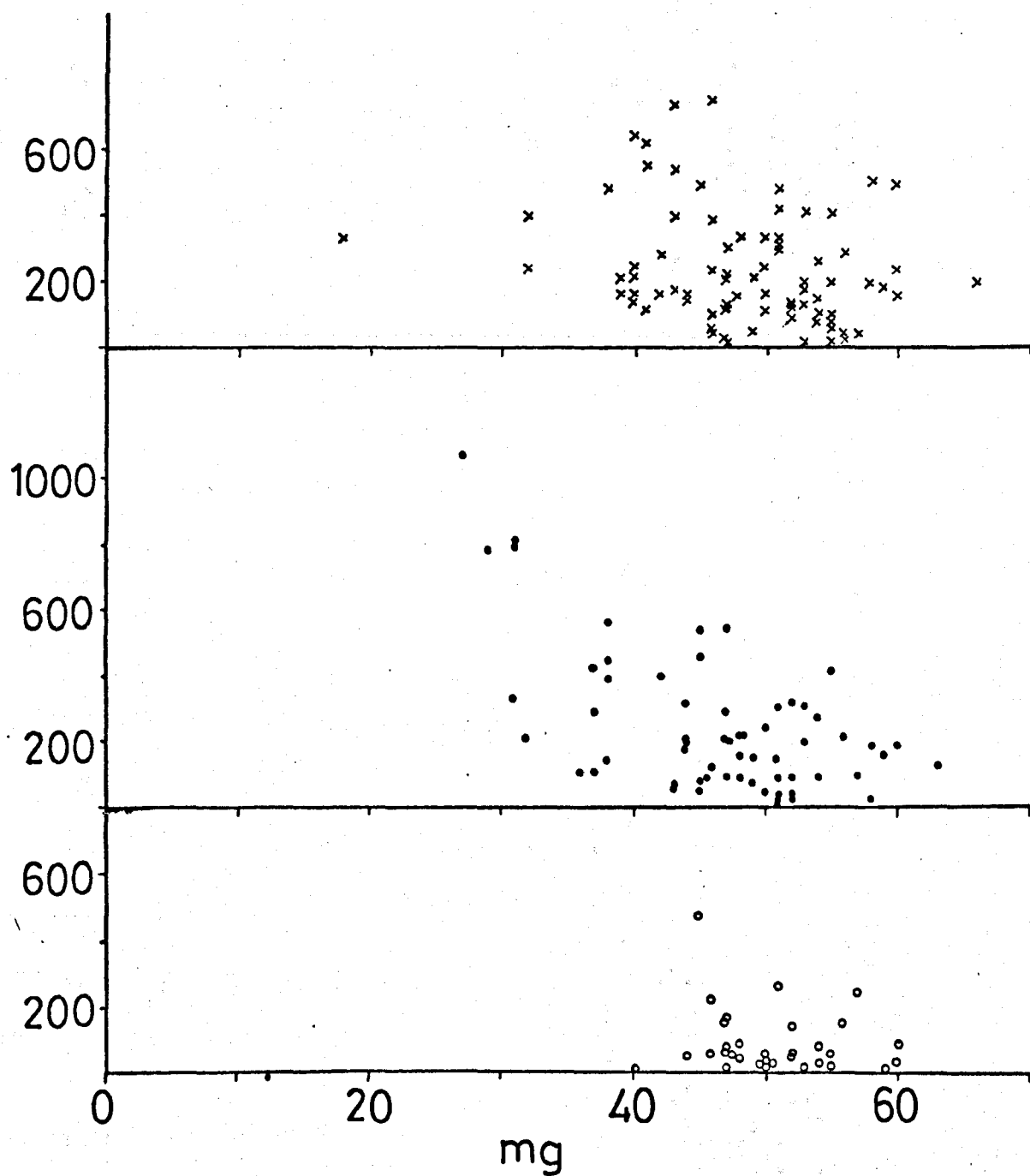


Figure 4.24: Ba p.p.m. v niggli $\text{mg} \cdot 10^2$.

Figure 4.23 (Previous page): Nb p.p.m. v niggli $\text{mg} \cdot 10^2$.

Nb
ppm

20

10

A

60

50

40

30

20

10

B

20

10

C

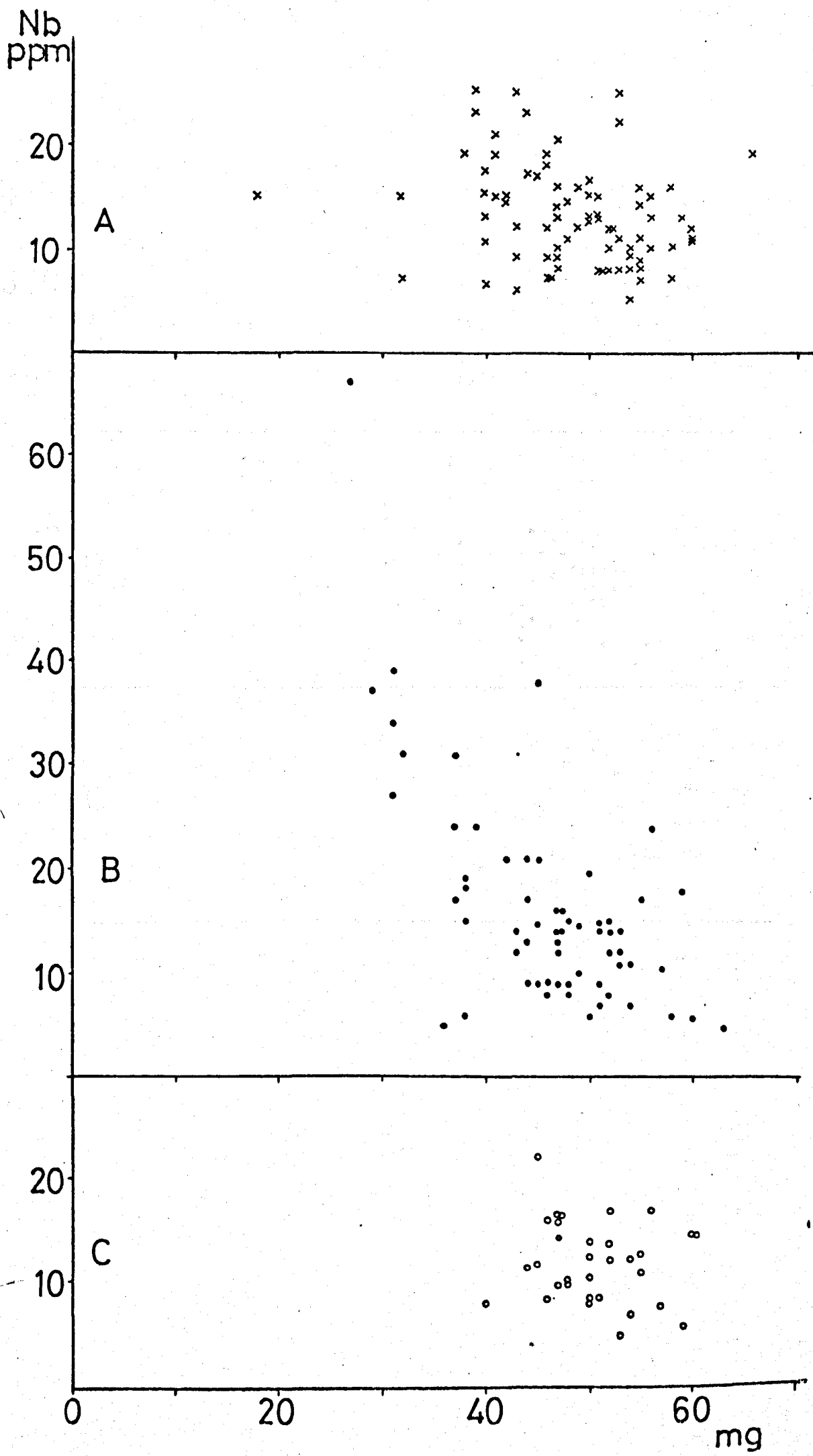
0

20

40

60

mg



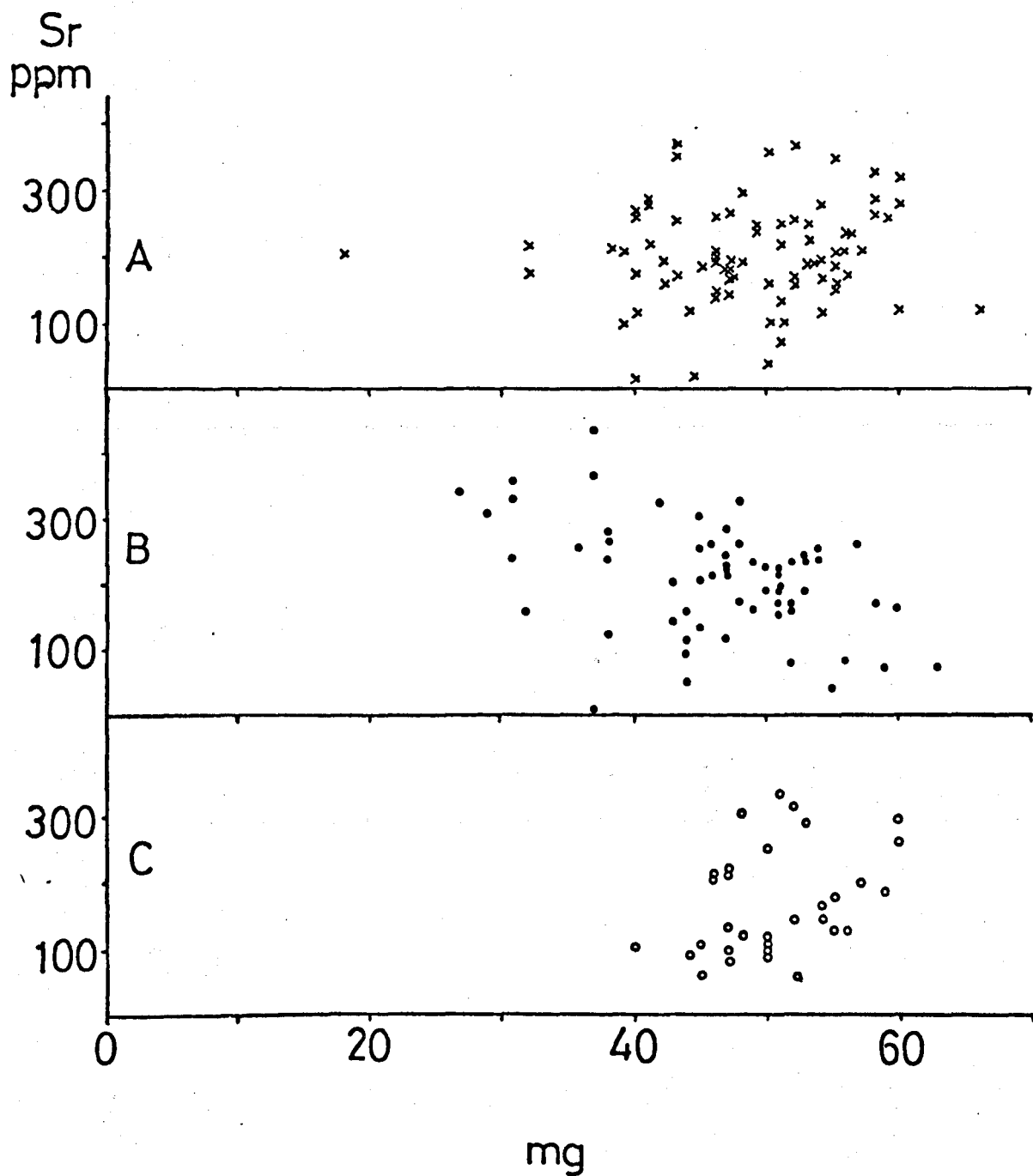


Figure 4.25: Sr p.p.m. v niggli $\text{mg} \cdot 10^2$

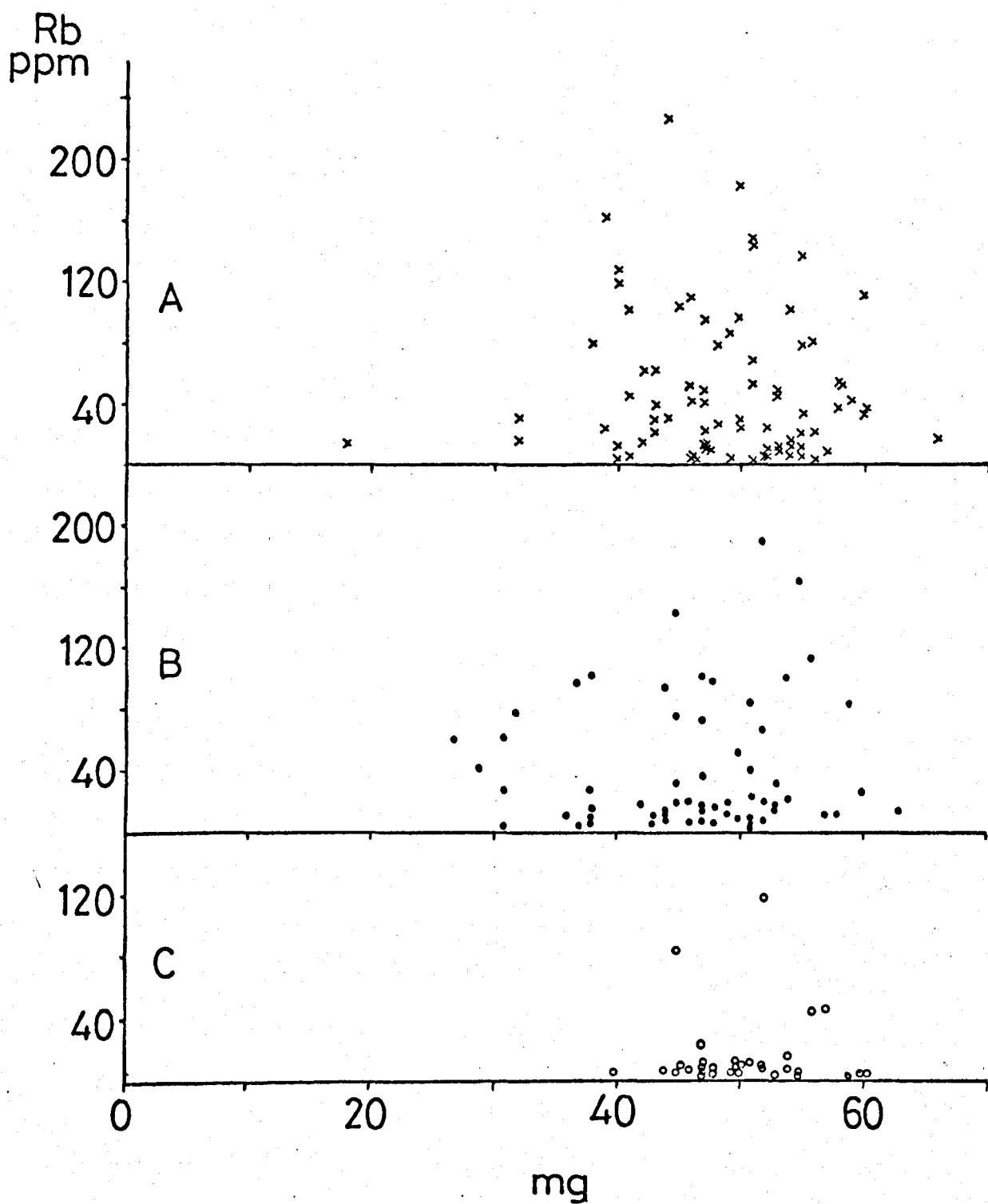


Figure 4.26: Rb p.p.m. v niggli $\text{mg} \cdot 10^2$.

Symbols in figures 4.20-4.26 as in figure 3.9.

F. Discussion.

Samples with high Fe content and consequent low niggli mg have an important influence on all trace element abundance levels, with the exception of Rb. The geographical location of most of these rocks, in zone B, causes the abundance levels in this zone to be particularly affected. Table 4.5 summarises the influence of the high-iron group on the average trace element chemistry of zone B. This also reaffirms the consistency of the remainder of the zone B samples with the average trace element values for zone A. (Table 4.4).

Most of the trace elements in the metabasites display behaviour patterns which are known to result from differentiation of igneous rocks. The overall decline in value in the transition metals with fractionation is well-documented in many suites, including Skaergaard (Wager and Brown 1968), the Nuanetsi basalts (Cox et al 1967) and tholeiitic plateau basalts from the North Atlantic province (Jakobsson 1972, Noe-Nygaard and Pedersen 1974).

The behaviour of the 'incompatible' elements is also significant. Zr, Nb, Ce and Y show marked and sometimes extreme enrichments in the high-iron samples. These trends most probably represent preservation or partial preservation of a primary igneous fractionation. This is consistent with the results of Cann (1970), Hart et al (1974) and Smith and Smith (1976) who have each shown that Nb, Zr and Y (among other elements) are not mobile under low-grade

TABLE 4.5Influence of differentiation on trace element chemistry in
Zone B.

Element.	1.	2.	3.
Sc	31	41	40
V	92	299	276
Cr	31	125	114
Co	27	48	46
Ni	48	90	85
Zn	139	127	128
Rb	40	41	41
Sr	324	194	209
Y	49	23	26
Ba	623	207	254
Ce	154	46	58
Zr	685	147	208
Nb	39	13	16
(P ₂ O ₅)	1.36	0.37	0.48
(TiO ₂)	3.10	2.16	2.27

All values are p.p.m., except for P₂O₅ and TiO₂ which are wt. %.

1. = Mean of 7 "highly evolved" samples (85, 90, 97, 100, 102, 105 and 747), with average niggli mg = 0.33.

2. = Mean of remainder of zone B samples (n = 55).

3. = Mean trace element chemistry, zone B (n = 62), from table 4.4, column 2.

metamorphism. From the current study, it seems that Ce may also be included as 'immobile', and that even granulite facies metamorphism may not entirely remove primary igneous geochemical characteristics (c.f. Windley et al 1973).

"Incompatible" elements, which do not readily enter the early-formed crystals in magma solidification have been recognised for many years. (Wager and Mitchell, 1951). Harris (1957) and Green and Ringwood (1967) have suggested that these elements may even be preferentially extracted into the late-stage differentiates, perhaps due to the small temperature gradient between low level magma chambers and the wall rocks. Ba, Rb and possibly Sr have all been included as incompatible fractions in such petrogenetic schemes, in addition to Zr, Nb, Ce and Y. In the present study Ba and Sr only show enrichments in the extreme differentiates, and there is no gradual build up of the elements with declining niggli mg. Moreover, no systematic relationship is seen between the differentiation index and Rb, an element which is always described as incompatible.

If the pattern of fractionation for other igneous suites was originally followed by the South Norway metabasites, Rb would have been enriched in the high-iron group in a manner similar to that of the Zr distribution.

No such relationship is preserved and the scattered plots are believed to indicate that there has been metasomatic redistribution.

The case for similar redistributions of Ba and Sr is weaker, because of their increased 'endstage' abundance levels (Table 4.5), which may represent partial preservation of an igneous trend. However, both elements are certainly lower in abundance in zone C, a feature also reported in the acid-intermediate charnockitic gneisses of this portion of the terrain. (Cooper and Field 1977). Chemical studies of the amphibolitization of the hyperite bodies in Bamble showed dispersion patterns for Ba and Sr suggestive of variable mobility. The possibility of Ba and Sr movement is considered in more detail in the next chapter.

G. Conclusions.

1. Overall abundance levels for trace elements in the metabasites compare broadly with both basalts and other metabasic series.
2. The Rb abundance decreases systematically with metamorphic grade. In addition, zone C samples are characterised by lower levels of Zr, Ni, Ba, Sr and higher Zn than the mainland.
3. The distribution of most of the analysed trace elements is influenced, at least in part, by differentiation. Cr and Ni display clear, gradual declines with decreasing mg; Co, V and to a lesser degree Sc decline in the ferrodifferentiates only. These features are probably related to primary fractionation of olivine and pyroxene (+ magnetite?)

The strong iron-enrichment of the most evolved samples is also accompanied by marked increases in Zr, Ce and Y, behaving as incompatible elements. Zn shows a similar, though less conspicuous trend. There are gradual increases in these elements in the less extreme differentiates in all three zones of the terrain. Sr, Ba and Nb show enriched levels in the most evolved samples, but no overall trends of variation against mg.

4. The Rb distribution is not related to differentiation despite its usual behaviour. Metasomatic redistribution of this element is likely to have occurred, and some Ba and Sr mobility may also have been involved.
5. Ni abundances in zone C are anomolous, and the reasons for this remain obscure.
6. Sc abundance levels may be confidently used as a chemical discriminant in distinguishing the metabasites from the later hyperites and their feeder dykes.

CHAPTER 5: The 'lithophile' elements, K, Rb, Ba and Sr.

A. Introduction.

In this chapter the inter-element relationships between the alkaline and alkaline earth metals, K, Rb, Sr and Ba are considered.

Current interest in the behaviour of these elements in granulite terrains is high (e.g. Tarney 1976). In recent years many surveys have concluded that there is a deficiency of K and Rb in granulites relative to average values in the amphibolite facies, and to "average crustal values" (Lambert and Heier 1968, Sighinolfi 1969, 1971, Eade and Fahrig 1971, Tarney et al. 1972, Lewis and Spooner 1973, Sheraton et al 1973, Holland and Lambert 1975, Collerson 1975). Consistent results have been noted from many geographically separated terrains, and sometimes from a wide spectrum of lithologies. Most of the studies quoted above relate to Archaean terrains, however.

In contrast, Ba and Sr are usually reported as normal or even enhanced in granulites relative to amphibolite facies equivalents (e.g. Sheraton et al 1973, Tarney 1976), although Cooper and Field (1977) have noted possible deficiencies in these two elements in the Tromsø charnockitic gneisses. The alkaline element ratios give useful information in such studies, and granulite facies terrains normally display relatively high Ba/Rb and low K/Sr, K/Ba and Rb/Sr. Whenever K and Rb have both been reported as deficient in granulites it has been noted that the deficiency in Rb is

proportionately the greater leading to high K/Rb ratios, (e.g. Whitney 1969, Drury 1973, Sheraton et al 1973).

These ratios are now examined for the metabasites within the established framework (chapters 3 and 4) that:

(i) K and Rb both vary systematically with metamorphic grade throughout the terrain, and show lowest values in the granulites of zone C. (ii) Neither element correlates with the iron-enrichment of the suite. (iii) Ba and Sr show no deficiency in the mainland granulite transition, but are relatively reduced in zone C.

B. Element ratios in the metabasites.

(i) K/Rb.

The importance of K/Rb ratios is emphasized by the considerable recent literature on their characteristics in both igneous and metamorphic suites. It has become increasingly evident, particularly since the work of Shaw (1968), that K-Rb relationships are more complex than Taylor (1965) envisaged when stating that: "normal (K/Rb) ratios are within the range of 150-300 and ratios definitely outside these limits call for special explanations".

Shaw (1968) showed that both K and Rb are somewhat fractionated in the upper crust, and that K/Rb decreases slightly with increasing K content. For most igneous suites he established a "Main Trend" (MT) along which the K/Rb varies from 433 to 195 with a concomitant increase in K% of 0.1% to 10.0%. In contrast, granulites often have much higher K/Rb ratios and generally lower K₂O%, often with a trend towards decreasing K/Rb in amphibolite facies equivalents.

The K/Rb ratios for the metabasites are plotted collectively and by metamorphic zone in the histograms of figure 5.1, and the summary data, using four possible measures of location, is presented in table 5.1. The mean K/mean Rb, which is often used in summarising K-Rb data (e.g. Sheraton et al 1973) can be greatly influenced by single outlying values (c.f. Cooper and Field 1977, p.109), and mean (K/Rb) or median locations are more representative of the data.

Table 5.1 and figure 5.1 show that the K/Rb ratios for the metabasites are distinctly higher in zone C than in zones A and B. The zone B samples are characterised by higher overall K/Rb ratios than those of zone A, although this difference is less marked than that between Tromp/ and the mainland. There is thus an increase in K/Rb with increasing grade, associated with declines in both K and Rb (chapters 3 and 4).

The K-Rb data are further illustrated by the log plot of K versus Rb (figure 5.2), from which the following features emerge:

(i) With increasing K and Rb there are well-defined decreases in the K/Rb ratio, both within the total sample, and also within each metamorphic zone.

(ii) For each zone, and for the total sample, the plots are approximately linear, and follow similar trends.

(iii) Despite a considerable overlap of the fields for the two facies, there is an overall decrease in K/Rb from granulites (zones B and C) to amphibolites (zone A). This is also shown by the histograms for K/Rb (figure 5.1).

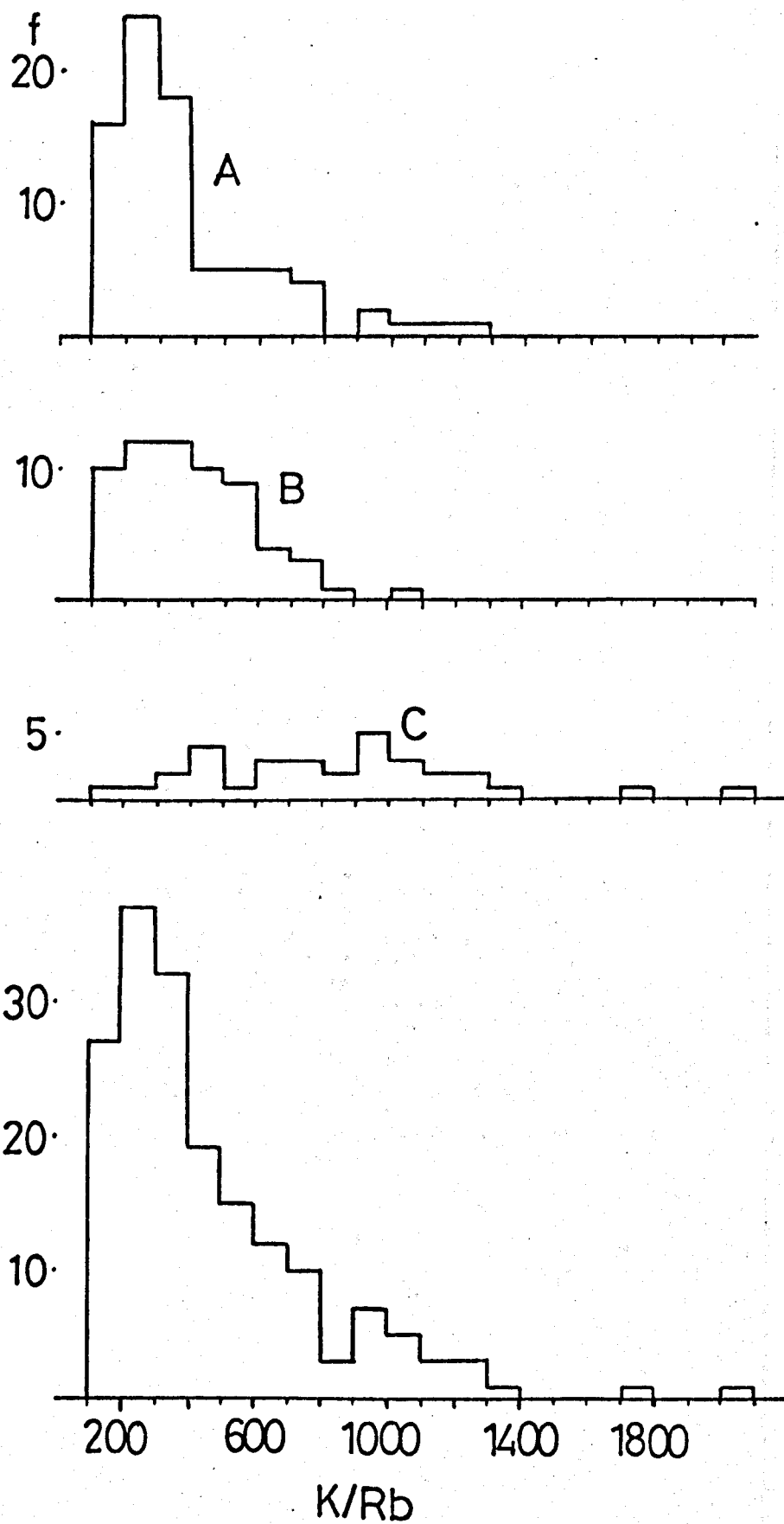


Figure 5.1: Histograms of K/Rb ratios for the metabasites in the whole suite (lower graph), and by metamorphic zone (A,B & C.) f = frequency.

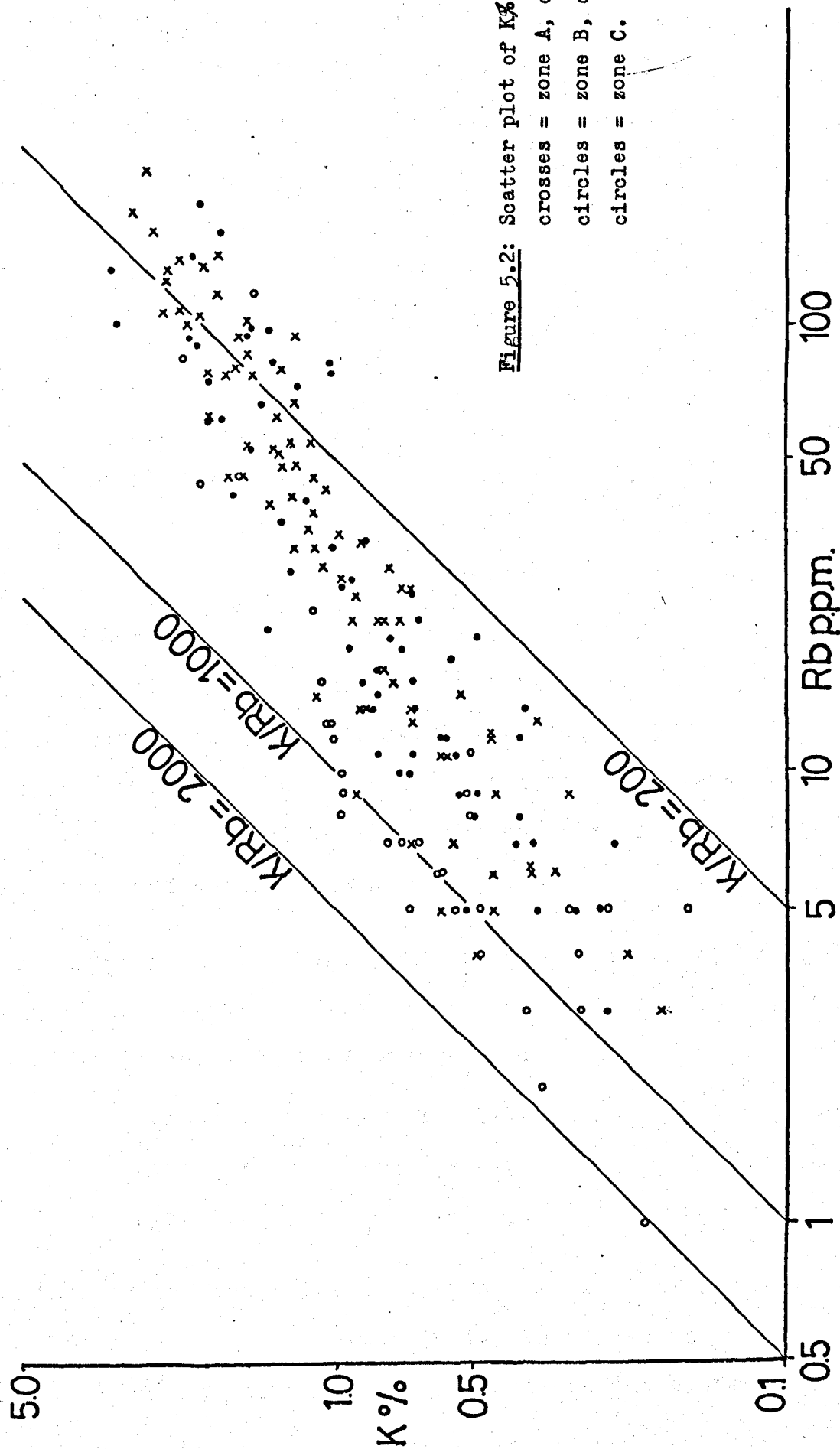


Figure 5.2: Scatter plot of K% V. Rb ppm.
 crosses = zone A, closed
 circles = zone B, open
 circles = zone C.

Correlation and regression analysis have been used to illustrate points (i) and (ii) above in more detail.

The coding method applied below follows the usage of Shaw (1968), and later authors (e.g. Lewis and Spooner 1973):

$$\text{i.e. } x = 1 + \log_{10} (K\%)$$

$$y = \log_{10} (\text{Rb p.p.m.}).$$

The product moment correlation coefficients, r_{xy} , for each group are:

$$r_{xy} \text{ total sample} = 0.858$$

$$r_{xy} \text{ Zone A} = 0.896$$

$$r_{xy} \text{ Zone B} = 0.861$$

$$r_{xy} \text{ Zone C} = 0.935.$$

The minimum values of r_{xy} required to establish statistically significant linear correlations at the 99% confidence level are 0.19, 0.22, 0.25 and 0.35 respectively. These values indicate that the plots may be considered linear, which allows the calculation of best-fit equations and comparisons between them.

For the present data, the reduced major axis (RMA) is the most suitable method of regression analysis (Miller and Kahn 1962), and the equations become:

$$\text{Zone A : } y = 1.60 x - 0.10$$

$$\text{Zone B : } y = 1.58 x - 0.08$$

$$\text{Zone C : } y = 1.48 x - 0.30$$

By inspection, the regression equations for the zonal sub-samples are practically identical. There are no statistically significant differences between the slope

values as confirmed by Z statistic calculations, (Miller and Kahn 1962, p.206). The three calculated values are, $Z_{A-B} = 0.16$, $Z_{B-C} = 0.67$ and $Z_{A-C} = 1.00$, and values of $Z = 1.96$ and $Z = 2.58$ are required to establish significant differences in slope at the 95% and 99% confidence levels. It is therefore justifiable to regard the sub-samples as homogeneous in terms of the rate of change of K relative to Rb, as represented by the (RMA) equation for the entire sample: $y = 1.69x - 0.24$. This regularity of the chemical changes underlines the transitional nature of the chemical gradient, as shown by the extensive overlap of the fields in figure 5.2.

Since it is possible to define all the metabasite samples by a single linear equation, valuable comparisons can be made with linear trends from other petrographic suites. In particular, a comparison can be made with the 'Main Trend' (MT) of Shaw (1968), which reflects normal magmatic K/Rb fractionation. Using covariance analysis, Shaw established a coded linear K/Rb trend of $y = 1.115x + 0.482$. This was calculated using an average of x on y and y on x regressions and not by the reduced major axis method. To allow a direct comparison with Shaw's Main Trend, the metabasite data have been recalculated and the regression values for the whole suite become as follows:

Averaged equation : $y = 1.77x - 0.32$.

This trend is plotted together with Shaw's Main Trend in figure 5.3. It is quite clear that the South Norway metabasites are characterised by a much more rapid decrease

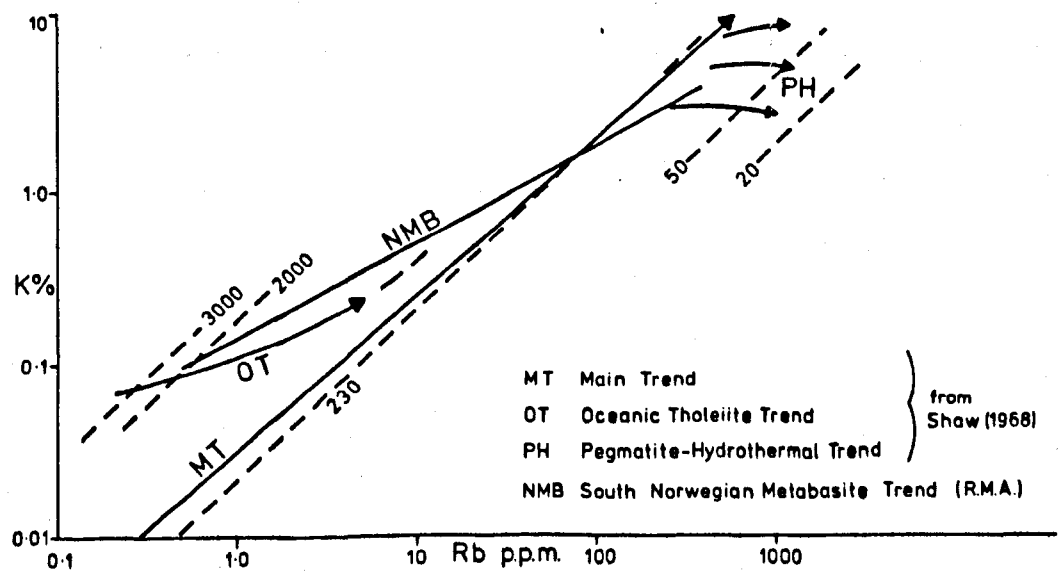


Figure 5.3: Comparison of the K/Rb trend in the metabasites with those established by Shaw (1968).

Table 5.1: K/Rb ratios: summary data.

Zone	1	2	3	4
A	381	235	309	337
B	404	258	381	374
C	860	488	866	889
All Rocks	476	263	370	452

1. = Mean (K/Rb); 2. = Mean K/mean Rb; 3. = Median (K/Rb);
 4. = Median K/median Rb.

in K/Rb with increasing K than the Main Trend.

It is therefore concluded that unless special igneous processes were operative, the metabasites do not reflect a normal igneous chemical variation pattern for K and Rb despite the clear field evidence documented earlier, and confirmed by Touret (1968) and Starmer (1972a). The results also conflict with the conclusions of Lambert and Heier (1968) and Collerson (1975), for Australian shield metabasites. These authors were unable to distinguish clear differences from established pre-metamorphic fractionation patterns, and the K/Rb ratios were believed to be inherited.

The present data for the metabasites are consistent with (i) the bulk chemical variation for each element, established in chapters 3 and 4, (ii) the absence of relationships for K and Rb with niggli mg, and (iii) the related trend established for the acid-intermediate charnockitic gneisses from Tromsø. (Cooper and Field 1977). Combined, these features are quite compatible with the concept of a metamorphically induced, vertical chemical fractionation between granulites and an originally overlying amphibolite facies zone, (e.g. Heier 1973 a, b.). Possible mechanisms for such fractionation are discussed in chapter 7, after consideration of the behaviour patterns of the remaining trace elements.

(ii) K/Ba.

The K-Ba diagram (figure 5.4), shows several features of interest. Firstly, there is a great deal of variation

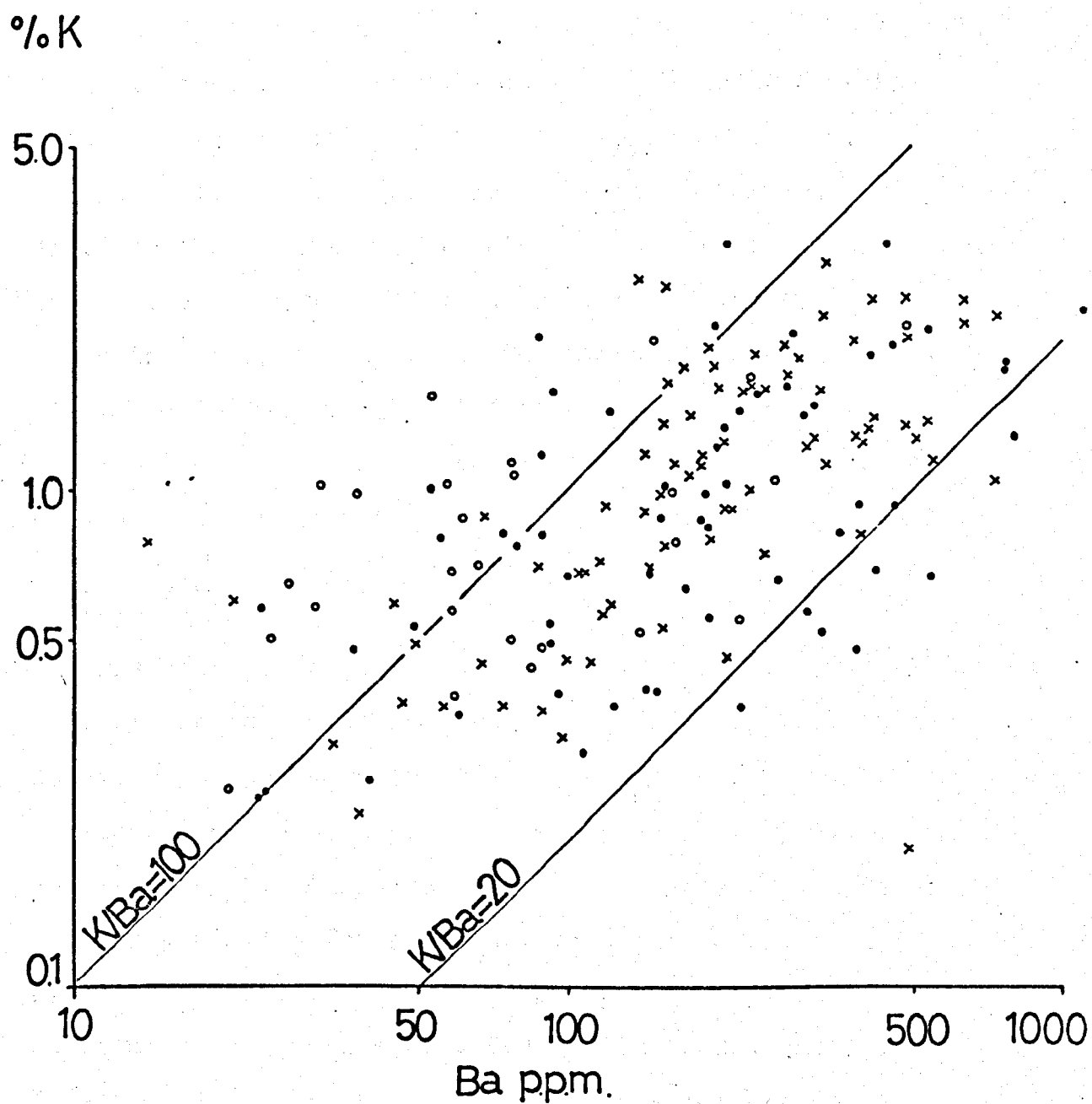


Figure 5.4: Scatter plot of K% v Ba ppm. Symbols as in figure 5.2.

in the K/Ba ratio, with a range of values from 3 to over 500. The majority of metabasites have K/Ba between 30 and 80, however. Secondly, the ratios for the zone C metabasites, whilst varying within the continuum of values are, overall, much higher than on the mainland. In zone C, K/Ba has mean and median values of 126 and 114 respectively, (table 5.2), and these Tromøy rocks have a somewhat displaced field on the scatter plot. Within the mainland transition, there is an increased K/Ba in the amphibolite facies, which is a reflection of the increased K₂O in this zone. The correlation coefficient for the mainland samples, (zones A and B; $r = 0.60$) is higher than that for Tromøy ($r = 0.39$), though both are significant at the 99% level.

(iii) Ba/Rb.

The mean Ba/Rb ratio for the whole suite is 10.3, although again there is a wide spectrum of values. In rocks with Rb below 30 ppm there is an average Ba/Rb of 14.6, and the points (figure 5.5) scatter evenly about this line of constant Ba/Rb. There is no regular change in the ratio with Rb variation for samples with under 30 ppm of this element. However, where Rb > 30 p.p.m. there is a noticeable and considerable decline in Ba/Rb, and this is also illustrated by table 5.3. This feature may be related to the behaviour of both Ba and Rb in entering the biotite lattice. Biotite will accept the Rb⁺ ion readily, but Ba²⁺ is less favoured (Nockolds and Mitchell 1948, Taylor 1965). Accordingly, an increase in modal biotite will tend to lower Ba/Rb.

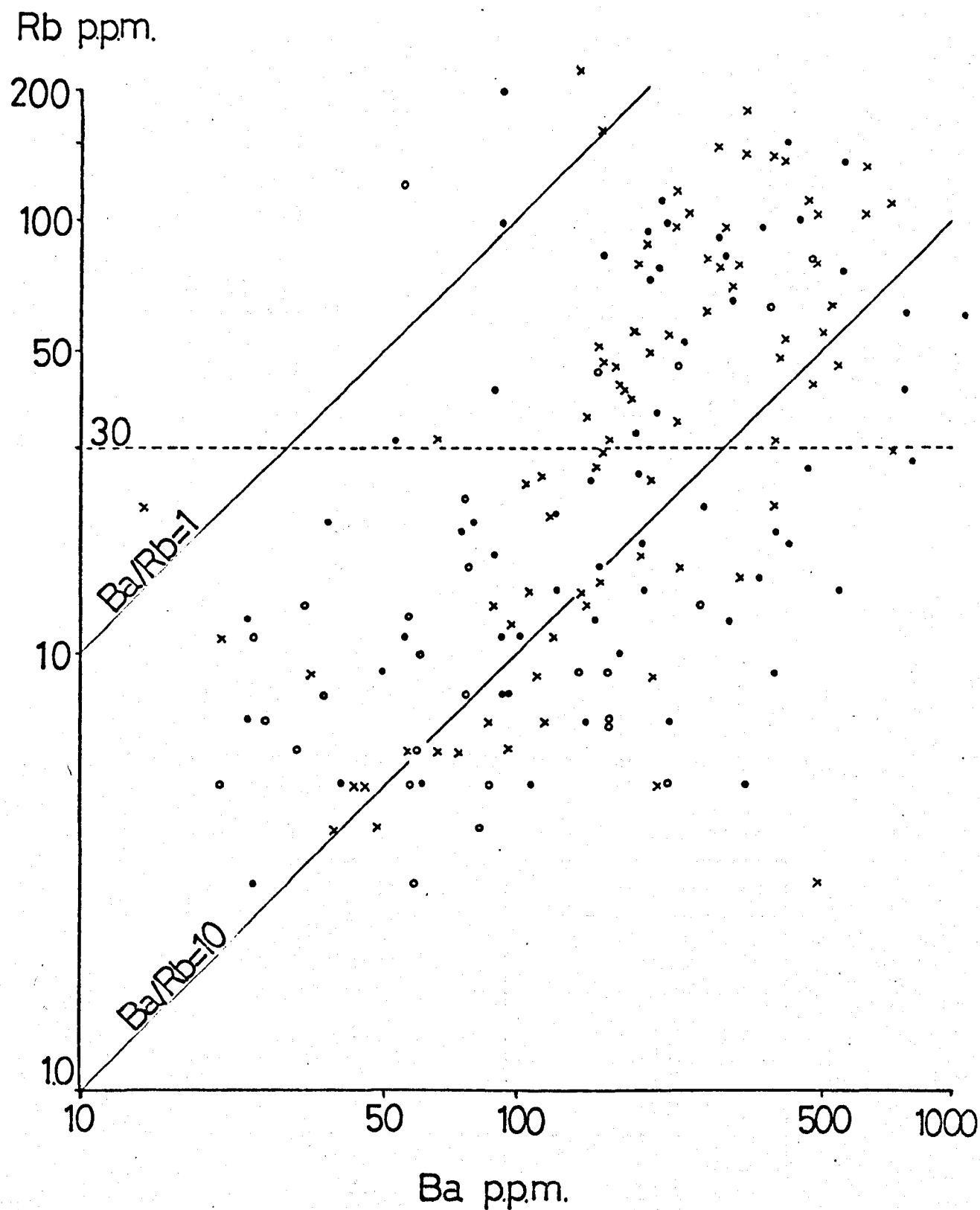


Figure 5.5: Scatter plot of Rb p.p.m. v. Ba p.p.m. Symbols as in figure 5.2. Broken line is 30 p.p.m. Rb.

Table 5.2: Alkali element ratios, by metamorphic zone.

Zone	K/Ba		Ba/Rb		Rb/Sr		Ba/Sr	
	x	m	x	m	x	m	x	m
A	69.3	60.1	9.5	5.5	0.62	0.17	1.6	1.2
B	66.0	52.7	11.3	6.0	0.47	0.11	1.8	1.0
C	125.6	114.2	10.6	6.0	0.16	0.05	0.8	0.5
All Rocks	76.9	60.1	10.3	5.8	0.48	0.11	1.5	1.0

x = mean

m = median

Table 5.3: Variation in Ba/Rb ratios by zone related to the whole-rock Rb abundance.

Zone	Over 30ppm Rb	Under 30ppm Rb
A	4.6	15.8
B	4.9	15.1
C	3.7	11.9
All Rocks	4.6	14.6

Values are mean Ba/Rb ratios.

(iv) Ba/Sr, K/Sr and Rb/Sr.

Figures 5.6, 5.7 and 5.8 illustrate the log-log plots for these three element pairs. Sr is slightly lower in overall abundance in zone C, and approximately constant within the mainland transition. Of the elements K, Rb, Ba and Sr, the latter shows proportionately the least variation in bulk chemistry. Thus, in each of these interelement relationships the trend of variation is dominated by the relatively large ranges of K, Rb and Ba, as are the quite remarkable ranges in ratio values for the whole suite. For example, Rb/Sr varies from 0.01 to over 5.0 and the mean of 0.47 is completely uncharacteristic for rocks of basaltic chemistry, with average SiO₂ under 50%. Rb/Sr values of ca. 0.05 are usual in fresh basalts, which also have a much more limited range than the South Norwegian metabasites. (Faure and Hurley 1963, Gast 1967). The K/Sr diagram shows variation broadly comparable with the data of Hart et al (1970) for Archaean metavolcanic rocks, with little change in Sr relative to large variations in K.

In table 5.2, the representative values for each alkali element ratio by zone are presented.

C. Discussion.

The alkaline element chemistry of the mainland granulite facies transition (zones A and B) is entirely consistent with the pattern of distribution established in other high grade terrains. K and Rb are depleted in zone B; Ba and Sr are not. Zone B is characterised by high K/Rb and Ba/Rb but low K/Sr, K/Ba and Rb/Sr relative to the

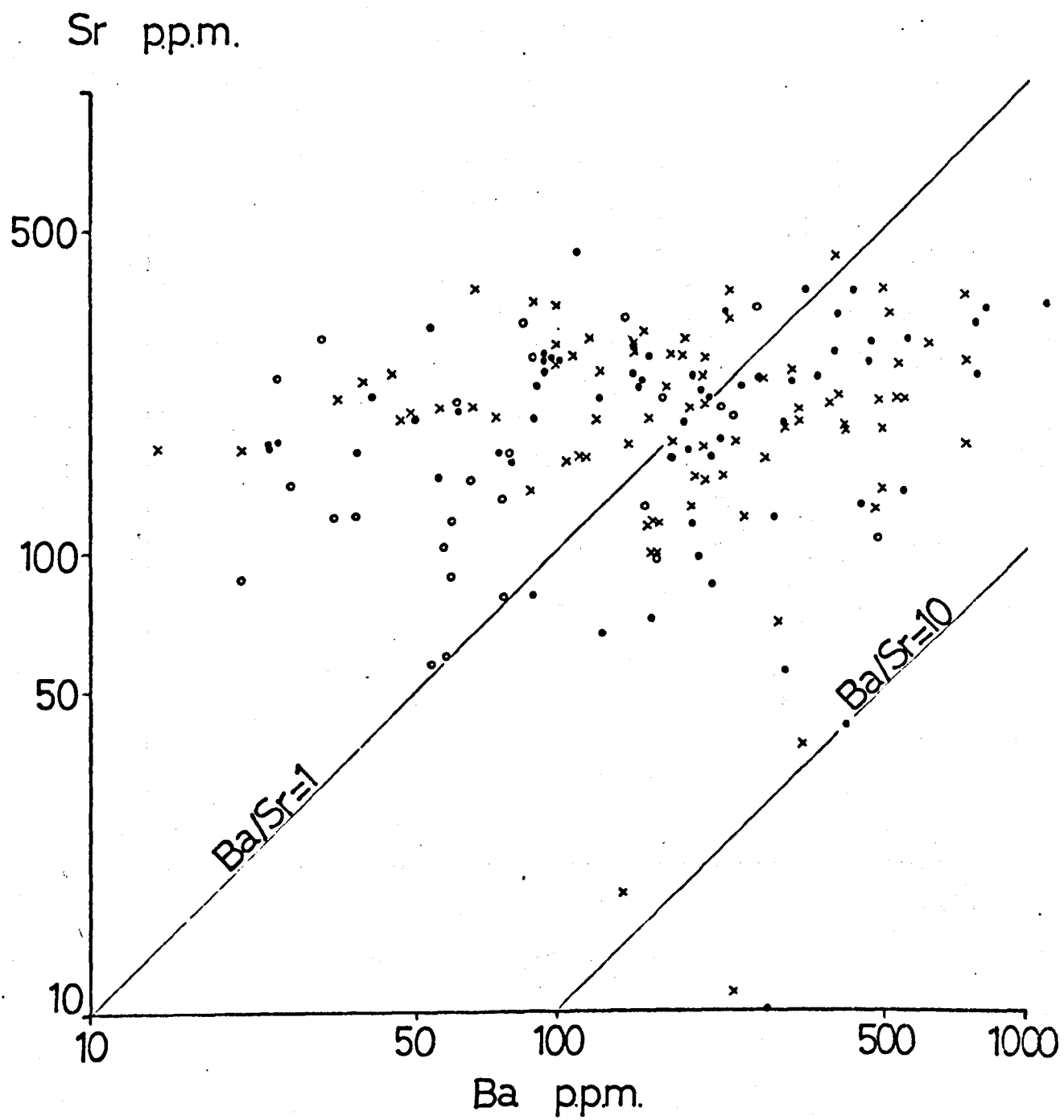


Figure 5.6: Norwegian metabasites: Sr ppm v. Ba ppm. Symbols as in figure 5.2.

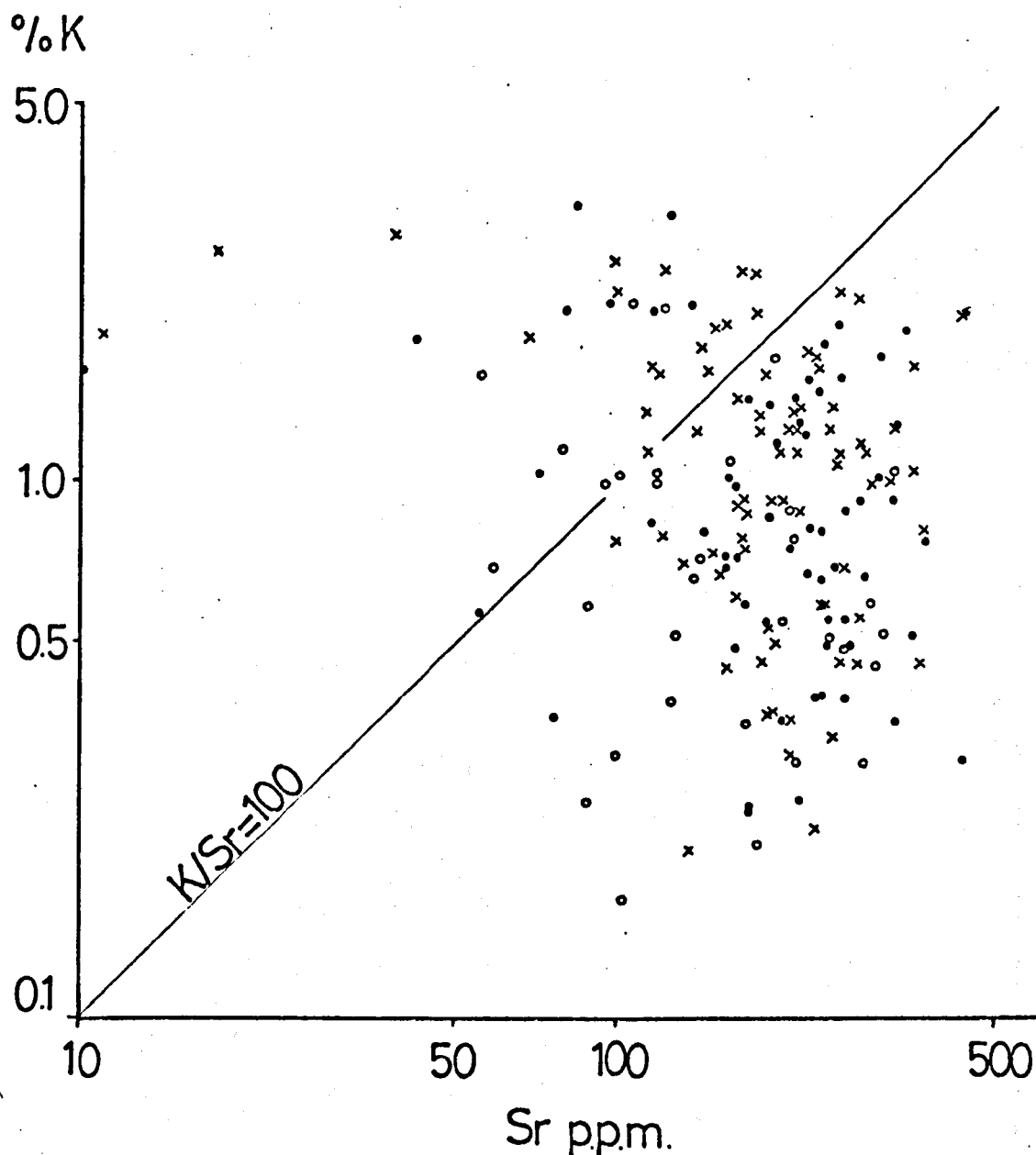
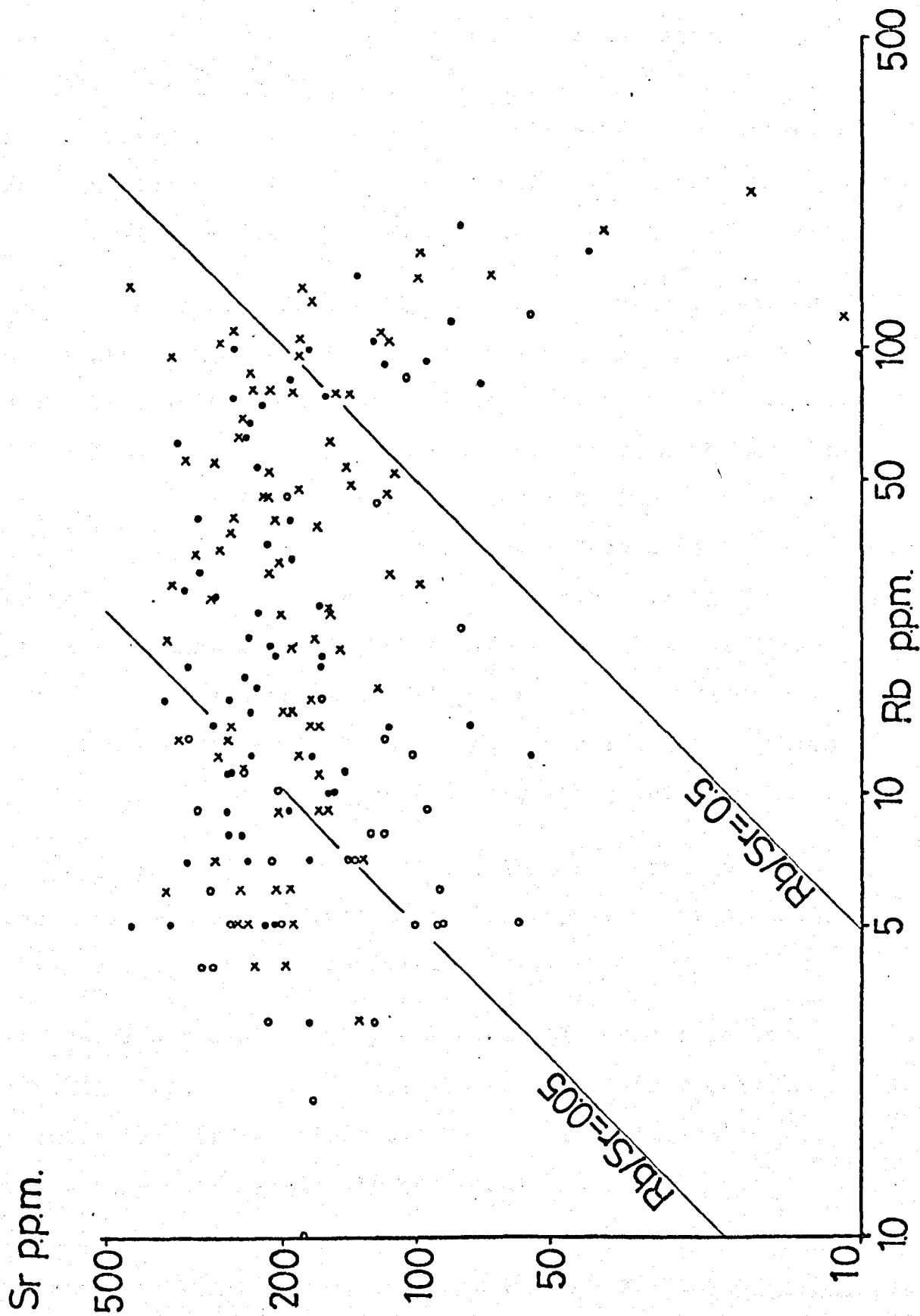


Figure 5.7: %K v. Sr ppm. Symbols as in figure 5.2.

Figure 5.8 (overleaf): Ba ppm v. Sr ppm. Symbols as in fig. 5.2,



amphibolite facies, (table 5.2).

For K-Rb, the metabasites exhibit a systematic fractionation with metamorphic grade over the entire terrain, with lowest K and Rb and highest K/Rb occurring in the Tromøy rocks. This is the first time that such a fractionation effect has been conclusively demonstrated for a low-intermediate pressure suite of basaltic chemistry.

A second aspect of alkaline element behaviour centres on the chemical discontinuity of zone C with respect to Ba and Sr levels. Thus, the trends to relatively lower K/Sr, K/Ba and Rb/Sr values and higher Ba/Rb in the mainland granulites (zone B) are not continued into Zone C, the highest grade portion of the terrain. Zone C ratios for K/Sr, Ba/Rb and Rb/Sr are intermediate between the values for zones A and B (Table 5.2), whilst the K/Ba in Zone C is the highest of all groups. These features reflect the declines in both Ba and Sr in Zone C, of which the decrease in Ba is proportionately the greater.

It is possible that these deficiencies represent a localised metamorphic redistribution, (perhaps even genetically separate from the K-Rb redistribution).

Cooper and Field (1977) have recently described the chemical character of the acid-intermediate charnockitic gneisses from Tromøy (Zone C), the complex into which the metabasites were originally intruded. Ba and Sr show significantly lower levels in the Tromøy charnockitic gneisses than in their equivalents in the adjacent mainland terrain. The Ba and Sr levels for this related suite

were reported by Beeson (1971). There is little overall variation in these elements in the gneisses of Zones A and B, and abundance levels are normal relative to other terrains. (Field, in prep.).

Consequently, parallel behaviour (i.e. relative deficiency on Tromøy) for both Ba and Sr exists in two genetically distinct lithologies - the metabasites and their gneissic wall rocks. On Tromøy, both Ba and Sr show low levels compared with metabasic equivalents, and these combined data suggest that these relative deficiencies represent actual net reductions in element abundance.

Further evidence for Ba mobility is circumstantial. The correlation coefficients for K vs. Ba and Rb vs. Ba are lower for the Zone C samples as a group than for the remainder of the metabasites (Zones A + B), and this may reflect the greater breakdown of a primary distribution in Zone C.

Finally, it should be noted that Field and Elliott (1974), in describing chemical changes between hyperite and amphibolite in Bamble, suggested variable mobility of both Ba and Sr. Regular distributions of both elements in the hyperites were changed into irregular ones in the amphibolite derivatives, though no addition or subtraction of material could be isolated.

D. Conclusions.

- (1) The chemical changes in the mainland transition are consistent with those established in other "depleted" granulite terrains.

- (2) Metasomatic fractionation of K and Rb has occurred in the metabasites, with K/Rb increasing with increased grade of metamorphism. Rb is fractionated relative to K. The linear K/Rb trend is oblique to Shaw's (1968) Main Trend, and is not a primary igneous feature.
- (3) Ba and Sr are reduced in zone C, reflecting possible metasomatic depletion at the highest grades of metamorphism.

CHAPTER 6: The "presumed immobile" elements - Ti, P, Zr, Y, Nb.

A. Introduction.

The present interest in the geochemistry of Ti, Zr, P, Y and Nb arises mainly from the work of Cann (1970) and Pearce and Cann (1973), who proposed a chemical scheme for relating basaltic rocks to their tectonic environments. Using a Ti-Zr-Y diagram, for example, they were able to discriminate between "within-plate" (continental or oceanic) basalts, and the magmas produced at plate margins. This work has been extended by Floyd and Winchester (1975) who used a set of simple binary plots incorporating these elements to attempt distinctions between fresh tholeiites and alkalic basalts. The discrimination diagrams are applicable to basic dykes as well as basaltic lavas.

An essential premise in these discrimination methods has been that the elements are considered to be immobile during alteration. It is well recognised that under sea-floor alteration or spilitization many major and trace elements may be redistributed (e.g. Vallance 1960, 1969; Matthews 1971, Hart 1969, 1970). However, in several studies of basaltic rocks no evidence of mobility for Ti, Zr, P, Nb and Y has been noted. (Nicholls and Islam 1971, Bloxham and Lewis 1972, Pearce and Cann 1973). Even elements known to be potentially mobile, when used in diagrams in conjunction with 'immobiles', have yielded data adequate for the distinction of magma types. Thus the $K_2O-TiO_2-P_2O_5$ plot (Pearce et al. 1975) has been successful in separating oceanic and continental basalts, and schemes involving Sr

have also been used effectively (Pearce and Cann 1973). However, low-grade metamorphism can cause extensive redistribution of K_2O and Sr and result in trends of variation which cross the "discrimination boundaries" within these tri-element diagrams. (Smith and Smith 1976).

In a logical extension of the previous work, Winchester and Floyd (1976) have applied magma type discrimination methods to metamorphosed basic igneous suites. This again assumes that the elements used have been chemically stable, and a second important qualification is that inherited trace element distribution patterns in basalts have remained relatively constant through geological time. Winchester and Floyd (1976) examined eight suites of "amphibolites" on the following discrimination diagrams (1) TiO_2 - Y/Nb (2) P_2O_5 -Zr (3) TiO_2 - Zr/ P_2O_5 and (4) Nb/Y - Zr/ P_2O_5 . The "amphibolites" were mainly from the amphibolite facies, but included metabasites of greenschist facies, (Misra and Griffin 1972) and retrogressed granulites (Drury, 1974). The P_2O_5 - Zr and TiO_2 - Zr/ P_2O_5 plots indicated that the amphibolites from the Lofoten islands could be ascribed to an alkalic source magma. This conclusion had also been reached by Misra and Griffin (1972), on different grounds. Of the remaining metabasic suites, all except the Dalradian metabasites (e.g. Wilson and Leake 1972) were assigned to a tholeiitic magma source. The high TiO_2 and P_2O_5 with low Y/Nb ratios of the Dalradian series suggested an alkalic source for this group, although

the series could not be unequivocally separated from tholeiites. From independent evidence, Graham (1976 a, b) has shown the Dalradian metabasites to have strongly tholeiitic tendencies. He has attributed the trend into an alkaline field on the Floyd-Winchester diagrams as being due to exceptional magmatic differentiation.

This case illustrates one of the difficulties in using discrimination diagrams for metabasic rocks. Graham (1976b) concluded that comprehensive petrochemical studies may be needed to achieve a confident original magma-type classification.

A further problem is that it may not always be valid to consider these elements as immobile, especially in the higher grades of metamorphism. It has been demonstrated in the South Norway terrain that P_2O_5 and Zr can increase during amphibolitization of gabbro (Elliott 1973, Field and Elliott 1974).

In this chapter the Pearce-Cann and Floyd-Winchester diagrams are applied to the metabasites. Particular difficulties in interpretation occur for the following reasons:

- (i) The rocks have been subjected to very high-grade metamorphism.
- (ii) Substantial metasomatic effects in the metabasites have already been noted (Chapter 5; Field and Clough 1976).
- (iii) The possibility of Zr and P_2O_5 variation during metamorphism (Field and Elliott 1974).

- (iv) The inconclusive nature of the alkalis - SiO_2 plot, described in chapter 3.
- (v) The differentiated nature of the suite, with increased abundances of Zr, P, Ti, Y and Nb associated with the iron-enrichment of the metabasites.

B. Y/Nb ratios.

The data of Pearce and Cann (1973) indicate that the Y/Nb ratio is useful in distinguishing fresh alkalic basalts from tholeiites. Alkalic continental basalts are characterised by Y/Nb of <1.0 while tholeiites have values >1.0 .

The Y/Nb data for the metabasites are presented in figures 6.1 and 6.2, and illustrate a wide span of present day ratios. 22% of the suite have an Y/Nb of less than 1.0, and as figure 6.2 indicates, most of these rocks have Y under 15 ppm.

Whilst this proportion of rocks is "alkalic" according to the criterion above, the majority of rocks have tholeiitic or transitional-tholeiitic Y/Nb values. (The mean Y/Nb for all rocks is 1.72; median = 1.54). Low ratios usually reflect relatively low Y, and not high Nb (figure 6.2).

C. The Zr-Ti/100 - Y.3 diagram (Pearce and Cann 1973).

The South Norwegian metabasites are plotted on this diagram in figure 6.3, while the fields of variation for each zone are outlined in figure 6.4, along with the Pearce-Cann discrimination fields.

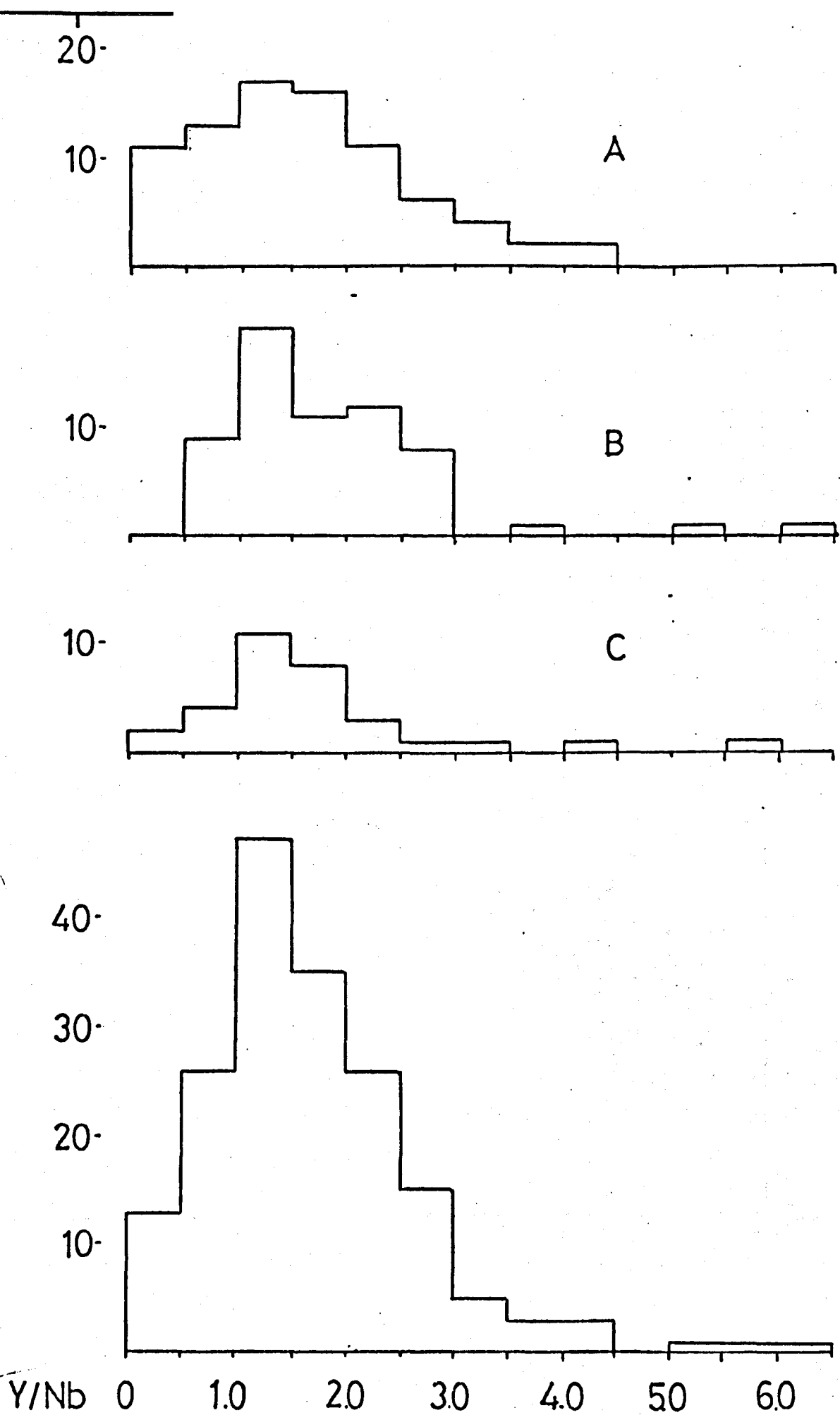


Figure 6.1: Histograms of Y/Nb in the metabasites. A, B & C refer to metamorphic zones.

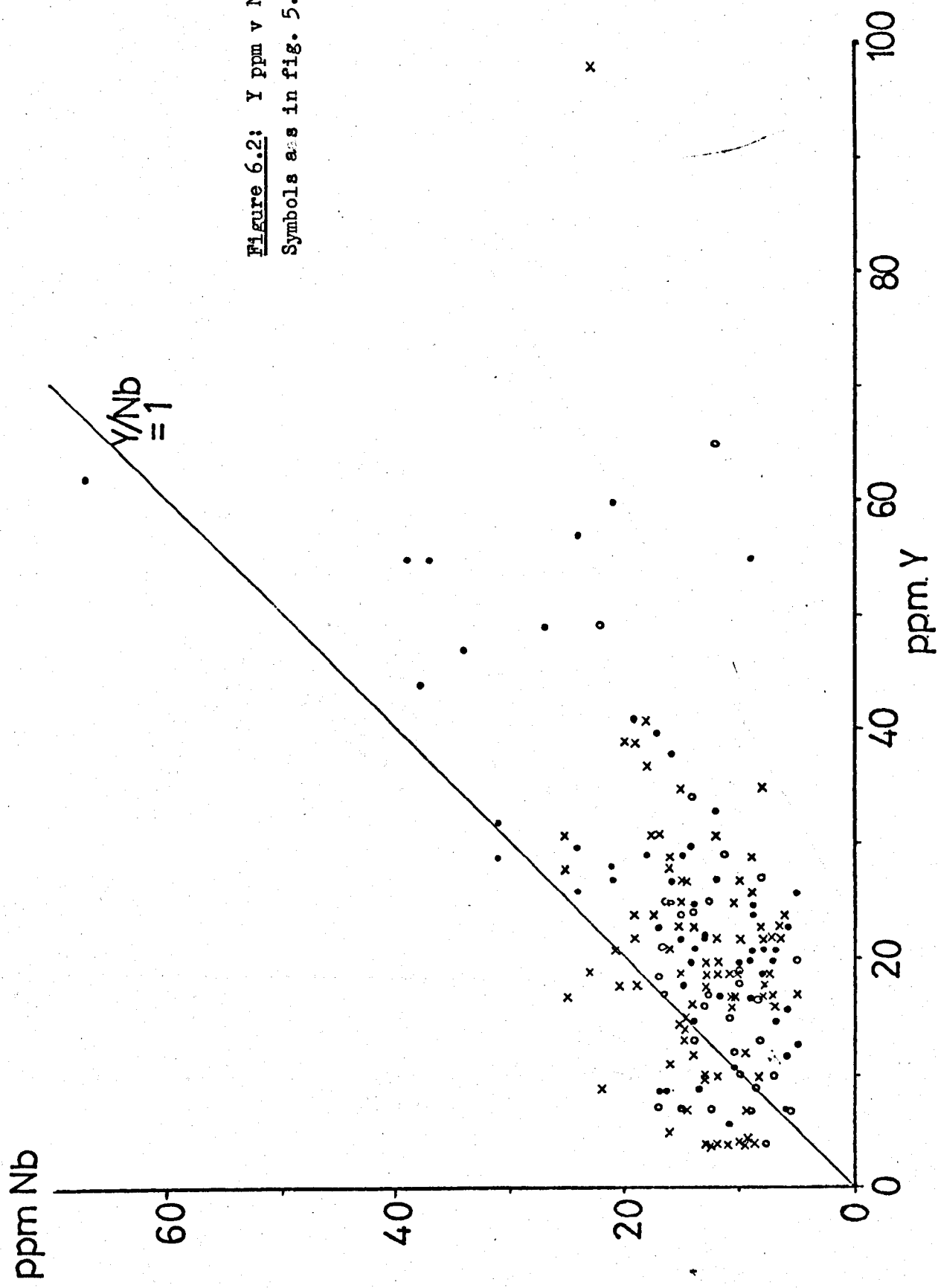


Figure 6.2: Y ppm v Nb ppm
Symbols as in fig. 5.2.

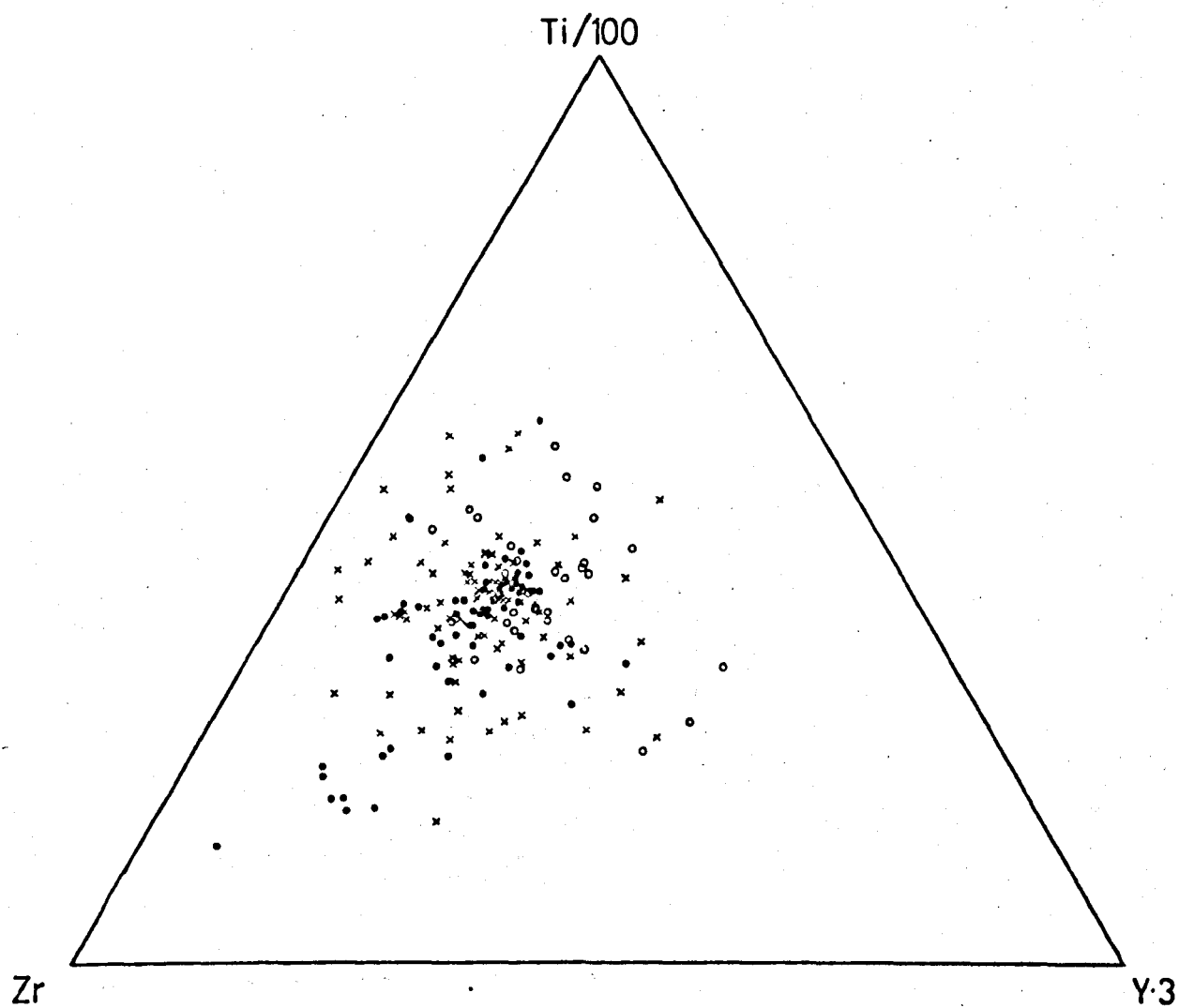


Figure 6.3: Ti/100-Zr-Y3 diagram. Symbols as in figure 5.2.

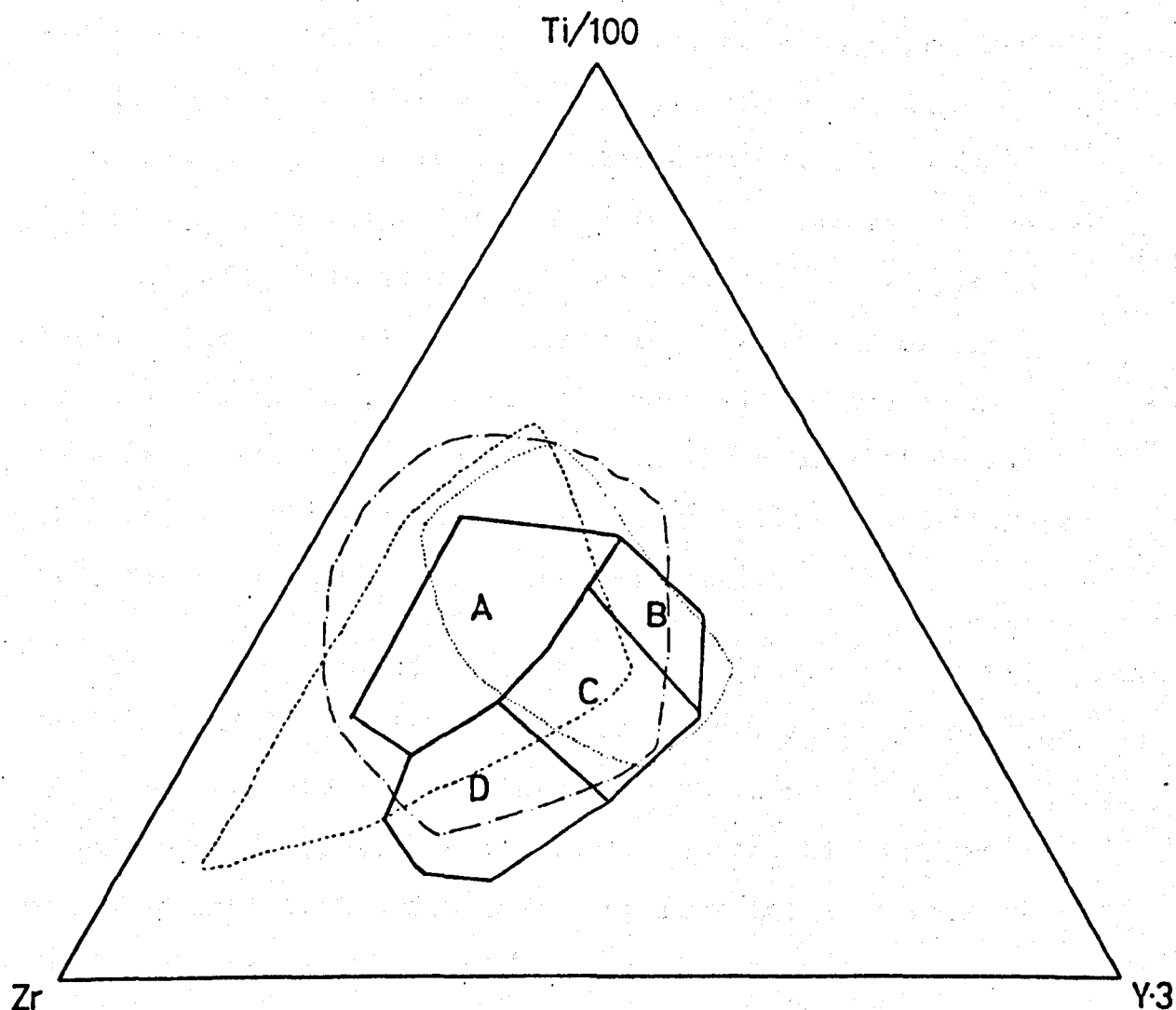


Figure 6.4: Schematic Ti/100-Zr-Y₃ diagram after Pearce and Cann (1973). A = Within plate basalts, including continental basalts. B. = Low potash tholeiites C = Ocean-floor basalts (+low K tholeiites). D = Calc-alkali basalts. Broken lines represent fields of variation for metabasites: Zone A = dashed/dotted line; Zone B = dashed line; Zone C = dotted line.

There is a well-defined cluster of points within the Pearce-Cann field for "within-plate" (continental or oceanic) basalts. 70% of the metabasites fall in this division, and there is a convergence within the area at approximately 20% (Y.3) - 40% (Ti/100) - 40% (Zr). However, the remaining 30% of the rocks scatter extensively. This variation is equally distributed in the triangle and there are sets of points trending to each of the three apices. Thus, whilst much of the scatter is outside any of the Pearce-Cann fields, some points occur within the calc-alkaline basalt area and the 'ocean floor basalt' area. (Figure 6.4). The exclusive low-K tholeiite field (Figure 6.4, field B) is virtually unrepresented.

There are some differences between the fields of variation for the individual zones, A, B and C in this diagram. The main features are the prominence of the zone B trend towards the Zr apex, and the fact that the highest grade rocks of zone C plot furthest away from the same corner. The zone B trend is caused by exceptional Zr levels of over 500 p.p.m. in 7 samples. Abundance levels for Zr in Zone C are relatively low, explaining the field of variation for Tromøy in this diagram.

D. Floyd/Winchester Diagrams.

(i) The TiO₂-Zr plot (figure 6.5).

There is considerable overlap in this diagram between the continental tholeiite field and the

alkalic basalt field (Floyd and Winchester 1975, figure 1(c).) These authors suggested that tholeiites usually develop a "proportional" trend (constant Ti/Zr) which, upon differentiation to high levels of Ti and Zr, tends to flatten out. Continental alkali basalts, with generally higher levels of both elements, show a "horizontal" trend, having a wide range of Zr relative to little change in TiO_2 . The metabasite data (figure 6.5) is most consistent with the behaviour of continental tholeiites, although a large proportion of metabasites (50%) have TiO_2 greater than 1.8%, a value considered high for tholeiites by Floyd and Winchester (1975). The metabasite trend is not strictly proportional, showing a slight decline in TiO_2/Zr with increased abundance levels, but is similar to both the Rhodesian Karroo basalts (Cox et al 1967), and the Baffin Bay tholeiites (Clarke 1970).

(ii) TiO_2 - Y/Nb (figure 6.6).

Whilst most metabasite samples again lie in the field for continental tholeiites, some of the most differentiated rocks describe a 'vertical' trend, characteristic of fresh alkali basalts. The average Y/Nb for these differentiates is over 1.0, however, and the samples with Y/Nb lower than unity are also low in TiO_2 . This latter group therefore plot beneath the alkalic basalt fields of Floyd and Winchester (1975).

(iii) P_2O_5 - Zr. (figure 6.7)

The majority of points plot beneath the alkalic-

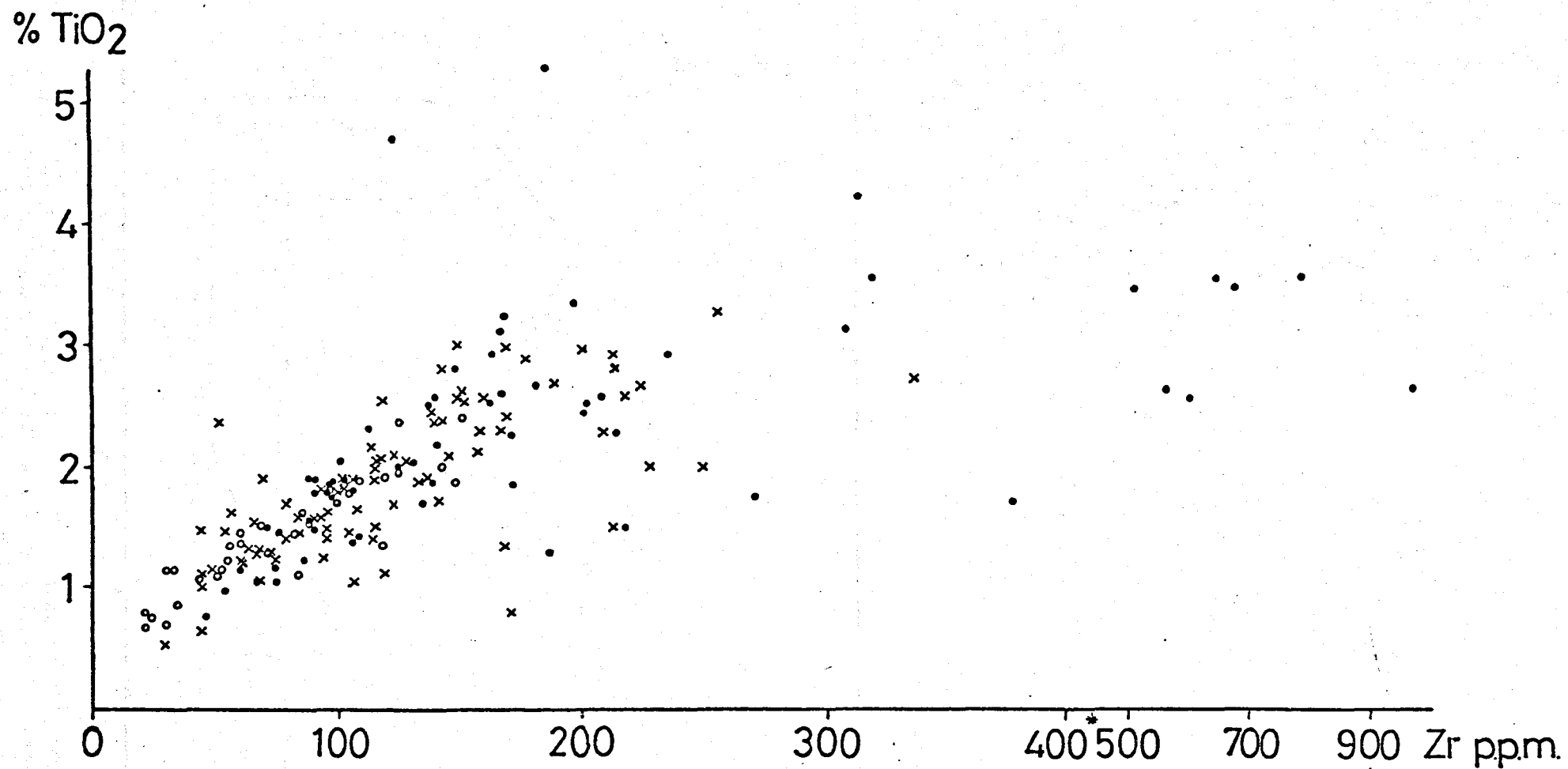


Figure 6.5: TiO₂ wt. % v. Zr ppm. Symbols as in figure 5.2 . Zr scale non-linear at high values.

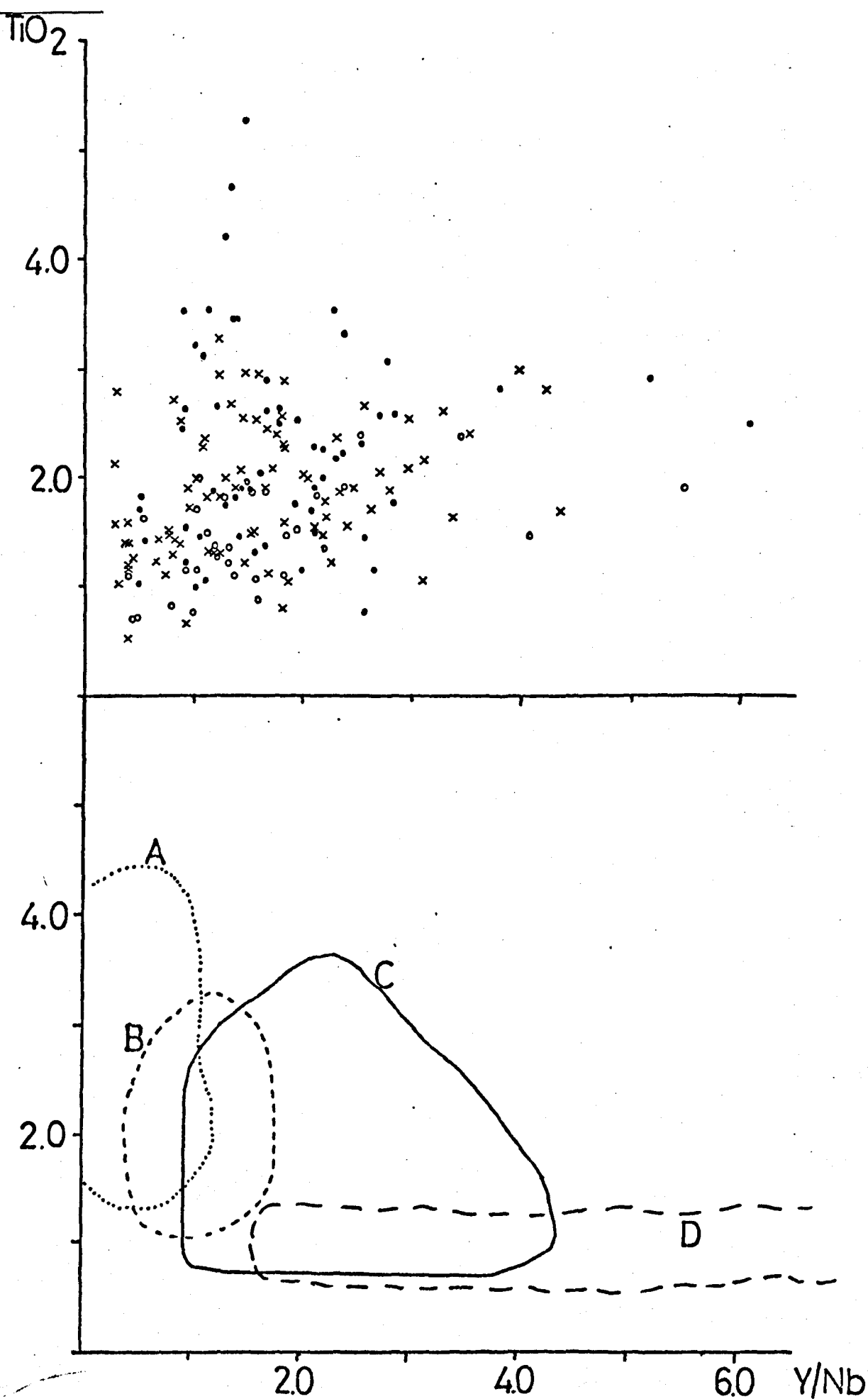


Figure 6.6: TiO_2 v. Y/Nb . Symbols as in fig. 5.2. Fields of variation in lower diagram are from Floyd & Winchester (1975): i.e. A = Oceanic alkali basalts. B = Continental alkali basalts. C = Continental tholeiites. D = Oceanic tholeiites.

tholeiitic divide, but there is a trend across this division combined with an increased scatter, into the "alkalic" field. These features are consistent with the progressive enrichment of both Zr and P_2O_5 with differentiation. The zone C samples partially separate out from the rest of the metabasite suite due to their relatively low Zr abundance.

(iv) $TiO_2 - Zr/P_2O_5$ (figure 6.8) .

From the criteria of Floyd and Winchester (1975) and Winchester and Floyd (1976), the alkali-tholeiitic divide in this plot bisects the metabasite data, and therefore provides no direct discrimination of magma type. A similarly indistinct distribution is shown by Dalradian metabasites (Wilson and Leake 1972, Graham 1976 a, b), which have apparent alkalic basalt affinities due to extreme TiO_2 enrichment during differentiation.

(v) $Nb/Y - Zr/P_2O_5$ (figure 6.9)

This diagram also fails to provide a complete magma type discrimination for the metabasites, although the majority of points fall in the tholeiitic field. The features are again analogous to the behaviour of the Dalradian suite (Wilson and Leake 1972).

E. Diagrams utilizing "mobile" elements.

Pearce et al (1975) have proposed using the $TiO_2 - P_2O_5 - K_2O$ diagram as a method of discriminating between oceanic and continental basalts, and have suggested that obviously continental suites displaying oceanic affinities in this diagram may represent incipient fragmentation and

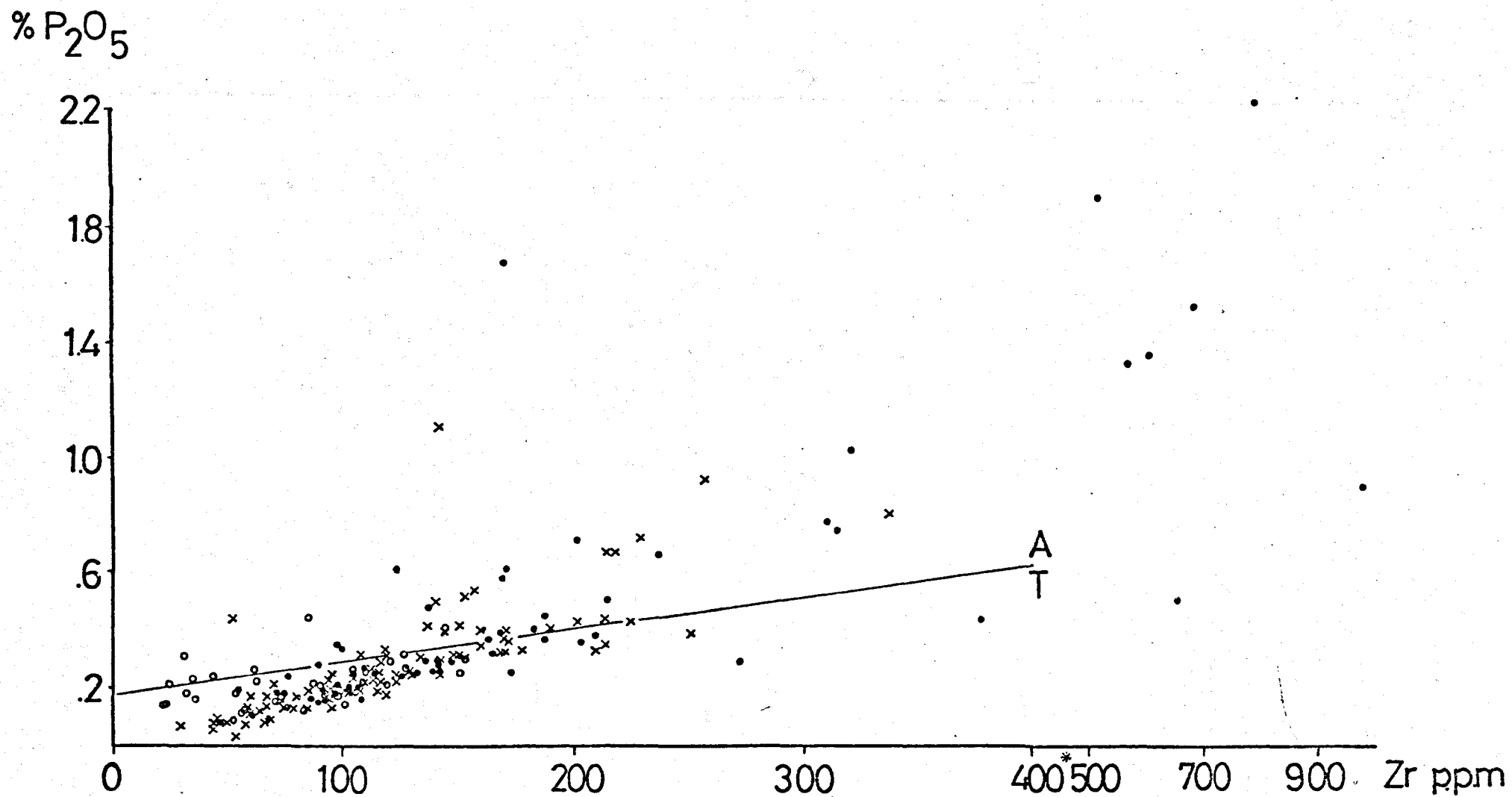


Figure 6.7: P_2O_5 v. Zr ppm. Symbols as in fig. 5.2. Zr scale non-linear at high values. A/T = alkaline-tholeiitic divide from Winchester & Floyd (1976).

% TiO₂

Figure 6.8: TiO₂ - Zr/P₂O₅.

Symbols as in fig. 5.2.
Zr/P₂O₅ scale non-linear
at high values. A/T =
alkaline-tholeiitic
division.

50

40

30

20

10

0

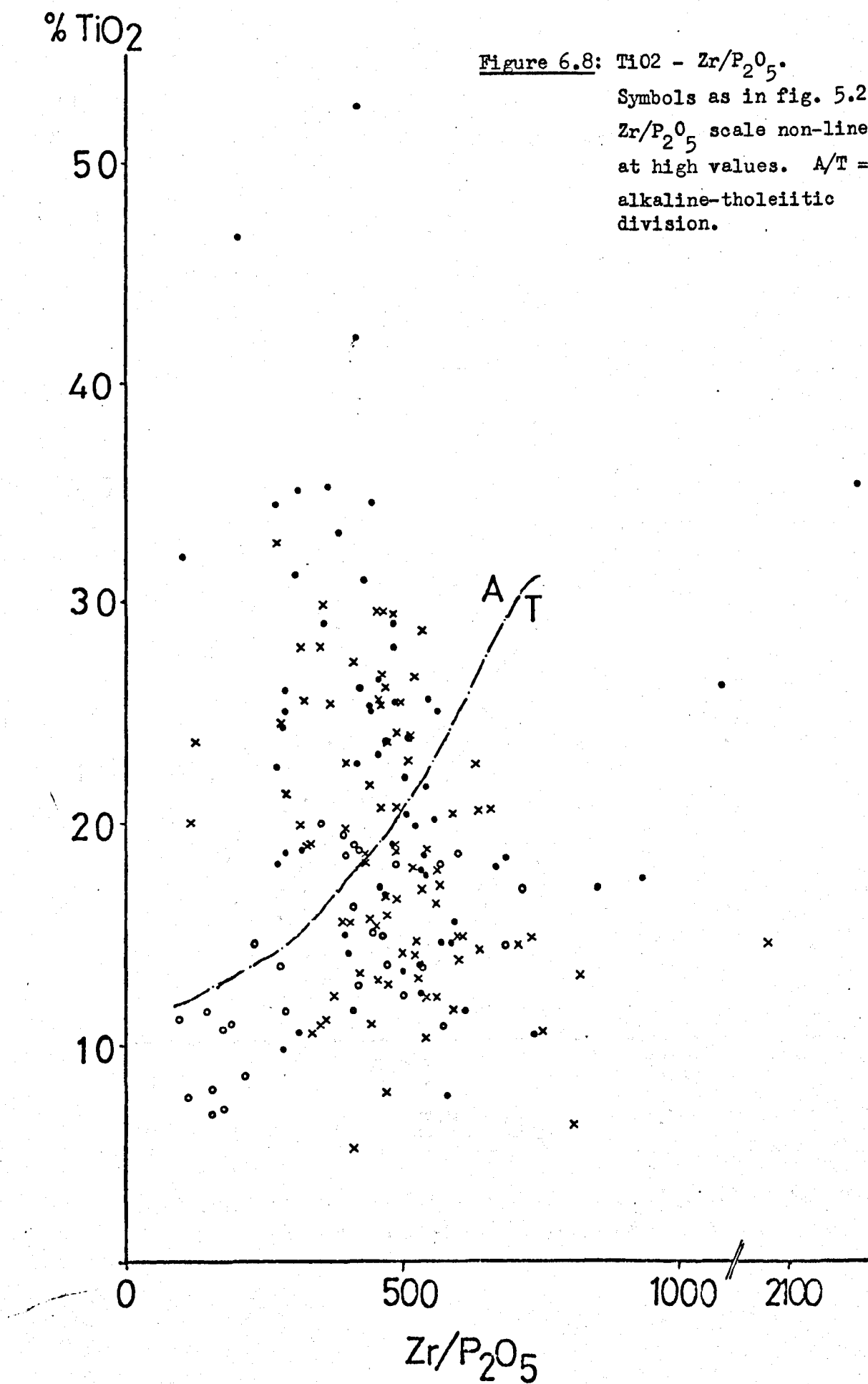
500

1000

2100

Zr/P₂O₅

A/T



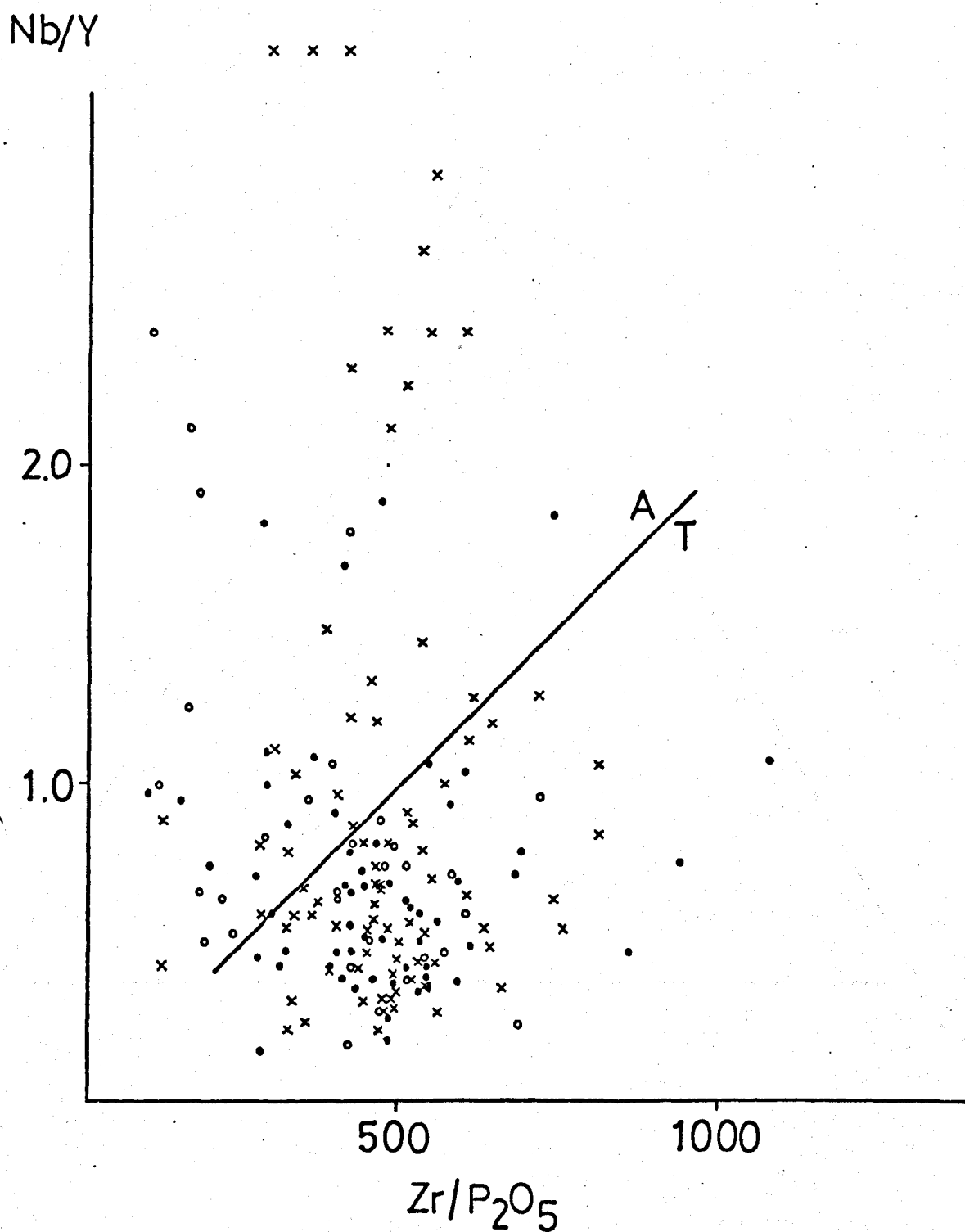


Figure 6.9: Nb/Y v. Zr/P₂O₅. Symbols as in fig. 5.2. A/T = alkaline-tholeiitic division of Winchester & Floyd (1976).

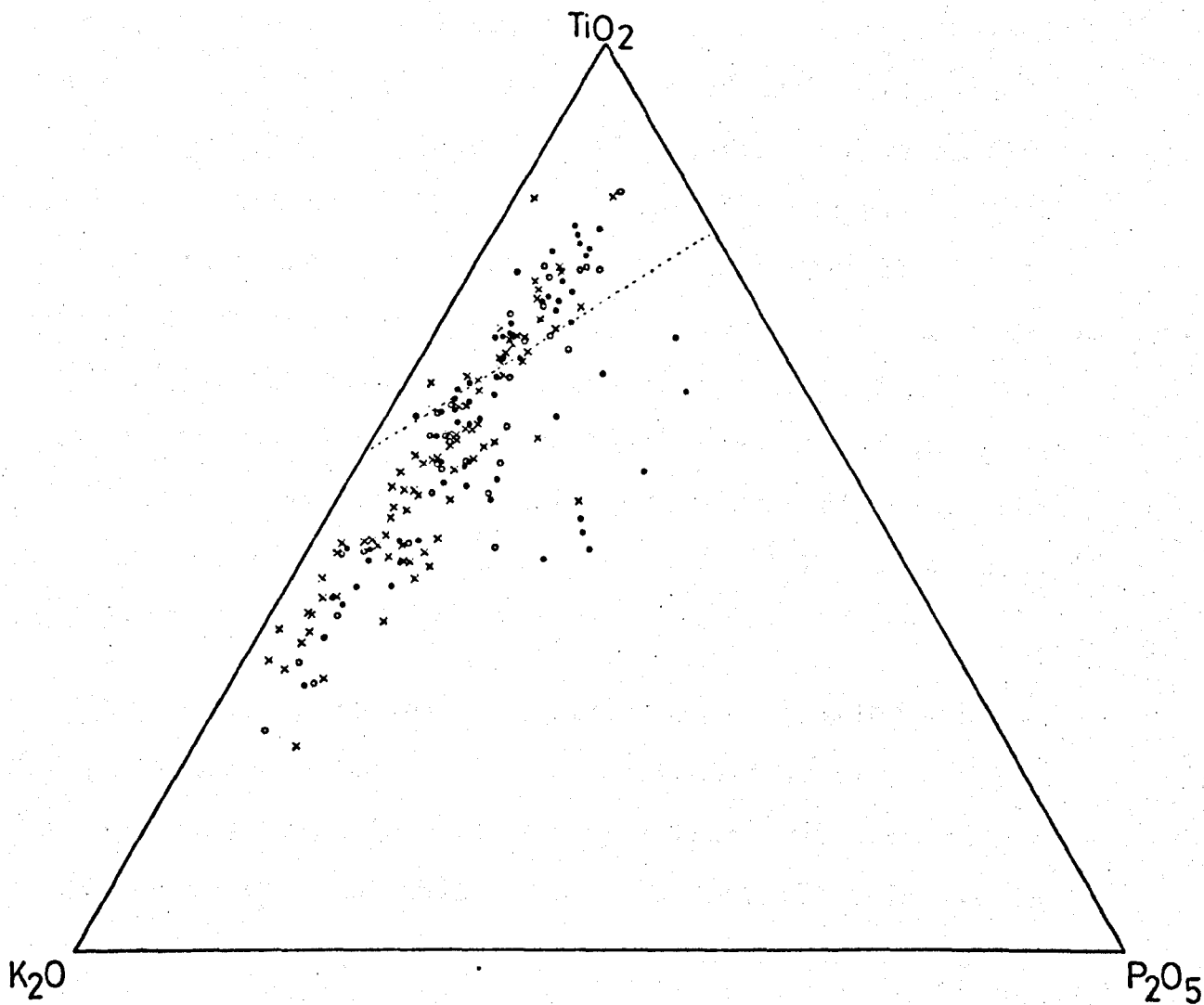


Figure 6.10: $\text{TiO}_2\text{-K}_2\text{O-P}_2\text{O}_5$ plot of the Norwegian metabasites
 Symbols as in figure 5.2.
 Dotted line separates fields of oceanic and non-oceanic basalts (Pearce et al. 1975). Field at TiO_2 apex is oceanic.

ocean-floor generation. Potash mobility and the differentiated nature of the suite make the interpretation of figure 6.10 hazardous. Whilst the $\text{TiO}_2/\text{P}_2\text{O}_5$ ratio is relatively constant in the metabasites, the spread of values reflects the variable K_2O . The overall trend of the metabasites is therefore from the "oceanic" field of Pearce et al (1975) towards the K_2O apex. The occurrence of a minority of points within the oceanic field could theoretically reflect igneous differentiation, with TiO_2 enrichment the dominant factor. Alternately, although the environment of intrusion of the metabasites was clearly not "oceanic", genesis of the rocks may possibly have occurred during an episode of continental rifting, according to the interpretation of Pearce et al (1975).

A discrimination diagram including Sr ($\text{Ti}/100 - \text{Zr} - \text{Sr}/2$), (Pearce and Cann 1973) is presented as figure 6.11. The wide scatter is focussed along a line away from the Sr apex, suggesting that this element is variable relative to an approximately constant Ti/Zr . The spread of values crosses the boundaries proposed by Pearce and Cann (1973) for discrimination purposes, and confirms that this diagram is of doubtful value in altered or metamorphosed suites. Similar conclusions were reached by Smith and Smith (1976). A "minority trend" towards the Zr corner reflects the samples with extreme values of this element due to fractionation.

Analogous features are shown by the $\text{Ti}/100 - \text{Zr} - \text{Ba}/2$ plot, and the scatter of points is even more evident in this diagram (figure 6.12).

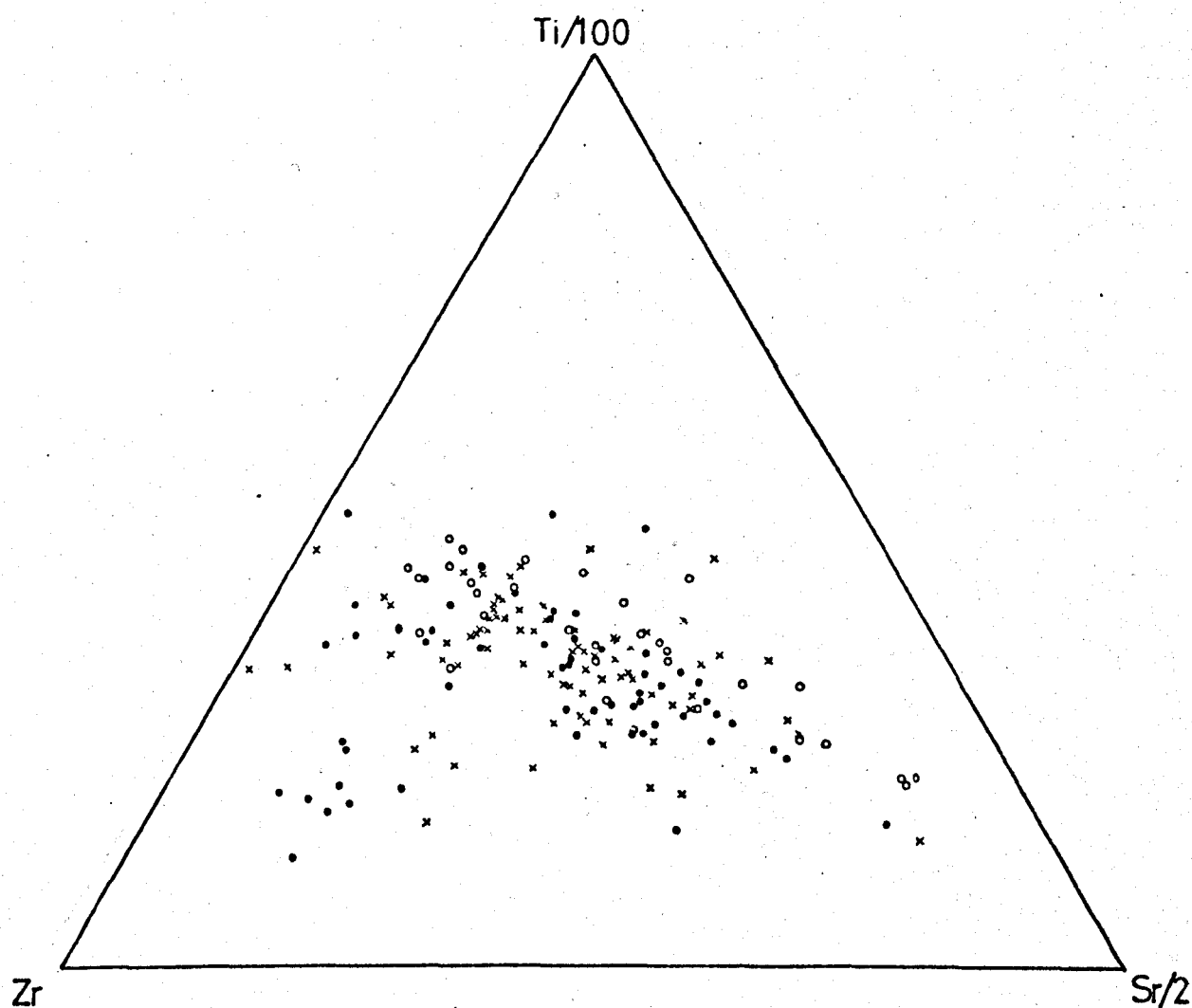


Figure 6.11: $Ti/100$ - Zr - $Sr/2$ diagram. Symbols as in figure 5.2

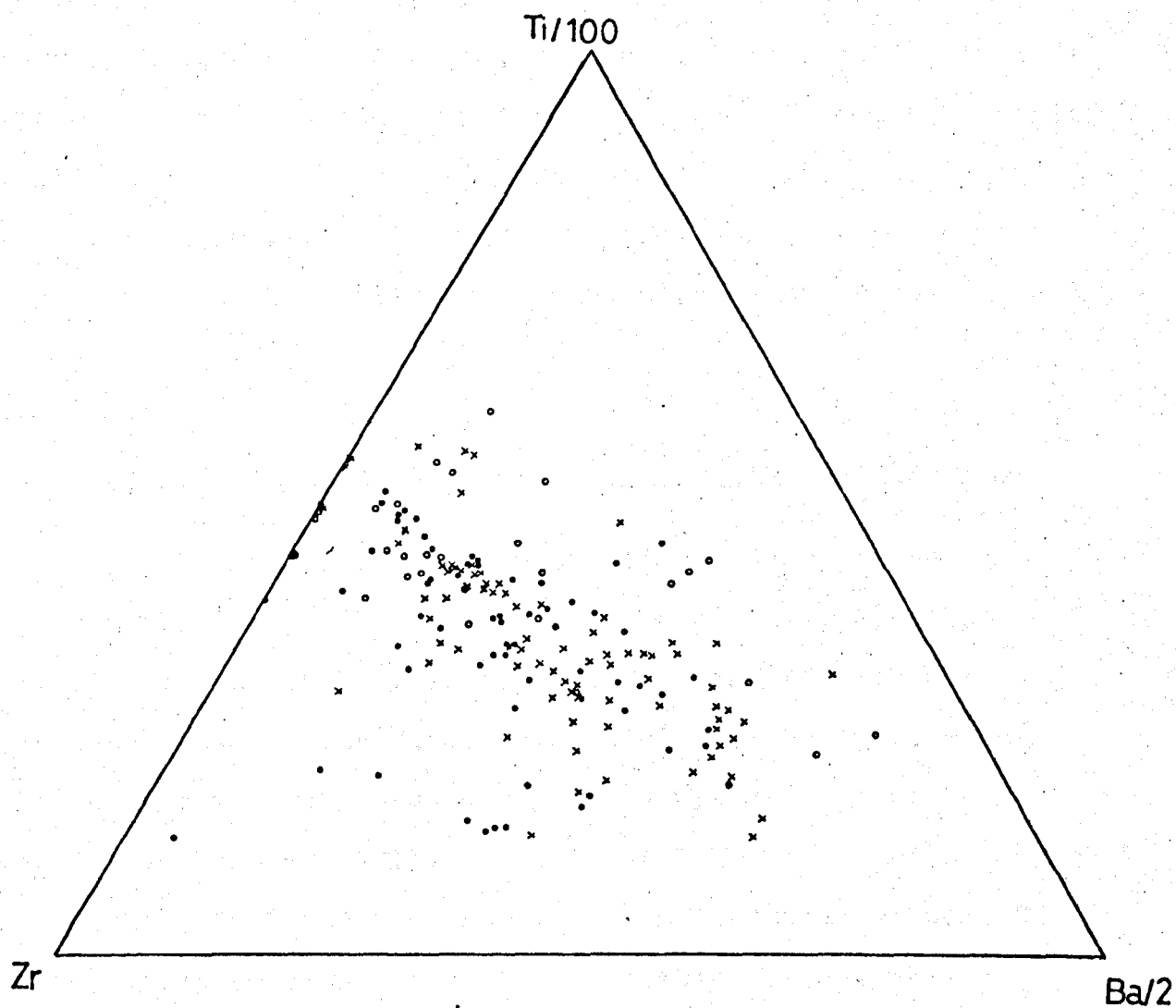


Figure 6.12: Ti/100-Zr-Ba/2 diagram. Symbols as in fig. 5.2

Trends of variation across triangular plots towards the apex representing a "mobile" element might be anticipated if the other two elements defined a constant or relatively constant ratio, and were themselves "immobile". Although such an assumption for Zr and P_2O_5 is not necessarily valid at high grades of metamorphism (c.f. Field and Elliott 1974), figures 6.10 - 6.12 provide additional evidence that K_2O , Ba and Sr have been metamorphically distributed.

F. Discussion.

(i) The tholeiitic/alkalic affinities of the metabasites.

The alkalis versus SiO_2 plot (figure 3.20) showed the present chemistry of the suite to be dominantly alkalic relative to the tholeiitic-alkalic division of MacDonald and Katsura (1964). The diagram is unreliable however, when altered and metamorphosed basic rocks are considered (e.g. Irvine and Baragar 1971). In chapter 3 it was concluded that soda enhancement had occurred in the metabasites of zone C, while K metasomatism has been established for the entire terrain (Field and Clough 1976).

In contrast to the $(Na_2O + K_2O)$ - SiO_2 diagram, the AFM plot shows a strong iron-enrichment trend, consistent with a tholeiitic affinity. The Floyd-Winchester plots described in this chapter also suggest a tholeiitic magma source for the metabasites, although a significant minority of rocks trend into alkalic fields, in each diagram.

It has been recently demonstrated that spurious alkalic

basalt trends can be generated in differentiated rocks from a tholeiite source. (Graham 1976b). For example, in the TiO_2 - $\text{Zr/P}_2\text{O}_5$ diagram, the Dalradian metabasaltic rocks (Wilson and Leake 1972, Graham 1976b) trend across the alkaline-tholeiitic divide as positioned by Floyd and Winchester (1975). The less-differentiated samples plot within the tholeiite field, whilst more evolved rocks trend vertically into the alkaline field due to TiO_2 enrichment at constant $\text{Zr/P}_2\text{O}_5$. It is therefore important that interpretation of Floyd-Winchester diagrams takes into account differentiation enrichment of Zr, P, Ti, Nb and Y. It is possible that some trends of differentiation for these elements may be such that the original tholeiitic or alkalic characteristics are retained throughout evolution of the magma (Floyd and Winchester 1976). Whether this occurs or not depends upon the proportionate rates of increase of the individual elements during differentiation. For example, if TiO_2 enrichment is extreme, whilst Zr and P_2O_5 are enriched such that the $\text{Zr/P}_2\text{O}_5$ ratio is relatively constant, then a vertical (alkalic) trend will be generated on the TiO_2 - $\text{Zr/P}_2\text{O}_5$ plot.

In chapters 3 and 4, it has been demonstrated that the iron-enrichment trend of the metabasites is characterised by concomitant increases in Ti, P, Zr, Nb and Y. In terms of abundance differences between (1) the "extreme differentiates" and (2) the average metabasite, Zr and P are fractionated more than Ti, Y or Nb. (Table 6.1). $\text{Zr/P}_2\text{O}_5$ shows on average a lower proportionate increase due to differentiation than TiO_2 , and this provides an explanation for the overall vertical trend into the 'alkalic' field in figure 6.8.

Table 6.1.

Variation of 'presumed immobile' elements and ratios with differentiation.

Element/Ratio.	1	2	3
P ₂ O ₅ %	1.36	0.35	3.9
TiO ₂ %	3.10	1.93	1.6
Y p.p.m.	49	22	2.2
Nb p.p.m.	40	14	2.9
Zr p.p.m.	685	147	4.7
Mean Zr/Mean P ₂ O ₅	504	420	1.2
Mean Nb/Mean Y.	0.82	0.64	1.3
Mean Y/Mean Nb.	1.23	1.57	0.8

1. = Mean of 7 "highly evolved" samples, with niggli mg average = 0.33.

2. = Mean for all 176 metabasites.

3. = "Differentiation factor"; i.e. Column 1 divided by Column 2.

The Y/Nb ratio is also decreased slightly during fractionation, and therefore caution should also be used in assigning magma type to suites from diagrams using this ratio or Nb/Y. The fact that a minority of metabasites plot in the alkaline basalt fields in all the Floyd-Winchester diagrams can therefore be ascribed to differentiation.

The closest analogues to the South Norwegian metabasites appear to be the Nuanetsi basalts (Cox et al. 1967) and the Dalradian metabasalts (Graham 1976 a, b). Both suites have clearly tholeiitic mineralogies, and high levels of "immobile elements", and have been described as "transitional tholeiitic" by Floyd and Winchester (1976). Since the South Norway metabasites have lower overall levels of immobile elements than either suite it is reasonable to conclude that the original mineralogy of the South Norway group was also tholeiitic. The Floyd-Winchester diagrams, when igneous fractionation is taken into account, are consistent with this conclusion.

(ii) Zr as an 'immobile' element.

In chapter 4 it has been shown that the main influence on Zr distribution in the metabasites is declining Mg, representing the iron-enrichment trend. Zones A and B show distinct increases in the element, which are thought to represent a primary igneous trend, with late-stage build-up of Zr as an incompatible element. The higher grade rocks of zone C however, are relatively deficient in Zr, even when the absence of low-Mg rocks is taken into account.

Recently, Cooper and Field (1977) have reported Zr values for the Zone C charnockitic gneisses. The overall values are lower than the abundances of Zr in most granulite terrains, and, more importantly, are lower than the adjacent mainland granulite facies charnockitic gneisses (Field, in prep.) and the amphibolite facies equivalents (Beeson 1971). The behaviour of Zr is thus analogous to that of Ba and Sr as reported in the previous chapter: in zone C, both the metabasites and their country rocks are deficient relative to their genetic equivalents in zones A and B. Partial separation of the field of variation for the Tromsø metabasites may be noted on the discrimination diagrams using Zr or Zr/P_2O_5 . In some instances the low values for Zr in zone C may be directly responsible for samples falling in an alkalic field instead of a tholeiitic field, (e.g. the Nb/Y - Zr/P_2O_5 plot).

Thus, although most studies of Zr have shown that it is relatively immobile during alteration and low-grade metamorphism, it would seem that its use in discrimination methods applied to high-grade rocks may be suspect.

G. Conclusions

- (1) Discrimination diagrams suggest that the metabasites were originally "within-plate" basaltic rocks of tholeiitic affinity.
- (2) Igneous differentiation, and possible metamorphic mobilization of elements must be taken into account when interpreting discrimination schemes.

- (3) The $\text{TiO}_2\text{-K}_2\text{O-P}_2\text{O}_5$ plot does not preclude "oceanic" affinities for the suite, (perhaps associated with ineffective continental rifting and ocean-floor formation), despite the 'continental' environment of the rocks.
- (4) Zr depletion probably occurred in zone C.

CHAPTER 7 Petrochemistry: Summary and Discussion.

The present whole rock chemistry of the metabasites is apparently a function of two separate processes, igneous differentiation and metamorphic redistribution. Despite the high grade of metamorphism to which the suite has been subjected, it has proved possible to distinguish the separate effects of each.

A. Primary Characteristics.

The primary igneous fractionation resulted in moderate to extreme enrichments of incompatible elements, although this was within the constraints of known basaltic chemistry. It was possibly caused by cumulus enrichment of ilmenite and/or apatite. Olivine fractionation at depth could account for the decline in both Cr and Ni with increasing iron-enrichment.

In chapter 6, the application of trace element discrimination diagrams showed that the metabasites were dominantly tholeiitic in magma type. "Alkalic" affinities for a minority of samples can be accounted for by the differentiated nature of the suite, or even by Zr movement for the zone C samples.

Many Precambrian igneous and meta-igneous suites are tholeiitic. Examples of Archaean greenstone belts which formed from this magma type are known in Australia (Hallberg 1972), and Canada (Baragar 1968). Most meta-igneous basic suites from the Archaean and Proterozoic have been shown to be tholeiitic by Winchester and Floyd (1976). Graham (1976 a, b) has concluded that the Dalradian epidiorites are also of this affinity. Tholeiitic magma seems predominant over

"alkalic" material over most of geological time, and one of the few examples of alkalic igneous activity from the Precambrian is the 1790 m.y. dolerite swarm from the Lofoten islands (Misra and Griffin 1972).

Thus the tholeiitic nature of the South Norwegian metabasites is unexceptional in the context of geological history.

The environment of intrusion of the metabasites was clearly continental. However, in the previous chapter the TiO_2 - K_2O - P_2O_5 plot (Pearce et al. 1975) showed a variation trend from the "oceanic field" along a line towards the K_2O apex. Similar trends have been observed in basaltic oceanic samples subject to weathering (Hart 1970) and low-grade metamorphism (Cann 1971). Pearce et al (1975) have suggested that metamorphosed basaltic rocks falling within the oceanic field of their diagram are very likely of oceanic origin. If this interpretation is correct, then the intrusion of the metabasites may well have represented an unsuccessful attempt to generate ocean floor, presumably associated with continental rifting. There is no other evidence to support this contention although it strengthens the analogy with the Dalradian metabasaltic rocks (Graham 1976a), which also show oceanic affinities on the TiO_2 - K_2O - P_2O_5 diagram. Interpretation of the tectonic environment from this plot must be highly cautious however, when dealing with a titania-enriched suite which has undergone fractional crystallisation.

The metabasites have no affinities with calc-alkaline or island-arc environments.

B. Metamorphic fractionation.

The behaviour of K and Rb reflects a fractionation which is effective over the entire South Norway transition. K and Rb both decline with increased grade, a pattern well-documented in other terrains (see introduction to chapter 5). Several theories have been invoked to account for the mechanism of this depletion, and these are now examined with reference to the metabasite data.

It is difficult to reconcile the consistently lower levels of K and Rb in granulites with primary, pre-metamorphic abundances, as suggested by Holland and Lambert (1973). The analogous patterns of deficiency in K and Rb in other high-grade terrains, and the present relative depletions in both mafic and genetically distinct acid/intermediate suites in the South Norway transition are features which mitigate against the primary abundance hypothesis.

Fyfe (1973) has suggested that granulite depletions may sometimes represent the residual component of widespread lower crustal melting, with the anatexite being correspondingly enriched in K and Rb. In the case of the Bamble sector it seems impossible that this could have been the exact mechanism of depletion, since the fractionation involves rocks of basaltic chemistry. The granulite facies on the mainland is not characterised by lower levels of Ba, an element which would be removed with K and Rb in granitic melts.

A third possible cause of the large-ion depletion is by removal from mineral sites which become energetically unfavourable at high pressures. Heier, as long ago as 1964,

pointed out that the lower crust would contain mineral structures unlikely to retain Rb. More recently, it has been suggested that such elements would then be subject to upward transport in a hydrous phase produced by the dehydration reactions, (Lambert and Heier 1968, Heier 1973a, b). However, these data suggested that the alkali element deficiencies were restricted to medium or high-pressure terrains, while the South Norwegian data (low-intermediate pressure) appear to substantiate the views of Sheraton et al (1973) that such a restriction need not apply.

With regard to the K/Rb relationships in the South Norway metabasites, a mineralogical control over chemistry during high grade metamorphism is suggested. In the absence of suitably accommodating minerals, decreasing amounts of hornblende and biotite (see chapter 2) would lead to expulsion of both K and Rb (e.g. Hart and Aldrich 1967, Whitney 1969, Drury 1973, Heier, op cit). Also, because biotite has the particular ability to concentrate Rb (low K/Rb), decreases in modal proportions tend to increase the whole rock K/Rb ratio (e.g. Shaw 1968, Sighinolfi 1969). The same mineralogical controls would be operative if primary, mantle-derived igneous differentiates crystallised directly under granulite facies conditions (Holland and Lambert 1975). In view of the associated regional dehydration during granulite formation a dispersed aqueous phase would necessarily be available as a transporting medium for this expelled material. For the Archaean Lewisian granulites, Tarney and co-workers (Tarney et al 1972, Sheraton et al 1973 and Tarney 1976) favour mantle-degassing, a specific Precambrian process, leading to the purging of 'incompatible' elements from granulite

terrains via a hydrous fluid phase. Any mantle-degassing occurring during the evolution of the Proterozoic Bamble sector would aid vertical transfer.

For the metabasites, it seems clear that the present linear trend of the K/Rb variation (figure 5.2) reflects a redistribution of K and Rb on a regional scale, although not necessarily involving movement over large distances (c.f. Roddick and Compston 1977).

As the elements show high overall abundances relative to both basalts and other metabasic suites, the redistribution probably resulted in net addition of alkalis to at least some of the higher level samples. This seems the more likely in the light of the demonstration that amphibolitization of gabbros can involve increases in both K and Rb (Elliott 1973, Field and Elliott 1974). If the present-day amphibolites once underwent an earlier granulite metamorphism involving depletion of K and Rb, then the subsequent influx of these alkalis must have been even greater.

A second aspect of metamorphic fractionation is that within the granulite facies (i.e. between zones B and C), quite marked variations in chemistry occur, and include features which are not distinguishable in the mainland transition. Thus, the Tromsø (zone C) metabasites display high levels of Na₂O, and low abundances of Sr, Zr and Ba relative to the mainland suite. The evidence that these are probably secondary enhancements and depletions and not primary features has been outlined in previous chapters. In addition, the zone C metabasites are characterised by lower levels of H₂O and higher oxidation ratios than the

mainland metabasites.

The present composition of many zone C metabasites is similar to that of spilites (Vallence 1965, 1969), which are characterised particularly by high Na_2O . Spilite genesis is usually attributed to secondary alteration involving hydrous fluid phases, perhaps under low grades of metamorphism (e.g. Smith 1968, Hughes 1972). While such a process could account for the present metabasite chemistry in zone C, a more pervasive introduction of soda is required to explain the Na_2O distribution in the more acid rocks of the Bamble sector. The concept of soda metasomatism at high-grades of metamorphism is in contrast to the views of Moine et al (1972). The latter authors did not consider the possibility of metasomatism, and described the Tromsø rocks as representing an isochemically metamorphosed greywacke-keratophyre-spilite sequence.

An important question concerns the relationship between the Ba, Sr (and Zr) depletions in the zone C metabasites and the systematic K/Rb relationships described above, relating to the entire amphibolite-granulite transition. Ba, Sr and Zr may be reflecting a localised event, perhaps genetically distinct from the K-Rb metasomatism. Alternatively, if the two redistributions are related, the differences in behaviour could be explained by K and Rb being more susceptible to fractionation over long distances than the other elements.

Regional movement of Ba might occur as a response to losses in K and Rb, which on Tromsø show the most extreme overall deficiencies yet reported for granulites (Cooper and Field 1977). A fractionation pattern with large

quantities of Rb removed relative to K might result in additional Ba mobility (from K sites, subsequent to the Rb^+ ions). Sr movement is more difficult to explain since plagioclase is a freely available host mineral. The only other analogous granulite terrains known to the author which have low Sr contents similar to the Tromsø rocks (including the charnockitic acid-intermediate gneisses) are the Cape Naturaliste and Southern Eyre Peninsula blocks of Australia (Lambert and Heier 1968). These are both low pressure suites, and it is probable that pressure has an important effect on Sr partitioning.

For the present terrain, an interesting and important factor is that fractionation occurs dominantly, though not entirely, within the granulite facies, and is not so marked between the granulite facies of zone B and the amphibolite facies (zone A).

Whilst fractionation effects for K and Rb between zone A and zone B metabasites are perceptible, the differences in abundances and in K/Rb are more pronounced between zones B and C. Moreover, although the acid-intermediate Tromsø gneisses show extreme depletion in these elements, the zone B charnockites are "normal" for K, Rb, (and Ba, Sr, Na and Zr.)

This is apparently the first terrain where "within-granulite facies" fractionation has been demonstrated, and it may explain for example why Heier (1973 a, b) has suggested low pressure terrains are not implicated in depletion processes. If the mainland transition in South Norway had been studied in isolation, little evidence for metamorphic fractionation would have been forthcoming.

The "within-granulite facies" chemical zonation for both the acid-intermediate and basic components of the Bamble sector might indicate a relatively steep temperature gradient, associated with increased dehydration, and the lower H₂O in zone C samples. Ba, Sr and Zr mobility, features which are apparently not characteristic of other high-grade terrains, might be associated with such an increased geothermal gradient.

These aspects of metamorphic fractionation need further scrutiny and it is clear that more detailed petrochemical studies of other high-grade terrains would be pertinent. In particular, surveys of the chemical behaviour of Ba, Sr and Zr within granulite facies terrains would be useful in determining whether the present area is exceptional in this manner.

For the present survey, the demonstration that the chemistry of the metabasites has been modified by metamorphic/metasomatic processes has important petrochemical implications. For example, the K-Rb data indicate that a linear variation pattern per se need not reflect an original igneous fractionation trend. The linearity of the K-Rb plot is of special interest from this point of view, for linear trends have also been established for certain other high-grade metamorphic suites of various lithologies (Sighinolfi 1969, 1971, Lewis & Spooner 1973). The data relating to these trends are compared with those for Shaw's (1968) Main Trend and the Norwegian metabasites in table 7.1. Whilst Lewis & Spooner's (1973) 'granulite trend' is "substantially parallel to the Main

TABLE 7.1 : K/Rb ratios related to K % for the South Norwegian metabasites and other suites.

K%	1	2	3	4	5
0.2	1075	304	1208	1279	398
0.5	573	275	688	860	352
1.0	355	254	450	637	320
1.5	269	241	352	535	303
2.0	220	234	295	472	291
5.0	*117	210	168	317	257

* Extrapolated value.

1. South Norwegian metabasites (R.M.A. regression).
2. Main Trend for igneous suites (Shaw 1968).
3. Alpine amphibolite (paragneiss) sequence (Sighinolfi 1969).
4. Brazilian acid-intermediate-basic granulites (Sighinolfi 1971).
5. Various granulites (Lewis and Spooner 1973).

Trend," their results are based on a composite sample ($n = 62$) involving seven different geological settings. The trends for individual suites from the Alps and Brazil are quite different, and these show the same marked decrease in K/Rb with increasing K as the Norwegian metabasites. Similar trends, although not quantified, have been identified within some lithological groups of the Lewisian of Assynt (Sheraton et al. 1973) and the Inner Hebrides (Drury 1974). This feature, shared by different lithologies from different areas, suggests that such essentially linear (metasomatic?) trends may prove to be characteristic of several terrains where granulite metamorphism has played an important role in the geological evolution.

Another aspect of the data is that the elements apparently most susceptible to fractionation include K , Rb and Sr , and that geochronological studies in high grade terrains should take into account the possibility of systematic metasomatism. The existence of erroneous ages due to metamorphic fractionation should not be precluded in granulite terrains (c.f. Roddick and Compston 1977).

CHAPTER 8.

Mineral Chemistry.

A. Introduction.

It is particularly advantageous to supplement whole-rock chemistry with individual mineral compositional data, and this chapter considers some partial and preliminary microprobe analyses of the metabasites. This approach allows a deeper understanding of the petrochemistry of the suite, as outlined in previous chapters.

In addition to the intrinsic value of the study, a knowledge of mineral chemistry may be particularly useful in assessing chemical equilibrium in the metamorphism. Several analyses of minerals coexisting in textures of petrographic equilibrium are included in this study. Textural equilibrium per se does not prove chemical equilibrium, but detailed studies of mineral chemistry in high-grade metamorphic terrains, and other suites, have indicated that such conditions may be related (e.g. Davidson 1968, 1971; Heitanan 1969, Rivalenti and Rossi 1973, Fleet 1974 a, b.). In addition major and minor element partitioning between coexisting phases has proved of great interest. The use of such distributions (particularly between Fe^{2+} and Mg in pyroxenes) has been invoked as a geothermometer since the work of Kretz (1961, 1963), and McIntire (1963). However, such coefficients may not be uniquely temperature dependant, and, for example, crystal field effects may partly or wholly determine the site distribution of transition metals in coexisting phases, (e.g. Schwarz 1967, Davidson 1968).

The first part of this chapter deals with hornblende, pyroxene and biotite analyses. The second contains a discussion of garnet paragenesis in the metabasites, in which petrographic and whole-rock chemical data^{are} supplemented by microprobe analyses.

B. Analytical techniques.

All analyses were obtained using a Cambridge Instruments "Geoscan" microprobe Mark V, using highly polished carbon-coated thin-sections. The standards used were artificial, homogeneous silicate glasses of known composition, produced according to the method of Smellie (1972). All raw count data were corrected directly for dead time, background and mass absorption effects, and iteratively for fluorescence and atomic number effects. Further details of standard composition, standard preparation and operating conditions of the microprobe are included in appendix 2. The method used unfortunately precluded the analysis of K_2O and Na_2O , since these oxides of high volatility could not be satisfactorily fused in the glass standards. The major oxides obtained were SiO_2 , Al_2O_3 , TiO_2 , FeO (Total Fe as FeO), MgO , CaO , and MnO .

C. Hornblendes.

The partial analyses for 12 hornblendes are presented in table 8.1, together with the atomic ratios for Fe, Mg and Ca. (The number of cations per unit cell on the basis of 23 (0) were not calculated due to the lack of data on Na_2O , K_2O , H_2O and F etc.). Most of the analysed hornblendes are chemically homogeneous, and variation between rim and core is reported for only three minerals. In these cases, the chemical

ZONE	A		B								
NO.	754	7319	83	85	86	88r.	88c.	101r.	101c.	748	7117
SiO ₂	42.80	43.56	43.34	42.97	41.63	41.89	39.91	44.73	42.87	45.76	42.48
Al ₂ O ₃	10.66	12.47	12.93	11.78	12.86	11.15	10.81	11.06	11.98	8.65	12.02
FeO*	18.78	16.43	17.25	22.19	18.94	19.79	23.51	20.56	18.93	17.90	22.13
MgO	9.74	11.95	10.18	6.54	9.66	8.20	7.71	8.54	9.66	10.70	9.45
CaO	10.65	10.81	11.56	10.79	10.62	11.97	11.51	10.66	11.70	9.37	8.71
TiO ₂	1.71	1.53	1.75	2.08	2.48	2.50	2.52	1.85	1.86	2.34	2.17
MnO	0.34	0.13	0.43	0.25	0.17	0.27	0.29	0.31	0.27	0.42	0.25
(TOTAL)*	(94.68)	(96.88)	(97.44)	(96.42)	(96.36)	(95.77)	(96.26)	(97.71)	(97.27)	(95.14)	(97.21)
<u>Atomic Ratios</u>											
Fe	37.7	31.8	34.4	46.6	38.1	39.8	45.2	41.6	37.0	36.6	44.1
Mg	34.9	41.3	36.1	24.4	34.6	29.4	26.4	30.8	33.7	38.9	33.6
Ca	27.4	26.9	29.5	29.0	27.3	30.8	28.4	27.6	29.3	24.5	22.3

* Total Fe as FeO.

r = rim

+ = total excludes alkalis, H₂O, etc.

c = core

TABLE 8.1: Partial Hornblende Analyses

ZONE	C			
NO.	7218	7221	7222r	7222c
SiO ₂	43.37	43.32	43.64	45.20
Al ₂ O ₃	11.96	9.72	9.13	7.90
FeO*	14.85	16.24	16.18	15.15
MgO	14.08	12.64	12.90	13.62
CaO	11.03	10.27	10.85	10.99
TiO ₂	1.70	1.10	1.43	1.34
MnO	0.43	0.50	0.51	0.51
(TOTAL)	(97.42)	(93.79)	(94.64)	(94.71)
<u>Atomic Ratios</u>				
Fe	27.5	31.3	30.5	28.3
Mg	46.4	43.4	43.3	45.4
Ca	26.1	25.3	26.2	26.3

TABLE 8.1 (Continued)

changes are not extreme, and there is no consistent pattern of variation. For example, specimens 88 and 101 are both slightly enriched in silica in the rim relative to the core, but in specimen 7220, SiO_2 is higher in the core.

In terms of the general chemistry of these analyses, SiO_2 , Al_2O_3 and CaO are relatively constant in the group. Although the rational nomenclature of Leake (1968) cannot be strictly applied to partial analyses, it is clear that the amphiboles are calciferous (Minimum $\text{CaO} = 8.71\%$ Maximum = 11.97%), and that Si in the half-unit cell will range approximately between 6.0 and 7.0. The main chemical variable in the mineral group is the magnesium to iron ratio and $\text{Mg}/\text{Mg} + \text{Fe}$ varies from 0.34 to 0.63. Thus, according to the criteria of Leake (1968), the likely nomenclature for the amphiboles will be: (Magnesio-or ferro-) hornblende - tschermakitic hornblende - tschermakite. Specimens 86, 88 and 748 should have the prefix titaniferous. The general term 'hornblende' is retained in subsequent discussion.

Figure 8.1 illustrates that the variation in magnesium and iron in the hornblendes is a reflection of the whole-rock magnesium-iron variation. Similar features have been described by Sen (1970, 1973). The small degree of scatter about the 45° line may be related to variations in the abundance or chemistry of other coexisting ferromagnesian minerals.

The TiO_2 content of the hornblendes is also influenced by whole-rock chemistry. (Figure 8.2). TiO_2 in hornblende gradually increases with whole rock TiO_2 until a value of approximately 2.5% in the amphibole is obtained. There is no further increase in TiO_2 in hornblende,

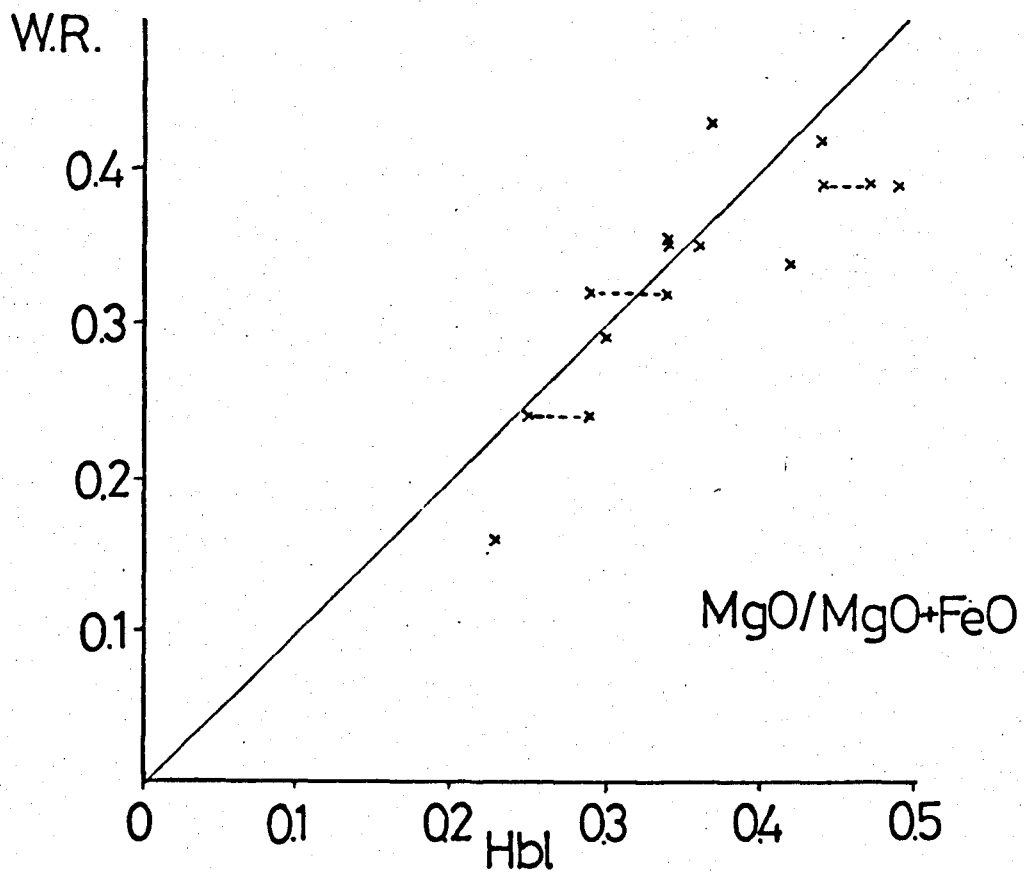


Figure 8.1: Caption overleaf.

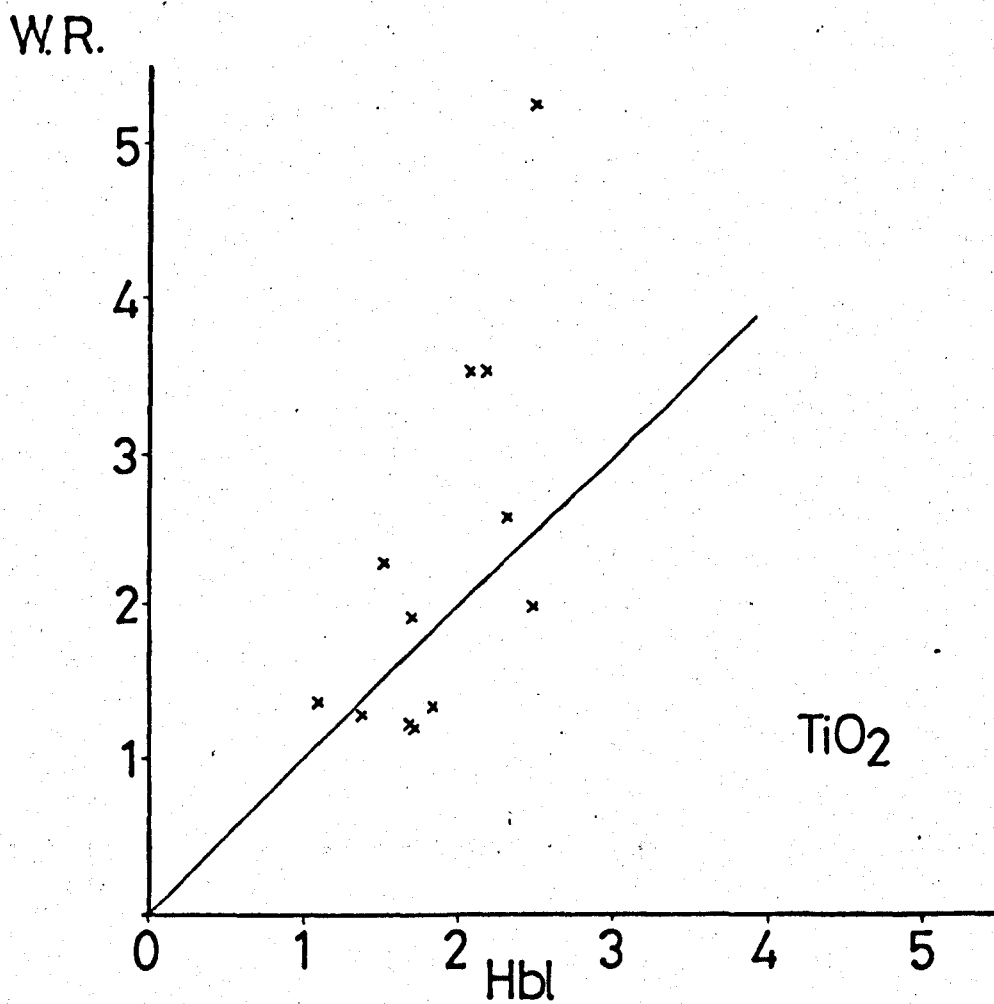


Figure 8.2: Caption overleaf.

Figure 8.1: (previous page) $\text{MgO}/\text{MgO}+\text{FeO}$ in hornblendes (hbl) versus $\text{MgO}/\text{MgO}+\text{FeO}$ in corresponding whole rocks (W.R.). Diagonal line has a slope of 1.0. Dashed lines represent variation between rim and core.

Figure 8.2: (previous page) TiO_2 in hornblendes (hbl) versus TiO_2 in whole rock (W.R.). Diagonal line has a slope of 1.0.

despite whole-rock values of over 5.0%, and kaersutite compositions are not attained in this suite.

MnO is variable in the hornblendes, increasing with whole-rock MnO% so that MnO (hornblende)/MnO whole rock is usually between 1.0 and 2.0 (figure 8.3).

D. Pyroxenes.

The microprobe analyses for 5 orthopyroxenes and 5 clinopyroxenes are given in tables 8.2 and 8.3.

The orthopyroxenes are hypersthene and ferrohypersthene, and their main characteristic as a group is a variation in iron and magnesium. $Mg/Mg+Fe$ ranges from 0.33 to 0.54, and again shows a clear relationship with whole-rock magnesium-iron variation. (Table 8.2). TiO_2 is low in the orthopyroxenes, showing values characteristic of metamorphic orthopyroxenes from other high-grade basic suites (e.g. Deer et al 1963; Davidson 1968). MnO (0.56 - 1.67%) is fairly high, and no clear relationship with whole rock values has been noted for this element.

Compositionally the clinopyroxenes straddle the salite-augite division on the pyroxene trapezium (Deer et al 1963), and display a less marked Fe/Mg variation than the hornblendes or orthopyroxenes.

E. Biotites.

Partial analyses for 3 biotites are presented in table 8.4. $Mg/Mg+Fe$ varies from 0.39 to 0.53. However the most interesting feature of these analyses is the high TiO_2 contents of specimens 101 and 88. The latter biotite contains 6.68% TiO_2 , and occurs in a rock with 5.25% of this oxide. These high titania values in biotites are presumably related

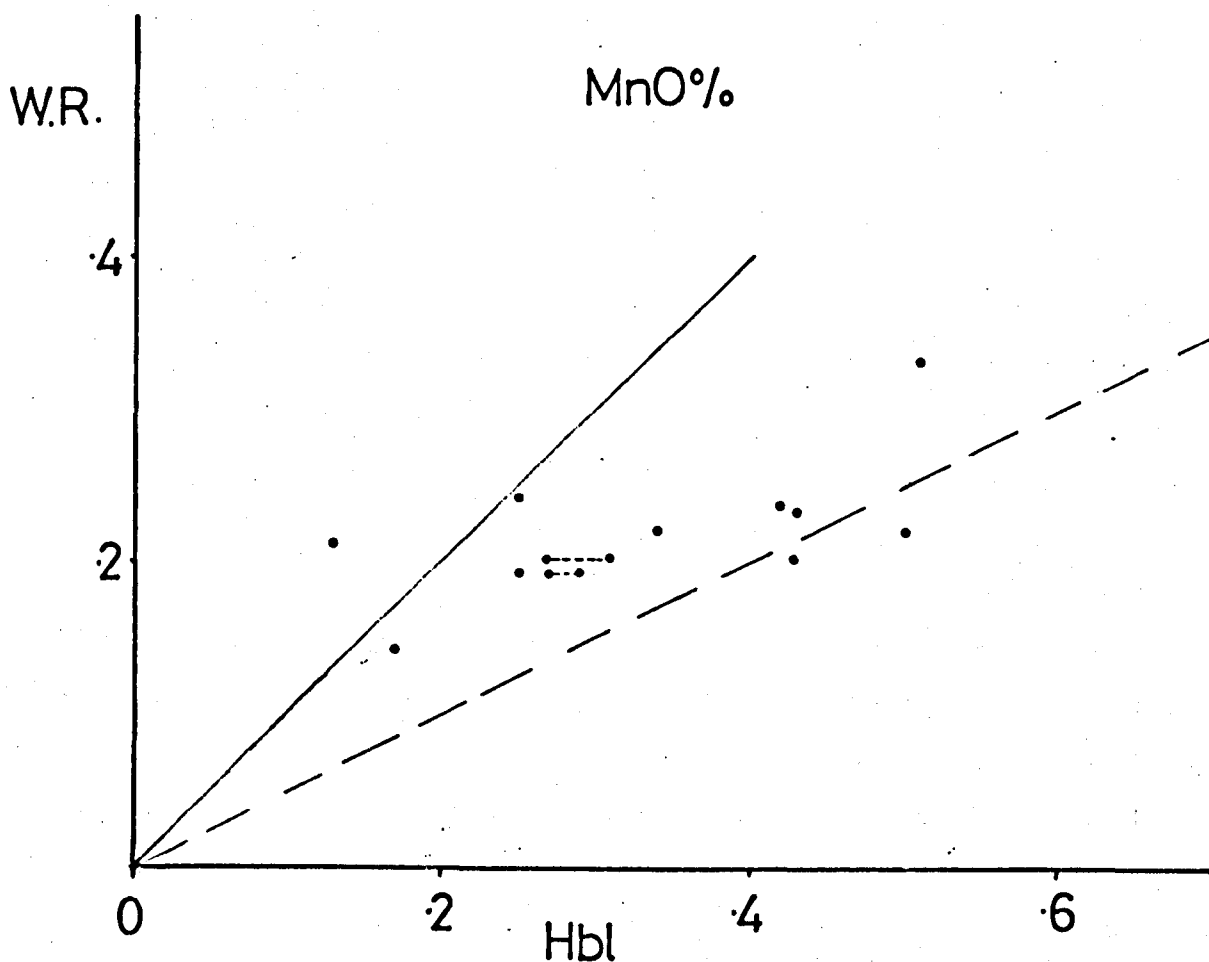


Figure 8.3: MnO% in hornblende versus MnO% in whole rock (W.R.). Solid diagonal line has a slope of 1.0; dashed line has slope 2.0. Dotted lines represent rim-core variation in minerals.

TABLE 8.2 : Orthopyroxene Analyses.

No.	83	85	86	101	7117
SiO ₂	52.27	52.29	50.75	51.80	47.60
Al ₂ O ₃	1.12	1.05	1.06	0.87	0.73
TiO ₂	0.10	0.20	0.14	0.12	0.10
FeO*	26.46	35.29	27.98	29.47	33.35
MgO	17.09	9.64	18.49	15.51	15.92
CaO	0.87	0.75	0.49	0.79	0.64
MnO	1.67	1.08	0.56	1.23	0.64
(Total)	99.58	101.19	99.47	99.79	98.98
<u>Atomic Ratios.</u>					
Fe	45.6	66.0	45.5	50.7	53.3
Mg	52.5	32.2	53.5	45.6	45.4
Ca	1.9	1.8	1.0	1.7	1.3
Mg/Mg+Fe	0.54	0.33	0.54	0.47	0.46
Mg (W.R)	0.43	0.27	0.51	0.47	0.44

TABLE 8.3 : Partial Clinopyroxene Analyses.

Spec.	83	101	218	220	221
SiO ₂	49.80	50.64	50.49	52.65	50.68
Al ₂ O ₃	2.40	1.48	2.61	1.96	1.99
TiO ₂	0.22	0.14	0.22	0.14	0.13
FeO*	12.48	13.21	11.22	9.51	10.34
MgO	13.40	11.74	14.67	12.66	12.96
CaO	20.70	20.62	21.56	19.84	20.33
MnO	0.77	0.57	0.53	1.24	0.76
(Total)	(99.77)	(98.40)	(101.08)	(98.00)	(97.19)
Atomic Propn.					
Fe	19.8	21.8	17.3	16.6	17.4
Mg	38.0	34.6	40.2	39.2	38.8
Ca	42.2	43.6	42.5	44.2	43.8

TABLE 8.4 : Biotites : Partial Analyses.

	754	101	88
SiO ₂	40.20	38.03	36.5
Al ₂ O ₃	16.07	14.22	14.03
TiO ₂	1.96	4.27	6.68
FeO*	20.45	25.31	25.48
MgO	12.75	11.64	9.05
CaO	0.01	0.09	0.06
MnO	0.12	0.12	0.07
(Total)	91.56	93.68	92.02
<u>Atomic Ratios</u>			
Fe	47.4	54.9	61.3
Mg	52.6	45.1	38.7

to the "saturation" of the element, in hornblende lattices since TiO_2 does not exceed 2.5% in the amphiboles, irrespective of the whole rock value (figure 8.2).

F. Coexisting Minerals.

The data presented above are inadequate in the number of analyses for a complete and systematic study of coexisting mineral relationships, and their implications to the South Norway suite. These implications include major and minor cation partitioning as a function of equilibrium (Fleet 1974a, b) and also the use of distribution coefficients as geothermometers (e.g. Kretz 1960, 1963; Heitanan 1969, Ray and Sen 1970, Sen 1973). An additional difficulty in the use of distribution coefficients is the absence of data on Fe^{2+} and Fe^{3+} in the Norwegian minerals. This precludes direct comparison with previous work, which has in particular emphasized the importance of Fe^{2+} and Mg distribution between orthopyroxene and clinopyroxene (e.g. Kretz (op cit.), Meuller 1960, 1962, Bartholomé 1962).

However, the data of tables 8.1 - 8.4 are now examined with respect to coexisting mineral relationships.

Figures 8.4 and 8.5 illustrate the compositions of coexisting pyroxenes and amphiboles referred to their Ca, Fe and Mg contents. The only specimens in which the triad orthopyroxene, clinopyroxene and hornblende has been analysed are numbers 83 and 101, and these are plotted separately in figure 8.4. This shows clearly an increased Fe/Mg from clinopyroxene to orthopyroxene, a pattern well-documented in the coexisting ferromagnesian minerals of

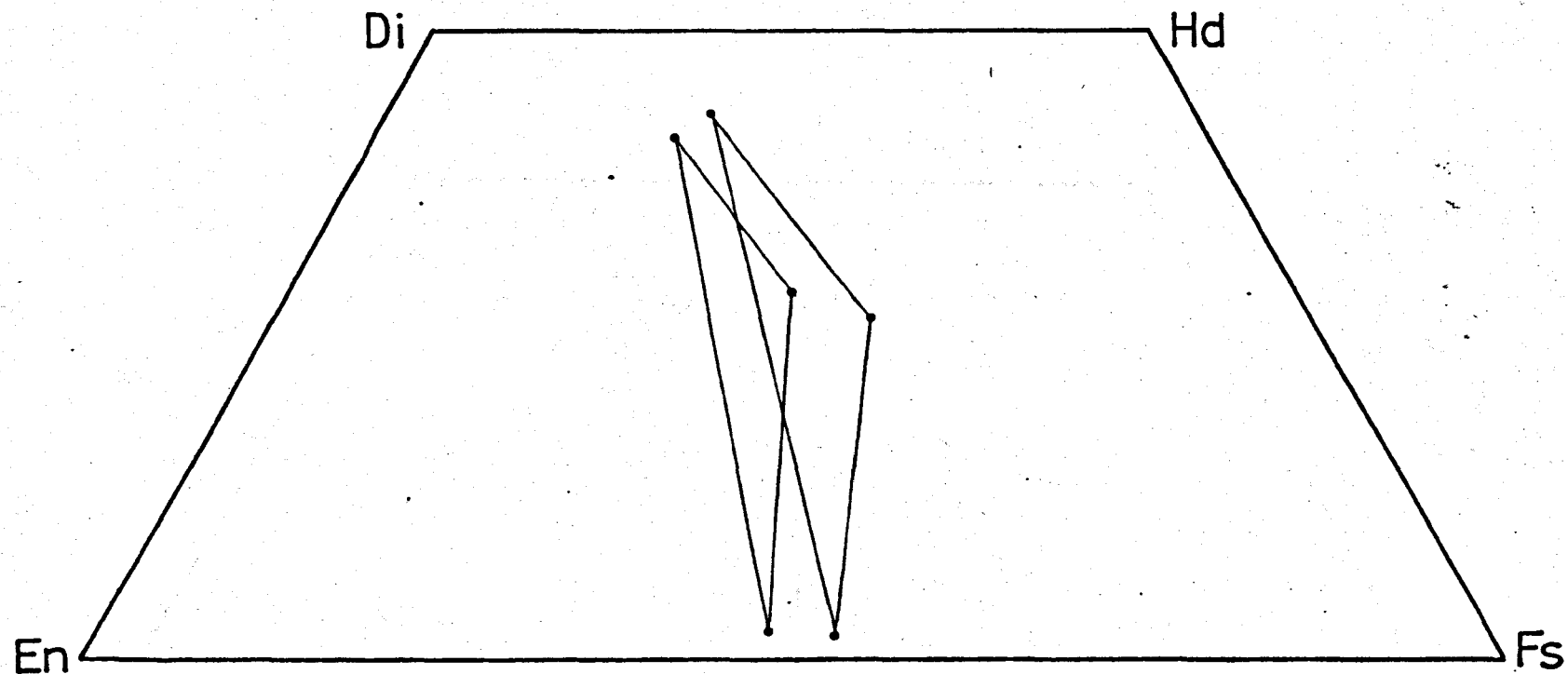


FIGURE 8.4: Coexisting orthopyroxene , hornblende and clinopyroxene triads (samples 83 and 101) in the Diopside (Di) - Hendenbergite (Hd) - Ferrosilite (Fs) - Enstatite (En) diagram.

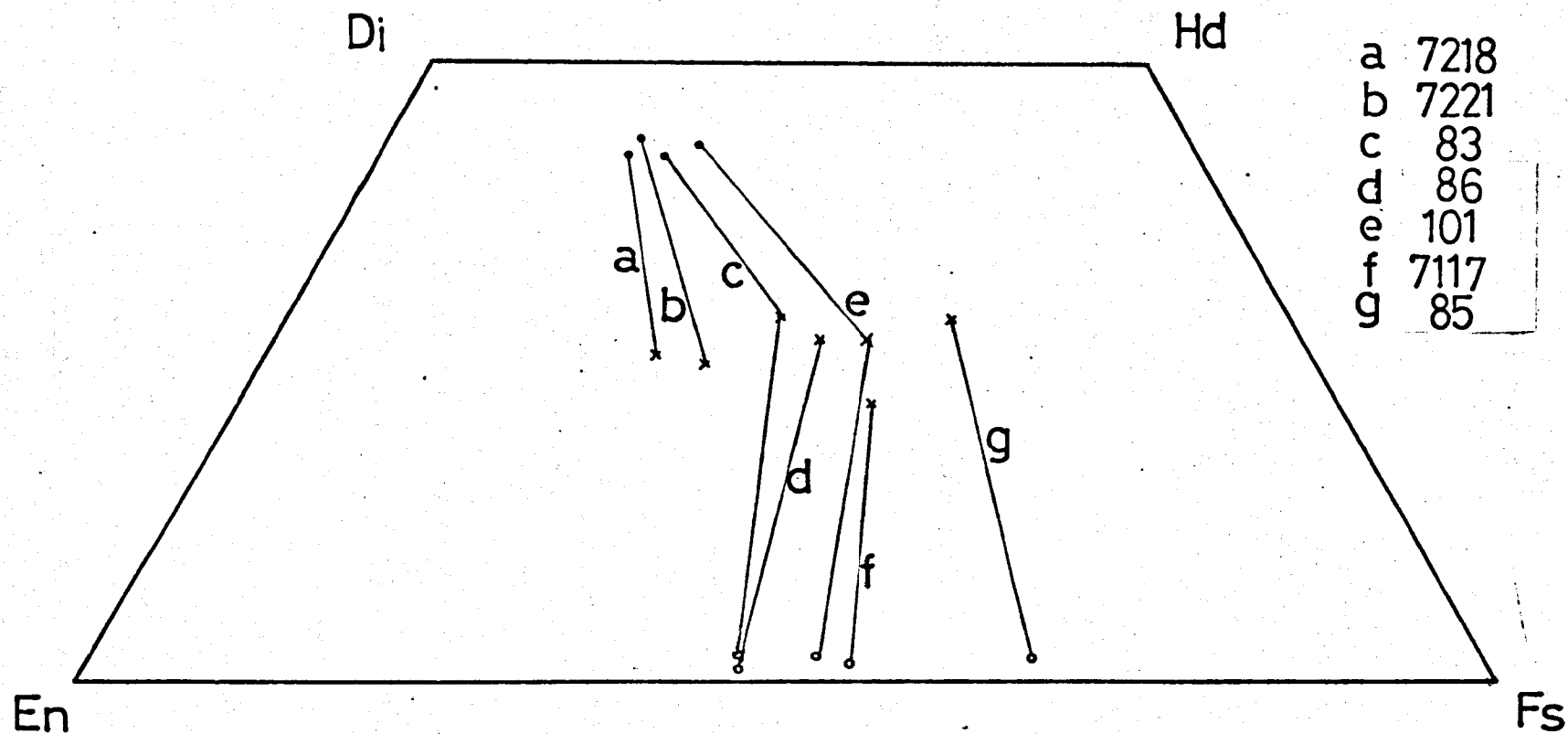


FIGURE 8.5: Coexisting orthopyroxene - hornblende and clinopyroxene-hornblende pairs. a-g refer to sample numbers in key. Closed circles = clinopyroxenes; crosses = hornblende; open circles = orthopyroxenes.

other high-grade basic rocks (e.g. Leelanandam 1967, Davidson 1968). The parallelism of the mineral tie-lines is suggestive of chemical equilibrium in both rocks.

The remaining diads (orthopyroxene-hornblende and clinopyroxene-hornblende) are plotted in figure 8.5. Although there is less regularity about the tie-lines in this diagram, there is no strong evidence for disequilibrium, with the possible exception of specimen 7117, in which the hornblende has a very low Ca content.

MnO usually shows a regular distribution in the coexisting ferromagnesian minerals. In particular, $\text{MnO}(\text{opx})/\text{MnO}(\text{cpx})$ is almost constant at 2.16 and 2.17 in samples 101 and 83. These values are virtually identical with the MnO distributions obtained in coexisting pyroxenes by Davidson (1968), despite a different range of MnO values for the minerals. In figure 8.6, Davidson's data are plotted for comparison alongside the Norwegian analyses.

MnO is also concentrated into orthopyroxenes relative to coexisting hornblendes, (figure 8.7) and the K_D (distribution coefficient) values range from 2.6 to 4.3 (Table 8.5).

The low values for TiO_2 in the pyroxenes give a degree of unreliability to distribution values using this oxide, since small analytical errors can result in relatively large fluctuations in K_D . Nevertheless, table 8.5 indicates a reasonable regularity in titania partitioning.

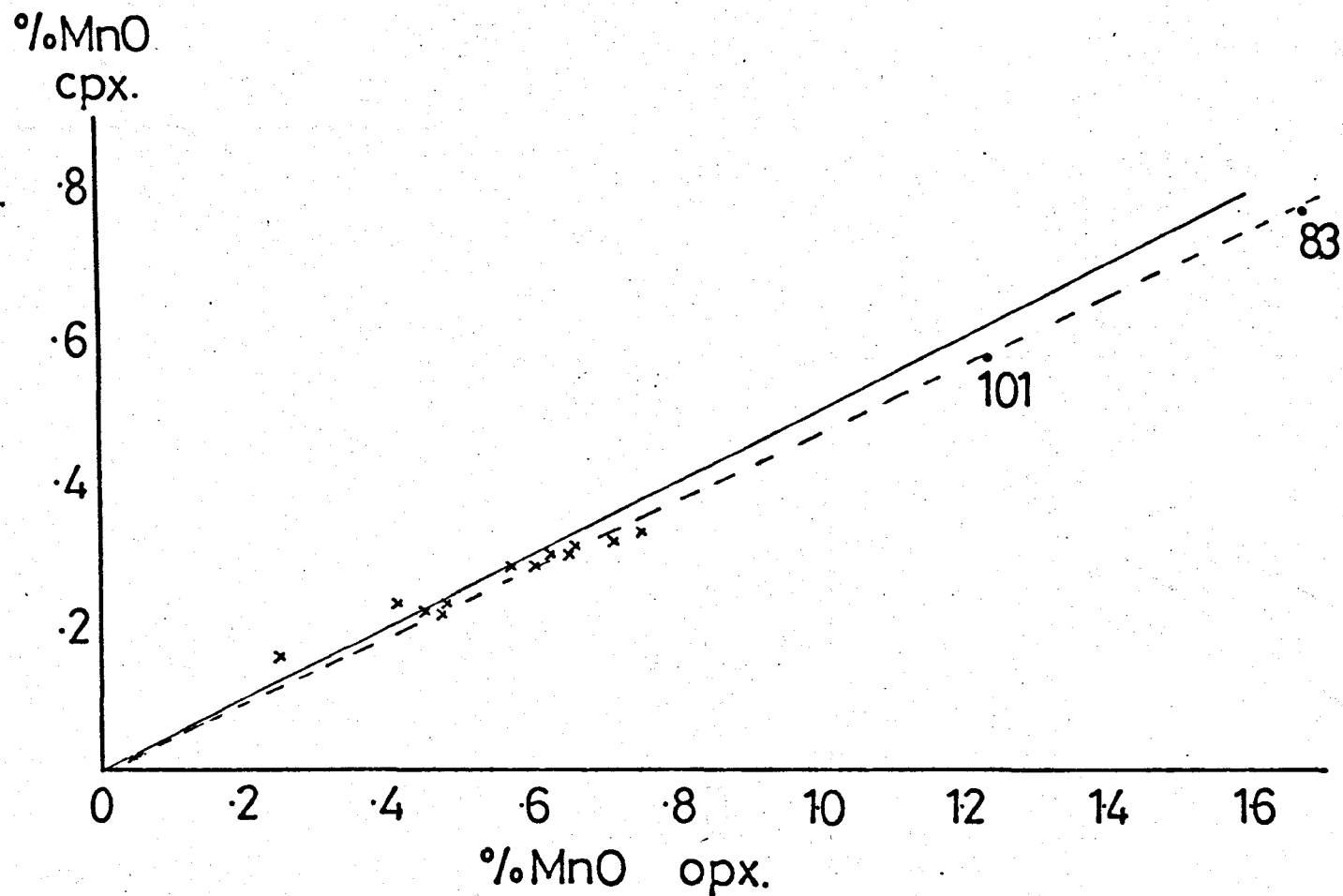


FIGURE 8.6: MnO% clinopyroxene (cpx) versus MnO% in orthopyroxene (opx). 83, and 101 are sample numbers of metabasites. Crosses = data of Davidson (1968, Table 1). Solid diagonal line has slope 2.0; dashed line has slope 2.15.

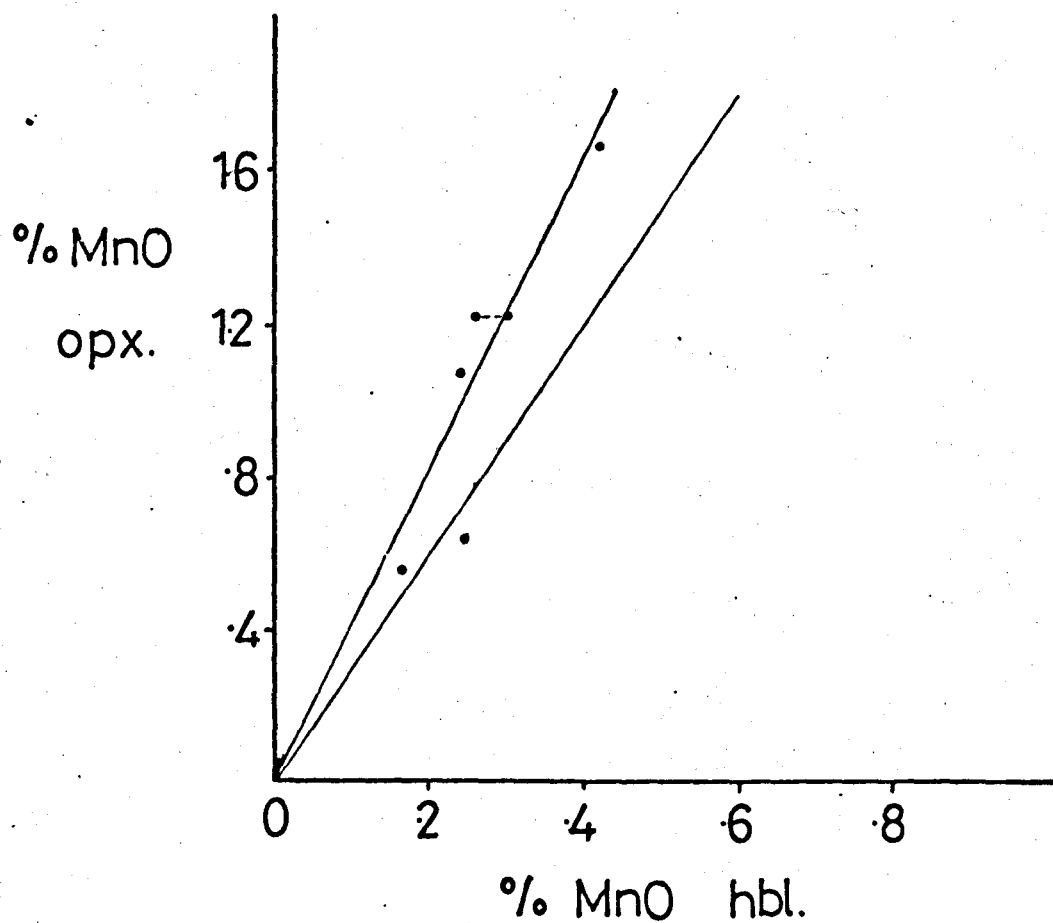


Figure 8.7: Caption overleaf

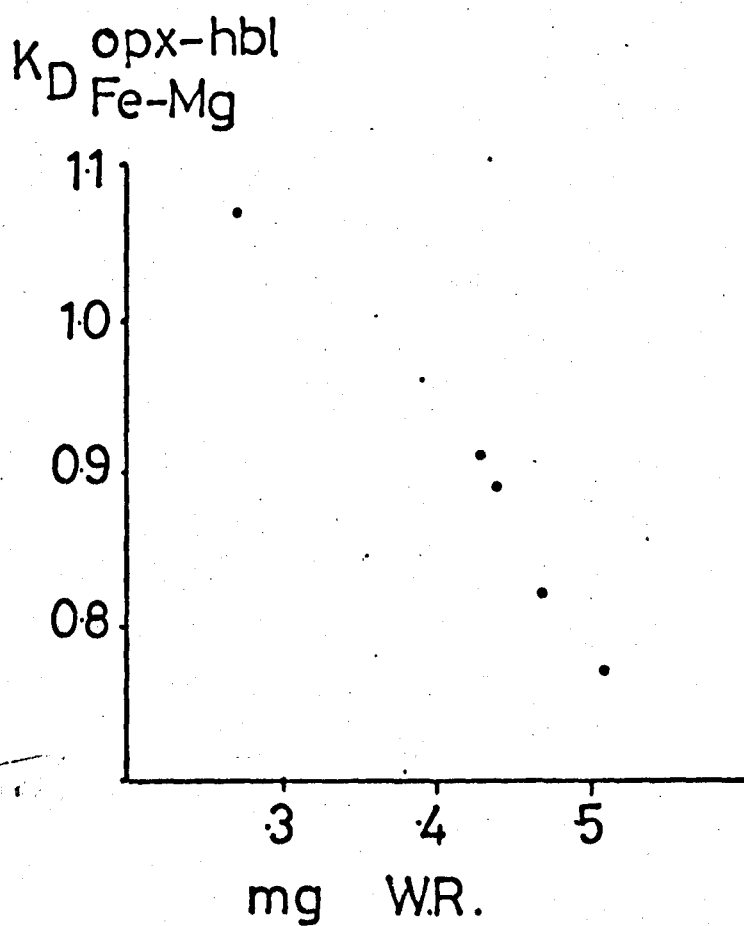


Figure 8.8: Caption overleaf

Figure 8.7: MnO% in orthopyroxene (opx) versus MnO% in hornblende (hbl). Solid diagonal lines represent K_D (MnO opx/ MnO hbl) of 3.0 and 4.0 respectively. Dashed line = core - rim variation.

Figure 8.8: Distribution coefficients K_D Fe-Mg between orthopyroxenes and hornblendes plotted against niggli mg of corresponding whole rock.

Table 8.5 summarises the iron-magnesium distribution coefficients for the hornblendes and pyroxenes, using total Fe as FeO. Comparison with previous work in which the temperature dependence of K_D has been invoked is strictly speaking invalidated by the absence of data on Fe^{3+} in the minerals. However, the K_D values for the two pyroxene pairs, at 1.67 and 1.77 are close to the range of K_D values (Using Fe^{2+}) which have been published for coexisting metamorphic pyroxenes (e.g. Kretz 1963, Davidson 1968). The latter author quotes K_D Fe^{2+} -Mg values of 1.70 to 1.87 for pyroxene pairs from Quairading, Western Australia. Distribution coefficients for igneous pyroxene pairs average 1.36 (Kretz 1963), and reflect much higher temperatures of equilibration.

The distribution coefficient, K_D Fe-Mg between orthopyroxene and hornblende varies from 0.77 to 1.07 in the Norwegian rocks. Figure 8.8 illustrates an excellent relationship between this variation and the whole-rock iron-magnesium content, as measured by niggli mg.

G. Discussion.

Although the mineral chemistry described above is of a preliminary nature, certain conclusions may be drawn. Several lines of evidence suggest that the metabasites have approached chemical equilibrium. These are as follows:

- (i) The tie lines for coexisting minerals in the Fe-Mg-Ca diagram are parallel or sub-parallel and not "cross-cutting".
- (ii) Whole rock chemistry has a strong control on mineral chemistry, particularly among the hornblendes. The relationship between Fe/Mg in hornblende and Fe/Mg in the whole rock (e.g. figure 8.1) is also

Table 8.5: Distribution Coefficients.

K_D	83	85	86	101	117	218	221
1	2.17	-	-	2.16	-	-	-
2	3.88	4.32	3.29	4.24	2.56	-	-
3	1.79	-	-	1.97	-	1.23	1.52
4	0.45	-	-	0.86	-	-	-
5	17.5 (0.06)	10.4 (0.10)	17.7 (0.06)	15.5 (0.06)	21.7 (0.05)	-	-
6	7.95 (0.13)	-	-	13.3 (0.08)	-	7.7 (0.13)	8.5 (0.12)
7	1.67	-	-	1.77	-	-	-
8	0.91	1.07	0.77	0.99	0.89	-	-
9	0.43	-	-	0.47	-	0.55	0.59

- 1 = $K_D \frac{\text{opx-cpx}}{\text{MnO}} = \text{MnO opx/MnO cpx}$
- 2 = $K_D \frac{\text{opx-hbl}}{\text{MnO}} = \text{MnO opx/MnO hbl}$
- 3 = $K_D \frac{\text{cpx-hbl}}{\text{MnO}} = \text{MnO cpx/MnO hbl}$
- 4 = $K_D \frac{\text{opx-cpx}}{\text{TiO}_2} = \text{TiO}_2 \text{ opx/TiO}_2 \text{ cpx}$
- 5 = $K_D \frac{\text{hbl-opx}}{\text{TiO}_2} = \text{TiO}_2 \text{ hbl/TiO}_2 \text{ opx}$
- 6 = $K_D \frac{\text{hbl-cpx}}{\text{TiO}_2} = \text{TiO}_2 \text{ hbl/TiO}_2 \text{ cpx}$
- 7 = $K_D \frac{\text{opx-cpx}}{\text{Fe-Mg}} = \text{Fe/Mg opx /Fe/Mg cpx}$
- 8 = $K_D \frac{\text{opx-hbl}}{\text{Fe-Mg}} = \text{Fe/Mg opx /Fe/Mg hbl}$
- 9 = $K_D \frac{\text{cpx-hbl}}{\text{Fe-Mg}} = \text{Fe/Mg cpx /Fe/Mg hbl}$

Figures in parentheses are reciprocals.

Numbers on top line are sample numbers.

good evidence for the primary nature of this mineral (c.f. Chapter 2). Sen (1970, 1973) has described similar correlations in other hornblende-pyroxene granulites and has suggested the Fe/Mg in hornblendes will place some constraint on this ratio in coexisting pyroxenes.

- (iii) Partition of the minor cations, Mn and Ti, is usually regular in the ferromagnesian minerals, a feature which suggests that these "dilute" constituents have attained equilibrium.
- (iv) Variation in the Fe-Mg distribution between orthopyroxenes and hornblendes is also a function of whole-rock chemistry.

It is inappropriate here to discuss in detail all the factors influencing cation distribution in coexisting minerals, partly due to the difficulties, described above, in comparing the microprobe data with "wet" chemical results. However, it has been shown that thermodynamic models (e.g. for orthopyroxene and clinopyroxene (Bartholomé 1962, Kretz 1961)) in which K_D is temperature dependant are somewhat oversimplified, and that ideal solution behaviour is not always a valid assumption. For example, Davidson (1968) has found a regular variation in the distribution coefficients of metamorphic pyroxenes, related to the ferrous iron of the system. Variation in relative bond energies in pyroxene lattice sites, perhaps directly related to crystal field stabilization energy, has been used to illustrate non-ideal behaviour of Fe^{2+} and Mg in pyroxenes. In Davidson's (1968) model, an increase in the iron content of the system is accompanied by an increased tendency for Fe^{2+} to enter orthopyroxene M_1 at the expense of Mg^{2+} . This causes the

$K_D^{\text{opx-cpx}}_{\text{Fe-Mg}}$ to vary with total iron, and casts some doubt on the temperature dependence of this coefficient.

Other studies have shown that $K_D^{\text{opx-cpx}}_{\text{Fe}^{2+}\text{-Mg}}$ can vary systematically with the Ca content of the clinopyroxene. (Ray and Sen 1970, Sen 1973). Moreover, the Al^{IV} content of hornblendes can influence the Mg-Fe variation between hornblende and either pyroxene (Sen 1973).

In the present work, figure 8.8 shows that $K_D^{\text{opx-hbl}}_{\text{Fe-Mg}}$ increases with the total Fe of the system. This is probably due to an effect similar to that of Davidson's model cited above. Crystal field stabilization energy may be the critical factor which causes Fe^{2+} to increasingly favour orthopyroxene over hornblende in systems with high iron.

It is concluded therefore that variation in whole-rock chemistry is liable to affect coexisting mineral cation distributions, at least in the case of major elements such as iron and magnesium. Calibration of geothermometers using distribution coefficients should take this factor into account.

H. The Garnetiferous metabasites.

The occurrence of garnet in the metabasites is sporadic. Of the 176 analysed rocks considered in this thesis, only 13 contain garnet (7.4%), and this is believed to reflect the minerals overall abundance in this rock group. Six of the thirteen garnetiferous assemblages are from zone A, and seven are from zone B. Garnet is absent in the 32 analysed metabasites from Tromsø, but has been recorded in metabasic material on the island. (Grid ref. 490 648). Two of the six

garnetiferous samples from zone A are also orthopyroxene-bearing.

Petrography.

The garnets are variable in size, ranging from 0.3 mm to over 12 mm in character. The smaller forms tend to be euhedral, with relatively few inclusions. However, the majority of garnets are large, highly poikiloblastic, and have anhedral, indentate or lobate margins with the surrounding matrix. Occasionally, these larger varieties are approximately euhedral, in overall shape, whilst in others small euhedral facets are developed in garnets which are otherwise anhedral in outline (figure 8.9).

The inclusions in the poikiloblastic garnets are large, usually randomly disposed, and of heterogeneous mineralogy. The commonest inclusions are hornblende, plagioclase and small grains of opaque ore, but quartz is also frequent, particularly at the margins of the garnet, and is usually vermicular. Quartz is apparently the only type of inclusion to be crystallographically controlled, since the vermicular forms are occasionally parallel to euhedral garnet faces (Figure 8.9).

A noteworthy feature of the poikiloblastic garnets is the occasional occurrence of "composite" inclusions, a phenomenon which is apparently undocumented in textures of regional metamorphism. Particles representing two or three mineral species are found to be included by some of the larger, more skeletal garnets, and their existence as true inclusions was confirmed by serial sectioning. The feature is illustrated in figure 8.10

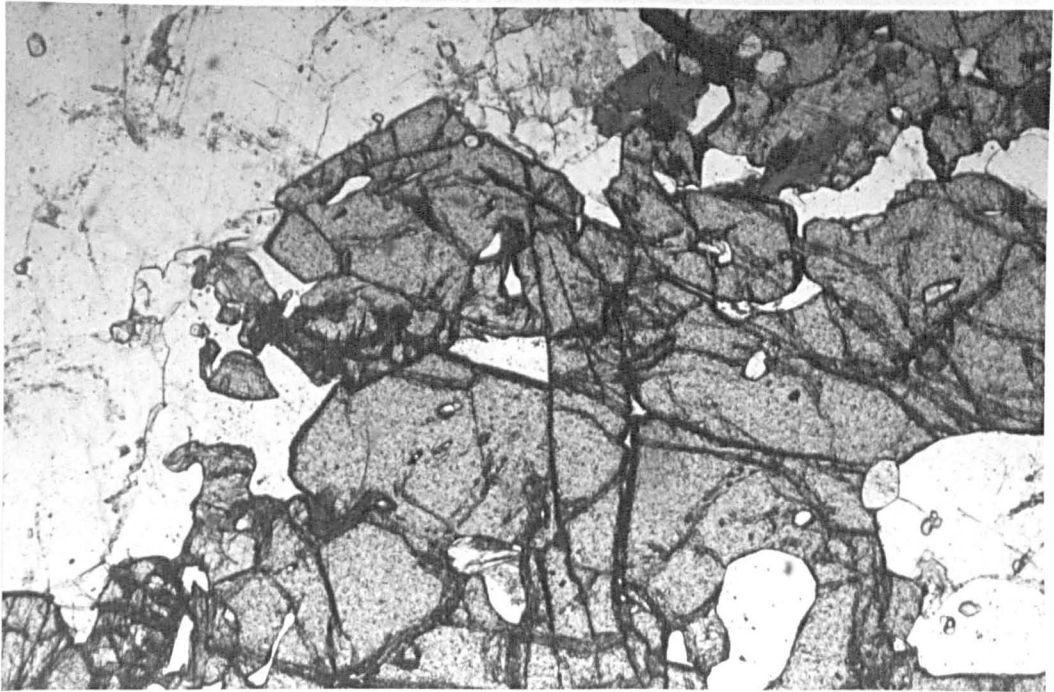


Figure 8.9: Anhedral garnet (No 750), showing euhedral facets with parallel vermicular quartz inclusions. (X 16)

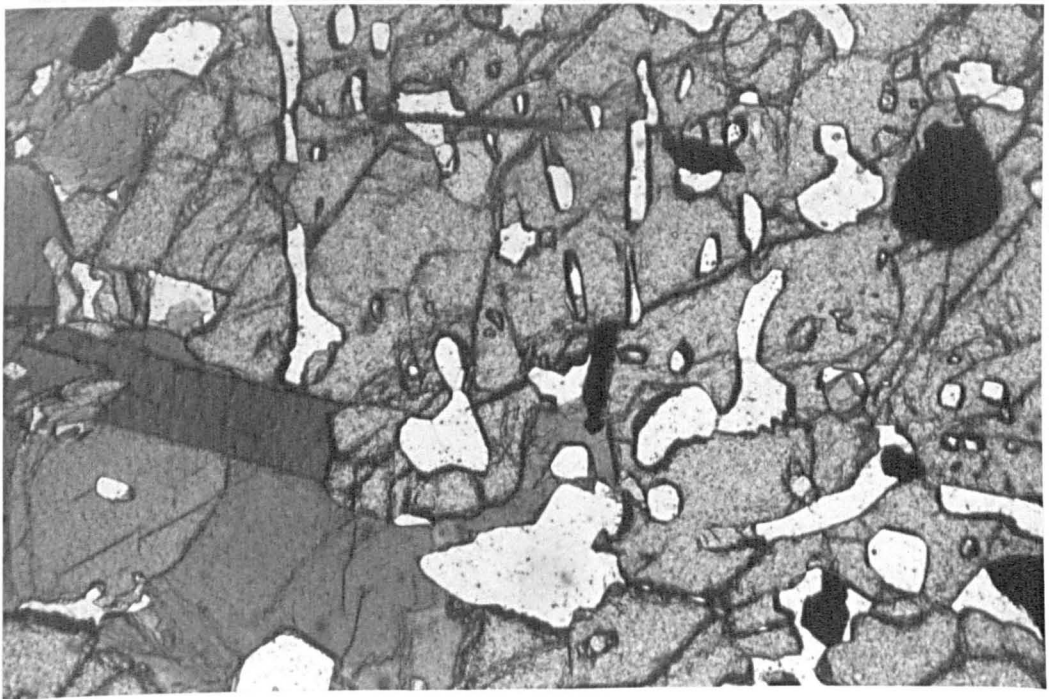


Figure 8.10: Highly poikiloblastic garnet with some composite inclusions. (No. 779). (X 16).

The frequency of large garnets with poikiloblastic textures, is good evidence for rapid growth of this mineral, (Spry 1969, p.70), and the existence of "composite inclusions" suggests that in certain instances the growth was particularly fast. In addition, the absence of orientation features (other than the vermicular quartz), suggests that garnet growth was a static, late-stage event.

Garnet analyses.

Microprobe data for garnets in samples 319 (zone A) and 117 (zone B) are presented in table 8.6, along with end-member compositions. Distribution coefficients between garnet and hornblende, and garnet and the whole rock are quoted in table 8.7.

Both garnet analyses are almandine rich. Each garnet is homogeneous, except that 319 has very small but consistent increases in MnO and Fe/Mg towards the rim.

Figure 8.11, an FeO*-MgO-CaO ternary plot, illustrates that both garnets are iron-enriched, relative to the whole rock chemistry. The whole rock-garnet tie-lines, trend almost directly towards the total Fe apex, and this feature is the dominant chemical characteristic for both minerals. MnO is enriched in the garnets relative to the bulk chemical values, by a factor of between 4.0 and 8.0. (Table 8.7).

Chemical control of garnet formation.

An examination of the whole-rock chemistry of the thirteen garnetiferous metabasites does not reveal any notable or consistent trends. The mean major element chemistry for the garnet-group is presented in table 8.8, and is

319

117

	Garnet rim	Garnet core	Whole rock	Garnet core	Whole rock
SiO ₂	38.31	38.64	47.52	38.76	42.72
Al ₂ O ₃	21.14	20.96	16.65	19.70	15.11
TiO ₂	0.08	0.06	2.27	0.06	3.52
FeO	27.13	26.28	13.10	28.59	17.08
MgO	5.85	6.48	8.02	4.69	7.62
CaO	5.46	5.47	9.18	5.32	10.05
MnO	1.14	0.85	0.21	1.52	0.19
(Total)	99.11	98.74		98.64	
Alm.	59.4	57.4		63.2	
Gr.	15.3	15.4		15.1	
Py.	22.8	25.4		18.4	
Sp.	2.5	1.9		3.3	

Total Fe as FeO

Alm. = Almandine

Py. = Pyrope

Gr. = Grossular

Sp. = Spessartine

Table 8.6: Garnet analyses (Specimens 319 and 117).

	Garnet-Hornblende Coefficients		
	319		117
	rim	core	
K_{MnO}	8.77	6.54	6.08
K_{TiO_2}	0.05	0.04	0.03
$K_{\text{Fe-Mg}}$	2.41	2.11	2.61
	Garnet-Whole rock coefficients		
	319		117
	rim	core	
K_{MnO}	5.43	4.05	8.00
K_{TiO_2}	0.04	0.03	0.02
$K_{\text{Fe-Mg}}$	2.84	2.48	2.72

Table 8.7: Distribution coefficients involving garnets

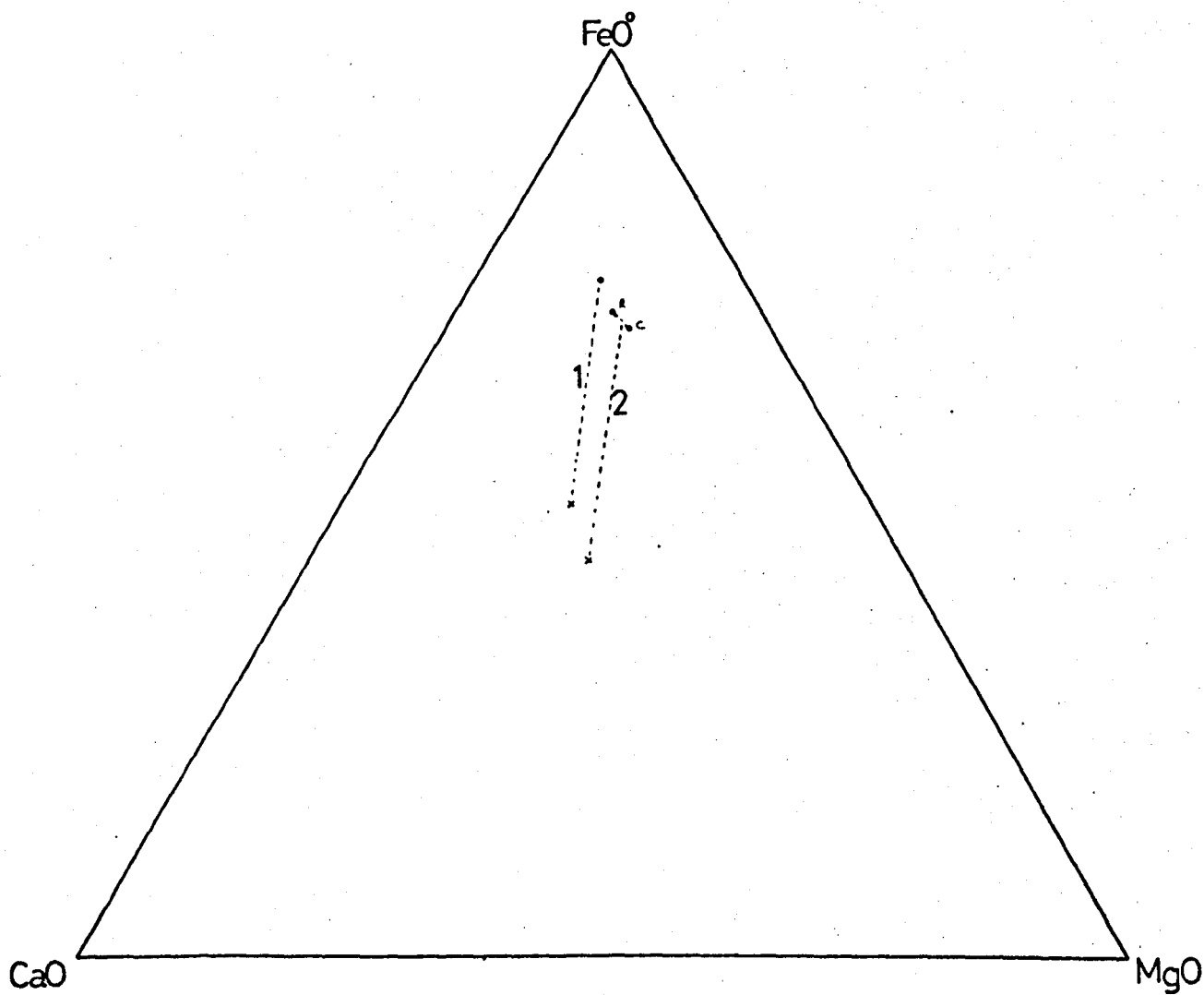


Figure 8.11:

FeO° - MgO - CaO diagram, showing the iron-enrichment in garnets (closed circles), relative to whole rock compositions (crosses). 1 = sample 117; 2 = sample 319. R = rim, C = core of 319.

	1	2
SiO ₂	48.33	47.89
Al ₂ O ₃	16.83	15.80
TiO ₂	2.33	1.93
Fe ₂ O ₃	3.64	3.52
FeO	10.07	9.68
MgO	6.18	6.88
CaO	8.57	8.97
Na ₂ O	2.39	2.77
K ₂ O	0.95	1.30
MnO	0.22	0.22
P ₂ O ₅	0.44	0.35
H ₂ O	0.58	0.62

1. = Mean of 13 garnetiferous metabasites

2. = Mean of 176 metabasites (Table 3.1)

Table 8.8: Mean chemistry of garnetiferous metabasites

compared with the overall metabasite chemistry (from table 3.1, Chapter 3). Al_2O_3 is slightly higher in the garnetiferous group, but total iron and MnO are indistinguishable in the two data sets. In addition, no major oxide is consistently high or low in the 13 garnet-metabasites, and there are no chemical differences between the six analyses from zone A and the seven from zone B.

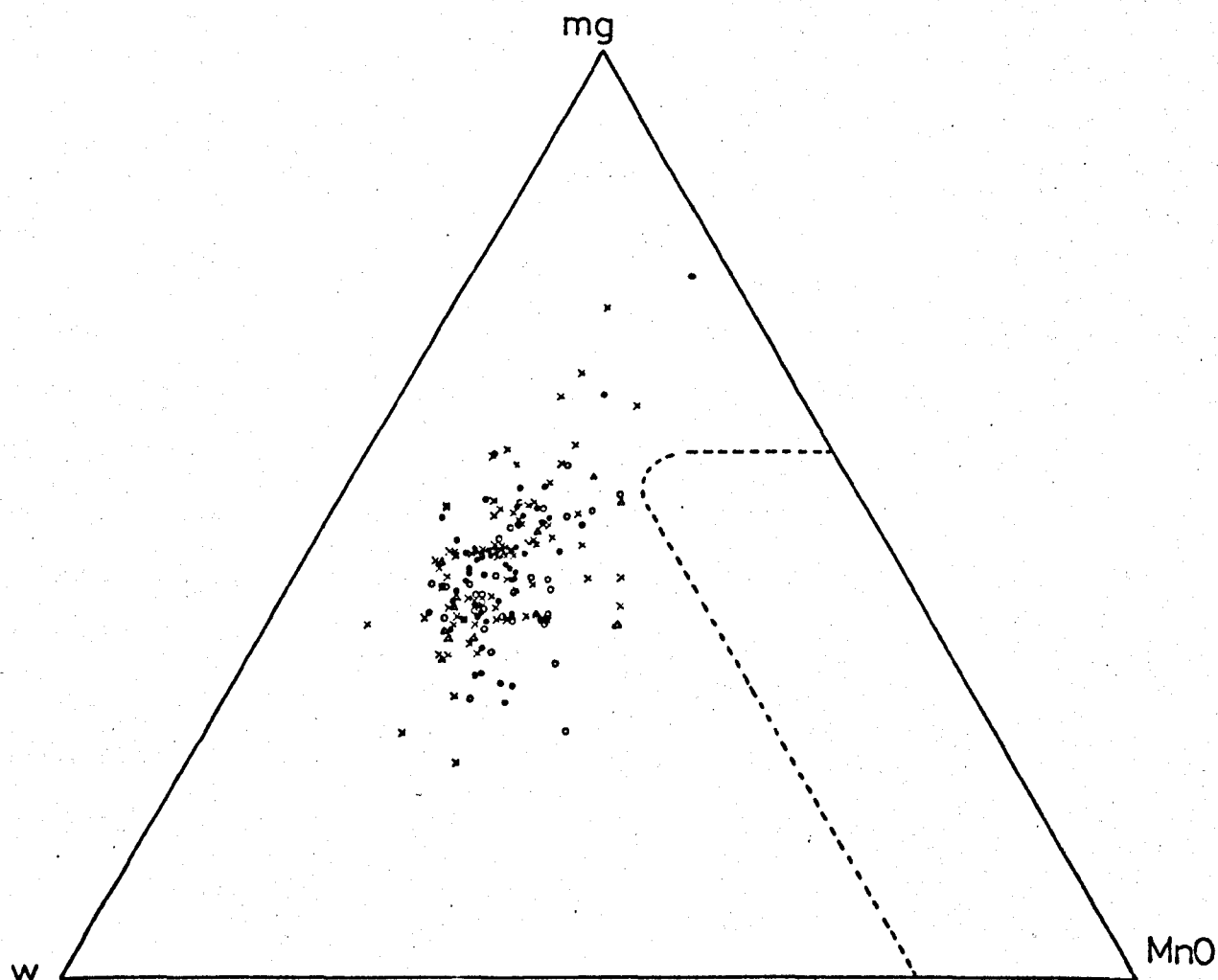
The whole rock trace element data for the garnet-bearing group is also consistent with that for the entire suite of metabasites.

Leake (1972) has shown that relatively low mg, low w and high MnO are the three dominant critical chemical factors controlling garnet paragenesis in amphibolites from Connemara. When these parameters are combined in a triangular plot, these garnetiferous amphibolites separate into the indicated field in figure 8.12. The South Norway metabasites are all plotted in this mg-w-MnO diagram, and it can be seen that no rock falls in the garnet-forming field critical for Connemara. Two garnetiferous samples approach Leake's division, but the remaining 11 samples are not separated from the bulk of the metabasite analyses. Thus, the chemical criteria for garnet formation in basic rocks from Connemara are not applicable to the higher grade rocks of South Norway.

The present whole rock chemistry of the metabasites does not allow the chemical controls (if any) of garnet formation to be isolated.

Discussion:

The occurrence of garnet in basic rocks of high-grade terrains has been the subject of some controversy in



12
Figure 8.12. Ternary plot of niggli mg, w ($= 2\text{Fe}_2\text{O}_3/2\text{Fe}_2\text{O}_3 + \text{FeO}$) and MnO for the South Norwegian metabasites, after Leake (1972). Crosses = zone A samples, closed circles = zone B samples, open circles = zone C samples. Triangles = garnetiferous metabasites. Dashed line is the garnetiferous field for Connemara amphibolites (Leake 1972.)

the past. For example, De Waard (1965) emphasized the role of composition in the development of garnet in the Adirondacks, whilst Buddington (e.g. 1966) suggested pressure and temperature were more dominant factors.

In the metabasites from South Norway, garnet is infrequently developed throughout the terrain.

Its occurrence shows an overall decline with increased grade of metamorphism, and in Zone C it is very rare in metabasites. However, the formation of garnet on the mainland is still sporadic, and no real pattern of distribution emerges from zones A and B, which represent a range of metamorphic conditions from the amphibolite facies to the granulite facies. Thus, although increased grade of metamorphism has some overall control on garnet formation, a wide field of pressure and temperature exists in which the mineral's paragenesis must be due to other factors.

Although the metabasite chemistry is relatively uniform, varying within the constraints of a basaltic composition, no whole-rock chemical factor can be isolated to account for garnet formation. This result differs from that of the garnetiferous amphibolites of Connemara, (in which mg, w and MnO were decisive chemical controls of garnet growth), (Leake 1972).

The few mineral data available for South Norway show that the garnets are iron-enriched relative to the host metabasite, and this result is in accordance with previous results in other high-grade terrains (e.g. Howie and Subramaniam 1957). Almandine-rich garnet is typical of granulite facies and charnockitic series (Deer et al. 1963).

Accordingly, it is possible to invoke a garnet forming reaction in which an iron oxide (e.g. magnetite) occurs as a reactant.

An example might be of the general form:

(Anorthite) + Hypersthene + Magnetite \longrightarrow Almandine + Hornblende + (Albite).

There is no textural evidence for the consistent occurrence of this or a similar reaction, but the garnets in sample 7117 have a narrow hornblende-rich surround.

A second aspect of garnet formation concerns the MnO distribution between the mineral and the host rock. The coefficient K_{Mn} (= MnO garnet/MnO whole rock) varies between 4.0 and 8.0, and is therefore similar in range to K_{Mn} for Moldanubian granulite facies rocks (3.5 - 7.7) (Kurat and Scharbert 1972). In contrast, Atherton (1968) reported much higher distribution values ($K_{Mn} = 28.0 - 81.0$) in Dalradian garnetiferous pelites. In these studies there is apparently some temperature dependence, with K_{Mn} decreasing systematically with increasing grade of metamorphism. Kurat and Scharbert (1972) also suggest that an absence of (Mn)- zonation is indicative of high temperatures of formation, with MnO equilibrating within the garnet by thermal diffusion.

The South Norwegian metabasite garnets have homogeneous chemistries, though sample 319 has minor MnO enrichment (reverse zoning) at its rim. This feature is also found in some Moldanubian garnets, and has been attributed to falling temperature during the later stages of crystallisation. (Kurat and Scharbert, Op. cit.)

Since the whole-rock chemistry has no apparently consistent influence on garnet formation, the reason for the sporadic growth of this mineral across the amphibolite-granulite facies transition is enigmatic. The microscopic textures suggest that garnets grew rapidly under static metamorphic conditions, while the mineral chemistry indicates formation at high temperatures with reaction involving an iron-rich mineral, such as magnetite.

However, these features are unlikely to have been exclusive to the rocks which now contain garnet. It is possible therefore that the physical or chemical factors affecting nucleation, perhaps including differential strain at grain boundaries (Spry 1969, p.119), were critical in garnet paragenesis. The detailed reasons for growth of this mineral remain obscure at this stage.

I. Conclusions.

- (i) Whole rock chemistry is a dominant control of the composition of most analysed ferromagnesian minerals.
- (ii) Hornblende - pyroxene relationships support the concept of chemical equilibrium in the metabasites.
- (iii) Cation distribution coefficients in coexisting minerals may also be influenced by host rock chemistry and should be interpreted with caution.
- (iv) The garnets are usually poikiloblastic, almandine-rich and relatively homogeneous, but whole rock chemistry has no consistent control on the sporadic growth of this mineral.

- (v) The temperature of formation of garnet was high, if the mineral - whole rock MnO distribution is a reliable temperature indicator.

Acknowledgements

The study was carried out during the tenure of an N.E.R.C. Research Studentship.

The author is especially and sincerely grateful to Dr. Dennis Field for his constant help, encouragement and friendship throughout the study.

Thanks are due to Professor the Lord Energlyn, Dr. R.B.Elliott, and other members of staff of the Geology department, Nottingham for their valuable assistance and useful discussions. Mr Roy Hendry and the technical staff also rendered considerable assistance.

Dr. A.J.Nehru and Mr. P.O'Byrne of the Wolfson Institute of Interfacial Technology, University of Nottingham gave assistance in the use of the electron probe.

The late Herr Gunnar Albring and Frau Albring provided warm hospitality during field work in Norway. Mrs S.Dodds typed the manuscript with patience and efficiency.

The advice and companionship, both in the field and in the laboratory, of Mr Colin Peter are acknowledged with gratitude. Similar thanks would have been due to Peter Lankshear, who died in November, 1975.

References

- ABBEY, S. 1973. Studies in 'standard samples' of silicate rocks and minerals. Part 3, Extension and 'revision of 'usable values'. Geol. Surv. Can. Paper 73-36, 25pp.
- AHRENS, L.H. 1964. Element distribution in igneous rocks - VII. A reconnaissance survey of the distribution of SiO_2 in granitic and basaltic rocks. Geochim. Cosmochim. Acta, 28, 271-290.
- AHRENS, L.H., PINSON, W.H. & KEARNS, M.M. 1952. Association of Rb and K and their abundance in common igneous rocks and meteorites. Geochim. Cosmochim. Acta, 2, 229-242.
- ANDRAE, M.O. 1974. Chemical and stable isotope composition of high-grade metamorphic rocks from the Arendal area, South Norway. Contr. Mineral. and Petrol. 47, 299-316.
- ATHERTON, M.P. 1968. The variation in garnet, biotite and chlorite compositions in medium grained pelitic rocks from the Dalradian, Scotland. Contr. Mineral. and Petrol. 18, 347-371.
- BARAGAR, W.R.A. 1968. Major element geochemistry of the Noranda volcanic belt, Quebec-Ontario. Can. J. Earth Sci., 5, 773-790.
- BARAGAR, W.R.A. 1969. Geochemistry of the Coppermine river basalts, Northwest Territories, Canada. Geol. Surv. Can. Paper 69-89pp.
- BARTHOLOMÉ, P. 1962. Iron-magnesium ratio in associated pyroxenes and olivines. Geol. Soc. Am. Buddington Volume, 1-20.
- BEACH, A. & FYFE, W.S.. 1972. Fluid transport and shear zones at Scourie, Sutherland: Evidence of overthrusting? Contr. Mineral and Petrol. 36, 175-180.
- BEESON, R. 1971. The geology of the country between Sogne and Ubergsmoen, South Norway. Unpubl. Ph.D. Thesis, Univ. of Nottingham.

- BINNS, R.A. 1964. Zones of progressive regional metamorphism in the Willyama complex, Broken Hill district, New South Wales. *Jl. Geol. Soc. Aust.* 11, 283-329.
- BLOXAM, T.W. & LEWIS, A.D. 1972. Ti, Zr and Cr in some British pillow lavas and their petrogenetic affinities. *Nature*, 237, 134-136.
- BORISENKO, L.F. & RODIONOV, D.A. 1961. The distribution of Sc in intrusive rocks. *Dokl. Akad. Nauk SSSR*, 138, 203-206. (In Russian).
- BRØGGER, W.C. 1935. On several Archaean rocks from the south coast of Norway. II. The south Norwegian hyperites and their metamorphism. *Skr. Norsk Vidensk. - Akad., I. Mat. - naturv. Kl.*, 1934, No. 1.
- BUDDINGTON, A.F. 1966. The occurrence of garnet in the granulite facies terrane of the Adirondack highlands. A discussion. *J. Petrol.* 7, 331-335.
- BUGGE, A. 1928. En forkastning i det syd-norske grundfjell. *Norges Geol. Unders.*, 130.
- BUGGE, A. 1965. Iakttagelser fra rektangelbladet Kragerø og den store grunnfjellsbreksje. *Norges Geol. Unders.*, 229.
- BUGGE, J.A.W. 1940. Geological and petrological investigations in the Arendal district. *Norsk Geol. Tidsskr.* 20, 71-111.
- BUGGE, J.A.W. 1943. Geological and petrological investigations in the Kongsberg-Bamble formation. *Norges Geol. Unders.*, 160.
- BURNS, R.G. 1970. Mineralogical applications of crystal field theory. Cambridge University Press, 224pp.

- CANN, J.R. 1969. Spilites from the Carlsberg ridge, Indian Ocean. J. Petrol. 10, 1-19.
- CANN, J.R. 1970. Rb, Sr, Y, Zr and Nb in some ocean-floor basaltic rocks. Earth Planet. Sci. Lett. 10, 7-11.
- CANN, J.R. 1971. Petrology of basement rocks from Palmer ridge, N.E. Atlantic. Phil. Trans. Roy. Soc. Lond. A268, 605-617.
- CARR, M.H. & TUREKIAN, K.K. 1961. The geochemistry of Cobalt. Geochim. Cosmochim. Acta. 23, 9-60.
- CLARKE, D.B. 1970. Tertiary basalts of Baffin bay: possible primary magma from the mantle. Contrib. Mineral. and Petrol. 25, 203-224.
- COLLERSON, K.D. 1965. Contrasting patterns of K/Rb distribution in Precambrian high-grade metamorphic rocks from Central Australia. Jl. Geol. Soc. Aust. 22, 145-158.
- COOPER, D.C. 1971. The geology of the area around Eydehavn, South Norway. Unpubl. Ph. D. thesis, Univ. of Nottingham.
- COOPER, D.C. & FIELD, D. 1977. The chemistry and origins of Proterozoic, low-potash, high-iron charnockitic gneisses from Tromsø, South Norway. Earth Planet. Sci. Lett. 35, 105-115.
- CORRENS, C.W. 1969. Introduction to Mineralogy. Allen and Unwin, London. (2nd edn.) 484pp.
- COX, K.G., MACDONALD, R., & HORNUNG, G. 1967. Geochemical and petrographic provinces in the Karroo basalts of Southern Africa. Am. Mineral. 52, 1451-1474.

- DAVIDSON, L.R. 1968. Variations in ferrous iron-magnesium distribution coefficients of metamorphic pyroxenes from Quairading, Western Australia. *Contr. Mineral and Petrol.* 19, 239-259.
- DAVIDSON, L.R. 1971. Metamorphic hornblendes from basic granulites of the Quairading district, Western Australia. *Neues Jahrb. Mineral. Monatsh.* 8, 344-359.
- DEER, W.A., HOWIE, R.A. & ZUSSMAN, J. 1963. Rock-forming minerals. (5 volumes). Longmans, London.
- DE WAARD, D. 1965. The occurrence of garnet in the granulite-facies terrane of the Adirondack highlands. *J. Petrol.* 6, 165-191.
- DRURY, S.A. 1972. The chemistry of some granitic veins from the Lewisian complex of Tiree, Argyllshire, Scotland. *Chem. Geol.* 9, 175-193.
- DRURY, S.A. 1973. The geochemistry of Precambrian granulite facies rocks from the Lewisian complex of Tiree, Inner Hebrides, Scotland. *Chem. Geol.* 11, 167-188.
- DRURY, S.A. 1974. Chemical changes during retrogressive metamorphism of Lewisian granulite facies rocks from Coll and Tiree. *Scott. J. Geol.* 10, 237-256.
- EADE, K.E. & FAHRIG, W.F. 1971. Geochemical evolutionary trends of continental plates - a preliminary study of the Canadian shield. *Geol. Surv. Can. Bull.* 179, 51pp.
- ELLIOTT, R.B. 1973. The chemistry of gabbro/amphibolite transitions in South Norway. *Contr. Mineral. and Petrol.* 38, 71-79.
- ENGEL, A.E.G. & ENGEL, C.G. 1958. Progressive metamorphism and granitization of the major paragneiss, Northwest Adirondack Mountains, New York, 1. *Bull. Geol. Soc. Am.* 69, 1369-1413.

- ENGEL, A.E.G. & ENGEL, C.G. 1960. Progressive metamorphism and granitization of the major paragneiss, northwest Adirondack mountains, New York, 2. Bull. Geol. Soc. Am. 71, 1-57.
- ENGEL, A.E.G. & ENGEL, C.G. 1962. Progressive metamorphism of amphibolite, northwest Adirondack mountains, New York. Geol. Soc. Am. Buddington volume, 37-62.
- FAURE G. & HURLEY, P.M. 1963. The isotopic composition of Sr in oceanic and continental basalts: application to the origin of igneous rocks. J.Petrol. 4, 31-50.
- FERRARA, G., INNOCENTI, F., RICCI, C.A., & SERRI, G. 1976. Ocean-floor affinity of basalts from north Appennine ophiolites: geochemical evidence. Chem. Geol., 17, 101-111.
- FIELD, D. 1969. The geology of the country around Tvedestrand, South Norway. Unpubl. Ph.D. thesis, Univ. of Nottingham.
- FIELD, D. & ELLIOTT, R.B. 1974. The chemistry of gabbro/amphibolite transitions in South Norway. II Trace elements. Contr. Mineral. and Petrol. 47, 63-76.
- FIELD, D. & CLOUGH, P.W.L. 1976. K/Rb ratios and metasomatism in metabasites from a Precambrian amphibolite-granulite transition zone. Jl. Geol. Soc. Lond. 132, 277-288.
- FLANAGAN, F.J. 1973. 1972 values for international geochemical reference samples. Geochim. Cosmochim. Acta 37, 1189-1200.
- FLEET, M.E. 1974a. Partition of Mg and Fe^{2+} in coexisting pyroxenes. Contr. Mineral. and Petrol. 44,
- FLEET, M.E. 1974b. Partition of major and minor elements and equilibration in coexisting pyroxenes. Contr. Mineral. and Petrol. 44, 259-274.

- FLOYD, P.A. & WINCHESTER, J.A. 1975. Magma type and tectonic setting discrimination using immobile elements. *Earth Planet. Sci. Lett.* 27, 211-218.
- FLOYD, P.A. & WINCHESTER, J.A. 1976. Petrochemical affinities of Dalradian metabasaltic rocks: a reply to C.M.Graham. *Earth Planet. Sci. Lett.* 32, 213-214.
- FREY, F., HASKIN, M.A., POETZ, J. & HASKIN, L.A. 1968. Rare earth abundances in some basic rocks. *J. Geophys. Res.* 73,
- FRODESEN, S. 1968a. Coronas around olivine in a small gabbro intrusion, Bamble area, South Norway. *Norsk Geol. Tidsskr.* 48, 201-206.
- FRODESEN, S. 1968b. Petrographical and chemical investigations of a Precambrian gabbro intrusion, Håsen, Bamble area, South Norway. *Norsk Geol. Tidsskr.* 48, 55-59.
- FRYKLUND, V.C. & FLEISCHER, M. 1963. The abundance of Scandium in volcanic rocks, a preliminary estimate. *Geochim. Cosmochim. Acta* 27, 643-664.
- FYFE, W.S. 1973. The granulite facies, partial melting and the Archaean crust. *Phil. Trans. Roy. Soc. Lond.* A273, 457-461.
- GAST, P.W. 1967. Isotope geochemistry of volcanic rocks. In: Hess, H.H. & Poldervaart, A. (eds.) *Basalts*. Volume 1, 325-358.
- GILL, R.C.O. & BRIDGWATER, D. 1976. The Ameralik dykes of West Greenland, the earliest known basaltic rocks intruding stable continental crust. *Earth Planet. Sci. Lett.* 29, 276-282.
- GOODWIN, A.M. 1968. Archaean protocontinental growth and early history of the Canadian shield. *Intn. Geol. Cong.* 23rd, 1 69-89.

- GRAHAM, C.McL. 1976a Petrochemistry and tectonic significance of Dalradian metabasaltic rocks of the southwest Scottish highlands. Jl. Geol. Soc. Lond., 132, 61-84.
- GRAHAM, C.McL. 1976b. Petrochemical affinities of Dalradian metabasaltic rocks: discussion of paper by J.A.Winchester and P.A.Floyd. Earth Planet. Sci. Lett. 32, 210-212.
- GREEN, D.H. & RINGWOOD, A.E. 1967. An experimental investigation of the gabbro to eclogite transformation and its petrological application. Geochim. Cosmochim. Acta 31, 767-833.
- HALLBERG, J.A. 1972. Geochemistry of Archaean volcanic belts in the Eastern Goldfields region of Western Australia. J. Petrol. 13, 45-56.
- HARKER, A. 1939. Metamorphism. Methuen, London.
- HARRIS, P.G. 1957. Zone refining and the origin of potassic basalts. Geochim. Cosmochim. Acta 12, 195-210.
- HART, S.R. 1969. K, Rb, Cs contents and K/Rb, K/Cs ratios of fresh and altered submarine basalts. Earth Planet. Sci. Lett. 6, 295-303.
- HART, S.R. 1970. Chemical exchange between sea-water and deep-ocean basalts. Earth Planet. Sci. Lett. 9, 269-279.
- HART, S.R. & ALDRICH, L.T. 1966. Fractionation of K/Rb by amphiboles: implications regarding mantle composition. Science, 155, 325-327.
- HART, S.R., BROOKS, C., KROGH, T.E., DAVIS, G.L. & NAVA, D. 1970. Ancient and modern volcanic rocks: a trace element model. Earth Planet. Sci. Lett. 10, 17-28.

- HART, S.R., ERLANK, A.J. & KABLE, E.J.D. 1974. Sea floor basalt alteration: some chemical and Sr isotopic effects. Contr. Mineral. and Petrol. 44, 219-230.
- HARVEY, P.K., TAYLOR, D.M., HENDRY, R.D. & BANCROFT, F. 1973. An accurate fusion method for the analysis of rocks and chemically related materials by X-ray fluorescence spectrometry. X-Ray Spectrometry, 2, 33-44.
- HEIER, K.S. 1964. Rb-Sr and $\text{Sr}^{87}/\text{Sr}^{86}$ ratios in deep crustal material. Nature 202, 477-478.
- HEIER, K.S. 1973a. A model for the composition of the deep continental crust. Fortschr. Mineral. 50, 174-187
- HEIER, K.S. 1973b. Geochemistry of granulite facies rocks and problems of their origin. Phil. Trans. Roy. Soc. Lond. A273, 429-442.
- HEIER, K.S. 1976. Chemical composition of Archaean granulites and charnockites. In: The Early History of the Earth, (ed. B.F.Windley), Leicester University Press, 159-164.
- HEIER, K.S., COMPSTON, W. & McDOUGALL, I. 1965. Th and U contents and the isotopic composition of Sr in the differentiated Tasmanian dolerites. Geochim. Cosmochim. Acta 29, 643-661.
- HEITANAN, A. 1969. Distribution of Fe^{2+} and Mg between garnet, staurolite and biotite in alumina-rich schists in various metamorphic zones, north of the Idaho batholith. Am. J. Sci. 267, 422-456.
- HOLLAND, J.G. & LAMBERT, R.StJ. 1973. Comparative major element geochemistry of the Lewisian of the mainland of Scotland. In: The Early Precambrian of Scotland and related rocks of Greenland. (eds. R.G.Park & J.Tarney), Univ. of Keele. 51-62.
- HOLLAND, J.G. & LAMBERT, R.StJ. 1975. The chemistry and origin of the Lewisian gneisses of the Scottish mainland: the Scourie and Inver assemblages and sub-crustal accretion. Precambrian Res. 2, 161-188.

- HOWIE, R.A. & SUBRAMANIAM, A.P. 1957. The paragenesis of garnet in charnockite, enderbite and related granulites. *Min. Mag.* 31, 565-579.
- HUGHES, C.J. 1972. Spilites, keratophyres and the igneous spectrum *Geol. Mag.* 109, 513-527.
- IRVINE, T.N. & BARAGAR, W.R.A. 1971. A guide to the chemical classification of the common igneous rocks. *Can. J. Earth Sci.* 8, 523-548.
- JAKOBSSON, S.P. 1972. Chemistry and distribution pattern of recent basaltic rocks of Iceland. *Lithos*, 5, 365-386.
- KALSBECK, F. & LEAKE, B.E. 1970. The chemistry and origin of some basement amphibolites between Ivigtut and Frederikshab, S.W. Greenland. *Bull Grønlands geol. Unders.* 90, 36pp.
- KAMP, P.C. van de 1969. Origin of amphibolites in the Beartooth mountains, Wyoming and Montana: new data. *Bull. Geol. Soc. Am.* 80, 1127-1136.
- KAMP, P.C. van de 1970. The green beds of the Scottish Dalradian series: geochemistry, origin and metamorphism of sediments. *J. Geol.* 78, 281-303.
- KRATZ, K.O., GERLING, E.K. & LOBACH-ZHUCHENKO, S.B. 1968. The isotope geology of the Precambrian of the Baltic shield. *Can. J. Earth Sci.* 5, 657-660.
- KROGH, T.E. & DAVIS, G.L. 1969. Isotopic ages along the Grenville Front in Ontario. *Ann. Rep. Geophys. Lab. Yrb.* 68, 309.
- KRETZ, R. 1960. The distribution of certain elements among coexisting pyroxenes, calcic amphiboles and biotites in skarns. *Geochim. Cosmochim. Acta* 20, 161-191.

- KRETZ, R. 1961. Some applications of thermodynamics to coexisting minerals of variable composition. Examples: orthopyroxene-clinopyroxene, and orthopyroxene-garnet. *J. Geol.* 69, 361-387.
- KRETZ, R. 1963. Distribution of magnesium and iron between orthopyroxene and calcic pyroxene in natural mineral assemblages. *J. Geol.* 71, 773-785.
- KULP, J.L. & NEUMANN, H. 1961. Some K-Ar ages from the Norwegian basement. *Ann. N.Y. Acad. Sci.* 91, 469-475.
- KUNO, H. 1967. Differentiation of basic magmas. *In: Hess, H.H. & Foldervaart, A. (eds.) Basalts, Interscience, New York. Vol. 2* 623-688.
- KURAT, G. & SCHARBERT, H.G. 1972. Compositional zoning in garnets from granulite facies rocks of the Moldanubian zone, Bohemian massif of Lower Austria, Austria. *Earth Planet. Sci. Lett.* 16, 379-387.
- LAMBERT, I.B. & HEIER, K.S. 1968. Geochemical investigations of deep-seated rocks in the Australian shield. *Lithos* 1, 30-53.
- LAMBERT, R.StJ., CHAMBERLAIN, V.E. & HOLLAND, J.G. 1976. The geochemistry of Archaean rocks. *In: The Early History of the Earth, B.F.Windley (ed.), Wiley, London.* 377-387.
- LEAKE, B.E. 1964. The chemical distinction between ortho- and para-amphibolites. *J.Petrol.* 5, 238-254.
- LEAKE, B.E. 1968. A catalog of analysed calciferous and sub-calciferous amphiboles together with their nomenclature and associated minerals. *Geol. Soc. Am. Spec. Paper* 98, 210pp.
- LEAKE, B.E. 1972. Garnetiferous striped amphibolites from Connemara, Western Ireland. *Min. Mag.* 38, 649-665.

- LEAKE, B.E., HENDRY, G.L., KEMP, A., PLANT, A.G., HARVEY, P.K., WILSON, J.R., COATS, J.S., AUCOTT, J.W., LUNEL, T. & HOWARTH, R.J. 1969. The chemical analysis of rock powders by automatic X-ray fluorescence. *Chem. Geol.* 5, 7-86.
- LEELANANDAM, C. 1967. Chemical study of pyroxenes from the charnockitic rocks of Kondapalli, India, with emphasis on the distribution of elements in coexisting pyroxenes. *Min. Mag.* 36, 153-179.
- LEWIS, J.D. & SPOONER, C.M. 1973. K/Rb ratios in Precambrian granulite terrains. *Geochim. Cosmochim. Acta* 37, 1111-1118.
- MacDONALD, G.A. & KATSURA, T. 1964. Chemical composition of some Hawaiian lavas. *J. Petrol.* 5, 82-133.
- McINTIRE, W.L. 1963. Trace element partition coefficients - a review of theory and application to geology. *Geochim. Cosmochim. Acta* 27, 1209-1264.
- MANSON, V. 1967. Geochemistry of basaltic rocks: major elements. In: Hess, H.H. & Poldervaart, A. (eds.) *Basalts*, Interscience, New York. Vol.1. 215-269.
- MATTHEWS, D.H. 1971. Altered basalts from Swallow bank, an abyssal hill in the N.E. Atlantic, and from a nearby seamount. *Phil. Trans. Roy. Soc. Lond.* A268, 551-571.
- MEULLER, R.F. 1960. Compositional characteristics and equilibrium relations in mineral assemblages of a metamorphosed iron formation. *Am. J. Sci.* 258, 449-493.
- MEULLER, R.F. 1961. Analysis of relations among Mg, Fe and Mn in certain metamorphic minerals. *Geochim. Cosmochim. Acta.* 25, 267-296.
- MILLER, R.L. & KAHN, J.S. 1962. Statistical analysis in the geological sciences. John Wiley, New York, 483pp.

- MISRA, S.N. & GRIFFIN, W.L. 1972. Geochemistry and metamorphism of dolerite dykes from Austraggy in Lofoten. Norsk Geol. Tidsskr. 52, 409-425.
- MIYASHIRO, A. 1967. Metamorphism of basaltic rocks. In: Hess, H.H. & Poldervaart, A. (eds.) Basalts. Interscience, New York. Vol. 2, 799-834.
- MIYASHIRO, A., SHIDO, F. & EWING, M. 1970. Crystallisation and differentiation in abyssal tholeiites and gabbros from mid-oceanic ridges. Earth Planet. Sci. Lett. 7, 361-365.
- MOINE, B., ROCHE, H. de la, & TOURET, J. 1972. Structures geochemiques et zonéographie métamorphique dans le Précambrien catazonal du Sud de la Norvège (Region d'Arendal). Sci. Terre 17, 131-141.
- MORTON, R.D., BATEY, B.H. & O'NIONS, R.K. 1970. Geological investigations in the Bamble sector of the Fennoscandian Shield, South Norway. 1. The geology of Eastern Bamble. Norges Geol. Unders. Nr. 263.
- MUIR, I.D. 1954. Crystallisation of pyroxenes in an iron-rich diabase from Minnesota. Min. Mag. 30, 376-388.
- NEUMANN, H. 1960. Apparent ages of Norwegian minerals and rocks. Norsk Geol. Tidsskr. 40, 173-189.
- NEUMANN, H. 1961. The Scandium content of some Norwegian minerals and the formation of Thortveitite - a reconnaissance survey. Norsk. Geol. Tidsskr. 41, 197-210.
- NICHOLLS, G.D. & ISLAM, M.R. 1971. Geochemical investigations of basalts and associated rocks from the ocean floor and their implications. Phil. Trans. Roy. Soc. Lond. A268, 469-486.
- NOCKOLDS, S.R. & MITCHELL, R.L. 1948. The geochemistry of some Caledonian plutonic rocks: A study in the relationship between the major and trace elements of igneous rocks and their minerals. Trans. Roy. Soc. Edinburgh. 61, 533-575.

- NOE-NYGAARD, A. & PEDERSEN, S. 1974. Progressive chemical variation in a tholeiitic lava sequence at Kap Stosch, North East Greenland. Bull. Geol. Soc. Den. 23, 175-190.
- NORMAN, J.C. & HASKIN, L.A. 1968. The geochemistry of Scandium : a comparison to the rare earths and Fe. Geochim. Cosmochim. Acta 32, 93-108.
- O'NIONS, R.K., MORTON, R.D., & BAADSGAARD, H. 1969. K-Ar ages from the Bamble sector of the Fennoscandian shield in South Norway. Norsk Geol. Tidsskr. 49, 171-190.
- O'NIONS, R.K. & BAADSGAARD, H. 1971. A radiometric study of polymetamorphism in the Bamble region, Norway. Contr. Mineral. and Petrol. 34, 1-21.
- ORVILLE, P.M. 1969. A model for metamorphic differentiation origin of thin-layered amphibolites. Am. J. Sci. 267, 64-86.
- OXBURGH, E.R. 1964. Petrological evidence for amphibolite in the upper mantle and its petrogenetic and geophysical implications. Geol. Mag. 101, 1-19.
- PANKHURST, R.J. & O'NIONS, R.K. 1973. Determination of Rb/Sr and $\text{Sr}^{87}/\text{Sr}^{86}$ ratios of some standard rocks, and evaluation of X-ray fluorescence spectrometry in Rb-Sr geochemistry. Chem. Geol. 12, 127-136.
- PARK, R.G. 1966. Nature and origin of Lewisian basic rocks of Gairloch, Wester Ross. Scott. J. Geol. 2, 179-199.
- PATCHETT, P.J. & BYLUND, G. 1977. Age of Grenville belt magnetisation. Rb-Sr and palaeomagnetic evidence from Swedish dolerites. Earth Planet. Sci. Lett. 35, 92-104.
- PEARCE, T.H. & CANN, J.R. 1973. Tectonic setting of basic volcanic rocks determined using trace element analyses. Earth Planet. Sci. Lett. 19, 290-300.

- PEARCE, T.H., GORMAN, B.E. & BIRKETT, T.C. 1975. The TiO_2 - K_2O - P_2O_5 diagram: a method of discriminating between oceanic and non-oceanic basalts. *Earth Planet. Sci. Lett.* 24, 419-426.
- PETTERSEN, M.J. 1964. The geology of the country around Sannidal, South Norway. Unpubl. Ph.D. Thesis, Univ. of Nottingham.
- PHAN, K.D. 1967. Le Sc dans certaines pegmatites Malagaches et roches encaissantes. *Bull. Bur. Recherches Geol. et Min.* (Paris), 3, 78-97.
- PRINZ, M. 1967. The geochemistry of basalts: trace elements. In: Hess, H.H. & Poldervaart, A. (eds.) *Basalts*, Interscience, New York. Vol. 1. 270-294.
- RAY, S. & SEN, S.K. 1970. Partitioning of major exchangeable cations among orthopyroxenes, clinopyroxene and hornblende in basic granulites from Madras. *Neues Jahr. Miner. Abh.* 114, 61-88
- RIVALENTI, G. 1970. Genetical problems of banded amphibolites in the Frederikshåb district, Southwest Greenland. *Atti Soc. Tosc. Sci. Nat. Mem., Serie A*, 77, 342-357.
- RIVALENTI, G. & ROSSI, A. 1972. The geology and petrology of the Precambrian rocks to the northeast of the fjord Qagssit, Frederikshåb district, Southwest Greenland. *Bull. Grønlands Geol. Unders.* 103, 98pp.
- RIVALENTI, G. & ROSSI, A. 1973. Amphiboles and biotites of the Hornblende gneisses in an area to the N.E. of the fjord Qagssit, Frederikshab district, S.W. Greenland. *Tschermaks Min. Petr. Mitt.* 20, 13-27.
- RODDICK, J.C. & COMPSTON, W. 1977. Strontium isotopic equilibration: a solution to a paradox. *Earth Planet. Sci. Lett.* 34, 238-246.
- SCHRIEVER, K. 1973a. Correlated changes in mineral assemblages and in rock habit and fabric across an orthopyroxene isograd, Grenville province, Quebec. *Am. J. Sci.* 273, 171-186.

- SCHRIVER, K. 1973b. Bimetasomatic plagioclase-pyroxene reaction zones in granulite facies. *Neues Jb. Miner. Abh.* 119, 1-19.
- SCHWARCZ, H.P. 1967. The effect of crystal field stabilization on the distribution of transition metals between metamorphic minerals. *Geochim. Cosmochim. Acta* 31, 503-517.
- SCHWARZER, R.R. & ROGERS, J.J.W. 1974. A worldwide comparison of alkali olivine basalts and their differentiation trends. *Earth Planet. Sci. Lett.* 23, 286-296.
- SEN, S.K. 1970. Mg^{2+} - Fe^{2+} compositional variation in hornblende-pyroxene granulites. *Contr. Mineral. and Petrol.* 29, 76-88.
- SEN, S.K. 1973. Compositional relations among hornblendes and pyroxenes in basic granulites, and an application to the origin of garnets. *Contr. Mineral. and Petrol.* 38, 299-306.
- SHAW, D.M. 1968. A review of K-Rb fractionation trends by covariance analysis. *Geochim. Cosmochim. Acta* 32, 573-601.
- SHAW, D.M., MOXHAM, R.L., FILBY, R.H. & LAPKOWSKY, W.W. 1963. The petrology and geochemistry of some Grenville skarns. *Canad. Mineral.* 7, 578-616.
- SHERATON, J.W., SKINNER, A.C. & TARNEY, J. 1973. The geochemistry of the Scourian gneisses of the Assynt district. *In: The Early Precambrian of Scotland and related rocks of Greenland.* R.G.Park & J.Tarney (eds.), Univ. of Keele.
- SIGHINOLFI, G.P. 1969. K/Rb ratios in high-grade metamorphism: A confirmation of the hypothesis of continued crustal evolution. *Contr. Mineral and Petrol.* 21, 346-356.
- SIGHINOLFI, G.P. 1971. Investigations into deep crustal levels: fractionating effects and geochemical trends related to high-metamorphism. *Geochim. Cosmochim. Acta* 35, 1005-1021.

- SMELLIE, J.A.T. 1972. Preparation of glass standards for use in X-ray microanalysis. *Min. Mag.* 38, 614-617.
- SMITH, R.E. 1968. Redistribution of major elements in the alteration of some basic lavas during burial metamorphism. *J. Petrol.* 9, 191-219.
- SMITH, R.E. & SMITH, S.E. 1976. Comments on the use of Ti, Zr, Y, Sr, K, P, and Nb in classification of basaltic magmas. *Earth Planet. Sci. Lett.* 32, 114-120.
- SMITHSON, S.B. & BROWN, S.K. 1977. A model for lower continental crust. *Earth Planet. Sci. Lett.* 35, 134-144.
- SPRY, A. 1969. *Metamorphic textures*. Pergamon, Oxford. 350pp.
- STARMER, I.C. 1969a. The migmatite complex of the Risør area, Aust Agder, Norway. *Norsk Geol. Tidsskr.* 49, 33-56.
- STARMER, I.C. 1969b. Basic plutonic intrusions of the Risør-Søndeled area, South Norway: the original lithologies and their metamorphism. *Norsk Geol. Tidsskr.* 49, 403-431.
- STARMER, I.C. 1972a. Polyphase metamorphism in the granulite facies terrain of the Risør area, South Norway. *Norsk. Geol. Tidsskr.* 52, 243-71.
- STARMER, I.C. 1972b. The Svecofennian regeneration and earlier orogenic events in the Bamble series, South Norway. *Norg. Geol. Unders.* 277, 37-52.
- TARNEY, J. 1976. Geochemistry of Archaean high-grade gneisses, with implications as to the origin of the Precambrian crust. In: *The Early History of the Earth.*, B.F.Windley (ed.) Wiley, London. 405-417.

- TARNEY, J., SKINNER, A.C. & SHERATON, J.W. 1972. A geochemical comparison of major Archaean gneiss units from Northwest Scotland and East Greenland. 24th Int. Geol. Congr., Montreal. Section 1, 162-174.
- TAYLOR, S.R. 1965. The application of trace element data to problems in petrology. Phys. Chem. Earth, 6, 133-213.
- THOMPSON, G. 1973. Trace-element fractionation in oceanic rocks. 2. Gabbros and related rocks. Chem. Geol. 12, 99-111.
- TILLEY, C.E. & SCOON, J.H. 1961. Differentiation of Hawaiian basalts: trends of Mauna Loa and Kilauea historic magma. Am. J. Sci. 259, 60-68.
- TOURET, J. 1962. Geological studies in the region Verarshei-Gjerstad. Norges. Geol. Unders. 215, 120-139.
- TOURET, J. 1967. Les gneiss oeilles de la region de Vegarshei-Gjerstad (Norvege meridionale). I. Etude petrographique. Norsk. Geol. Tidsskr. 47, 131-148.
- TOURET, J. 1968. The Precambrian metamorphic rocks around the lake Vegar (Aust Agder, Southern Norway). Norge Geol. Unders. 257, 45pp.
- TOURET, J. 1971. Le facies granulite en Norvege meridionale. 1. Les associations mineralogiques. Lithos 4, 239-249.
- TUREKIAN, K.K. & CARR, M.H. 1960. The geochemistry of Chromium, Cobalt and Nickel. 21st Intern. Geol. Congr., Norden, Section 1. 14-28.

- TURNER, F.J. & VERHOOGEN, J. 1960. Igneous and Metamorphic Petrology. McGraw-Hill, New York. (2nd edn.) 694pp.
- VALLANCE, T.G. 1960. Concerning spilites. Proc. Linn. Soc. N.S.W. 85, 8-52.
- VALLANCE, T.G. 1965. On the chemistry of pillow lavas and the origin of spilites. Min. Mag. 34, 471-481.
- VALLANCE, T.G. 1969. Spilites again: some consequences of the dehydration of basalts. Proc. Linn. Soc. N.S.W. 94, 8-51.
- VILJOEN, M.J. & VILJOEN, R.P. 1969. The geology and geochemistry of the lower ultramafic unit of the Onverwacht group, and a proposed new class of igneous rock. Spec. Pub. Geol. Soc. S.Africa 2, 245-274.
- VISWANATHAN, S. 1975. Rocks of unusual chemistry in the charnockitic terrains of India, and their geological significance. Geol. Mag. 112, 63-69.
- WAGER, L.R. & MITCHELL, R.L. 1951. The distribution of trace elements during strong fractionation of basic magma - a further study of the Skaergaard intrusion, East Greenland. Geochim. Cosmoch. Acta 1, 129-208.
- WAGER, L.R. & BROWN, G.M. 1968. Layered igneous rocks. Oliver & Boyd, Edinburgh. 588pp.
- WALKER, F. & POLDERVAART, A. 1949. The Karroo dolerites of South Africa. Bull. Geol. Soc. Am. 60, 591-706.
- WATTERSON, J. 1968. Plutonic development of the Ilordleq area, South Greenland. Part II. Late-kinematic basic dykes. Medd. om Grønland, Bd 185, Nr 3. 104pp.

- WEDEPOHL, K.H. 1967. Geochemistry. Holt, Rinehart & Winston. New York. 231pp.
- WEDEPOHL, K.H. 1970. Handbook of Geochemistry, 2. Springer-Verlag. New York.
- WHITNEY, P.R. 1969. Variations of K/Rb ratio in migmatitic paragneisses of the Northwest Adirondacks. Geochim. Cosmochim. Acta 33, 1203-1211.
- WINCHESTER, J.A. & FLOYD, P.A. 1976. Geochemical magma type discrimination: application to altered and metamorphosed basic igneous rocks. Earth Planet. Sci. Lett. 28, 459-469.
- WILSON, A.D. 1955. A new method for the determination of ferrous iron in rocks and minerals. Bull. Geol. Surv. Gt. Britain 2, 56-58.
- WILSON, J.R. & LEAKE, B.E. 1972. The petrochemistry of the epidiorites of the Tayvallich peninsula, North Knapdale, Argyllshire. Scott. J. Geol. 8, 215-252.
- WINDLEY, B.F., HERD, R.K. & BOWDEN, A.A. 1973. The Fiskenaasset complex, West Greenland. 1. A preliminary study of the stratigraphy, petrology and whole-rock chemistry from Qeqertarssuatsiaq. Bull. Grønlands Geol. Unders. 106, 80pp.

APPENDIX 1

Modal Analyses

Zone A

<u>Spec.</u>	57	58	59	60	61	62	63	64
Hb	59.6	59.9	63.8	47.8	46.8	43.4	45.4	60.0
Opx	-	-	-	-	-	-	-	-
Cpx	2.3	-	-	-	-	-	-	-
Plag	27.3	26.6	31.0	27.2	36.5	30.5	42.4	35.3
Qtz	8.6	6.4	-	9.0	9.4	-	0.7	1.6
Kfd	-	-	-	-	-	-	-	-
Bi	-	3.0	tr	10.3	5.3	25.2	11.1	0.2
Ch	-	-	tr	-	-	-	tr	tr
Op	2.2	4.0	tr	5.1	2.9	0.6	tr	2.5
Ap	tr	0.1	tr	0.6	0.1	0.3	0.4	0.4
Ct	-	-	-	-	-	-	0.2	-

<u>Spec.</u>	65	66	67	68	69	70	71	72
Hb	67.5	50.5	66.3	53.4	52.3	63.2	57.2	50.7
Opx	-	-	-	-	-	-	-	-
Cpx	0.2	-	-	-	-	-	-	-
Plag	23.8	28.7	32.2	28.0	34.2	33.7	37.2	36.8
Qtz	5.8	6.2	-	4.9	9.9	-	-	6.7
Kfd	-	-	-	-	-	-	-	-
Bi	1.0	9.6	0.5	9.8	0.6	tr	-	-
Ch	tr	-	-	0.2	-	0.3	2.7	-
Op	1.6	4.1	0.9	0.4	1.3	1.8	2.6	5.6
Ap	0.3	0.9	0.1	0.5	1.7	0.7	0.3	0.2
Ct	-	-	0.2	-	-	0.2	-	-

Spec.	73	76	753	754	755	756	759	760
Hb	54.7	53.5	43.1	50.2	74.2	35.3	65.0	36.3
Opx	-	-	8.0	-	-	-	-	-
Cpx	-	-	-	-	-	-	-	-
Plag	23.7	23.5	35.9	33.8	23.9	31.8	28.4	38.7
Qtz	-	9.1	-	-	0.6	-	-	-
Kfd	-	-	-	-	-	-	-	-
Bi	18.9	12.8	12.0	14.9	-	30.1	0.4	14.3
Gt	-	-	-	-	-	-	-	4.5
Ch	-	tr	tr	tr	-	-	5.1	0.1
Op	1.9	1.0	0.5	0.6	1.1	2.2	tr	4.9
Ap	0.8	0.1	0.1	0.5	tr	0.6	0.1	1.2
Ct	-	tr	-	-	0.2	-	1.0	-
Sp	-	-	0.4	-	-	-	-	-

Spec.	761	762	766	768	771	772	773	774
Hb	48.7	74.0	71.4	28.0	72.3	58.6	42.1	57.2
Opx	-	-	tr	16.4	-	-	-	-
Cpx	-	-	3.0	-	-	-	-	-
Plag	22.6	24.1	25.1	43.1	27.7	28.5	41.4	31.4
Qtz	3.7	-	-	-	-	1.3	-	-
Kfd	-	-	-	-	-	-	-	-
Bi	23.0	-	-	-	-	10.0	14.8	8.8
Gt	-	-	-	12.1	-	-	-	-
Ch	-	1.9	-	0.4	tr	-	-	-
Op	1.3	tr	0.5	tr	tr	1.0	0.2	2.6
Ap	0.7	-	-	tr	tr	0.6	0.8	tr
Ct	-	-	-	-	-	-	-	-
Sp	-	-	-	-	-	-	0.7	-

Spec.	779	780	783	784	785	786	787	788
Hb	43.6	69.5	59.1	63.5	40.4	48.1	70.4	49.1
Opx	-	-	-	-	-	-	-	4.7
Cpx	-	-	-	-	-	-	-	-
Plag	36.9	27.9	-	34.7	41.4	31.4	28.8	45.7
Qtz	2.4	-	31.2	-	-	-	tr	-
Krd	-	-	-	-	-	-	-	-
Bi	3.6	tr	1.5	1.4	18.3	20.2	-	-
Ch	-	-	6.9	0.4	-	-	-	-
Op	3.7	2.4	1.3	tr	-	0.3	0.6	0.5
Ap	0.4	0.2	tr	-	0.1	-	-	-
Ct	-	tr	tr	tr	-	tr	tr	-
Sp	-	-	-	-	-	-	0.1	-
Gt	9.4	-	-	-	-	-	-	-

Spec.	789	101	103	107	110	114	115	116
Hb	42.6	56.0	53.4	60.0	54.1	48.7	49.5	32.7
Opx	14.0	-	-	-	-	-	-	-
Cpx	-	-	-	-	-	-	-	-
Plag	37.0	33.7	39.9	37.1	36.7	42.7	30.9	35.1
Qtz	2.1	-	-	-	-	-	-	-
Kfd	-	-	-	-	-	-	-	-
Bi	3.2	9.0	7.8	-	4.6	2.1	15.2	27.9
Ch	-	-	-	-	-	tr	3.2	0.2
Op	1.1	1.3	0.1	2.9	4.6	6.3	1.2	4.0
Ap	-	tr	tr	tr	tr	tr	-	0.1
Ct	-	-	-	-	tr	0.2	-	tr
Sp	-	-	-	-	-	-	-	-
Gt	-	-	-	-	-	-	-	-

Spec.	118	120	121	124	129	132	303	305
Hb	39.1	48.9	57.8	69.2	53.9	59.0	56.8	52.6
Opx	-	-	-	-	-	-	-	-
Cpx	-	-	-	-	-	-	-	-
Plag	42.1	32.0	30.6	28.8	37.2	35.7	31.6	26.6
Qtz		0.9	0.4	-	-	-	-	2.6
Kfd	-	-	-	-	-	-	-	-
Bi	17.7	18.2	11.1		8.5	5.1	9.4	16.6
Ch	0.3		tr		0.1	0.2		
Op	0.6	tr	tr	1.9	tr	tr	0.2	1.4
Ap	0.2	tr	0.1	0.1	0.1	tr	-	0.2
Ct	tr	-	-	-	tr	-	-	-
Sp	-	-	-	-	0.2	-	-	-
Gt	-	-	-	-	-	-	-	-

Spec.	306	309	311	312	314	315	316	317
Hb	40.8	45.3	61.4	59.2	58.1	47.0	45.4	66.0
Opx	9.2	-	-	-	-	-	-	-
Cpx	tr	-	-	-	-	-	-	-
Plag	36.6	40.7	33.4	36.8	35.1	35.2	44.7	32.9
Qtz	-	1.4	3.6	1.8	-	-		-
Kfd	-	-	-	-	-	-	-	-
Bi	1.6	7.8	tr	0.2	6.1	15.4	9.9	-
Ch	0.6	-	0.8	-	-	-	tr	-
Op	4.3	4.0	0.6	1.4	0.4	1.8	tr	1.1
Ap	0.6	0.8	tr	0.6	0.3	0.6	tr	tr
Ct	-	-	-	-	-	-	tr	-
Sp	-	-	-	-	-	-	-	-
Gt	6.7	-	-	-	-	-	-	-

Spec.	319	320	321	322	324	325	326	327
Hb	64.2	61.9	48.9	41.8	48.6	61.6	60.2	45.9
Opx	-	-	-	-	-	-	-	-
Cpx	-	-	-	tr	-	-	-	-
Plag	18.3	38.0	43.6	32.8	35.6	30.2	22.9	49.7
Qtz	tr	-	1.7	4.8	-	-	2.1	-
Kfd	-	-	-	-	-	-	-	-
Bi	0.3	tr	1.4	13.4	13.2	3.2	11.4	0.1
Ch	-	tr	=	-	-	-	-	0.2
Op	-	0.1	4.2	4.4	2.6	3.8	3.4	4.1
Ap	-	tr	tr	-	-	0.2	tr	-
Ct	tr	-	0.2	2.8	tr	1.0	-	-
Sp	tr	-	-	-	-	-	-	-
Gt	17.2	-	-	-	-	-	-	-

Spec.	328	329	331	332	333	334
Hb	34.2	35.4	48.8	62.4	58.8	52.3
Opx	-	-	-	-	-	-
Cpx	-	-	-	-	-	-
Plag	47.8	50.0	46.4	22.5	38.8	33.6
Qtz	6.0	2.4	-	-	-	-
Kfd	-	-	-	-	-	-
Bi	8.6	9.6	3.0	-	2.0	14.1
Ch	-	tr	-	tr	-	-
Op	4.4	2.0	1.4	0.2	0.4	tr
Ap	-	0.2	0.2	-	-	-
Ct	-	0.4	0.2	-	-	-
Sp	-	-	-	-	-	-
Gt	-	-	-	7.9	-	-
Cum	-	-	-	7.0	-	-

ZONE B

Spec.	78	81	82	83	84	85	86	87
Hb	60.8	38.7	55.2	54.9	44.4	17.8	57.7	38.3
Opx	-	-	5.3	7.9	5.6	13.4	3.1	17.4
Cpx	-	-	-	0.5	-	-	4.6	-
Plag	19.8	38.4	34.5	34.0	46.4	44.2	34.3	42.5
Qtz	7.2	9.7	2.1	-	-	2.8	-	-
Kfd	-	-	-	-	-	15.6	-	-
Bi	10.8	4.5	-	0.2	0.6	tr	tr	tr
Gt	-	-	-	-	-	-	-	-
Ch	tr	tr	0.3	-	-	0.4	0.1	tr
Op	1.2	6.0	2.7	2.1	2.8	3.6	0.2	0.8
Ap	0.2	1.9	tr	0.4	0.2	2.2	tr	tr
Ct	-	0.8	-	-	-	-	-	-

Spec.	88	89	90	92	93	95	96	97
Hb	53.0	57.6	3.0	47.0	46.8	35.5	42.4	22.2
Opx	1.4	5.0	28.4	15.4	16.0	12.8	13.9	18.2
Cpx	-	-	-	-	-	-	-	-
Plag	33.0	35.6	53.6	30.6	37.2	35.3	41.5	41.2
Qtz	6.8	-	8.8	-	-	-	-	-
Kfd	-	-	-	-	-	-	-	7.2
Bi	3.4	0.4	1.6	6.2	tr	-	0.4	6.4
Gt	-	-	1.0	-	-	10.2	-	-
Ch	-	-	-	tr	-	-	-	tr
Op	2.0	1.2	3.2	0.8	tr	6.2	1.8	1.8
Ap	0.4	0.2	0.4	tr	tr	tr	tr	tr
Ct	-	-	-	-	-	-	-	-

Spec.	98	99	100	101	102	105	106
Hb	53.4	33.0	6.4	33.1	33.8	18.0	65.2
Opx	3.2	17.0	29.6	7.9	7.0	16.6	4.4
Cpx	-				-	-	-
Plag	28.4	44.6	55.8	49.8	46.8	50.8	27.4
Qtz	-		-			9.7	-
Kfd	-	-	-	-	4.2	1.3	-
Bi	10.2	1.2	1.2	9.0	3.0	0.6	tr
Gt	-	-	-	-	-	-	-
Ch	tr	-	0.2	-	-	-	-
Op	1.2	3.2	5.6	0.2	2.4	1.2	2.8
Ap	0.2	1.0	1.2	tr	2.6	1.8	0.2
Ct	3.3	-	-	-	-	-	-

Spec.	705	707	710	711	723	725	734	738
Hb	49.2	60.0	58.4	24.0	45.8	39.0	57.8	52.8
Opx	9.3	0.7	-	18.0	19.1	17.6	2.3	-
Cpx			-					-
Plag	33.8	39.3	21.3	48.3	33.4	36.5	37.6	35.4
Qtz	-	-	-	-	-	-	1.2	1.0
Bi	3.6	-	18.3	7.9	-	6.0	-	7.0
Ch	-	-	-	-	-	-	-	-
Op	4.1	-	1.4	1.3	1.7	-	1.1	3.0
Ap	tr	-	0.6	0.5	tr	0.9	-	0.4
Ct	-	-	-	-	-	-	-	0.4
Gt	-	-	-	-	-	-	-	-

Spec.	741	744	745	746	747	748	750	113
Hb	51.1	30.1	43.5	42.9	36.9	45.1	14.3	64.4
Opx	7.6		-	10.0	1.2	12.3	28.2	-
Cpx	3.9	15.6	-				-	-
Plag	36.9	37.8		31.7	41.5	40.1	31.2	33.1
Qtz	-	tr	39.2	-	-	-	5.1	-
Bi	-	tr	14.3	12.7	14.3	-	0.2	-
Ch	0.5	-	-	-	-	1.3	-	-
Op	tr	3.9	2.8	2.3	6.1	1.2	2.9	2.1
Ap	-	0.2	0.2	0.3	tr	-	0.6	-
Ct	-	-	-	0.1	tr	-	-	-
Sp	-	-	-	-	-	-	-	0.4
Gt	-	12.4	-	-	-	-	17.5	-

Spec.	133	401	402	403	404	405	406
Hb	63.7	16.2	46.2	46.2	41.3	54.7	28.2
Opx	0.6	22.4		-	1.0	1.3	
Cpx	-	3.2	10.9	-	-	-	17.9
Plag		33.4	42.7	45.8		40.7	44.3
Qtz	33.7	-	-	-	44.1	-	-
Bi	0.8	23.6	tr	7.6	12.9	-	9.6
Ch	-	-	-	tr	-	0.5	-
Op	1.2	tr	0.2	0.4	tr	2.5	tr
Ap	-	1.0	-	-	0.3	0.3	-
Ct	-	-	-	-	0.3	-	-
Gt	-	-	-	-	-	-	-
Pr	-	-	-	-	0.1	-	-

ZONE C

Spec.	713	215	216	218	221	222	225	226
Hb	19.9	34.2	20.4	42.4	68.4	52.1	61.3	42.4
Opx		5.0	9.2	9.2			-	4.3
	16.1				1.0	2.0		
Cpx		8.2	12.2	6.0			-	1.4
Plag	61.9	45.4	51.2	40.6	29.4	44.2	36.9	47.9
Bi	0.4	-	-	-	-	-	tr	-
Ch	-	-	-	-	-	-	0.7	3.3
Op	1.4	6.6	6.2	1.4	1.0	0.9	1.1	0.6
Ap	-	0.6	0.8	0.4	tr	0.7	0.2	-
Ct	-	-	-	-	-	-	-	-

Spec.	209	227
Hb	18.2	40.6
Opx	13.4	0.8
Cpx	2.8	0.2
Plag	64.6	57.2
Op	0.8	1.2
Bi	0.2	-

APPENDIX 2

Analytical Techniques

ANALYTICAL TECHNIQUES

A. X-Ray Fluorescence Spectrometry.

The whole rock chemical analyses were obtained using a Philips P.W.1212 automatic spectrograph. A Torrens TE 108 automatic sample loader, which allows up to 108 samples to be run sequentially without interruption was employed for some elements.

1. Major elements.

For major elements (except Na) the specimen preparation technique was the fusion bead method described by Harvey et al. (1972), in which the salient details are as follows:

2.000g of flux and 0.3700g rock powder (crushed to \leq 250 mesh) were fused together at 1000°C in a furnace. Appropriate corrections for individual weight losses on both flux and rock powder were made by cooling and reweighing. Final fusion was achieved in a blast burner and the homogeneous melt was pressed on duralumin plattens using a plunger assemblage; this method simultaneously quenches and moulds the melt into a glass disc or 'bead'. The beads were labelled on their lower surfaces prior to storage.

Calibration lines for X-ray fluorescence were obtained using the 5 U.S.G.S. International standards, DTS-1, BCR-1, PCC-1, GSP-1 and AGV-1, and taking their composition as the 'usable' values of Abbey (1973).

The unknown samples (analysed immediately afterwards) were referred to the calibration coefficients obtained for each element. The uncorrected abundance data for the major elements were thus obtained, using a computer program (X09). Inter-element correction of this abundance data was obtained by a second computer routine (X02).

The operating conditions used for the XRF analysis of

Element	Target	Kv	mA	Crystal	Bkg	Counter
Si	Cr	60	24	PE	-2.20	F
Al	Cr	60	24	PE	-6.95	F
Ti	Cr	60	24	LiF 200	-2.98	F
Fe	Cr	60	24	LIF 200	-2.23	F
Mg	Cr	50	40	KAP	+1.75	F
Ca	Cr	40	8	LiF 200	+11.20	F
Mn	W	60	32	LiF 200	-2.00	S
K	Cr	60	24	PE	+4.12	F
P	Cr	50	40	Ge	+2.00	F
(Na)	Cr	50	40	KAP	-1.52	F

Table A2.1: Operating conditions for XRFs analysis
(Major Elements)

Other operating conditions corresponded to those tabulated in Harvey et al (1972).

major elements in this study are tabulated in table A2.1.

Precision and Accuracy.

Instrumental precision was simply evaluated by replicate measurements of beads. The results are in accordance with those reported by Harvey et al. (1972), and indicate that the coefficient of variation for each major element is under 1%. Duplicate beads of Nottingham University standard 1000 were analysed as a further test of the method. 1000 is an olivine gabbro, and the mean composition is tabulated in table A2.2.

Table A2.2

	Mean	s.d.	%c.v.
SiO ₂	50.28	1.15	2.3
Al ₂ O ₃	15.96	0.11	0.7
TiO ₂	0.44	0.03	6.8
Fe ₂ O ₃	6.68	0.10	1.5
MgO	9.18	0.20	2.2
CaO	11.40	0.08	0.7
K ₂ O	0.27	0.02	7.4
MnO	0.12	0.01	8.3
P ₂ O ₅	0.04	0.005	12.5

Between-bead precision is indicated by the standard deviation and coefficient of variation in table A2.2 (n = 5).

Accuracy was monitored using U.S.G.S. standard samples, run at the same time as the unknowns. Particular emphasis was placed on the results for G2, a sample which was not used in determining calibration lines. The results were in excellent agreement with the values published by Abbey (1973) and Flanagan(1973) and are also similar to those tabulated by Harvey et al. (1972).

For several unknown samples in this study the SiO_2 and Al_2O_3 determinations were checked using standard 'wet' chemical techniques, following Shapiro and Brannock (1956). No significant variation was noted between this method and the XRF results.

Sodium was determined by the same method as the other major elements, except that rock powder pellets were used for both calibration standards and unknowns.

2. Trace Elements.

Rock powder pellets were prepared by adding 6g of rock powder (crushed to ≤ 250 mesh) to 1g of phenol-formaldehyde resin. The powders were thoroughly mixed in a mechanical shaker and pressed under vacuum between tungsten carbide platens, at 30 tons pressure, using a hydraulic press. The resultant pellet was then heated for 40 minutes at 85°C .

Calibrations used for trace element analysis were obtained by 'spiking' samples of the Nottingham laboratory standard 1000. A dried, known amount of a spec-pure compound of a particular trace element was added to 30g of the standard rock powder, giving a concentration of ca. 10000 ppm of that element. Thorough mixing of this spike was followed by progressive dilution with further rock powder. Powders, and subsequently pellets, were thus produced with added concentrations of from 5ppm to 10000ppm of each trace element.

The operating conditions for trace element analysis are presented in table A2.3. Interferences resulting from line overlap were corrected by analysing the spiked powders of the interfering element at the angle of the element suffering interference. Thus the overlaps of Cr by V, Y by Rb, Zr by Sr, Ba by Ce and Ce by Cr lines were corrected.

In the case of V K_{α} which is overlapped by Ti K_{β} , the increased count rate due to Ti was calculated using the U.S.G.S. international standards. These were also used to correct the Cr results for tube contamination.

The background position for Ni is enhanced by a Tungsten tube line. This was eliminated by subtracting the enhancement from results obtained by running a Ni-free matrix (distilled water). The background counts were consequently multiplied by a factor of 0.74 to remove this interference.

Since the olivine gabbro (Standard 1000) has a similar composition to the metabasite samples, mass absorption differences are minimised. Remaining mass absorption effects were corrected using the values of Heinrich (1966) via a computer routine (X03).

Precision and Accuracy.

The 6 U.S.G.S. standards, DTS-1, BCR-1, PCC-1, GSP-1, AGV-1, and G-2 were analysed for each element at the same time as the unknowns. The results on these standards are in good agreement with the recently published values of Abbey (1973) and Flanagan (1973). Results for Rb and Sr are also compared with the data of Pankhurst and O'Nions (1973), and with recent unpublished isotope dilution results, obtained in Oslo by Dr. D.Field (July-August, 1977). These are presented in tables A2.4 and A2.5.

Element	tg	Pk. 1.	kV	ma	Peak20	Bg 1	Bg 2	cry.	ct
Sc	Cr	K α	60	24	97.73	-3.00	-	1	F
V	Cr	K α	60	24	76.94	+5.21	-	1	F
Cr	W	K α	60	32	69.30	-1.92	-	1	F
Co	W	K α	60	32	77.79	-0.53	+0.72	2	S
Ni	W	K α	60	32	71.19	+0.88	-	2	S+F
Zn	Mo	K α	100	20	60.49	+1.45	-	2	S+F
Rb	Mo	K α	100	20	37.88	-0.88	+0.12	2	S
Sr	Mo	K α	100	20	35.76	-0.76	+1.11	2	S
Y	Mo	K α	100	20	33.75	-1.00	+1.04	2	S
Ba	W	L $\beta_{1,4}$	50	40	128.85	+3.00	-	2	S+F
Ce	W	L $\beta_{1,4}$	60	32	111.70	+2.55	-	2	S+F
Zr	W	K α	100	16	31.97	-1.00	+1.00	2	S
Nb	W	K α	60	32	30.45	+0.64	-	2	S

Table A2.3: Operating conditions for XRF analysis of trace elements.

tg = Target; Pk.1. = Peak line; Bg 1 = Background 1; Bg 2 = Background 2; cry. = Crystal (1 = LiF200, 2 = LiF220) ct. = counter (F= flow, S= Scintillation.)

Table A2.4: Results on U.S.G.S Standards for trace elements.

	Scandium				Vanadium			
	1.	2.	3.	4.	1.	2.	3.	4.
DTS-1	3.6	4.?	3	9.6%	10	13	31	4.4%
BCR-1	33	34	34	2.0 %	399	410	349	4.6%
PCC-1	6.9	9	8	2.7%	30	31	53	7.0%
GSP-1	7.1	8	8.5	7.5%	53	49	65	7.3%
G-2	3.7	4.	3.5	5.4%	35	34	35	19.3%
AGV-1	13.4	12	9	3.0%	125	125	123	6.4%

	Chromium				Cobalt			
	1	2	3	4	1	2	3	4
DTS-1	4000		4200	1.1%	133	135	140	6.9%
BCR-1	18	16	28	3.1%	38?	37	42	28.8%
PCC-1	2730		3000	1.0%	112	110	115	12.7%
GSP-1	12.5	13	15	7.0%	6.4	7	15	35.2%
G-2	7?	9	11	8.5%	5.5	6	9	7.5%
AGV-1	12.2	12	16	4.7%	14.1	17	19	40.1%

	Nickel				Zinc			
	1	2	3	4	1	2	3	4
DTS-1	2269		2400	1.4%	45	45	46	2.3%
BCR-1	16	13	18	9.1%	120	120	121	1.2%
PCC-1	2339		2350	1.1%	36	36	44	3.3%
GSP-1	12.5	9	12	8.5%	98	98	101	1.3%
G-2	5.1	6	4.8	-	85	85	83	4.3%
AGV-1	18.5	17	19	14.1%	84	84	84	0.7%

	Rubidium				Strontium			
	1	2	3	4	1	2	3	4
DTS-1	0.05	0.05	0.75	60%	0.35	0.35	0	
BCR-1	46.6	47	47.3	4.3%	330	330	328	0.7
PCC-1	0.06	0.06	0.4	67.5%	0.41	0.4	0	
GSP-1	254	250	251.7	0.9%	233	230	207	0.5
G-2	168	170	167.5	0.8%	479	480	490	0.4
AGV-1	67	67	66.3	2.1%	657	660	671	0.4

	Yttrium				Barium			
	1	2	3	4	1	2	3	4
DTS-1	0.05	-	4	4.9%	2.4	-	n.d.	
BCR-1	37	46	29	1.9%	675	680	727	2.7
PCC-1		-	4	4.9%	1.2	--	n.d.	
GSP-1	30.4	32	40	0.8%	1300	1300	1230	2.8%
G-2	12	12	18	0.6%	1870	1850	1848	2.3%
AGV-1	21.3	26	19	1.6%	1208	1200	1225	1.4%

	Cerium				Zirconium			
	1	2	3	4	1	2	3	4
DTS-1	0.06	-	n.d.		3?	-	3	90%
BCR-1	53.9	54	42	19.1%	190	185	177	3.3%
PCC-1	0.09	-	n.d.		7?	-	4	81%
GSP-1	394	390	373	3.7%	500	500	493	2.3%
G-2	150	150	167	5.8%	300	300	307	3.5%
AGV-1	63	63	52	18.5%	225	220	231	1.5%

Table A.24 (cont):

	Niobium			
	1	2	3	4
DTS-1	3	-	1	75%
BCR-1	13.5	14	18	23.4%
PCC-1	2	-	-	
GSP-1	29	29	24	12.8%
G-2	13.5	14	17	22.1%
AGV-1	15	15	19	13.7%

1. Published values of Flanagan (1973).
2. Published values of Abbey (1973).
3. Results this survey.
4. Coefficient of variation % (8 determinations on each standard).

Table A2.5: Comparison of results with a) Pankhurst & O'Nions (1973).
and b) isotope dilution results. (Rb and Sr.)

	1	2
DTS-1	0.057	0.75
BCR-1	47.3	47.3
PCC-1	0.055	0.4
GSP-1	254.7	251.7
G-2	169.0	167.5
AGV-1	67.1	66.2

sample	3	4	5	6
713	3.7	4	293.4	304
733	23.2	23	-	
201	4.5	5	-	
209	3.6	5	194.4	203

1. Results of Pankhurst & O'Nions (1973) for Rb
2. Rb, this study
3. Rb, isotope dilution
4. Rb, XRF, this study
5. Sr, isotope dilution
6. Sr, XRF, this study.

B. Electron probe microanalysis.

The instrument used was a Cambridge Instruments Geoscan mark V, housed in the Wolfson Institute of Interfacial technology, University of Nottingham.

Preparation of Standards.

The method employed for the preparation of glass standards follows that of Smellie (1972), in which homogeneity is obtained by careful grinding, mixing and fusion of powders of known composition.

Spec-pure oxide powders were ground, under ether, in a pestle and mortar to obtain as uniform a grain size as possible. The powders were then dried and weighed accurately to a suitable standard composition of approximately 1g total weight. This composite powder was then ground under ether again, and mixed for several hours using a mechanical shaker. An extremely well-mixed powder of uniform grain size and known composition was thus obtained.

Fusion was carried out by the following procedure: The powder was placed in a 1cm diameter molybdenum 'boat' situated between the electrodes of a vacuum coating unit. Under high vacuum, the powders were then heated to temperatures in the range of 1200°-1700°C by increasing the voltage. Complete fusion was achieved, and the occurrence of bubbles in the melt was minimised by slowly increasing the temperature. Rapid quenching produced a clear, lens-shaped glass, which was easily removed from the molybdenum boat. The glass was then mounted in a perspex block for polishing. A disadvantage of the method is that oxides of high volatility, notably Na_2O and K_2O , cannot be satisfactorily included in the standard.

The standards and the polished slides for analysis were carbon-coated simultaneously, with care being taken to ensure an even coating.

Table A2.6 gives the composition of three artificial standards used in the present study. Each of these was tested by the electron probe for homogeneity for each element. The maximum % variation in the count rate throughout the standards is quoted in table A2.7. The greatest variation was obtained between the edge of the lens-shaped standard and its centre, which varied well within the limits of table A2.7. Replicate analyses of the same spot on the standard before and after analysis of the unknowns was always within the limits of homogeneity.

	A	B	C
SiO ₂	50.57	51.90	34.92
Al ₂ O ₃	9.84	2.36	23.18
TiO ₂	0.33	0.25	1.97
FeO	11.65	8.17	28.86
MgO	14.98	14.73	3.05
CaO	12.39	22.38	7.28
MnO	0.24	0.21	0.74

Table A2.6: Composition in wt. % of artificial glass standards.

SiO ₂	5.0%
Al ₂ O ₃	4.2%
TiO ₂	5.1%
FeO	1.4%
MgO	2.9%
CaO	3.4%
MnO	2.9%

Table A2.7: Homogeneity of standards. (Maximum % variation of count rate throughout the standard.)

The operating conditions for electron probe microanalysis in this study are presented in table A2.8, below.

Element	Crystal	Peak 2 θ	Bkg	Counter	Beam current μ a	Kv.
Si	KAP	31°5'	$\pm 2^\circ$	Flow	75	20
Al	KAP	36°33'	$\pm 2^\circ$	Flow	75	20
Ti	QTZ	48°33'	$\pm 2^\circ$	Flow	75	20
Fe	QTZ	33°40'	$\pm 2^\circ$	Flow	75	20
Mg	KAP	43°40'	$\pm 2^\circ$	Flow	75	20
Ca	QTZ	60°19'	$\pm 2^\circ$	Flow	75	20
Mn	QTZ	36°39'	$\pm 2^\circ$	Flow	75	20

Additional references:

HEINRICH, K.F.J. 1966. X-ray absorption uncertainty. In:
Electron microprobe, McKinley, T.D., Heinrich, K.J.F.,
& Wittry, D.B. (eds.) Wiley, New York. p 296-377.

SHAPIRO, L. & BRANNOCK, W. 1956. Rapid analysis of silicate
rocks. U.S. Geol. Surv. Bull. 1036C.

APPENDIX 3

Major Elements

ZONE A

Spec.	57	58	59	60	61	62	63	64
SiO ₂	47.93	49.01	47.25	46.17	51.34	46.14	48.90	48.09
Al ₂ O ₃	14.28	14.87	15.21	14.18	16.51	16.92	18.17	16.42
TiO ₂	2.15	2.06	1.54	2.93	1.70	1.66	1.04	1.52
Fe ₂ O ₃	2.44	6.75	2.83	7.87	4.26	3.83	3.96	4.40
FeO	11.80	7.37	11.56	9.22	7.81	10.00	6.10	7.60
MgO	6.09	6.42	6.97	5.93	4.70	7.85	7.54	7.84
CaO	10.14	9.21	9.55	8.63	9.01	7.57	9.17	9.34
Na ₂ O	2.42	2.58	3.23	2.36	3.15	2.20	2.45	2.96
K ₂ O	0.90	0.84	0.44	1.09	0.67	2.70	1.53	0.55
MnO	0.23	0.24	0.21	0.28	0.25	0.18	0.16	0.18
P ₂ O ₅	0.26	0.25	0.17	0.44	0.25	0.17	0.32	0.20
H ₂ O	0.66	0.61	0.84	0.66	0.39	0.78	1.05	0.79
Total	99.30	100.21	99.80	99.76	100.04	100.00	100.39	99.89
FeO*	14.00	13.45	14.11	16.31	11.65	13.45	9.67	11.56

Spec.	65	66	67	68	69	70	71	72
SiO ₂	46.66	45.58	46.86	49.61	49.21	46.21	46.19	47.76
Al ₂ O ₃	15.71	15.83	17.90	16.48	13.41	14.91	16.97	15.21
TiO ₂	1.62	2.98	1.21	1.10	2.35	2.65	1.77	2.05
Fe ₂ O ₃	2.94	5.84	2.12	2.98	4.69	2.30	4.87	7.65
FeO	10.12	10.36	9.98	6.77	13.23	11.98	8.02	6.04
MgO	8.69	6.82	8.27	8.11	2.22	6.72	7.63	7.63
CaO	9.34	8.39	9.99	9.31	9.06	9.44	9.90	9.41
Na ₂ O	2.67	2.07	2.43	2.11	2.46	2.32	3.18	2.95
K ₂ O	0.45	1.27	0.45	1.20	1.34	1.53	0.40	0.23
MnO	0.20	0.24	0.20	0.13	0.20	0.24	0.18	0.13
P ₂ O ₅	0.17	0.42	0.13	0.33	1.11	0.43	0.19	0.18
H ₂ O	0.99	0.71	0.62	0.94	0.45	0.87	0.93	0.34
Total	99.56	100.51	100.16	99.07	99.73	99.60	100.23	99.58
FeO*	12.77	15.62	11.89	9.45	17.46	14.05	12.41	12.93

Spec.	73	76	753	754	755	756	758	759
SiO ₂	45.23	47.01	49.91	46.87	48.71	46.53	47.68	48.43
Al ₂ O ₃	15.04	16.09	15.66	15.60	15.69	15.35	16.93	16.57
TiO ₂	2.55	2.06	1.22	1.89	1.48	2.80	1.57	1.09
Fe ₂ O ₃	4.84	2.58	3.09	2.83	3.59	3.51	4.12	3.89
FeO	10.60	10.54	8.05	9.91	9.58	11.52	8.17	8.29
MgO	6.94	6.92	7.08	7.47	8.22	5.35	8.38	8.70
CaO	9.32	9.34	8.99	9.06	9.89	7.15	7.05	9.96
Na ₂ O	1.96	2.25	2.99	2.75	2.34	2.18	2.39	2.37
K ₂ O	2.43	1.93	1.34	1.51	0.55	3.10	2.90	0.95
MnO	0.25	0.17	0.14	0.22	0.21	0.24	0.16	0.19
P ₂ O ₅	0.67	0.32	0.25	0.42	0.13	0.67	0.23	0.10
H ₂ O	0.81	0.53	0.53	0.76	1.01	1.13	0.81	0.70
Total	100.64	99.74	99.75	99.29	101.40	99.54	100.39	101.24
FeO*	14.96	12.86	10.83	12.46	12.81	14.68	11.88	11.79

Spec.	760	761	762	766	768	770	771	772
SiO ₂	50.28	47.50	47.45	46.36	47.96	51.21	50.13	46.19
Al ₂ O ₃	15.35	13.62	16.06	15.78	17.85	16.05	17.92	18.29
TiO ₂	3.25	2.95	1.19	1.45	1.88	1.32	1.29	2.51
Fe ₂ O ₃	4.18	1.56	1.80	3.47	6.66	3.20	2.07	5.76
FeO	9.64	14.73	10.48	11.05	8.32	6.86	7.28	9.46
MgO	4.73	6.26	8.36	7.03	8.20	4.78	5.70	5.74
CaO	7.37	9.27	10.68	11.62	9.00	7.00	11.85	7.75
Na ₂ O	2.49	1.93	2.40	2.01	0.87	3.11	2.47	3.01
K ₂ O	1.59	1.96	0.87	0.82	0.93	2.71	0.54	2.64
MnO	0.21	0.26	0.19	0.18	0.23	0.22	0.12	0.22
P ₂ O ₅	0.93	0.43	0.17	0.06	0.19	0.40	0.16	0.52
H ₂ O	0.45	0.58	0.58	0.51	0.57	1.89	0.52	0.66
Total	100.37	101.05	100.23	100.34	100.86	100.22	100.05	99.81
FeO*	13.40	16.13	12.10	14.17	14.31	9.74	9.14	14.64

Spec.	773	774	779	780	783	784	785	786
SiO ₂	49.17	49.49	49.45	47.09	47.84	53.05	49.08	47.64
Al ₂ O ₃	15.05	16.65	16.64	15.07	18.33	14.91	14.04	17.09
TiO ₂	1.99	1.42	2.95	2.39	1.58	0.63	1.30	1.19
Fe ₂ O ₃	3.25	3.96	3.30	2.18	2.57	2.86	3.41	2.52
FeO	10.06	8.08	10.84	12.57	8.80	5.39	8.74	8.74
MgO	7.47	8.17	6.96	7.39	7.33	8.89	7.97	7.14
CaO	6.73	9.17	7.09	9.84	6.99	9.14	10.47	9.54
Na ₂ O	1.48	2.14	1.56	2.76	1.85	3.27	2.35	2.00
K ₂ O	3.45	1.07	1.47	0.72	1.93	0.95	1.08	2.12
MnO	0.21	0.17	0.19	0.22	0.17	0.14	0.21	0.20
P ₂ O ₅	0.72	0.13	0.37	0.33	0.12	0.07	0.12	0.11
H ₂ O	1.09	0.52	0.67	0.35	2.21	0.66	0.57	0.97
Total	100.67	100.97	101.49	100.91	99.72	99.96	99.34	99.26
FeO*	12.99	11.64	13.81	14.53	11.11	7.96	11.81	11.01

Spec.	787	788	789	C101	103	104	107	110
SiO ₂	47.39	48.26	47.62	49.13	47.33	45.44	45.47	45.33
Al ₂ O ₃	15.99	16.44	15.47	16.87	15.63	16.67	17.16	15.99
TiO ₂	1.87	1.38	1.79	1.04	1.26	2.78	1.97	2.27
Fe ₂ O ₃	1.96	0.88	2.38	1.82	3.04	2.46	4.76	4.18
FeO	11.56	10.51	10.84	8.98	9.07	12.75	8.25	9.94
MgO	6.42	8.52	6.46	7.69	8.47	5.72	6.63	7.05
CaO	9.78	9.33	10.02	7.46	9.71	8.28	9.22	9.46
Na ₂ O	3.09	2.44	3.11	2.99	2.44	2.06	3.47	2.32
K ₂ O	0.59	0.37	1.04	2.14	2.04	2.92	1.18	1.46
MnO	0.12	0.17	0.22	0.23	0.18	0.26	0.20	0.23
P ₂ O ₅	0.23	0.13	0.18	0.09	0.14	0.41	0.29	0.33
H ₂ O	0.63	0.51	0.63	0.83	0.86	1.34	0.64	0.40
Total	99.63	98.84	99.76	99.27	100.17	101.09	99.24	98.96
FeO*	13.32	11.30	12.98	10.62	11.81	14.96	12.53	13.70

Spec.	114	115	116	118	120	121	124	129
SiO ₂	44.96	48.14	44.99	44.67	47.14	46.69	50.44	46.76
Al ₂ O ₃	17.20	15.94	14.65	15.47	15.35	14.37	14.60	15.62
TiO ₂	1.89	1.40	2.72	2.12	1.40	1.81	1.89	1.43
Fe ₂ O ₃	6.48	2.12	3.02	3.67	3.55	3.62	3.32	3.28
FeO	6.95	9.01	12.87	10.81	8.74	10.36	9.61	9.13
MgO	8.15	9.48	7.10	8.22	8.21	7.89	6.91	7.72
CaO	9.84	8.51	8.17	9.80	9.24	9.20	9.58	9.43
Na ₂ O	3.08	1.27	1.99	1.93	3.36	2.80	1.33	3.77
K ₂ O	0.70	2.96	3.21	2.22	2.41	1.98	0.71	1.58
MnO	0.20	0.14	0.36	0.20	0.21	0.20	0.17	0.20
P ₂ O ₅	0.22	0.22	0.81	0.54	0.19	0.24	0.21	0.20
H ₂ O	0.51	1.84	0.53	0.97	0.64	0.53	0.47	0.59

Total	100.18	101.03	100.42	100.62	100.44	99.69	99.24	99.71
FeO*	12.78	10.92	15.59	14.11	11.94	13.62	12.87	12.08

Spec.	132	303	305	306	309	311	312	314
SiO ₂	45.99	46.32	47.10	46.26	52.76	51.88	45.03	48.40
Al ₂ O ₃	16.03	16.88	15.48	16.00	14.94	14.23	16.09	15.65
TiO ₂	1.64	1.30	0.77	2.86	2.44	1.68	1.56	2.26
Fe ₂ O ₃	1.81	2.32	3.23	1.60	1.65	3.62	2.75	3.19
FeO	12.19	9.46	12.15	13.71	12.93	9.85	11.56	10.20
MgO	7.26	8.01	6.33	6.19	3.95	6.71	8.82	5.77
CaO	9.01	9.12	8.66	8.75	7.63	8.82	10.23	9.19
Na ₂ O	2.56	2.47	2.15	3.14	2.65	2.69	2.12	3.02
K ₂ O	1.62	2.33	2.35	0.67	1.50	1.09	0.86	1.35
MnO	0.23	0.20	0.23	0.22	0.23	0.25	0.19	0.21
P ₂ O ₅	0.22	0.08	0.36	0.33	0.50	0.23	0.19	0.33
H ₂ O	1.17	0.47	0.70	0.63	0.63	0.63	0.56	0.56
Total	99.73	98.96	99.51	100.33	101.81	101.68	99.96	100.13
FeO*	13.82	11.55	15.06	15.15	14.42	13.11	14.04	13.07

Spec.	315	316	317	319	320	321	322	324
SiO ₂	48.30	53.79	46.79	47.52	47.11	51.37	47.38	50.95
Al ₂ O ₃	14.01	15.74	16.19	16.65	16.39	16.34	15.28	16.04
TiO ₂	2.66	1.48	1.45	2.27	1.48	1.85	2.55	2.03
Fe ₂ O ₃	3.99	1.12	4.74	5.11	0.68	3.69	4.60	2.62
FeO	11.98	8.68	7.90	8.50	10.78	9.10	9.10	9.55
MgO	5.88	5.78	8.79	8.02	9.15	4.65	7.03	5.71
CaO	7.74	7.40	9.56	9.18	9.68	7.47	9.98	7.11
Na ₂ O	2.08	2.93	3.06	1.75	2.48	3.21	1.93	3.15
K ₂ O	2.26	1.67	0.27	0.54	1.28	0.55	1.91	1.92
MnO	0.23	0.17	0.17	0.21	0.12	0.21	0.22	0.20
P ₂ O ₅	0.41	0.35	0.03	0.40	0.19	0.31	0.35	0.26
H ₂ O	1.20	0.41	0.40	0.51	0.63	0.56	0.57	0.73
Total	100.74	99.52	99.35	100.66	99.97	99.31	100.90	100.27
FeO*	15.57	9.69	12.17	13.10	11.39	12.42	13.24	11.91

Spec.	325	326	327	328	329	330	331	332
SiO ₂	46.05	45.23	46.80	56.18	53.14	46.03	46.12	50.14
Al ₂ O ₃	15.90	15.08	17.47	16.47	16.26	16.11	18.43	20.32
TiO ₂	2.54	2.60	2.40	2.35	1.99	2.05	2.53	0.51
Fe ₂ O ₃	4.57	4.23	4.39	0.54	2.23	2.73	4.36	3.34
FeO	10.24	12.22	9.73	8.74	9.52	11.86	8.95	5.93
MgO	7.17	6.96	5.09	4.04	4.58	8.29	5.46	6.14
CaO	9.14	8.17	9.53	7.24	7.78	8.60	9.85	9.39
Na ₂ O	2.91	2.50	3.53	2.89	3.00	2.83	2.92	3.55
K ₂ O	1.11	1.70	0.82	1.66	1.34	0.82	0.97	0.43
MnO	0.24	0.29	0.19	0.16	0.18	0.22	0.19	0.16
P ₂ O ₅	0.32	0.31	0.30	0.44	0.39	0.25	0.32	0.07
H ₂ O	0.45	0.53	0.46	0.53	0.46	1.17	0.36	0.58
Total	100.64	99.82	100.68	101.24	100.87	100.96	100.46	100.56
FeO*	14.35	16.03	13.68	9.23	11.53	14.32	12.87	8.94

Spec.	333	334
SiO ₂	47.82	47.04
Al ₂ O ₃	20.05	20.03
TiO ₂	1.14	1.01
Fe ₂ O ₃	3.34	2.03
FeO	5.93	6.89
MgO	6.98	7.60
CaO	8.39	9.05
Na ₂ O	3.09	2.75
K ₂ O	1.37	1.40
MnO	0.18	0.17
P ₂ O ₅	0.08	0.08
H ₂ O	0.87	0.77
Total	99.24	98.82
FeO*	8.94	8.72

ZONE B

Spec.	78	80	81	82	83	84	85	86
SiO ₂	48.38	46.10	47.96	47.53	45.98	48.16	49.15	47.45
Al ₂ O ₃	12.54	15.07	13.83	16.38	14.61	16.88	12.89	16.38
TiO ₂	3.21	2.49	4.20	1.77	2.50	1.88	3.52	1.98
Fe ₂ O ₃	4.59	2.17	4.30	4.98	4.63	5.11	4.15	2.45
FeO	11.72	12.16	10.24	8.68	10.36	7.66	12.46	9.16
MgO	4.19	6.97	5.86	7.69	6.35	6.51	3.36	6.74
CaO	8.04	9.00	8.91	9.92	9.77	9.24	7.29	10.82
Na ₂ O	2.38	2.41	2.00	2.44	2.78	3.11	2.60	3.23
K ₂ O	1.22	1.74	1.13	0.30	0.98	0.44	2.33	0.82
MnO	0.27	0.23	0.17	0.20	0.23	0.18	0.24	0.14
P ₂ O ₅	1.68	0.48	0.75	0.18	0.36	0.28	2.14	0.24
H ₂ O	0.92	0.98	0.67	0.70	0.53	0.37	0.46	0.81
Total	99.14	99.80	100.02	100.77	99.08	99.82	100.59	100.22
FeO*	15.85	14.11	14.11	13.16	14.53	12.26	16.20	11.37

Spec.	87	88	89	90	92	93	95	96
SiO ₂	47.26	46.79	45.85	48.08	46.08	48.53	45.87	49.12
Al ₂ O ₃	16.40	12.96	16.71	19.53	16.53	16.50	16.16	16.91
TiO ₂	2.01	5.25	2.16	2.62	1.49	1.15	2.78	1.85
Fe ₂ O ₃	1.60	3.98	2.46	4.09	3.20	2.13	3.57	3.41
FeO	11.62	12.16	11.94	7.78	11.26	9.58	12.57	9.46
MgO	7.09	5.45	7.21	3.77	9.55	6.64	5.46	6.07
CaO	9.17	8.99	9.45	7.98	8.51	11.08	9.17	9.29
Na ₂ O	2.73	2.14	2.87	4.03	2.05	2.59	2.95	3.09
K ₂ O	0.47	1.12	0.59	0.36	0.80	0.65	0.48	0.47
MnO	0.21	0.19	0.20	0.19	0.20	0.19	0.24	0.19
P ₂ O ₅	0.25	0.45	0.26	0.90	0.18	0.18	0.31	0.26
H ₂ O	0.69	0.48	0.59	0.27	0.75	0.68	0.51	0.36
Total	99.50	99.96	100.29	99.60	100.60	99.90	100.07	100.48
FeO*	13.06	15.74	14.15	11.46	14.14	11.50	15.78	12.53

Spec.	97	98	99	100	F101	102	105	F106
SiO ₂	47.06	46.38	45.58	46.89	49.80	50.15	52.04	45.24
Al ₂ O ₃	14.05	15.51	15.54	15.52	16.72	15.28	15.22	15.80
TiO ₂	3.44	2.26	4.66	3.45	1.36	2.54	2.61	2.90
Fe ₂ O ₃	2.68	3.57	2.87	4.14	2.12	2.00	2.39	4.63
FeO	13.05	9.04	12.46	11.14	9.88	11.02	10.48	11.56
MgO	3.94	7.22	4.93	3.83	5.88	2.99	3.28	5.10
CaO	7.55	9.59	9.26	8.82	9.18	7.32	7.69	9.53
Na ₂ O	2.68	2.19	3.10	3.25	3.18	3.91	3.33	3.12
K ₂ O	2.18	1.69	0.82	0.63	1.61	2.07	1.54	0.82
MnO	0.21	0.19	0.18	0.22	0.20	0.19	0.18	0.22
P ₂ O ₅	1.90	0.51	0.61	1.53	0.20	1.36	1.33	0.34
H ₂ O	0.53	0.81	0.40	0.60	0.53	0.48	0.43	0.60
Total	99.27	98.96	100.42	100.02	100.66	99.31	100.52	99.86
FeO*	15.46	12.25	15.04	14.87	11.79	12.82	12.63	15.73

Spec.	705	707	710	711	712	723	725	734
SiO ₂	49.15	50.34	47.47	45.13	46.23	47.77	47.41	49.33
Al ₂ O ₃	15.56	15.24	15.34	15.03	12.71	15.97	15.21	15.15
TiO ₂	2.56	0.76	2.24	2.42	2.30	1.76	2.90	1.45
Fe ₂ O ₃	3.12	3.31	4.04	3.67	6.81	3.88	3.10	6.15
FeO	11.17	6.05	9.40	10.99	8.32	9.70	11.62	7.12
MgO	6.19	8.58	6.57	7.39	6.45	8.26	7.27	7.92
CaO	8.17	10.48	8.97	9.23	11.77	10.05	8.17	8.57
Na ₂ O	3.08	2.86	2.79	2.21	3.30	2.54	2.53	4.18
K ₂ O	0.69	0.44	1.48	1.74	0.88	0.29	0.81	0.58
MnO	0.17	0.14	0.18	0.17	0.31	0.19	0.21	0.25
P ₂ O ₅	0.38	0.08	0.63	0.71	0.25	0.17	0.66	0.13
H ₂ O	1.00	0.45	1.11	1.36	1.65	0.55	0.60	0.55
Total	101.24	98.73	100.22	100.05	100.98	101.13	100.49	101.38
FeO*	13.98	9.03	13.04	14.29	14.45	13.19	14.41	12.66

Spec.	738	739	740	741	744	745	746	747
SiO ₂	47.87	48.64	48.79	47.06	43.80	46.53	42.96	46.81
Al ₂ O ₃	14.42	15.88	17.33	16.40	16.51	16.41	13.73	14.57
TiO ₂	2.65	1.84	0.97	1.14	2.51	1.83	3.32	3.53
Fe ₂ O ₃	2.91	2.80	2.03	2.70	3.08	3.30	6.24	3.30
FeO	10.60	8.86	8.05	8.65	11.26	8.47	12.69	11.14
MgO	7.50	6.75	7.42	8.86	6.56	7.81	6.09	6.60
CaO	8.97	10.65	9.97	9.95	11.31	9.42	7.89	8.15
Na ₂ O	2.91	2.51	2.87	2.81	1.93	2.64	2.83	2.56
K ₂ O	1.88	0.83	0.66	0.70	1.23	1.90	1.94	2.36
MnO	0.19	0.19	0.18	0.20	0.39	0.21	0.29	0.21
P ₂ O ₅	0.40	0.25	0.19	0.10	0.37	0.35	0.51	0.19
H ₂ O	0.46	0.81	0.63	0.69	0.65	0.97	0.65	0.85
Total	100.76	100.01	99.09	99.26	99.60	99.84	99.14	100.27
FeO*	13.22	11.38	9.88	11.08	14.03	11.44	18.31	14.11

Spec.	748	749	750	C106	112	113	117	125
SiO ₂	48.06	46.97	56.31	48.37	46.67	48.05	42.72	45.45
Al ₂ O ₃	14.95	15.61	16.28	14.95	15.99	15.94	15.11	15.20
TiO ₂	2.55	1.86	1.33	1.04	1.89	2.03	3.52	1.79
Fe ₂ O ₃	2.66	4.67	3.56	3.75	3.72	4.28	3.11	5.23
FeO	12.51	9.31	7.75	7.19	9.64	8.65	14.28	10.78
MgO	7.00	8.06	3.84	9.08	8.42	8.07	7.62	7.83
CaO	9.41	10.02	6.72	11.38	9.71	9.39	10.05	9.38
Na ₂ O	2.90	1.98	3.21	2.84	2.42	2.53	1.64	2.42
K ₂ O	0.92	1.43	0.58	1.18	0.67	1.04	1.01	0.98
MnO	0.23	0.26	0.19	0.17	0.19	0.20	0.19	0.22
P ₂ O ₅	0.29	0.34	0.37	0.24	0.19	0.20	1.03	0.16
H ₂ O	0.48	0.76	0.21	0.34	0.65	0.62	0.45	0.37
Total	101.96	101.27	100.35	100.53	100.16	101.00	100.73	99.81
FeO*	14.90	13.51	10.95	10.57	12.99	12.50	17.08	15.49

Spec.	128	133	134	136	138	141	401	402
SiO ₂	53.16	47.33	49.26	44.50	46.15	52.64	47.14	45.74
Al ₂ O ₃	14.79	16.78	16.16	15.46	15.23	15.93	15.01	17.79
TiO ₂	1.69	1.75	1.54	2.58	3.12	1.73	1.67	1.46
Fe ₂ O ₃	3.20	2.69	0.93	3.80	2.36	4.13	4.51	3.52
FeO	8.56	9.76	11.91	12.51	10.36	8.68	10.84	8.44
MgO	4.02	6.52	7.09	7.06	8.94	5.71	10.55	7.42
CaO	6.39	9.97	8.52	8.51	7.01	6.24	6.01	10.49
Na ₂ O	4.17	2.65	2.23	2.26	1.34	1.13	1.58	2.54
K ₂ O	3.78	1.06	0.87	2.61	3.91	2.55	2.25	0.98
MnO	0.18	0.20	0.15	0.21	0.12	0.19	0.24	0.18
P ₂ O ₅	0.44	0.21	0.15	0.58	0.78	0.29	0.29	0.16
H ₂ O	0.56	0.63	0.39	0.72	0.95	1.33	0.56	0.57
Total	100.94	99.55	99.20	100.80	100.27	100.55	100.65	99.29
FeO*	11.44	12.18	12.75	15.93	12.48	12.40	14.90	11.61

Spec.	403	404	405	406	407	409
SiO ₂	49.00	46.07	44.72	50.34	47.09	45.77
Al ₂ O ₃	16.11	16.55	15.68	16.14	16.10	17.72
TiO ₂	1.22	2.19	3.09	1.03	1.41	1.88
Fe ₂ O ₃	3.34	2.03	4.63	0.17	3.75	4.26
FeO	8.14	11.44	11.44	11.08	9.64	9.70
MgO	6.86	6.65	6.82	9.33	8.16	8.05
CaO	8.74	8.39	9.81	8.37	7.97	9.12
Na ₂ O	3.06	1.79	2.46	1.14	2.10	3.03
K ₂ O	1.80	2.50	0.43	1.24	2.44	0.31
MnO	0.17	0.17	0.21	0.16	0.24	0.19
P ₂ O ₅	0.16	0.29	0.39	0.09	0.27	0.25
H ₂ O	0.68	0.98	0.79	1.50	1.60	0.39
Total	99.28	99.05	100.47	100.59	100.77	100.48
FeO*	11.15	13.27	15.61	11.23	13.02	13.53

ZONE C

Spec.	713	715	716	722	726	727	728	730
SiO ₂	52.65	45.77	49.42	51.77	49.77	46.91	48.55	50.13
Al ₂ O ₃	16.74	16.35	14.35	13.87	14.74	15.73	15.05	16.19
TiO ₂	0.75	1.69	1.46	1.44	1.86	1.62	1.36	0.79
Fe ₂ O ₃	3.26	4.43	3.18	2.43	4.26	1.80	4.80	5.26
FeO	7.19	9.52	10.00	9.70	9.34	10.72	8.14	6.62
MgO	5.38	6.61	6.67	7.65	6.67	7.65	8.32	6.86
CaO	9.01	9.47	9.63	9.27	8.02	9.82	10.05	8.12
Na ₂ O	4.50	3.41	3.18	2.87	4.52	2.45	2.57	3.97
K ₂ O	0.54	1.06	1.20	0.35	0.35	1.90	0.79	1.23
MnO	0.22	0.26	0.27	0.21	0.28	0.19	0.23	0.22
P ₂ O ₅	0.21	0.14	0.26	0.12	0.17	0.21	0.12	0.14
H ₂ O	0.32	0.26	0.44	0.39	0.48	0.80	0.63	0.85
Total	100.77	98.97	100.06	100.07	100.46	99.80	100.61	100.38
FeO*	10.12	13.51	12.86	11.89	13.17	12.34	12.46	11.35

Spec.	733	201	202	203	205	206	207	209
SiO ₂	48.43	45.78	47.85	51.04	49.30	50.02	47.23	51.24
Al ₂ O ₃	13.69	13.51	17.08	16.47	15.33	15.09	15.48	16.46
TiO ₂	1.87	1.90	1.99	1.15	1.86	2.38	1.94	1.07
Fe ₂ O ₃	1.68	9.12	4.77	2.09	2.64	3.82	5.04	4.16
FeO	12.60	8.50	7.39	9.16	10.53	10.36	9.58	7.60
MgO	7.08	7.89	7.25	6.93	7.26	6.11	7.12	5.59
CaO	9.84	8.34	9.21	8.24	9.01	8.24	9.09	8.09
Na ₂ O	2.92	3.66	3.40	3.86	3.37	3.42	4.01	4.87
K ₂ O	1.37	0.83	0.62	0.86	1.23	0.73	0.61	0.66
MnO	0.24	0.56	0.18	0.24	0.18	0.30	0.23	0.40
P ₂ O ₅	0.26	0.29	0.41	0.18	0.25	0.30	0.32	0.24
H ₂ O	0.49	0.39	0.14	0.42	0.80	0.39	0.39	0.36
Total	100.47	100.77	100.29	100.64	101.76	101.16	101.04	100.74
FeO*	14.11	16.71	11.68	11.04	12.91	13.80	14.12	11.34

Spec.	210	211	212	213	214	215	216	217
SiO ₂	46.63	50.33	46.54	48.52	45.34	50.86	48.82	49.44
Al ₂ O ₃	14.34	14.07	14.66	16.61	16.48	14.57	13.25	16.14
TiO ₂	1.81	1.49	1.81	1.08	1.15	1.51	2.37	1.34
Fe ₂ O ₃	4.93	4.01	4.11	3.43	4.83	5.74	7.45	4.51
FeO	8.83	9.58	9.94	8.47	9.04	7.07	8.56	9.23
MgO	6.86	7.44	7.88	7.92	7.60	7.09	5.80	6.32
CaO	9.88	8.94	9.08	9.28	9.56	8.42	8.73	7.67
Na ₂ O	3.51	3.76	3.44	3.29	3.74	4.63	4.74	2.23
K ₂ O	1.18	0.37	1.24	1.32	0.61	0.30	0.20	2.67
MnO	0.26	0.26	0.22	0.28	0.24	0.33	0.31	0.22
P ₂ O ₅	0.22	0.15	0.17	0.09	0.23	0.20	0.27	0.22
H ₂ O	0.64	0.52	0.45	0.88	0.55	0.56	0.35	0.45
Total	99.09	100.92	99.54	101.17	99.37	101.28	100.85	100.44
FeO*	13.27	13.19	13.64	11.56	13.39	12.24	15.26	13.29

Spec.	218	221	222	223	224	225	226	227
SiO ₂	49.99	49.08	50.06	49.73	48.42	54.52	51.05	52.65
Al ₂ O ₃	14.94	16.25	15.96	17.42	15.85	16.74	16.29	16.86
TiO ₂	1.22	1.36	1.27	1.12	0.70	1.10	0.86	0.68
Fe ₂ O ₃	2.72	3.56	3.33	4.07	5.02	3.31	1.74	3.85
FeO	8.32	8.20	8.08	7.13	7.18	6.64	7.78	4.19
MgO	7.55	9.34	7.87	7.85	8.72	4.86	8.15	6.50
CaO	10.06	9.46	9.31	6.91	8.38	7.36	9.15	8.48
Na ₂ O	3.15	3.08	3.73	3.13	3.29	4.17	3.94	5.01
K ₂ O	0.42	0.25	0.46	2.42	2.04	0.95	0.58	0.71
MnO	0.20	0.22	0.33	0.37	0.26	0.16	0.30	0.19
P ₂ O ₅	0.11	0.22	0.17	0.31	0.18	0.44	0.16	0.14
H ₂ O	0.51	0.31	0.46	0.69	0.44	0.53	0.69	0.46
Total	99.19	101.33	101.03	101.15	100.48	100.78	100.69	99.72
FeO*	10.77	11.40	11.08	10.79	11.70	9.62	9.35	7.66

Trace Elements

Spec.	57	58	59	60	61	62	63	64	65	66
Sc	53	53	41	48	40	43	39	39	35	36
V	338	295	319	127	137	348	236	236	198	212
Cr	136	153	123	110	73	99	230	189	107	80
Co	43	36	86	38	40	36	55	25	49	46
Ni	66	86	125	87	80	131	127	121	168	128
Zn	86	63	83	123	280	123	26	45	52	34
Rb	16	7	5	25	7	143	55	12	6	29
Sr	171	135	190	202	281	99	327	278	194	352
Y	22	21	17	31	21	35	22	17	17	24
Ba	239	87	46	204	116	330	505	97	74	732
Ce	28	40	12	52	32	13	13	33	18	53
Zr	115	124	67	213	143	80	108	91	96	151
Nb	7	7	7	25	21	8	7	8	5	6

Spec.	67	68	69	70	71	72	73	76	753	754
Sc	36	38	50	49	41	53	40	38	32	37
V	211	233	25	257	243	230	333	309	303	345
Cr	140	315	7	237	94	136	162	70	274	220
Co	46	31	9	40	43	36	52	33	45	41
Ni	151	160	18	67	115	84	150	104	107	107
Zn	47	33	78	87	67	4	108	46	85	154
Rb	6	34	15	42	6	3	104	87	38	69
Sr	204	316	200	208	251	135	181	237	260	248
Y	16	19	35	31	18	22	31	28	11	14
Ba	56	232	329	380	97	483	489	201	185	315
Ce	21	35	53	26	33	14	40	22	53	43
Zr	74	120	142	225	101	119	218	148	95	138
Nb	7	11	15	12	8	8	17	16	16	15

Spec.	755	756	758	759	760	761	762	766	768	770
Sc	53	31	31	45	32	52	45	51	41	29
V	209	335	267	234	100	398	268	657	322	187
Cr	322	57	45	92	88	81	121	12	164	27
Co	45	49	56	57	35	38	35	57	58	37
Ni	101	61	153	96	72	44	91	11	127	16
Zn	91	159	108	91	146	148	112	100	113	93
Rb	12	163	136	22	80	47	21	14	29	110
Sr	185	99	180	170	212	116	150	263	99	256
Y	17	98	5	10	24	23	17	7	18	22
Ba		156	411	14	480	160		109	159	742
Ce	31	134	41	15	68	55	17	13	43	58
Zr	96	215	94	45	257	202	60	43	104	170
Nb	11	23	16	13	19	15	11	9	13	19

Spec.	771	772	773	774	779	780	783	784	785	786
Sc	50	30	44	38	36	47	37	37	50	37
V	255	235	397	230	342	46	124	207	367	334
Cr	193	37	186	101	65	137	126	469	143	53
Co	45	55	39	48	14	44	49	45	46	49
Ni	44	51	81	134	85	90	158	146	97	102
Zn	28	180	192	87	118	155	91	74	118	125
Rb	6	101	182	33	49	11	102	17	14	46
Sr	364	278	38	205	140	168	117	122	167	222
Y	10	13	21	12	23	29	4	18	12	9
Ba	67	616	332	66	203	21	250	193	141	170
Ce	33	57	88	15	48	38	17	37	30	24
Zr	73	154	229	84	170	171	57	57	64	60
Nb	12	15	17	14	14	16	10	19	10	22

Spec.	787	788	789	c101	103	104	107	110	114	115
Sc	41	38	54	43	43	33	40	44	43	37
V	368	363	443	400	315	496	268	378	282	389
Cr	99	129	65	91	102	66	71	114	112	352
Co	40	70	73	53	53	49	45	55	68	46
Ni	49	122	55	81	101	80	96	86	93	142
Zn	55	93	128	143	112	255	130	131	108	53
Rb	4	9	14	78	81	128	27	95	11	109
Sr	198	208	173	143	233	170	294	183	247	121
Y	26	18	16	39	7	4	5	14	19	4
Ba	48	34		199	277	635	152	302	122	476
Ce	30	20	36	74	21	41	32	44	27	32
Zr	114	79	94	68	67	144	117	169	108	116
Nb	9	21	14	20	15	13	15	13	8	11

Spec.	116	118	120	121	124	129	132	303	305	306
Sc	42	37	41	45	58	43	45	34	39	38
V	507	368	235	419	555	249	399	289	1361	292
Cr	99	123	206	139	144	218	187	35	51	89
Co	49	40	51	62	47	46	57	49	42	60
Ni	121	135	108	86	82	93	83	97	77	74
Zn	924	103	167	142	81	144	193	130	144	120
Rb	225	147	137	95	5	48	52	79	62	15
Sr	18	69	435	355	242	185	112	151	158	192
Y	19	4	4	19	20	17	41	10	27	27
Ba	139	297	379	235	44	403	155	191	275	156
Ce	73	38	36	26	22	45	65	20	48	54
Zr	337	158	96	105	70	106	109	66	172	178
Nb	23	13	9	15	12	25	18	8	15	15

Spec.	309	311	312	314	315	316	317	319	320	321
Sc	42	52	50	41	51	30	34	36	34	42
V	422	384	350	276	561	294	361	264	318	430
Cr	72	115	221	134	112	220	216	81	123	29
Co	51	76	70	50	21	38	74	65	50	47
Ni	22	46	118	42	45	91	205	87	101	23
Zn	182	119	88	99	145	121	114	98	808	275
Rb	32	9	26	32	199	53	4	9	43	5
Sr	215	168	159	114	11	216	233	160	258	258
Y	25	27	19	31	24	20	22	22	10	25
Ba	399	205	115	163	239	412	38	111	175	208
Ce	73	46	28	48	51	50	29	36	134	64
Zr	141	124	85	209	190	213	54	160	116	135
Nb	15	10	10	17	18	13	10	12	13	11

Spec.	322	324	325	326	327	328	329	330	331	332
Sc	43	34	39	42	39	33	34	42	35	18
V	327	352	259	378	240	128	287	307	273	56
Cr	102	75	40	39	53	148	52	101	97	34
Co	49	40	53	60	47	29	41	45	48	41
Ni	78	76	88	86	59	19	30	99	77	61
Zn	132	143	123	162	111	115	124	101	109	70
Rb	79	54	22	40	13	63	46	25	22	13
Sr	189	147	193	169	265	251	215	157	369	344
Y	16	37	23	29	23	28	39	19	19	4
Ba	326	228	120	176	145	536	552	105	394	89
Ce	33	51	25	26	31	47	59	21	28	11
Zr	161	130	151	153	143	52	251	116	119	29
Nb	11	18	8	9	7	25	19	13	12	9

Spec. 333 334

Sb	31	30
V	189	168
Cr	116	86
Co	42	72
Ni	102	76
Zn	84	100
Rb	55	35
Sr	286	278
Y	4	4
Ba	188	147
Ce	14	
Zr	48	44
Nb	10	12

ZONE B

Spec. 78 80 81 82 83 84 85 86 87 88

Sc	38	48	40	44	43	36	30	38	39	48
V	222	467	277	193	218	138	27	278	281	403
Cr	216	64	77	107	104	73	12	94	106	111
Co	40	36	45	47	58	42	10	33	24	45
Ni	105	64	80	115	83	127	26	102	102	53
Zn	124	81	86	68	85	70	192	22	71	93
Rb	78	21	19	3	11	7	61	25	12	27
Sr	160	213	325	174	145	329	340	225	234	280
Y	32	55	27	20	25	17	62	20	20	22
Ba	211	122	399	25	55	223	1074	149	151	462
Ce	49	122	88	10	40	20	214	23	24	49
Zr	170	139	315	97	204	90	791	127	133	188
Nb	31	9	21	7	14	8	67	9	10	15

Spec.	89	90	92	93	95	96	97	98	99	100
Sc	39	29	26	52	44	34	31	39	39	34
V	237	95	249	255	272	193	143	268	253	125
Cr	108	25	233	142	102	94	17	126	20	26
Co	55	44	85	47	29	33	24	50	27	28
Ni	93	83	192	64	87	102	31	110	40	51
Zn	73	57	88	67	104	72	142	70	86	147
Rb	8	5	22	9	7	8	62	84	16	5
Sr	245	437	239	193	240	262	241	190	364	355
Y	21	29	15	16	23	19	55	30	23	47
Ba	93	109	269	49	145	96	794	301	427	333
Ce	20	82	24	7	26	29	166	32	65	136
Zr	143	976	72	75	151	141	517	215	124	682
Nb	9	31	7	6	6	8	39	14	17	34

Spec.	f101	102	105	f106	705	707	710	711	712	723
Sc	39	29	30	43	48	40	39	40	59	44
V	303	75	65	297	259	223	321	336	368	245
Cr	39	6	26	64	109	403	72	123	65	100
Co	26	25	15	42	69	50	43	62	51	58
Ni	67	27	31	75	70	129	107	113	61	127
Zn	96	126	123	89	82	79	110	111	158	105
Rb	36	42	28	11	12	14	73	98	10	7
Sr	213	309	331	259	55	76	223	175	157	173
Y	22	55	49	26	60	13	27	14	24	21
Ba	210	784	810	101	307	125	202	221	174	24
Ce	30	189	140	29	36	34	41	41	1	31
Zr	107	604	570	165	209	47	173	202	115	92
Nb	13	37	27	5	21	5	12	15	9	8

Spec.	725	734	738	739	740	741	744	745	746	747
Sc	35	47	37	44	41	41	54	33	40	33
V	157	348	288	415	271	298	538	216	458	112
Cr	114	79	208	164	191	93	103	111	83	107
Co	63	50	50	51	41	55	54	50	52	44
Ni	90	94	121	52	87	127	54	99	69	90
Zn	147	187	130	126	92	129	127	139	243	186
Rb	14	20	53	10	11	12	32	99	96	76
Sr	287	164	227	158	262	172	303	258	10	257
Y	27	17	24	30	11	12	29	6	57	44
Ba	553	37	245		93	24	53	94	281	459
Ce	62	36	57	56	16	15	39	43	81	149
Zr	237	77	184	173	55	61	164	98	198	653
Nb	16	12	20	24	11	6	15	11	24	38

Spec.	748	749	750	c106	112	113	117	125	128	133
Sc	45	41	33	50	40	51	54	41	36	38
V	277	272	145	256	251	312	355	254	173	299
Cr	141	160	67	295	105	125	141	46	82	47
Co	55	46	19	75	43	54	68	84	48	46
Ni	59	108	14	119	113	67	89	100	39	91
Zn	129	170	107	80	99	74	133	117	169	102
Rb	20	41	9	26	18	33	14	17	102	16
Sr	209	196	269	165	244	190	115	229	126	262
Y	25	18	29	7	16	20	40	20	41	17
Ba	80	89	388	190	195	188	196	90	446	156
Ce	26	39	39	30	7	8	68	38	83	37
Zr	142	100	188	76	92	103	321	108	378	98
Nb	9	15	18	6	11	12	17	14	19	9

Spec.	134	136	138	141	401	402	403	404	405	406
Sc	41	37	37	42	40	42	36	46	54	39
V	428	326	434	355	438	314	302	370	374	313
Cr	92	66	123	164	381	115	42	78	121	395
Co	67	57	52	33	55	55	73	9	5	61
Ni	108	78	81	70	157	122	47	56	43	156
Zn	116	289	90	110	229	93	116	109	119	133
Rb	19	94	133	143	163	15	67	91	5	83
Sr	163	96	84	135	42	238	237	117	203	72
Y	14	22	26	28	9	15	13	38	33	9
Ba	75	200	213	541	416	357	319	289	61	159
Ce	4	44	78	52	47	29	37		45	38
Zr	90	169	310	272	137	92	86	148	168	67
Nb	15	13	24	21	17	14	14	16	12	17

Spec.	407	409
Sc	41	42
V	361	280
Cr	80	99
Co	48	68
Ni	94	110
Zn	861	103
Rb	189	5
Sr	80	218
Y	9	21
Ba	88	40
Ce	21	17
Zr	110	105
Nb	15	14

ZONE C

Spec.	713	715	716	722	726	727	728	730	733	201
Sc	40	55	52	55	51	48	51	43	51	85
V	230	472	377	333	333	433	328	327	417	285
Cr	55	85	79	239	180	154	152	94	180	156
Co	49	49	61	58	62	66	41	47	69	35
Ni	36	61	44	57	67	93	91	61	68	65
Zn	196	179	293	103	130	97	168	207	174	242
Rb	4	10	8	4	3	119	7	13	23	5
Sr	304	209	119	289	217	56	140	330	79	59
Y	10	17	19	20	25	7	17	7	34	65
Ba	84	61	37			53	27	264	76	58
Ce	20	30	26	31	25	26	14	22	50	41
Zr	24	101	61	83	104	87	57	22	110	121
Nb	10	16	10	5	16	12	13	9	14	12

Spec.	202	203	205	206	207	209	210	211	212	213
Sc	33	44	49	52	50	41	48	53	44	46
V	182	325	355	212	358	255	404	373	360	293
Cr	143	72	193	103	139	80	150	121	99	151
Co	46	47	59	51	57	14	33	34	13	65
Ni	93	43	68	41	57	27	75	68	81	124
Zn	98	168	148	183	162	226	143	194	109	238
Rb	9	7	12	6	8	5	9	5	13	16
Sr	312	143	101	88	129	203	95	90	119	162
Y	18	13	24	29	25	13	21	12	17	10
Ba	139	65	57	59	76	221	163		33	78
Ce	52	24	32	46	38	29	46	55	36	18
Zr	145	53	151	154	127	43	108	70	97	52
Nb	17	14	14	11	17	8	17	11	8	7

Spec.	214	215	216	217	218	221	222	223	224	225
Sc	41	58	51	40	52	48	49	40	42	35
V	335	328	407	342	398	335	291	275	311	218
Cr	48	120	50	49	139	130	241	144	32	70
Co	55	56	38	32	48	43	58	44	33	28
Ni	114	51	43	39	77	109	109	95	61	25
Zn	170	220	222	163	123	86	116	175	271	141
Rb	11	5	5	84	2	1	3	44	46	7
Sr	247	87	102	106	173	182	126	122	196	212
Y	9	25	27	49	15	7	16	7	4	18
Ba	25	21		483			59	153	236	164
Ce	22		32	80	25	5	23	37	36	49
Zr	34	90	128	119	56	62	72	31	32	85
Nb	9	13	8	22	11	6	13	17	8	10

Spec.	226	227
Sc	56	43
V	341	300
Cr	205	29
Co	27	39
Ni	68	16
Zn	196	148
Rb	5	6
Sr	261	291
Y	24	7
Ba	87	32
Ce	31	24
Zr	35	22
Nb	15	15

Niggli Norms

ZONE A

Spec.	57	58	59	60	61	62	63	64
si	94.53	114.82	105.07	106.64	128.93	102.45	112.83	108.29
al	16.60	20.53	19.93	19.30	24.44	22.14	24.71	21.79
fm	56.21	49.23	49.73	52.45	42.58	51.29	44.89	48.42
c	21.43	23.12	22.75	21.36	24.25	18.01	22.67	22.54
alk	5.76	7.12	7.59	6.89	8.74	8.56	7.73	7.25
ti	3.19	3.63	2.58	5.09	3.21	2.77	1.80	2.57
p	0.22	0.25	0.16	0.43	0.27	0.16	0.31	0.19
mg	0.32	0.46	0.46	0.39	0.41	0.51	0.58	0.54
w	0.68	0.65	0.33	0.63	0.52	0.43	0.56	0.54
k	0.20	0.18	0.08	0.23	0.12	0.45	0.29	0.11

Spec.	65	66	67	68	69	70	71	72
si	101.57	102.28	101.14	116.45	126.43	104.79	100.76	107.71
al	20.15	20.94	22.77	22.80	20.30	19.93	21.82	20.22
fm	51.80	52.57	48.42	47.19	46.43	49.82	47.76	50.27
c	21.79	20.17	23.10	23.42	24.94	22.94	23.14	22.74
alk	6.26	6.32	5.70	6.60	8.32	7.31	7.28	6.78
ti	2.65	5.03	1.96	1.94	4.54	4.52	2.90	3.48
p	0.16	0.40	0.12	0.33	1.21	0.41	0.18	0.17
mg	0.54	0.43	0.55	0.60	0.18	0.46	0.52	0.51
w	0.37	0.53	0.30	0.47	0.41	0.28	0.55	0.72
k	0.10	0.29	0.11	0.27	0.26	0.30	0.08	0.05

Spec.	73	76	753	754	755	756	758	759
si	99.71	106.56	122.21	105.88	106.81	112.80	107.74	104.54
al	19.54	21.49	22.60	20.77	20.28	21.93	22.55	21.08
fm	50.84	48.09	44.62	49.10	50.74	49.58	50.97	49.62
c	22.01	22.69	23.59	21.93	23.24	18.57	17.07	23.04
alk	7.61	7.74	9.19	8.20	5.74	9.92	9.42	6.27
ti	4.23	3.51	2.25	3.21	2.44	5.10	2.67	1.77
p	0.63	0.31	0.26	0.40	0.12	0.69	0.22	0.09
k	0.45	0.36	0.23	0.27	0.13	0.48	0.44	0.21
mg	0.45	0.49	0.58	0.51	0.53	0.39	0.55	0.56
w	0.48	0.33	0.21	0.36	0.43	0.38	0.50	0.48

Spec.	760	761	762	766	768	770	771	772
si	129.57	107.65	101.98	99.26	106.76	133.84	118.07	107.57
al	23.31	18.19	20.34	19.91	21.06	27.60	25.39	21.07
fm	47.50	52.22	48.87	48.14	54.28	40.39	38.26	48.88
c	20.35	22.51	24.59	26.66	21.47	19.60	29.91	19.34
alk	8.83	7.07	6.19	5.29	3.20	12.40	6.45	10.72
ti	6.30	5.03	1.92	2.33	3.15	2.59	2.28	4.40
p	1.01	0.41	0.15	0.05	0.18	0.44	0.16	0.51
k	0.30	0.40	0.19	0.21	0.41	0.36	0.13	0.37
mg	0.38	0.40	0.55	0.47	0.50	0.46	0.52	0.41
w	0.46	0.17	0.26	0.39	0.62	0.48	0.36	0.55

Spec.	773	774	779	780	783	784	785	786
si	117.39	111.33	117.92	102.56	114.78	125.16	110.56	109.26
al	21.18	22.07	23.38	19.34	25.92	20.73	18.64	23.10
fm	52.93	49.62	52.66	50.86	48.85	47.25	49.40	45.91
c	17.22	22.10	18.12	22.96	17.97	23.11	25.27	23.44
alk	8.68	6.20	5.84	6.83	7.26	8.91	6.68	7.55
ti	3.57	2.40	5.29	3.91	2.85	1.12	2.20	2.05
p	0.73	0.12	0.37	0.30	0.12	0.07	0.11	0.11
k	0.61	0.25	0.38	0.15	0.41	0.16	0.23	0.41
mg	0.50	0.55	0.47	0.47	0.54	0.66	0.54	0.53
w	0.39	0.50	0.38	0.26	0.37	0.51	0.44	0.37

Spec.	787	788	789	101	103	104	107	110
si	107.49	108.25	107.73	115.03	103.04	103.71	101.86	100.96
al	21.37	21.73	20.63	23.27	20.05	22.42	22.65	20.99
fm	47.21	50.01	46.76	48.05	49.31	48.52	45.99	49.35
c	23.77	22.42	24.29	18.70	22.65	20.25	22.13	22.58
alk	7.65	5.84	8.32	9.97	7.98	8.81	9.22	7.08
ti	3.19	2.33	3.05	1.83	2.06	4.77	3.32	3.80
p	0.22	0.12	0.17	0.08	0.13	0.40	0.27	0.31
k	0.11	0.09	0.18	0.32	0.35	0.48	0.18	0.29
mg	0.46	0.57	0.47	0.56	0.56	0.40	0.48	0.47
w	0.25	0.14	0.31	.	0.40	0.28	0.54	0.46

Spec.	114	115	116	118	120	121	124	129
si	95.42	106.95	99.34	94.79	102.22	102.34	121.28	102.20
al	21.51	20.87	19.06	19.35	19.61	18.50	20.69	20.12
fm	48.82	51.94	52.82	51.40	48.54	51.11	50.44	47.60
c	22.38	20.26	19.33	22.28	21.46	21.61	24.68	22.09
alk	7.29	6.93	8.78	6.98	10.39	8.72	4.19	10.19
ti	3.02	2.34	4.52	3.38	2.28	2.98	3.42	2.35
p	0.20	0.21	0.76	0.49	0.17	0.22	0.21	0.19
k	0.13	0.61	0.51	0.43	0.32	0.32	0.26	0.22
mg	0.53	0.60	0.44	0.51	0.55	0.50	0.49	0.53
w	0.65	0.32	0.32	0.40		0.41	0.41	0.42

Spec.	132	303	305	306	309	311	312	314
si	101.82	102.10	106.55	104.29	136.53	122.61	93.63	113.70
al	20.91	21.93	20.64	21.26	22.78	19.82	19.72	21.67
fm	49.95	47.98	50.27	49.78	46.93	50.04	52.07	46.30
c	21.36	21.54	20.99	21.14	21.16	22.33	22.79	23.13
alk	7.78	8.55	8.11	7.83	9.12	7.81	5.41	8.90
ti	3.63	2.16	1.31	4.85	4.75	2.99	2.44	3.99
p	0.21	0.07	0.34	0.31	0.55	0.23	0.17	0.33
k	0.29	0.38	0.42	0.12	0.27	0.21	0.21	0.23
mg	0.48	0.55	0.42	0.42	0.32	0.47	0.52	0.44
w		0.33	0.35	0.19	0.20	0.42	0.32	0.38

Spec.	315	316	317	319	320	321	322	324
si	115.03	141.66	100.97	106.13	101.27	133.11	106.41	127.41
al	19.66	24.43	20.59	21.92	20.76	24.95	20.23	23.64
fm	52.35	44.40	50.53	51.56	50.01	45.33	48.82	46.61
c	19.75	20.88	22.10	21.97	22.30	20.74	24.02	19.05
alk	8.24	10.29	6.77	4.56	6.92	8.97	6.94	10.70
ti	4.76	2.93	2.35	3.81	2.39	3.61	4.31	3.82
p	0.41	0.39	0.03	0.38	0.17	0.34	0.33	0.28
k	0.42	0.27	0.05	0.17	0.25	0.10	0.39	0.29
mg	0.40	0.51	0.56	0.52	0.59	0.40	0.48	0.46
w	0.40	0.21	0.55	0.55	0.11	0.45	0.50	0.35

Spec.	325	326	327	328	329	330	331	332
si	101.02	100.13	107.24	159.61	138.75	99.01	104.99	117.94
al	20.56	19.67	23.59	27.58	25.02	20.42	24.73	28.17
fm	50.22	53.18	43.97	39.41	43.39	52.73	43.40	39.42
c	21.48	19.38	23.40	22.04	21.77	19.82	24.03	23.67
alk	7.74	7.77	9.04	10.97	9.83	7.03	7.85	8.74
ti	4.19	4.33	4.14	5.02	3.91	3.32	4.33	0.90
p	0.30	0.29	0.29	0.53	0.43	0.23	0.31	0.07
k	0.20	0.31	0.13	0.27	0.23	0.16	0.18	0.07
mg	0.47	0.43	0.40	0.43	0.41	0.50	0.43	0.55
w	0.47	0.41	0.47	0.11	0.32	0.32	0.49	0.53

Spec.	333	334	335	336	337	338	339	340
si	111.98	107.35	110.12	110.12	110.12	110.12	110.12	110.12
al	27.67	26.94	27.67	27.67	27.67	27.67	27.67	27.67
fm	42.22	42.81	42.22	42.22	42.22	42.22	42.22	42.22
c	21.05	22.13	21.05	21.05	21.05	21.05	21.05	21.05
alk	9.06	8.12	9.06	9.06	9.06	9.06	9.06	9.06
ti	2.01	1.73	2.01	2.01	2.01	2.01	2.01	2.01
p	0.08	0.08	0.08	0.08	0.08	0.08	0.08	0.08
k	0.23	0.25	0.23	0.23	0.23	0.23	0.23	0.23
mg	0.58	0.60	0.58	0.58	0.58	0.58	0.58	0.58
w	0.53	0.37	0.53	0.53	0.53	0.53	0.53	0.53

ZONE B

Spec.	78	80	81	82	83	84	85	86
si	124.63	103.93	116.88	104.52	104.01	111.35	128.77	106.46
al	19.04	20.02	19.86	21.23	19.48	23.00	19.90	21.66
fm	50.82	50.47	50.39	49.78	49.33	46.49	49.13	44.13
c	22.19	21.74	23.27	23.37	23.68	22.89	20.46	26.01
alk	7.95	7.77	6.48	5.62	7.51	7.62	10.50	8.20
ti	6.22	4.22	7.70	2.93	4.25	3.27	6.94	3.34
p	1.83	0.46	0.77	0.17	0.34	0.27	2.37	0.23
k	0.25	0.32	0.27	0.07	0.19	0.09	0.37	0.14
mg	0.32	0.46	0.42	0.51	0.43	0.48	0.27	0.51
w	0.44	0.26	0.46	0.53	0.47	0.57	0.40	0.35

Spec.	87	88	89	90	92	93	95	96
si	107.16	112.73	99.93	121.53	96.84	109.81	104.12	114.50
al	21.91	18.40	21.46	29.09	20.47	22.00	21.62	23.23
fm	49.13	51.67	49.58	38.84	55.12	44.51	48.89	45.89
c	22.28	23.21	22.07	21.61	19.16	26.86	22.30	23.20
alk	6.68	6.72	6.88	10.46	5.25	6.62	7.19	7.68
ti	3.43	9.51	3.54	4.98	2.35	1.96	4.75	3.24
p	0.24	0.46	0.24	0.96	0.16	0.17	0.30	0.26
k	0.10	0.26	0.12	0.06	0.20	0.14	0.10	0.09
mg	0.49	0.38	0.47	0.37	0.54	0.50	0.38	0.46
w	0.22	0.40	0.29	0.51	0.36	0.31	0.36	0.42

Spec.	97	98	99	100	F101	102	105	F106
si	119.62	105.92	106.77	115.84	116.93	134.46	140.56	102.79
al	21.05	20.88	21.45	22.60	23.14	24.14	24.23	21.16
fm	48.25	48.34	47.04	45.28	44.12	41.12	42.15	47.58
c	20.56	23.47	23.24	23.35	23.10	21.03	22.26	23.20
alk	10.14	7.31	8.27	8.78	9.65	13.70	11.37	8.06
ti	6.58	3.88	8.21	6.41	2.40	5.12	5.30	4.96
p	2.04	0.49	0.60	1.60	0.20	1.54	1.52	0.33
k	0.35	0.34	0.15	0.11	0.25	0.26	0.23	0.15
mg	0.31	0.51	0.37	0.31	0.47	0.29	0.31	0.36
w	0.29	0.44	0.32	0.43	0.30	0.27	0.31	0.44

ZONE B

Spec.	705	707	710	711	712	723	725	734
si	115.89	115.14	110.02	100.04	100.89	103.11	108.36	109.30
al	21.62	20.54	20.95	19.64	16.35	20.31	20.49	17.10
fm	49.66	46.79	48.31	51.23	47.92	50.73	52.72	50.07
c	20.64	25.68	22.28	21.92	27.52	23.24	20.01	20.35
alk	8.08	6.98	8.46	7.21	8.21	5.71	6.79	9.80
ti	4.54	1.31	3.90	4.03	3.78	2.86	4.98	2.42
p	0.38	0.08	0.62	0.67	0.23	0.16	0.64	0.12
k	0.13	0.09	0.26	0.34	0.15	0.07	0.17	0.08
w	0.36	0.52	0.46	0.40	0.62	0.44	0.35	0.63
mg	0.44	0.63	0.47	0.48	0.44	0.52	0.47	0.52

Spec.	738	739	740	741	744	745	746	747
si	107.52	111.89	111.98	102.00	94.51	103.58	95.13	108.56
al	19.09	21.53	23.44	20.95	20.99	21.53	17.92	19.91
fm	50.30	45.40	44.69	49.07	47.13	47.60	54.54	50.59
c	21.59	26.25	24.52	23.11	26.15	22.47	18.72	20.25
alk	9.03	6.82	7.35	6.87	5.73	8.40	8.82	9.25
ti	4.48	3.18	1.67	1.86	4.07	3.06	5.53	6.16
p	0.38	0.24	0.18	0.09	0.34	0.33	0.48	0.19
k	0.30	0.18	0.13	0.14	0.30	0.32	0.31	0.38
mg	0.50	0.51	0.57	0.58	0.45	0.54	0.37	0.45
w	0.35	0.39	0.34	0.38	0.35	0.44	0.50	0.37

Spec.	748	749	750	C106	112	113	117	125
si	105.90	101.45	59.42	102.87	101.08	106.25	89.54	97.14
al	19.41	19.87	27.16	18.74	20.41	20.77	18.67	19.15
fm	50.88	50.83	42.59	47.87	51.05	50.09	54.08	53.02
c	22.22	23.19	20.39	25.93	22.53	22.25	22.57	21.48
alk	7.49	6.12	9.86	7.46	6.01	6.89	4.68	6.35
ti	4.23	3.02	2.83	1.66	3.08	3.38	5.55	2.88
p	0.27	0.31	0.44	0.22	0.17	0.19	0.91	0.14
k	0.17	0.32	0.11	0.21	0.15	0.21	0.29	0.21
mg	0.45	0.51	0.38	0.60	0.53	0.53	0.44	0.47
w	0.30	0.50	0.48	0.51	0.44	0.50	0.30	0.49

ZONE B

Spec.	128	133	134	136	138	141	401	402
si	140.90	107.84	115.30	96.51	104.54	139.13	101.07	100.02
al	23.10	22.53	22.89	19.76	20.33	24.81	18.97	22.93
fm	41.64	45.73	49.98	52.10	54.06	50.32	60.86	45.74
c	18.15	24.34	21.37	19.78	17.01	17.67	13.81	24.58
alk	17.11	7.39	6.36	8.36	8.59	7.19	6.36	6.75
ti	3.37	3.00	2.71	4.21	5.32	3.44	2.69	2.40
p	0.49	0.20	0.15	0.53	0.75	0.32	0.26	0.15
mg	0.37	0.21	0.20	0.43	0.66	0.60	0.48	0.20
k	0.38	0.48	0.49	0.44	0.56	0.45	0.55	0.53
w	0.43	0.36	0.14	0.38	0.31	0.49	0.45	0.45

Spec.	403	404	405	406	407	409
si	114.85	106.59	97.63	114.90	104.95	97.74
al	22.25	22.57	20.17	21.71	21.15	22.30
fm	46.15	48.93	51.07	53.49	51.81	50.13
c	21.95	20.80	22.95	20.47	19.03	20.87
alk	9.64	7.70	5.81	4.33	8.01	6.70
ti	2.15	3.81	5.07	1.77	2.36	3.02
p	0.16	0.28	0.36	0.09	0.25	0.23
mg	0.28	0.48	0.10	0.42	0.43	0.06
k	0.52	0.47	0.43	0.59	0.52	0.51
w	0.45	0.26	0.45	0.03	0.44	0.47

ZONE C

Spec.	713	715	716	722	726	727	728	730
si	128.74	101.41	113.48	121.43	115.53	103.64	106.36	117.18
al	24.12	21.35	19.42	19.17	20.16	20.48	19.43	22.30
fm	40.76	47.34	48.05	50.48	49.20	48.35	50.42	46.53
c	23.61	22.48	23.69	23.30	19.95	23.25	23.59	20.34
alk	11.51	8.82	8.84	7.05	10.69	7.93	6.56	10.83
ti	1.38	2.82	2.52	2.54	3.25	2.69	2.24	1.39
p	0.22	0.13	0.25	0.12	0.26	0.20	0.11	0.14
k	0.07	0.17	0.20	0.07	0.05	0.34	0.17	0.17
mg	0.48	0.46	0.48	0.53	0.47	0.52	0.54	0.51
w	0.48	0.48	0.39	0.33	0.48	0.25	0.54	0.61

Spec.	733	201	202	203	205	206	207	209
si	107.93	97.03	107.88	119.84	110.77	117.96	103.23	122.97
al	17.98	16.88	22.69	22.79	20.30	20.97	19.94	23.28
fm	50.27	55.54	46.73	46.41	48.90	49.29	49.42	43.57
c	23.50	18.94	22.25	20.73	21.69	20.82	21.29	20.80
alk	8.26	8.64	8.32	10.07	9.10	8.92	9.35	12.34
ti	3.13	3.03	3.37	2.03	3.14	4.22	3.19	1.93
p	0.25	0.26	0.39	0.18	0.24	0.30	0.30	0.24
k	0.24	0.13	0.11	0.13	0.19	0.12	0.09	0.08
mg	0.47	0.45	0.52	0.52	0.50	0.44	0.47	0.46
w	0.21	0.68	0.56	0.31	0.33	0.42	0.51	0.52

Spec.	210	211	212	213	214	215	216	217
si	104.24	114.15	101.55	106.71	97.10	117.28	112.08	116.84
al	18.89	18.81	18.85	21.53	20.80	19.80	17.93	22.48
fm	48.15	50.66	50.92	47.74	48.67	48.60	49.75	48.96
c	23.67	21.73	21.23	21.87	21.94	20.80	21.48	19.42
alk	9.29	8.80	9.00	8.87	8.60	10.79	10.84	9.13
ti	3.04	2.54	2.97	1.79	1.85	2.62	4.09	2.38
p	0.21	0.14	0.16	0.08	0.21	0.20	0.26	0.22
k	0.18	0.06	0.19	0.21	0.10	0.04	0.03	0.44
mg	0.47	0.50	0.50	0.54	0.50	0.50	0.40	0.45
w	0.53	0.46	0.45	0.45	0.52	0.62	0.64	0.49

ZONE C

Spec.	218	221	222	223	224	225	226	227
si	115.36	105.54	112.33	114.88	105.70	144.14	116.52	129.74
al	20.32	20.59	21.11	23.72	20.39	26.08	21.91	24.48
fm	47.14	50.84	47.73	48.60	50.20	40.78	46.14	40.04
c	24.88	21.80	22.39	17.10	19.60	20.85	22.38	22.39
alk	7.67	6.76	8.77	10.58	9.80	12.29	9.56	13.08
ti	2.12	2.20	2.14	1.95	1.15	2.19	1.48	1.26
p	0.11	0.20	0.16	0.30	0.17	0.49	0.15	0.15
k	0.08	0.05	0.08	0.34	0.29	0.13	0.09	0.09
mg	0.55	0.59	0.55	0.56	0.57	0.47	0.60	0.60
w	0.40	0.46	0.45	0.53	0.58	0.50	0.31	0.65

CIPW Norms

ZONE A

Spec.	57	58	59	60	61	62	63	64
Q	0.00	3.70	0.00	2.65	4.04	0.00	0.00	0.00
Ab	20.48	21.83	27.33	19.97	26.65	17.27	20.73	25.05
An	25.45	26.51	25.71	24.88	28.93	28.32	34.06	29.89
Or	5.32	4.96	2.60	6.44	3.96	15.96	9.04	3.25
Ne	0.00	0.00	0.00	0.00	0.00	0.73	0.00	0.00
Di	19.22	14.04	16.99	12.13	11.57	6.63	7.49	12.20
Hy	13.79	14.28	0.03	15.04	14.51	0.00	14.07	11.70
Ol	6.17	0.00	18.88	0.00	0.00	21.22	5.48	7.29
An%	55.41	54.84	48.47	55.47	52.05	62.13	62.17	54.41

Spec.	65	66	67	68	69	70	71	72
Q	0.00	0.00	0.00	0.42	5.96	0.00	0.00	1.82
Ab	22.59	17.52	20.56	17.85	20.82	19.63	26.44	24.96
An	29.55	30.15	36.61	31.95	21.59	25.75	30.85	27.58
Or	2.66	7.51	2.66	7.09	7.92	9.04	2.36	1.36
Ne	0.00	0.00	0.00	0.00	0.00	0.00	0.25	0.00
Di	12.78	7.09	9.91	9.73	13.81	15.10	13.72	14.08
Hy	7.13	20.24	6.32	23.90	15.35	4.26	0.00	14.04
Ol	16.12	2.19	17.81	0.00	0.00	15.58	14.80	0.00
An%	56.67	63.25	64.03	64.15	50.91	56.74	53.85	52.49

Spec.	73	76	753	754	755	756	758	759
Q	0.00	0.00	0.00	0.00	0.00	0.00	0.00	0.00
Ab	16.59	19.04	25.30	23.27	19.80	18.45	20.22	20.05
An	25.06	28.11	25.35	25.76	30.69	22.94	26.90	31.77
Or	14.36	11.41	7.92	8.92	3.25	18.32	17.14	5.61
Ne	0.00	0.00	0.00	0.00	0.00	0.00	0.00	0.00
Di	13.72	13.27	14.40	13.45	14.28	6.76	5.30	13.75
Hy	1.55	2.96	9.97	0.29	18.64	8.54	2.04	10.49
Ol	15.13	16.04	9.30	18.17	5.42	11.44	18.49	10.93
An%	60.18	59.62	50.05	52.54	60.78	55.43	57.09	61.30

Spec.	760	761	762	766	768	770	771	772
Q	6.24	0.00	0.00	0.00	6.49	0.00	0.25	0.00
Ab	21.05	16.33	20.31	17.01	7.36	26.32	20.90	22.63
An	26.01	22.71	30.48	31.61	37.14	26.93	37.23	20.58
Or	9.40	11.58	5.14	4.85	5.50	16.02	3.19	15.60
Ne	0.00	0.00	0.00	0.00	0.00	0.00	0.00	1.54
Di	3.67	17.12	17.55	21.12	5.03	4.23	16.77	11.79
Hy	19.25	10.85	0.58	3.12	25.11	14.84	15.74	0.00
Ol	0.00	13.02	20.32	14.20	0.00	2.31	0.00	12.69
An 7	55.25	58.17	60.01	65.02	83.46	50.58	64.04	47.62

Spec.	773	774	779	780	783	784	785	786
Q	0.00	0.00	4.46	0.00	0.00	0.00	0.00	0.00
Ab	12.52	18.11	13.20	23.35	15.65	27.67	19.89	16.92
An	24.23	32.67	32.76	26.61	33.89	23.20	24.57	31.39
Or	20.39	6.32	8.69	4.26	11.41	5.61	6.38	12.53
Ne	0.00	0.00	0.00	0.00	0.00	0.00	0.00	0.00
Di	3.64	9.68	0.00	16.57	0.00	17.34	21.62	12.44
Hy	25.72	24.22	29.99	2.81	25.49	18.34	12.81	4.68
Ol	2.91	0.71	0.00	18.50	3.28	1.62	5.82	14.15
An 7	65.93	64.34	71.28	53.25	68.41	45.61	55.27	64.97

Spec.	787	788	789	C101	103	104	107	110
Q	0.00	0.00	0.00	0.00	0.00	0.00	0.00	0.00
Ab	26.15	20.65	23.67	25.30	16.53	14.51	22.22	19.63
An	28.02	32.81	25.18	26.29	25.67	27.62	27.76	28.91
Or	3.49	2.19	6.15	12.65	12.06	17.26	6.97	8.63
Ne	0.00	0.00	1.43	0.00	2.23	1.58	3.87	0.00
Di	15.74	10.36	19.29	8.29	17.56	8.98	13.03	12.95
Hy	1.15	15.89	0.00	0.22	0.00	0.00	0.00	2.77
Ol	17.52	12.34	16.14	20.87	18.14	20.01	13.43	14.53
An 7	51.73	61.38	51.55	50.96	60.84	65.55	55.54	59.55

Spec.	114	115	116	118	120	121	124	129
Q	0.00	0.00	0.00	0.00	0.00	0.00	7.35	0.00
Ab	22.85	10.75	12.80	12.36	13.44	17.94	11.25	17.23
An	31.05	29.05	21.56	26.99	19.69	20.80	31.77	21.93
Or	4.14	17.49	18.97	13.12	14.24	11.70	4.20	9.34
Ne	1.74	0.00	2.19	2.15	8.12	3.11	0.00	7.95
Di	12.99	9.52	11.31	14.78	20.22	19.02	11.76	19.92
Hy	0.00	11.34	0.00	0.00	0.00	0.00	23.55	0.00
Ol	13.41	14.80	21.64	19.65	15.84	17.34	0.00	15.71
An%	57.60	73.00	62.75	68.59	59.43	53.68	73.84	54.96

Spec.	132	303	305	306	309	311	312	314
Q	0.00	0.00	0.00	0.00	4.42	2.03	0.00	0.00
Ab	17.89	13.11	18.19	26.57	22.42	22.76	16.95	25.55
An	27.47	28.09	25.65	27.59	24.44	23.54	31.85	25.16
Or	9.57	13.77	13.89	3.96	8.86	6.44	5.08	7.98
Ne	2.05	4.22	0.00	0.00	0.00	0.00	0.54	0.00
Di	13.08	13.59	12.45	11.40	8.58	15.35	14.48	15.06
Hy	0.00	0.00	2.59	0.09	24.27	21.96	0.00	6.30
Ol	22.26	19.69	19.06	21.61	0.00	0.00	23.11	9.84
An%	60.56	68.19	58.50	50.94	52.15	50.84	65.27	49.61

Spec.	315	316	317	319	320	321	322	324
Q	0.00	3.07	0.00	2.62	0.00	4.92	0.00	0.00
Ab	17.60	24.79	25.89	14.81	18.19	27.16	16.33	26.65
An	22.22	24.87	29.64	35.98	29.81	28.55	27.39	23.96
Or	13.36	9.87	1.60	3.19	7.56	3.25	11.29	11.35
Ne	0.00	0.00	0.00	0.00	1.52	0.00	0.00	0.00
Di	11.17	7.88	14.15	5.59	13.91	5.35	16.08	7.92
Hy	22.18	23.39	3.46	25.31	0.00	19.93	11.91	17.81
Ol	1.22	0.00	14.52	0.00	24.12	0.00	5.01	3.59
An%	55.80	50.07	53.38	70.84	62.11	51.25	62.65	47.34

Spec.	325	326	327	328	329	330	331	332
Q	0.00	0.00	0.00	8.54	4.35	0.00	0.00	0.00
Ab	24.62	21.15	27.81	24.45	25.39	23.95	24.71	30.04
An	27.05	24.91	29.40	27.07	26.95	28.83	34.32	38.24
Or	6.56	10.05	4.85	9.81	7.92	4.85	5.73	2.54
Ne	0.00	0.00	1.11	0.00	0.00	0.00	0.00	0.00
Di	13.21	11.20	13.09	4.98	7.56	10.02	10.17	6.38
Hy	0.11	1.40	0.00	19.60	20.34	0.29	1.63	8.96
Ol	16.45	18.80	12.36	0.00	0.00	23.43	11.67	7.84
An%	52.34	54.07	51.39	52.53	51.49	54.63	58.14	56.01

Spec.	333	334
Q	0.00	0.00
Ab	26.15	21.81
An	36.79	38.18
Or	8.10	8.27
Ne	0.00	0.79
Di	3.46	5.02
Hy	2.19	0.00
Ol	14.49	18.93
An%	58.46	63.64

ZONE B

Spec.	78	80	81	82	83	84	85	86
Q	7.18	0.00	5.36	0.00	0.00	0.00	5.30	0.00
Ab	20.14	20.39	16.92	20.65	23.52	26.32	22.00	22.82
An	19.93	25.16	25.42	32.86	24.49	30.80	16.62	27.78
Or	7.21	10.28	6.68	1.77	5.79	2.60	13.77	4.85
Ne	0.00	0.00	0.00	0.00	0.00	0.00	0.00	2.44
Di	7.48	13.51	11.29	12.28	17.71	10.66	4.69	19.90
Hy	19.63	0.85	17.73	18.98	4.17	15.64	20.09	0.00
Ol	0.00	19.63	0.00	2.54	10.57	1.81	0.00	13.75
An%	49.74	55.24	60.04	61.41	51.01	53.93	43.04	54.89

Spec.	87	88	89	90	92	93	95	96
Q	0.00	3.20	0.00	0.00	0.00	0.00	0.00	0.00
Ab	23.10	18.11	23.72	34.10	17.35	21.92	24.96	26.15
An	31.11	22.45	30.97	33.71	33.54	31.48	29.44	30.88
Or	2.78	6.62	3.49	2.13	4.73	3.84	2.84	2.78
Ne	0.00	0.00	0.31	0.00	0.00	0.00	0.00	0.00
Di	10.54	15.77	11.73	0.00	6.13	18.37	11.67	11.09
Hy	10.75	16.55	0.00	16.03	12.67	7.32	7.30	16.46
Ol	13.82	0.00	21.22	0.21	17.55	10.60	12.18	3.71
An%	57.39	55.35	56.63	49.71	65.91	58.95	54.11	54.15

Spec.	97	98	99	100	F101	102	105	106
Q	0.06	0.00	0.00	1.63	0.00	0.00	4.71	0.00
Ab	22.68	18.53	26.23	27.50	26.91	33.09	28.18	25.76
An	19.87	27.50	26.07	25.90	26.59	18.03	22.04	26.69
Or	12.88	9.99	4.85	3.72	9.51	12.23	9.10	4.85
Ne	0.00	0.00	0.00	0.00	0.00	0.00	0.00	0.35
Di	4.36	13.61	13.18	6.55	14.59	7.96	6.25	15.21
Hy	24.08	7.87	5.09	18.02	0.95	12.18	18.32	0.00
Ol	0.00	10.01	10.18	0.00	15.45	4.48	0.00	13.40
An%	46.70	59.74	49.84	48.50	49.71	35.27	43.88	50.88

Spec.	705	707	710	711	712	723	725	734
Q	0.00	0.00	0.00	0.11	0.00	0.00	0.00	0.00
Ab	26.06	24.20	23.61	18.70	21.69	21.49	21.41	34.85
An	26.60	27.45	24.96	25.95	17.27	31.32	27.75	20.86
Or	4.08	2.60	8.75	10.28	5.20	1.71	4.79	3.43
Ne	0.00	0.00	0.00	0.00	3.38	0.00	0.00	0.28
Di	9.45	19.27	12.58	11.83	31.79	14.18	6.95	16.64
Hy	21.08	15.33	9.21	12.92	0.00	13.97	23.06	0.00
Ol	2.72	3.00	8.43	0.00	5.19	8.55	4.40	12.80
An%	50.51	53.14	51.40	58.12	44.33	59.30	56.45	37.45

Spec.	738	739	740	741	744	745	746	747
Q	0.00	0.00	0.00	0.00	0.00	0.00	0.00	0.00
Ab	23.27	21.24	24.29	22.99	13.48	18.87	19.30	21.66
An	20.73	29.61	32.46	30.07	32.76	27.32	19.03	21.30
Or	11.11	4.91	3.90	4.14	7.27	11.23	11.46	13.95
Ne	0.73	0.00	0.00	0.43	1.54	1.88	2.52	0.00
Di	17.30	17.63	12.86	15.13	17.26	13.89	13.82	14.67
Hy	0.00	12.87	8.17	0.00	0.00	0.00	0.00	0.64
Ol	16.98	4.81	11.56	19.50	16.55	16.62	15.82	15.28
An%	47.12	58.23	57.20	56.67	70.84	59.14	49.65	49.57

Spec.	748	749	750	C106	112	113	117	125
Q	0.00	0.00	12.60	0.00	0.00	0.00	0.00	0.00
Ab	24.54	16.75	27.16	20.00	20.48	21.41	13.88	20.48
An	25.06	29.48	28.30	24.56	30.79	29.07	30.89	27.72
Or	5.44	8.45	3.43	6.97	3.96	6.15	5.97	5.79
Ne	0.00	0.00	0.00	2.19	0.00	0.00	0.00	0.00
Di	16.31	14.60	2.17	24.39	13.12	13.10	10.12	14.51
Hy	5.18	10.86	17.94	0.00	9.23	12.29	8.27	4.11
Ol	15.58	9.27	0.00	14.12	12.51	7.84	17.58	15.48
An%	50.52	63.77	51.03	55.12	60.06	57.59	69.00	57.51

Spec.	128	133	134	136	138	141	401	402
Q	0.00	0.00	0.00	0.00	0.00	10.68	0.00	0.00
Ab	32.13	22.42	18.87	13.43	11.34	9.56	13.37	19.47
An	10.48	30.76	31.52	24.33	24.00	29.06	27.22	34.25
Or	22.34	6.26	5.14	15.42	23.11	15.07	13.30	5.79
Ne	1.71	0.00	0.00	3.08	0.00	0.00	0.00	1.10
Di	15.21	14.24	8.10	11.63	4.62	0.00	0.57	13.61
Hy	0.00	4.10	25.18	0.00	6.41	24.24	23.07	0.00
Ol	9.65	13.42	5.38	20.43	18.70	0.00	12.19	16.26
An%	24.59	57.84	62.55	64.44	67.91	75.24	67.06	63.76

Spec.	403	404	405	406	407	409
Q	0.00	0.00	0.00	0.04	0.00	0.00
Ab	25.89	15.15	20.82	9.65	17.77	25.64
An	24.91	29.74	30.74	35.26	27.30	33.84
Or	10.64	14.77	2.54	7.33	14.42	1.83
Ne	0.00	0.00	0.00	0.00	0.00	0.00
Di	14.18	8.25	12.82	4.66	8.54	7.95
Hy	1.51	5.31	9.71	39.74	5.05	2.01
Ol	13.94	17.07	9.84	0.00	17.36	18.69
An%	49.03	66.26	59.41	78.52	60.57	56.89

ZONE C

Spec.	713	715	716	722	726	727	728	730
Q	0.00	0.00	0.00	1.11	0.00	0.00	0.00	0.00
Ab	38.08	21.39	26.91	24.29	38.25	16.13	21.75	33.59
An	23.88	26.18	21.34	23.93	18.90	26.31	27.20	22.72
Or	3.19	6.26	7.09	2.07	2.07	11.23	4.67	7.27
Ne	0.00	4.04	0.00	0.00	0.00	2.49	0.00	0.00
Di	15.92	16.27	20.34	17.42	15.67	17.30	17.65	13.40
Hy	5.86	0.00	3.67	24.33	0.98	0.00	12.46	1.56
Ol	6.88	14.61	12.28	0.00	13.90	19.37	6.44	11.53
An%	38.55	55.03	44.23	49.63	33.07	62.00	55.57	40.35

Spec.	733	201	202	203	205	206	207	209
Q	0.00	0.00	0.00	0.00	0.00	0.00	0.00	0.00
Ab	22.80	29.53	28.77	32.66	28.19	28.94	28.44	39.65
An	20.20	17.98	29.51	25.08	23.07	23.67	22.44	21.11
Or	8.10	4.91	3.66	5.08	7.27	4.31	3.60	3.90
Ne	1.03	0.78	0.00	0.00	0.17	0.00	2.98	0.85
Di	22.33	17.19	10.84	12.01	16.42	12.54	16.74	14.27
Hy	0.00	0.00	5.91	5.43	0.00	17.86	0.00	0.00
Ol	18.93	12.49	9.80	14.33	17.89	2.70	14.72	12.00
An%	46.97	37.85	50.64	43.43	45.00	44.99	44.10	34.74

Spec.	210	211	212	213	214	215	216	217
Q	0.00	0.00	0.00	0.00	0.00	0.00	0.00	0.00
Ab	22.78	31.82	21.74	23.95	21.43	39.18	39.54	18.87
An	19.89	20.42	20.90	26.66	26.38	18.09	14.29	26.15
Or	6.97	2.19	7.33	7.80	3.60	1.77	1.18	15.78
Ne	3.75	0.00	3.99	2.11	5.53	0.00	0.31	0.00
Di	22.50	18.79	18.78	15.28	15.90	17.97	21.98	8.57
Hy	0.00	8.12	0.00	0.00	0.00	3.51	0.00	15.80
Ol	18.93	12.49	9.80	14.33	17.89	2.70	14.72	12.00
An%	46.61	39.09	49.01	52.68	55.17	31.59	26.54	58.08

Spec.	218	221	222	223	224	225	226	227
Q	0.00	0.00	0.00	0.00	0.00	3.29	0.00	0.00
Ab	26.65	26.06	31.56	26.49	22.51	35.29	33.34	41.19
An	25.39	29.78	25.45	26.34	22.46	24.15	25.05	21.42
Or	2.48	1.48	2.72	14.30	12.06	5.61	3.43	4.20
Ne	0.00	0.00	0.00	0.00	2.89	0.00	0.00	0.65
Di	19.38	12.68	15.93	4.78	14.43	7.74	15.70	15.70
Hy	11.62	10.64	3.54	4.20	0.00	16.26	0.13	0.00
Ol	6.65	12.12	13.74	15.62	16.68	0.00	17.83	8.91
An ^g	48.78	53.33	44.64	49.86	49.94	40.64	42.90	34.21

ZONE A

Spec.	K/Rb	K/Ba	Ba/Rb	Rb/Sr	Y/Nb	Zr/P ₂ O ₅	Ni/Co
57	467	31.3	14.9	0.09	3.14	440	1.5
58	996	80.1	12.4	0.05	3.00	490	2.4
59	731	79.3	9.2	0.03	2.43	390	1.5
60	362	44.4	8.2	0.12	1.24	480	2.3
61	795	47.9	16.6	0.02	1.00	570	2.0
62	157	67.9	2.3	1.44	4.38	470	3.6
63	231	25.1	9.2	0.17	3.14	330	2.3
64	381	47.1	8.1	0.04	2.13	450	4.8
65	623	50.4	12.3	0.03	3.40	560	3.4
66	364	14.4	25.2	0.08	4.00	350	2.8
67	623	66.8	9.3	0.03	2.29	560	3.3
68	293	42.9	6.8	0.11	1.73	360	5.2
69	742	33.8	21.9	0.08	2.33	120	2.0
70	302	33.4	9.0	0.20	2.59	520	1.7
71	553	34.0	16.2	0.02	2.25	530	2.7
72	636	3.9	161.0	0.02	2.75	660	2.3
73	194	41.2	4.7	0.57	1.82	320	2.9
76	184	79.7	2.3	0.37	1.75	460	3.2
753	293	60.1	4.9	0.15	0.67	380	2.4
754	182	39.8	4.6	0.28	0.96	330	2.6
755	380	-	-	0.06	1.56	740	2.2
756	158	164.9	1.0	1.65	4.30	320	1.2
758	177	58.6	3.0	0.76	0.30	410	2.7
759	358	563.2	0.6	0.13	0.75	450	1.7
760	165	27.5	6.0	0.38	1.24	275	2.1
761	346	101.7	3.4	0.41	1.49	470	1.2
762	344	-	-	0.14	1.50	350	2.6

Spec.	K/Rb	K/Ba	Ba/Rb	Rb/Sr	Y/Nb	Zr/P ₂ O ₅	Ni/Co
766	486	62.4	7.8	0.05	0.78	715	0.2
768	266	48.5	5.5	0.29	1.42	745	2.2
770	205	30.3	6.7	0.43	1.15	425	0.4
771	747	66.9	11.2	0.02	0.83	455	1.0
772	217	35.6	6.1	0.36	0.89	295	0.9
773	157	86.3	1.8	4.79	1.27	320	2.1
774	269	134.6	2.0	0.16	0.84	645	2.8
779	249	60.1	4.1	0.35	1.61	460	6.1
780	543	284.6	1.9	0.07	1.78	520	2.0
783	157	64.1	2.5	0.87	0.41	475	3.2
784	464	40.9	11.4	0.14	0.94	815	3.2
785	640	63.6	10.1	0.08	1.26	535	2.1
786	383	103.5	3.7	0.21	0.41	545	2.1
787	1224	102.0	12.0	0.02	2.83	495	1.2
788	341	90.3	3.8	0.04	0.88	610	1.7
789	617	-	-	0.08	1.14	520	0.8
0101	228	89.2	2.6	0.55	1.91	755	1.5
103	209	61.2	3.4	0.35	0.47	480	1.9
104	189	38.2	5.0	0.75	0.31	350	1.6
107	363	64.5	5.6	0.92	0.33	405	2.1
110	128	40.1	3.2	0.52	1.08	510	1.6
114	527	47.5	11.1	0.04	2.38	490	1.4
115	225	51.6	4.4	0.90	0.37	525	3.1
116	118	191.7	0.6	12.5	0.82	415	2.5
118	125	62.0	2.0	2.13	0.30	295	3.4
120	146	52.8	2.8	0.31	0.44	505	2.1
121	173	70.0	2.5	0.27	1.24	440	1.4

Spec.	K/Rb	K/Ba	Ba/Rb	Rb/Sr	Y/Nb	Zr/P ₂ O ₅	Ni/Co
124	1179	134.1	8.8	0.02	1.69	335	1.7
129	273	32.5	8.4	0.26	0.69	530	2.0
132	259	86.8	3.0	0.46	2.24	495	1.5
303	245	101.3	2.4	0.52	1.19	825	2.0
305	315	70.9	4.4	0.39	1.86	480	1.8
306	354	34.1	10.4	0.08	1.84	540	1.2
309	389	31.2	12.5	0.15	1.70	280	0.4
311	1005	44.1	22.8	0.05	2.67	540	0.6
312	275	62.2	4.4	0.16	1.86	450	1.7
314	350	68.7	5.1	0.28	1.85	630	0.8
315	158	78.5	2.0	10.8	1.36	460	2.1
316	262	33.6	7.8	0.25	1.55	610	2.4
317	560	59.2	9.5	0.17	2.20	1800	2.8
319	498	40.3	12.3	0.06	1.83	400	1.3
320	247	60.7	4.1	0.17	0.78	610	2.0
321	913	22.0	41.6	0.02	2.38	435	0.5
322	201	48.6	4.1	0.42	1.48	460	1.6
324	295	70.0	4.2	0.37	2.02	500	1.9
325	419	76.7	5.5	0.11	2.99	470	1.7
326	353	80.1	4.4	0.24	3.33	494	1.4
327	524	46.9	11.2	0.05	3.54	475	1.3
328	219	25.7	8.5	0.25	1.12	120	0.7
329	242	20.2	12.0	0.21	2.07	645	0.7
330	272	64.8	4.2	0.16	1.46	465	2.2
331	366	20.4	17.9	0.06	1.60	370	1.6
332	275	40.2	6.8	0.04	0.43	415	1.5
333	207	60.5	3.4	0.19	0.41	600	2.4
334	332	79.1	4.2	0.13	0.34	550	1.1

Spec.	Zone B						
	K/Rb	K/Ba	Ba/Rb	Rb/Sr	Y/Nb	Zr/P ₂ O ₅	Ni/Co
78	130	48.0	2.7	0.49	1.03	100	2.6
80	688	118.0	5.8	0.10	6.11	280	1.8
81	494	23.6	21.0	0.06	1.29	420	1.8
82	830	99.6	8.3	0.02	2.86	530	2.4
83	740	147.8	5.0	0.08	1.79	560	1.4
84	522	16.4	31.9	0.02	2.13	320	3.0
85	317	18.1	17.6	0.18	0.93	360	2.6
86	272	45.6	6.0	0.11	2.22	520	3.1
87	325	25.8	12.6	0.05	2.00	530	4.3
88	344	20.1	17.1	0.10	1.47	410	1.2
89	612	52.7	11.6	0.03	2.33	550	1.7
90	598	27.5	21.8	0.01	0.94	1080	1.9
92	302	24.5	12.2	0.09	2.14	400	2.3
93	600	110.2	5.4	0.05	2.67	410	1.4
95	569	27.6	20.7	0.03	3.83	480	3.0
96	488	40.6	12.0	0.03	2.38	540	3.1
97	292	22.8	12.8	0.26	1.41	270	1.3
98	167	46.5	3.6	0.44	2.14	420	2.2
99	425	15.9	26.7	0.04	1.35	200	1.5
100	1046	15.6	66.6	0.01	1.38	440	1.8
F101	371	63.8	5.8	0.17	1.69	530	2.6
102	409	21.9	18.7	0.14	1.49	440	1.1
105	457	15.8	28.9	0.08	1.81	420	2.1
F106	619	67.3	9.2	0.04	5.20	480	1.8
705	477	18.7	25.6	0.22	2.86	550	1.0
707	261	29.2	8.9	0.18	2.60	590	2.6
710	168	60.8	2.8	0.33	2.20	275	2.5
711	147	65.3	2.3	0.56	0.91	285	1.8
712	731	42.0	17.4	0.06	2.55	460	1.2
723	344	100.3	3.4	0.04	2.59	540	2.2
725	480	12.2	39.5	0.05	1.69	360	1.4

Spec.	K/Rb	K/Ba	Ba/Rb	Rb/Sr	Y/Nb	Zr/P ₂ O ₅	Ni/Co
734	241	130.1	1.9	0.12	1.44	590	1.9
738	294	63.7	4.6	0.23	1.23	460	2.4
739	689	-	-	0.06	1.27	690	1.0
740	498	58.9	8.5	0.04	1.05	290	2.1
741	484	242.1	2.0	0.07	2.03	610	2.3
744	319	192.6	1.7	0.11	1.97	443	1.0
745	159	167.8	0.9	0.38	0.55	280	2.0
746	168	57.3	2.9	9.6	2.38	390	1.3
747	258	42.7	6.0	0.30	1.15	3440	2.0
748	382	95.6	4.0	0.10	2.72	490	1.1
749	290	133.4	2.2	0.21	1.22	295	2.3
750	535	12.4	43.1	0.03	1.58	510	0.7
C106	377	51.6	7.3	0.16	1.17	320	1.6
112	309	28.5	10.8	0.07	1.45	485	2.6
113	262	46.0	5.7	0.17	1.67	515	1.2
117	599	42.9	14.0	0.12	2.30	310	1.3
125	479	90.6	5.3	0.07	1.41	675	1.2
128	308	70.3	4.4	0.81	2.11	860	0.8
133	550	56.4	9.8	0.06	1.95	465	2.0
134	380	96.3	3.9	0.12	0.97	600	1.6
136	230	108.3	2.1	0.98	1.68	290	1.4
138	244	152.3	1.9	1.35	1.10	400	1.6
141	148	39.1	3.8	1.06	1.33	940	2.1
401	115	44.9	2.6	3.89	0.53	470	2.9
402	542	22.8	23.8	0.06	1.07	575	2.2
403	223	46.9	4.8	0.28	0.94	540	0.6
404	228	71.8	3.2	0.78	2.39	510	6.2
405	714	58.6	12.2	0.02	2.80	430	8.6
406	124	64.8	1.9	1.15	0.54	745	2.6
407	107	230.1	0.5	2.36	0.59	405	2.0
409	515	64.4	8.0	0.02	1.53	420	1.6



IMAGING SERVICES NORTH

Boston Spa, Wetherby

West Yorkshire, LS23 7BQ

www.bl.uk

**3RD PARTY COPYRIGHT
MATERIAL EXCLUDED
FROM DIGITISED THESIS**

**PLEASE REFER TO THE
ORIGINAL TEXT TO SEE
THIS MATERIAL**